Brain wiring and neuronal dynamics : advances in MR imaging of focal epilepsy

Brain wiring and neuronal dynamics

advances in MR imaging of focal epilepsy

ISBN 978-94-6203-552-2
Printed by CPI – Royal Wöhrmann

The printing of this thesis was financially supported by the following organizations: epilepsiecentrum Kempenhaeghe, Nederlands Epilepsiefonds, School for Mental Health and Neuroscience (Maastricht University), Epilepsievereniging Nederland, UCB Pharma

Brain wiring and neuronal dynamics

advances in MR imaging of focal epilepsy

PROEFSCHRIFT

ter verkrijging van de graad van doctor aan de Universiteit Maastricht,
op gezag van de Rector Magnificus, Prof. Dr. L. L. G. Soete,
volgens het besluit van het College van Decanen,
in het openbaar te verdedigen
op vrijdag 4 april 2014 om 12.00 uur

door

René Mathieu Hubertus Besseling
Geboren op 10 oktober 1984 te Maastricht

Promotores
Prof. Dr. A. P. Aldenkamp
Prof. Dr. Ir. W. H. Backes

Co-promotor
Dr. J. F. A. Jansen

Beoordelingscommissie
Prof. Dr. R. van Oostenbrugge (voorzitter)
Prof. Dr. Ir. J. W. M. Bergmans, TU Eindhoven
Prof. Dr. F. M. Mottaghy, RWTH Aachen/ UM
Prof. Dr. K. Nicolay, TU Eindhoven
Prof. Dr. J. E. Wildberger

Table of contents

CHAPTER 1

General introduction

R.M.H. Besseling

Brain wiring and neuronal dynamics
advances in MR imaging of focal epilepsy

1.1 The brain

1.1.1 Brain networks

The brain is organized as a network (van den Heuvel and Hulshoff Pol 2010); it consists of specialized ensembles of neurons, which are interconnected. This network organization is evident at several levels (Figure 1.1). At the largest scale, the brain consists of cortical and subcortical gray matter, which contains the neuronal cell bodies; and of white matter, which is composed of bundles of interconnecting axons. Within specialized regions such as the visual cortex, a network organization is also evident, in which information is relayed from primary to higher visual areas. On the smallest scale, the cortex is organized into neuronal columns. These consist of vertically orientated pyramidal cells and interconnecting interneurons. Also specialized afferent and efferent connections are present at specific depths, giving the whole a layered organization (Zigmond, Bloom et al. 1999).

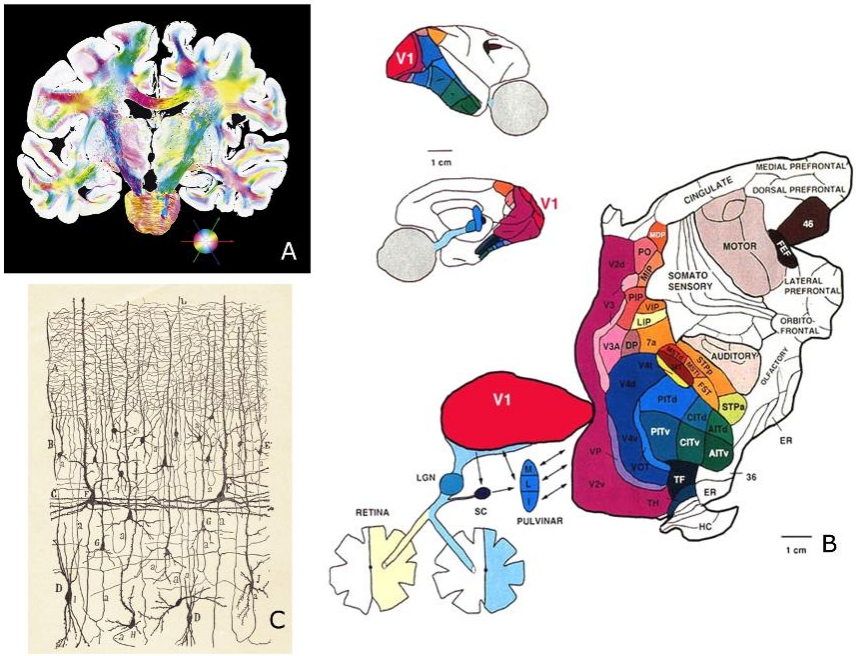

Figure 1.1: The brain is a multilevel network. Macroscopically, it consists of cortical and subcortical gray matter areas, interconnected by white matter bundles as visualized by polarized light imaging (PLI; (Axer, Amunts et al. 2011)) in A (fiber orientation color coded; see inset). On the meso scale, specialized subnetworks processes specific information, such as the visual stream linking the primary visual cortex (V1) to higher visual areas (V2-4) in B, (Van Essen, Anderson et al. 1992). Microscopic cortical columns as depicted in C represent the smallest network scale (original drawing by Ramón y Cajal, 1899).

1.1.2 Neurons and synapses

The smallest functional unit of the brain is the neuron, which consists of a cell body, one or more dendrites, and a single axon (Figure 1.2). In essence, a neuron is an electro-chemical relay unit.

Neurons connect to each other through so called synapses, in which the presynaptic axon signals to the postsynaptic neuron by excretion of chemical substances called neurotransmitters. Neurons maintain an electrical resting potential over their membrane, which is transiently disturbed by these neurotransmitters in two ways: depolarization by excitatory post synaptic potentials (PSPs) and hyperpolarization by inhibitory PSPs. The exact effect a neurotransmitter exerts depends on its type, the neuronal circuit involved (and its ion channel types), as well as the developmental stage. For example, the role of γ-aminobutyric (GABA) shifts from excitatory to inhibitory during brain maturation. Other important neurotransmitters are glutamate (typically excitatory) and acetylcholine (dual role) (Zigmond, Bloom et al. 1999).

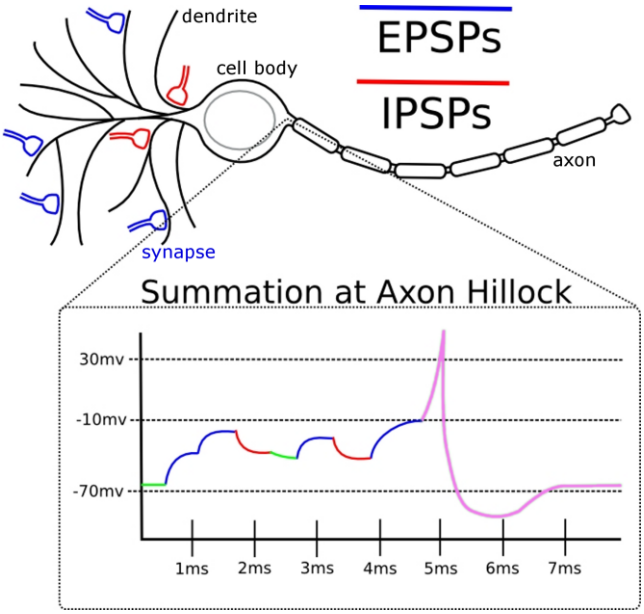

Figure 1.2: Neurons connect to each other in synapses, which may deliver either excitatory (blue) or inhibitory (red) post-synaptic potentials (EPSPs and IPSPs, respectively). These transiently disturb the equilibrium resting potential of -70 mV that the post-synaptic neuron actively maintains (green) over its membrane. The combined effect of EPSPs and IPSPs may at a certain moment depolarize the post-synaptic neuron beyond its threshold of about -10 mV, which triggers an action potential (pink) of signaling to the next neuron.
Figure adapted from Matlab file exchange #25788; www.mathworks.com

1.1.3 Action potentials and information processing

A neuron may receive input from as many as several thousands of synapses, each of which may be either excitatory or inhibitory (DeFelipe, Marco et al. 1999; Drachman 2005). The combined effect of the resulting PSPs over time may at a certain moment depolarize the neuron beyond a certain threshold. When this happens, an action potential occurs, which is the propagation of a depolarization along the cell membrane. When this action potential reaches the axonal terminus, it will trigger the release of neurotransmitters into the synapse with the next neuron, etc.

Effectively, each neuron thus performs a spatio-temporal integration of information (i.e. it combines inputs from distributed other neurons over time), and networks of neurons can therefore display very complicated dynamics indeed. In a sense, it is the complicated interactions between neuronal networks of specialized topologies and over several spatio-temporal scales that give rise to complex dynamic phenomena such as behavior, cognition, and emotion (Deco, Jirsa et al. 2008). In fact, abnormalities in neuronal dynamics and/or neuronal network topology may give rise to neurological diseases, for example epilepsy.

1.2 Epilepsy

1.2.1 Epidemiology and diagnosis

Epilepsy is the most prevalent neurological disease worldwide, and is estimated to affect 4-10 of every 1000 people at some point in their lives (Banerjee, Filippi et al. 2009; WHO October 2012). About 40% of the newly diagnosed cases are children under 18 years of age (Shinnar and Pellock 2002). In fact, epilepsy is a spectrum disease, which makes concise description and categorization very challenging, and even subject to regular revision due to progressive insights (Berg, Berkovic et al. 2010).

The common characteristic of epilepsy is recurrent unprovoked seizures. These represent transient episodes of abnormal neuronal activity, which are accompanied by characteristic abnormalities on electroencephalography (EEG). Seizure-concordant EEG abnormalities are an important aspect of the clinical diagnosis of epilepsy (Hauser and Kurland 1975; Banerjee, Filippi et al. 2009).

1.2.2 Causes

Epilepsy can have a variety of causes, including cortical and vascular malformations, brain tumors or other lesions, stroke, brain trauma, infections of the brain such as meningitis, encephalitis, neurocysticercosis, as well as genetic factors (WHO October 2012).

In all cases, there is a disbalance between excitation and inhibitions within the brain, leading to transient episodes of abnormal neuronal activity. More specifically, clusters of neurons display a tendency of hyperexcitability, and transient episodes of hypersynchronisation. This presents clinically as seizures, during which normal information processing is temporarily disrupted (Morimoto, Fahnestock et al. 2004; Jacobs MP, Leblanc GG et al. 2009).

As an underlying cause for this disbalance, abnormalities in the non-neuronal glial cells that support and nourish the neurons have been proposed (de Lanerolle, Lee et al. 2010; Devinsky, Vezzani et al. 2013). Recently, awareness has increased that inflammatory processes may also play an important role (Devinsky, Vezzani et al. 2013). Furthermore, oxidative stress and mitochondrial dysfunction have been suggested both as consequences and as causes of epileptic seizures (Patel 2004; Kudin, Zsurka et al. 2009).

1.2.3 Epileptogenesis

It is assumed that preceding the first seizure, a process of epileptogenesis occurs within the brain (J Engel 2007). During this period, normal brain tissue is transformed into tissue capable of generating unprovoked seizures (Jacobs MP, Leblanc GG et al. 2009). This involves changes in neurotransmitter and receptor levels and distributions, as well as rewiring of neuronal circuits (Morimoto, Fahnestock et al. 2004). In the course of the epileptogenic period, the EEG will develop sub-clinical epileptiform activity which at some point exceeds a certain threshold and triggers the first seizure.

1.2.4 Seizures

The type and severity of the seizures depends on which region of the cortex is involved (epileptogenic zone), and to what extent the epileptiform activity spreads over the cortex (Berg, Berkovic et al. 2010). In focal epilepsy, the epileptiform activity and seizures originate from one or several specific cortical areas; if subsequent spread to the rest of the brain is observed, this is called secondary generalization. In primary generalized epilepsy, it is not possible to pinpoint the exact region of seizure onset. Seizures may range from relatively subtle absence seizures in children, with short spells (seconds) of reduced consciousness, to full-blown tonic-clonic seizures (several minutes), in which the subject displays jerks of the limbs, falls to the ground, and loses consciousness completely.

Although some subjects report “feeling strange” directly prior to a seizure (epileptic aura), the seizures are unpredictable by definition, and may occur at any moment. However, certain provocative factors may increase the seizure likelihood, such as sleep deprivation (also used in diagnostic settings), stress, fever, hyperventilation, specific cognitive tasks, and visual stimulation (Kasteleijn-Nolst

Trenite, de Weerd et al. 2013). Obviously, epileptic seizures can greatly interfere with daily activities and have a profound impact on the quality of life.

1.2.5 Interictal epileptiform activity

Also in between seizures (i.e. interictally), subtle but still typical EEG abnormalities may be observed; this is known as epileptiform activity. By definition, epileptiform activity is sub-clinical, in the sense that it is insufficient in amplitude or extent to trigger a seizure (ictus). If at a certain point the epileptiform activity exceeds a certain threshold, this results in a (clinical) seizure.

1.2.6 Anti-epileptic drugs

Epilepsy may be treated using a variety of anti-epileptic drugs (AEDs). Especially over the last decades a multitude of new AEDs has become available, and AED development remains a very active field of research (Das, Dhanawat et al. 2012; Simonato, Loscher et al. 2012). This poses a clinical challenge, since a priori it is difficult to establish which AED will be effective in which patient, and this typically needs to be tested in practice (Simonato, Loscher et al. 2012). If the efficacy of a certain AED is insufficient, another may be considered. However, the likelihood of therapeutic success reduces each time an alternative AED is prescribed, and is only a few percent for the third AED in line (Kwan and Brodie 2000; Callaghan, Anand et al. 2007).

1.2.7 Epilepsy, cognition, and AEDs

Epilepsy is associated with neuropsychological comorbidities including cognitive complaints (Rudzinski and Meador 2013). Furthermore, AEDs influence neuronal signaling, and thereby may impact cognitive abilities as well (Ijff and Aldenkamp 2013). As a consequence, not only seizure control, but also preservation of cognitive abilities is an important clinical goal (Lin, Mula et al. 2012; Ijff and Aldenkamp 2013; Witt and Helmstaedter 2013). Epilepsy treatment is convoluted by this complex interaction between epilepsy, cognition, and medication. A trade-off is to be found between the degree of seizure control and the extent of cognitive problems and/or complaints, in close dialogue with the patient, and including factors such as type and severity of the epilepsy.

As mentioned, the exact interaction between epilepsy and cognition is a complicated matter. Status epilepticus, a life-threatening state of persistent seizure, has been shown to cause both transient and chronic brain damage (Morimoto, Fukuda et al. 2002; van Eijsden, Otte et al. 2011). On the other hand, typical seizures are much milder. Furthermore, seizures are rare, and interleaved with long (days-months) seizure-free interictal periods. However, in the inter-ictal state, epileptiform activity may still be present, which may interfere with neuronal circuits. It is known that brain network formation (and consolidation) depends on

the presence of suitable neuronal cues, such as adequate neuronal signaling (Andersen 2003). It has been suggested that epileptiform activity represents a pathological cue which disrupts brain networks, and that this is the actual cause of cognitive problems (Shewmon and Erwin 1988; Seri, Cerquiglini et al. 1998; Lin, Mula et al. 2012).

1.2.8 Rolandic epilepsy

Rolandic epilepsy (RE) is the most common focal childhood epilepsy, with a prevalence of 10-20/10.000 children aged 0-15 years and a typical age at onset of 7-10 years (Panayiotopoulos, Michael et al. 2008). It is an idiopathic disorder of unknown cause, which probably has a genetic basis of which the genes are as yet unknown.

RE is characterized by epileptiform activity originating from the centro-temporal (rolandic) cortex on EEG and typically mild and nocturnal seizures (Panayiotopoulos, Michael et al. 2008; Hughes 2010). As the rolandic cortex is involved with sensorimotor function, seizures typically involve hemifacial spasms, oromotor symptoms and speech arrest (Loiseau P and Duché B 1989; Hughes 2010).

RE is also known as benign epilepsy (of childhood) with centro-temporal spikes (BECTS), and seizures spontaneously resolve before the age of 16 years (Panayiotopoulos, Michael et al. 2008). Because of its mild seizure nature and this spontaneous seizure remission, in clinical practice RE is often left untreated (Hughes 2010).

Over the last years, RE has been associated with a variety of visuomotor, neuropsychological and cognitive complaints (Deltour L, Barathon M et al. 2007; Deltour L, Querné L et al. 2008), mostly language problems (Jocic-Jakubi B and Jovic NJ 2006; Liasis A, Bamiou DE et al. 2006; Clarke, Strug et al. 2007; Lillywhite, Saling et al. 2009). These findings have put RE's assumedly benign character under debate (Hughes 2010). EEG criteria have been established for cognitive impairment risk over a decade ago, and the neuropsychological profile of impairment has been extensively described (Gündüz E, Demirbilek V et al. 1999; Massa R, de Saint-Martin A et al. 2001). However, the underlying brain mechanisms and the structural and/or functional connections that are involved have as yet received little attention.

During childhood, essential neuronal networks for cognitive processing are established. It is assumed that this network formation is under guidance of neuronal cues such as neurotransmitters and growth factors, but also depends on adequate network dynamics, such as learning (Andersen 2003). In RE, epileptiform activity may interfere with normal signaling in neuronal networks, and as such may lead to deviant development of these networks.

A key question is how epileptiform activity originating from the rolandic (sensorimotor) cortex may cause not only speech (which is a motor function) to be affected, but also other (cognitive) aspects of language, such as reading, verbal memory, and speech comprehension (Jocic-Jakubi B and Jovic NJ 2006; Liasis A, Bamiou DE et al. 2006; Clarke, Strug et al. 2007; Lillywhite, Saling et al. 2009). In a previous thesis by our group, the special role of language impairments amongst the cognitive complaints in RE was established from a neuropsychological point of view (Overvliet GM, Besseling RM et al. 2010; Overvliet GM, Aldenkamp AP et al. 2011; Overvliet GM, Aldenkamp AP et al. 2011; Overvliet GM, Besseling RMH et al. 2011; Overvliet, Besseling et al. 2013). Employing advanced neuroimaging methods, the current thesis aims to shed light on the underlying brain abnormalities, among which patterns of aberrant brain connectivity.

1.2.9 Focal cortical dysplasia

Focal cortical dysplasia (FCD) is a type of congenital malformation of cortical development which is highly epileptogenic (Taylor, Falconer et al. 1971; Blumcke, Thom et al. 2011). It involves cortical lesions in which the normal (layered) cytoarchitecture of the cortex is disturbed (Palmini, Najm et al. 2004). FCD actually extends into the underlying white matter, where ectopic neurons as well as abnormal so-called balloon cells may be found (Palmini, Najm et al. 2004; Blumcke, Thom et al. 2011). The patch of cortex concerned is prone to hypersynchronisation of neuronal activity, which may trigger seizures (Jacobs MP, Leblanc GG et al. 2009; de Lanerolle, Lee et al. 2010).

The basis of FCD is aberrant neuronal migration during cortex formation. The cortex is established in an inside-out fashion, with newly formed neurons migrating from the germ layer near the ventricle along already established cortical layers towards the outer surface. In FCD, this complex process is locally disturbed.

FCD typically gives rise to medically refractory epilepsy, for which resective surgery may be the only therapeutic option (Taylor, Falconer et al. 1971). The neurosurgical challenge is to remove as much abnormal cortex as possible while sparing eloquent cortex to prevent loss of function. Histopathological examination of surgical specimens can be used to investigate to what extent the abnormal tissue has been removed (Taylor, Falconer et al. 1971). It has been estimated that 80% of patients become seizure free after full resection, compared to only 20% in case of incomplete resection (Hauptman and Mathern 2012).

Accurate neuro-imaging is essential in the presurgical work-up to assess the extent of the abnormal tissue. Conventional magnetic resonance imaging (MRI) is important to detect and characterize structural FCD features, such as increased cortical thickness, abnormalities in the gyral pattern, blurring of the gray matter-white matter interface, as well as structural abnormalities of the underlying white matter (Hofman, Fitt et al. 2011). In MRI-negative cases, e.g. fluorodeoxyglucose

positron emission tomography (FDG-PET) may be used to delineate characteristic hypometabolic cortex (Chassoux, Landre et al. 2012). Magnetoencephalography (MEG) has also been proven of value for detecting cortical abnormalities beyond the structural lesion (Widjaja, Zarei Mahmoodabadi et al. 2009).

In addition to these focal characterizations, it would be interesting to study the (local) connectivity of FCDs to understand how the epileptiform activity is distributed through (part of) the brain network. This may provide alternative approaches to delineate (more) aberrant cortex, potentially improving surgical outcome. Ultimately, this may lead to the development of alternative surgical approaches, in which the epileptic tissue is not removed but merely electrically insolated by resection of selected connections. Such surgical procedures may be less invasive and might especially be useful in the proximity of eloquent cortex.

1.3 Magnetic resonance imaging

MRI is a very versatile and non-invasive medical imaging technique, which allows the in vivo assessment of (abnormalities of) soft tissues such as the brain in exquisite detail. Its settings can be tuned to create a whole range of clinically relevant image contrasts, and in advanced approaches it can even be used to open windows on brain physiology (functional MRI) and microstructure (diffusion weighted imaging).

1.3.1 Nuclear magnetic resonance

MRI is based on the principle of nuclear magnetic resonance (NMR; Figure 1.3). NMR exploits the fact that certain atomic nuclei (certain isotopes, to be precise) possess a magnetic property called spin. When placed in an external magnetic field, these atoms will start to precess around their axis. Furthermore, they will line up with the field in either of 2 orientations, spin-up or spin-down. Spin flips (from spin-up to spin-down) can be induced by exposing the spins to electromagnetic (EM) radiation of a certain frequency, the resonance or Larmor frequency. For in vivo applications, these frequencies are within the radio band, and this process is known as excitation, see Figure 1.3A. Flipped spins will fall back to the energetically more favorable spin-up state (relaxation) at a rate which is defined by the T1 relaxation time. When doing so, they will re-emit the radio waves they previously absorbed.

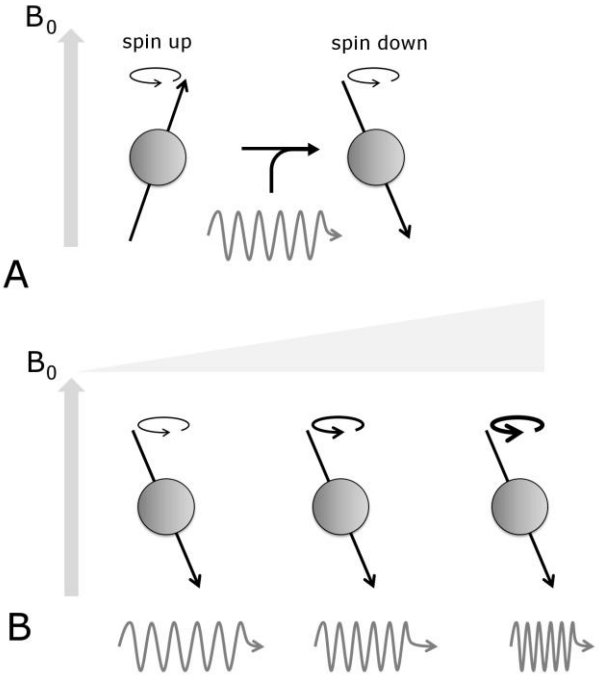

Figure 1.3: The principle of nuclear magnetic resonance (NMR): when placed in an external magnetic field B_0, spins will precess around their axis and will align with this field in either of 2 orientations, spin-up or spin-down. Spin flips (from spin-up to spin-down) can be induced by radio waves of the Larmor frequency of spin precession (excitation; A). Governed by a time constant T1, these radio waves are subsequently re-emitted in a process called relaxation. As the Larmor frequency increases with the field strength, field gradients can be used to encode the position of the spins in the frequency of these radio waves; this is known as frequency encoding (B).

1.3.2 Imaging and contrast mechanisms

MRI is based on inducing spin flips within the tissue and detecting the subsequently re-emitted radio waves (read-out). To identify from which position within the tissue the radio signals originate, spatial encoding is needed. For this, during read-out the main magnetic field B_0 is modulated by an additional field called a gradient, to make the total field vary linearly over space. As the Larmor frequency increases with the field strength, the frequency of the re-emitted radio waves thus contains information on the spin locations (Figure 1.3B). This is known as frequency encoding. An encoding that is mathematically equivalent can be applied in the second dimension to build a 2D image. This involves temporarily switching on a gradient perpendicular to the frequency encoding gradient and before read-out, which is known as phase encoding. 3D image volumes can be built by stacking 2D images or by extending the phase-encoding scheme to 3D. The resulting cubic image elements are known as voxels.

In order for the signals of the individual spins to make up a signal that is macroscopically measurable, the spins within a voxel need to precess synchronously (in phase). Directly after excitation, spins will start to dephase due to dynamic spin-spin interactions and within-voxel field inhomogeneities. Depending on the acquisition scheme, the effect of static field inhomogeneities may or may not be compensated for, resulting in T2 or T2* relaxation, respectively.

In medical MRI, typically the Larmor frequency of hydrogen nuclei (^1H) is used, which implies that the signal is (mostly) derived from tissue water (H_20). Since tissue consists for 55-75% of water (Dubinskaya, Eng et al. 2007), this yields a relatively high signal, and ^1H-MRI is especially useful to depict soft ("watery") tissue such as muscle, liver and brain.

Based on the exact excitation and acquisition scheme, MR images can be T1-, T2- or T2*-weighted (low signal in voxels of long T1 or short T2/T2*, respectively), proton density (^1H) weighted, or any combination. The introduction of additional gradients (e.g. in diffusion weighted imaging) or excitation pulses (e.g. inversion recovery) further broadens the range of possibilities, yielding a sheer infinite variety of clinically relevant image contrasts.

1.3.3 Functional MRI

While constituting only 2% of the total body weight, the brain accounts for 20% of the total oxygen expenditure (Raichle and Gusnard 2002; Tomasi, Wang et al. 2013). Not surprisingly, it is supplied with a very elaborate vasculature, and blood perfusion is regulated based on local metabolic demands. This dynamic relation between neuronal activity and perfusion is known as neuro-vascular coupling.

When neuronal activity increases, not only is the local perfusion (and volume) of blood increased, but also the ratio between oxygenated and deoxygenated hemoglobin changes. Actually an overshoot of oxygenated hemoglobin is delivered. Since oxygen magnetically shields hemoglobin's ion-containing heme groups, this reduces local dynamic field inhomogeneities caused by passing red blood cells. As a consequence, T2*-relaxation is reduced. Effectively this meant that the T2*-weighted signal goes up and down in accordance with the neuronal activity. This is known as the blood oxygen level dependent (BOLD) effect.

In task fMRI, a series of T2*-weighted images of the brain is acquired over time while the subject is presented with a task that modulates neuronal activity. Dedicated statistics are applied to identify those voxels for which the time series significantly resembles the task design (R.S.J. Frackowiak 2003). In this way, distributed brain regions can be found that define the network that processes the task under investigation (Figure 1.4A).

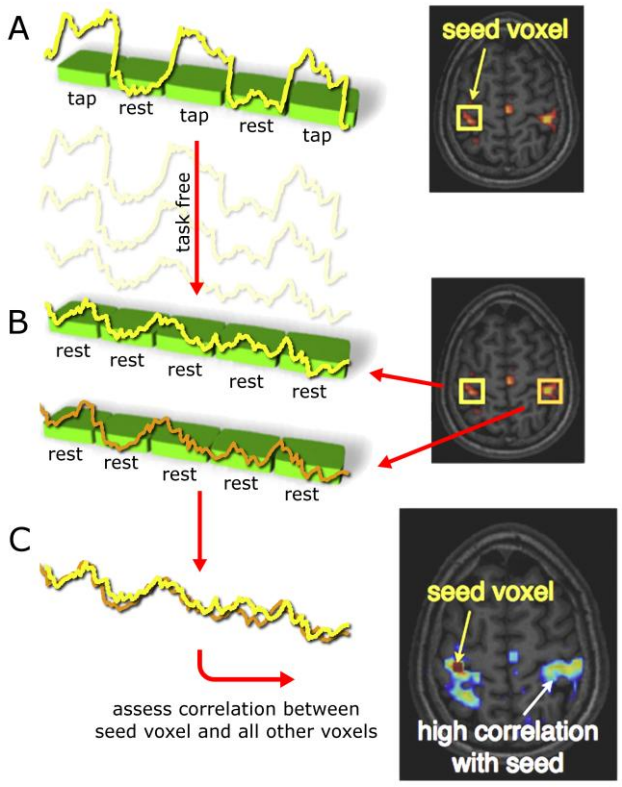

Figure 1.4: Task and resting-state fMRI. In task fMRI, voxels are identified for which the time series resembles the task design (A), in this case a finger tapping paradigm. In resting-state fMRI, this task-induced modulation in neuronal activity is omitted. The remaining spontaneous signal fluctuations have been demonstrated to be of neuronal origin and contain information on the intrinsic functional architecture of the brain (B). For example, correlation analysis of resting-state time series can be used to construct functional connectivity maps for seed voxels of interest (C), in this case the motor network. Figure based on (Biswal, Yetkin et al. 1995; van den Heuvel and Hulshoff Pol 2010).

Over the last two decades, resting-state fMRI (rs-fMRI) has been developed (Biswal, Yetkin et al. 1995). The same acquisition paradigm can be applied as in task fMRI, only now the neuronal activity is not modulated by a task. Resting-state fMRI is based on the observation that even at rest, spontaneous fluctuations of the BOLD signal can be observed, and that these reflect the intrinsic functional architecture of the brain (van den Heuvel and Hulshoff Pol 2010). A seminal study in this context is the work by Biswal et al, who showed that at rest the spontaneous BOLD signal fluctuations of the left motor cortex resemble those of other motor regions, including contralateral homotopic cortex, and as such can be used to map functional networks (Biswal, Yetkin et al. 1995). See also Figure 1.4B and C.

Because of the absence of a task, rs-fMRI can be applied in clinical populations for which task compliance may be a problem, such as elderly or mentally disabled subjects, and infants (Fox and Greicius 2010). Furthermore, while task fMRI only allows for the investigation of the task related network(s), in rs-fMRI the full repertoire of functional networks may be investigated from the a single dataset (Beckmann, DeLuca et al. 2005; Smith, Fox et al. 2009).

Interestingly, the signal of interest in rs-fMRI is essentially that part of the signal which was considered noise in task fMRI (compare Figure 1.4A and B). This brings forward important challenges of rs-fMRI analysis, among which a reduction of the signal-to-noise ratio and the estimation of suitable time signature templates (due to the lack of a predefined task). Removal of non-neuronal sources of signal variation such as cardioballistic or breathing artifacts becomes of major importance, as well as correction for global signal fluctuations (Chang and Glover 2009; Smith, Miller et al. 2011; Smith 2012). The potential mixing or overlap of multiple functional networks is also an important issue, and dedicated and statistically stringent methodological approaches are needed to address these issues (Beckmann, DeLuca et al. 2005).

It is interesting to realize that over the last few years, the term resting-state fMRI is being replaced in the literature and at conferences by task-free fMRI. This underlines that in the brain there is no such condition as a resting state, and that task-directed activity is always superimposed on a considerable neuronal activity baseline. In line with this, it has been estimated that task-induced increases in neuronal oxygen consumption are only around 5% (Fox, Raichle et al. 1988; Raichle and Gusnard 2002). It is speculated that this high baseline activity serves to consolidate and maintain the intrinsic functional architecture of the brain between tasks (Buckner and Vincent 2007; Smith, Fox et al. 2009).

1.3.4 Diffusion weighted imaging

Diffusion weighted imaging (DWI) can be used to probe tissue microstructure and its directionality. In the brain it can be used to assess the orientation of white matter fibers. It is complementary to fMRI in the sense that it may be used to study the structural connections between distributed regions of similar neuronal dynamics.

In DWI, the diffusion of tissue water is probed. Diffusion is the random and spontaneous (Brownian) motion of molecules that is observed in any system above absolute zero (i.e. 0 K or -273 °C), which comfortably includes all living tissues (Brown 1828). Diffusion may occur in every direction, but preferentially occurs along the direction of tissue microstructure such as membranes or macromolecules, rather than perpendicular to these.

In DWI, diffusion sensitizing gradients are incorporated in the acquisition scheme to make the MR signal diffusion dependent. If within a voxel diffusion takes place within the direction of these gradients, increased spin dephasing occurs, which results in signal loss. To investigate the full directional profile of diffusion, several image volumes need to be acquired, each sensitized to diffusion in a different direction. This is known as high angular resolution diffusion weighted imaging (HARDI; Figure 1.5A).

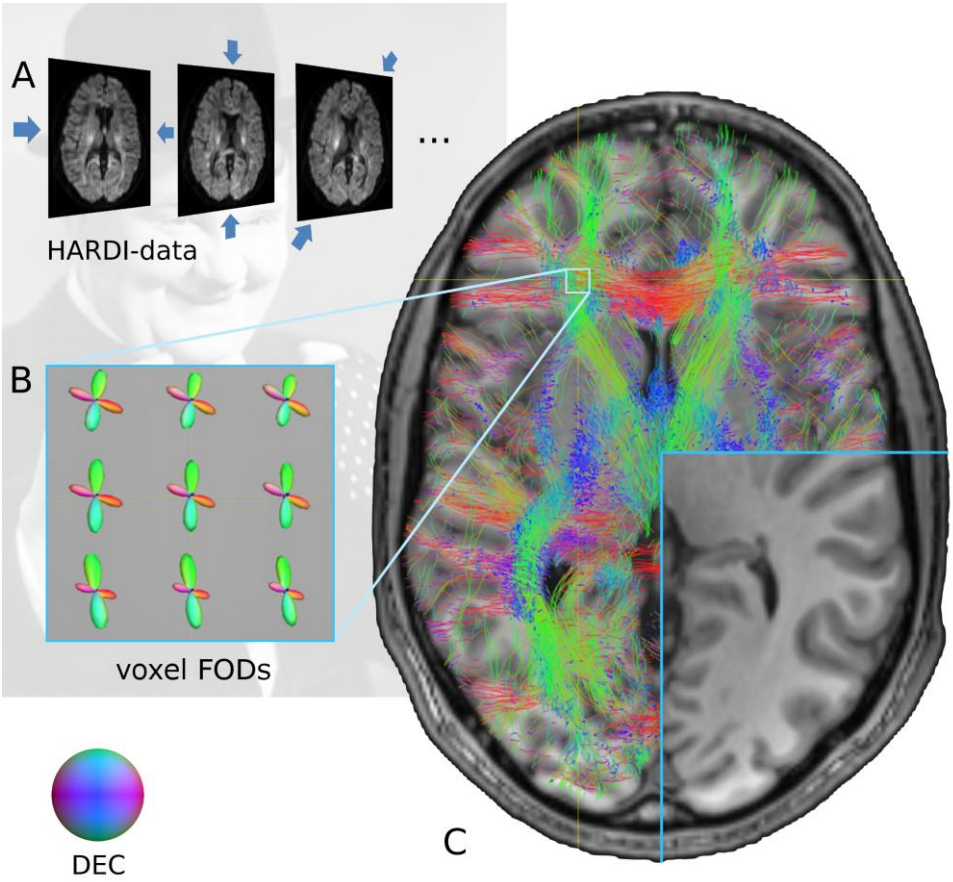

Figure 1. 5: High angular resolution diffusion weighted imaging (HARDI): a stack of MRI volumes is acquired, each probing diffusion in a different direction (arrows in A). Advanced modeling is used to derive fiber orientation distributions (FODs) reflecting voxel-wise white matter fiber orientation (B); in this case a model is used that resolves crossing fibers (Constrained Spherical Deconvolution). FODs can be interpolated over voxels to construct (semi-)continuous streamlines representing white matter tracts; this is known as tractography (C). Note that in conventional structural imaging, the internal organization of white matter is not visible (lower quadrant).
Fiber and FOD orientations comply with direction encoded coloring (DEC), see bottom left inset.

HARDI-data of the brain can be used to derive the orientation of white matter fibers per voxel, see Figure 1.5B (Beaulieu 2002). These local estimates of fiber orientation can be interpolated over voxels to construct (semi-)continuous streamlines, a technique that is called tractography (Figure 1.5C). A multitude of models exist to derive fiber orientation distributions (FODs) and to perform tractography. Important distinctions are deterministic versus probabilistic approaches, as well as single versus multiple fiber approaches. It is impossible to

give a full overview of all the algorithms available, but in general probabilistic multi-fiber approaches have gained interest over the last few years (Parker, Haroon et al. 2003; Tuch 2004; Tournier, Yeh et al. 2008; Jones, Knosche et al. 2012). These aim to take into account the uncertainty that is accumulated along streamlines due to local inaccuracies in fiber orientation estimates, as well as the fact that within voxels, multiple fiber populations of distinct orientation may exist (Tournier, Yeh et al. 2008; Vos, Jones et al. 2011).

Rather than for the reconstruction of global white matter pathways, DWI data can be used to characterize tissue microstructure at the voxel level. The best known diffusion metrics are derived from the oldest and arguably most robust model for diffusion weighted data, called diffusion tensor imaging (DTI) (Le Bihan, Breton et al. 1986; Basser, Mattiello et al. 1994). An important voxel-wise metric than can be derived from DTI is fractional anisotropy (FA), which reflects the coherence of fiber orientation and is assumed to be a measure of white matter integrity. Aberrant FA values reflective of microstructural abnormalities have been demonstrated in a multitude of neurological diseases, among which epilepsy, for overviews see e.g. Gross et al and Engel et al (Gross 2011; Engel, Thompson et al. 2013).

That said, it is a complicated matter how exactly FA relates to tissue microstructure. It is modulated by a multitude of tissue parameters, such as axonal density, packing, and diameter, as well as the presence of crossing fibers. Therefore, FA is a measure that should be interpreted with care (Beaulieu 2002; Jones, Knosche et al. 2012).

1.4 Connectomics

Functional MRI can be used to investigate the dynamic interactions between gray matter areas; DWI and tractography can be used to study the underlying white matter connections. These concepts are known as functional and structural connectivity, respectively, and can be subjected to what is called network analysis. The field of study of the brain by investigation of its connections is known as connectomics (Sporns, Tononi et al. 2005; Sporns 2013).

1.4.1 Brain graphs

The notion of a network is quite broad. In general it describes some pattern of association between distributed entities or regions. A possible neuroscientific interpretation of this concept is to think of the brain as being composed of a set of distributed, specialized gray matter regions termed nodes, and a set of (functional or structural) connections between these nodes called edges (Watts and Strogatz 1998). Such a network description is called a graph and can be represented by a

matrix, in which rows/columns represent nodes, and matrix entries represent connection strengths between pairs of nodes, see Figure 1.6.

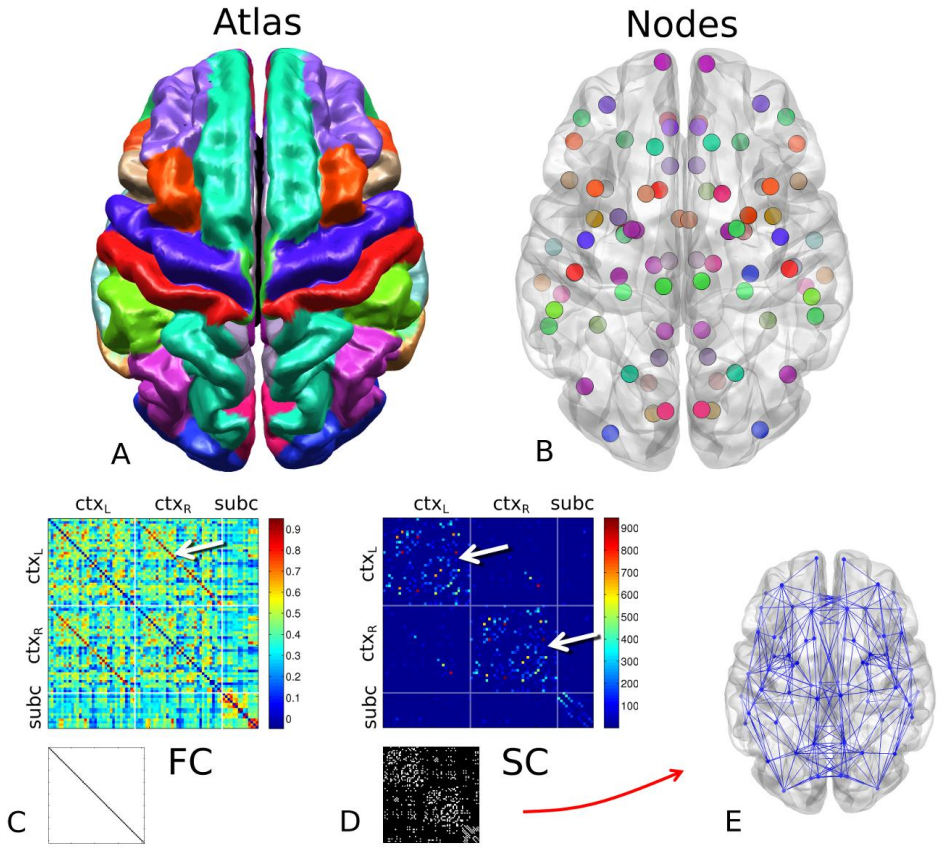

Figure 1.6: In graph analysis, the brain is parcellated into a set of distinct regions; here the Freesurfer atlas is used to segment the cortical (ctx) and subcortical (subc) gray matter (A). For visualization purposes, these regions (nodes) are typically represented as spheres at their centre (B; same color coding as A). For each pair of regions, both functional and structural connectivity (FC and SC) may be assessed and stored in so called connectivity matrices (C and D; insets are binarized versions). Given a sensible ordering of the nodes along the rows/columns of these matrices, intrinsic organization is immediately visible. For example, for cortical areas high functional connectivity between contralateral homotopic regions is seen (high valued diagonal in FC submatrix ctx$_L$-ctx$_R$; white arrow in C), as well as a predominance of within-hemisphere structural connectivity (relatively high number of non-zero entries in SC submatrices ctx$_L$-ctx$_L$ and ctx$_R$-ctx$_R$; white arrows in D). FC typically yields a full (fully connected) matrix (inset in C), whereas SC is sparse; only a limited set of all possible structural connections actually exists (inset in D, and subfigure E).

1.4.1.1 Nodes

The definition of brain nodes and edges is far from trivial, and a multitude of methods have been suggested for this. Nodes can for example be derived from a variety of essentially morphological features, such as gyral parcellations (either deterministic; e.g. Freesurfer (Fischl, van der Kouwe et al. 2004) and Automated Anatomical Labeling (AAL) (Tzourio-Mazoyer, Landeau et al. 2002); or probabilistic (Gaël Varoquaux, Alexandre Gramfort et al. 2010)), or brain histology (the historical Brodmann atlas; (Brodmann 1909; Pearce 2005)). Also characteristics more related to physiology may be employed to delineate regions, such as automated detection of transitions in cortical cytoarchitectonics and receptor densities/distributions (Zilles and Amunts 2009).

Alternatively, since nodes are supposed to represent functionally distinct units, it has recently been suggested to parcellate the cortex based on functional architecture as derived from rs-fMRI data itself (Naveau, Doucet et al. 2012).

Also on the number (and size) of nodes, no consensus has as yet been reached; these may range from several dozen (Freesurfer, AAL) to as many as several 100,000 if each voxel is considered as a distinct node (Baldassano, Iordan et al. 2012). Smaller nodes reduce the risk of lumping together functionally distinct regions at the cost of higher demands on data quality and lower signal-to-noise ratios.

1.4.1.2 Edges

For the characterization of edges (i.e. connection strength), also a wide variety of measures is in use.

Structural connectivity may for example be characterized by the number of streamlines between a pair of nodes; this may be normalized by the size of the nodes since larger nodes contain more streamlines (van den Heuvel and Sporns 2011). Also an edge may be quantified by its mean FA, or by what may be considered its "multi-fiber" equivalent, apparent fiber density (AFD; (Raffelt, Tournier et al. 2012)).

Functional connectivity may be characterized by the correlation or covariance of the time series of the pair of nodes under investigation, but also partial correlation and more advanced measures have been considered. For a comparison, see the review by Smith et al (Smith, Miller et al. 2011).

As an illustration, in Figure 1.6 the Freesurfer atlas of gyral regions was used; 82 cortical and subcortical gray matter regions were included (van den Heuvel and Sporns 2011). Functional connectivity was determined using correlations of region-averaged time series; structural connectivity was quantified as the number of streamlines between each pair of regions. From Figure 1.6, an important distinction between functional and structural connectivity becomes apparent. Functional connectivity typically yields fully connected (completely

filled) connectivity matrices (binary inset Figure 1.6C), whereas structural connectivity typically yields sparse graphs as only for a limited set of pairs of regions, interconnecting streamlines are found (Figure 1.6D and E). This is related to the fact that tractography will typically only find direct connections, whereas functional connectivity is prone to also detect indirect (multi-synaptic) connections, for instance relayed via subcortical structures such as the thalamus (Honey, Sporns et al. 2009).

1.4.2 Graph theory

Have established either functional or structural connectivity matrices, these may be studied using graph theory. Graph theory represents a set of mathematical tools to characterize networks based on the topology (and strength) of their connections (Watts and Strogatz 1998; Rubinov and Sporns 2010). Summary measures of overall network organizations may be derived, such as clustering coefficient or average path length. Numerous studies have demonstrated that such measures of network organization are compromised in epilepsy patients compared to healthy controls (van Diessen, Diederen et al. 2013).

Compared to (mass-univariate) edge-wise inference on connectivity abnormalities, comparison of graph measures may be statistically less complicated. Another potential benefit is that the connectivity structure (of non-zero connections) does not need to be consistent over subjects. Possible drawbacks include reduced spatial precision, as global network organization rather than local connectivity is investigated.

1.4.3 Association between network structure and function

It has been argued that white matter connectivity represents the structural substrate (wiring) on which functional connectivity unfolds (Rubinov, Sporns et al. 2009). Put differently, functional connectivity is determined (and constrained) by structural connections.

Indeed studies have been performed in which realistic functional dynamics have been simulated by interconnecting distinct neuronal mass models following structural network topologies derived from macaque and human brains (Honey, Kotter et al. 2007; Honey, Sporns et al. 2009; Honey, Thivierge et al. 2010). Furthermore, rather than in reference to both structural and functional connectivity, the term connectome is sometimes used to indicate the structural connections of the brain only (Sporns, Tononi et al. 2005; Sporns 2013). The implicit assumption is that detailed knowledge of brain structure will also provide information on brain function.

Taking the reverse approach, simulations of functional dynamics over an initially random structural network have been carried out, in which the network was progressively rewired based on self-structuring features of the functional data.

The result was that the initially random network progressed into a topology showing graph properties similar to the brain (Rubinov, Sporns et al. 2009).

Probably functional and structural connectivity of the brain are in constant interaction; this has even been dubbed a "symbiotic relationship" by Rubinov et al (Rubinov, Sporns et al. 2009). As windows on the brain, structural and functional connectivity can be assumed to provide complementary insights.

1.4.4 Alternative network descriptions

An alternative to the nodes-and-edges network concept has been developed for fMRI data and is based on independent component analysis (ICA) (Beckmann, DeLuca et al. 2005; Beckmann, Mackay et al. 2009). The underlying idea is that the brain is not as much ordered in specialized *regions*, but in specialized *networks*. Depending on the task that is performed, certain gray matter regions are recruited to form a dedicated network, optimized for that task. This also implies that regions may participate in multiple networks. As a consequence networks are (to a certain extent) allowed to overlap. Mathematically, the resting-state data is decomposed into maximally independent spatio-temporal patterns. In this framework, a network represents a set of distributed brain regions with a common time signature.

One of the benefits of this ICA-approach is that any set of regions with a distinct time signature is singled out. If the spatial pattern and/or the time signature is obviously not of neuronal origin, the corresponding component can be discarded as noise. An example is movement artifacts clustering at the rim of the brain or the ventricles. This means that insufficiencies in data preprocessing will be "absorbed" in certain non-neuronal ICA-components which may be excluded from further analysis.

Although the node-and-edge description of functional networks may seem very different from the ICA model, similarities may be found. Graph theory includes what is called modularity analysis, which clusters nodes based on having relatively high mutual connectivity and low connectivity with other clusters. In functional data, it effectively clusters distributed nodes of similar time signature, which may yield spatial patterns comparable to well-known large-scale ICA components, see Figure 1.7 (Beckmann, DeLuca et al. 2005; Smith, Fox et al. 2009).

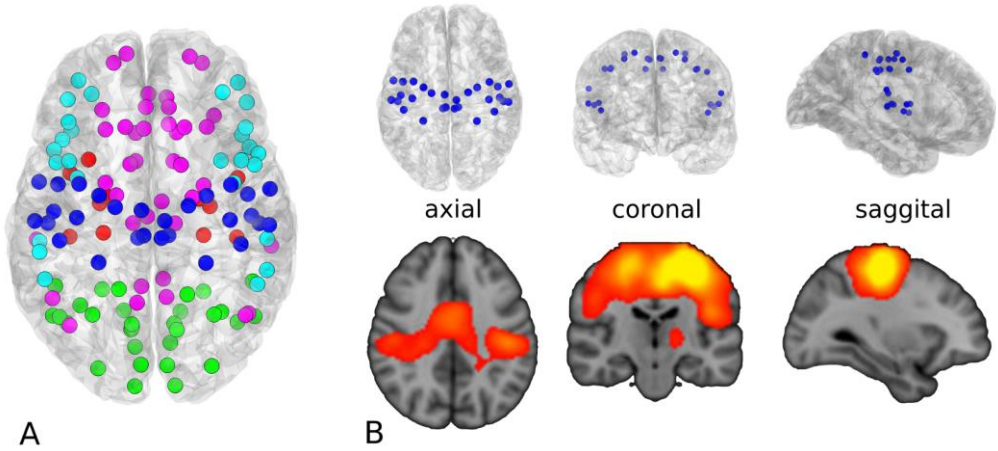

Figure 1.7: Graph cluster analysis groups nodes based on high mutual connectivity. An example is given in A (FC based on correlation of time series), in which clusters are color coded. The spatial distribution of nodes within a cluster may resemble networks as found using independent component analysis (ICA); the cluster of blue nodes for example (B, top row) resembles the ICA sensorimotor-network (B, bottom row).
ICA network (bottom row in B) adapted from (Smith, Fox et al. 2009).

1.5 Aim and outline of this thesis

The overall aim of this thesis is to establish neuroimaging correlates for epilepsy characterized by focal seizures. In other words, using advanced neuroimaging methods, can we find brain abnormalities that are related to the epilepsy as well as the associated cognitive impairments?

The outline is as follows. After this introductory Chapter 1 and in a methodological framework, Chapter 2 deals with the reproducibility of several tractography derived measures for structural connectivity. The goal of this chapter is to obtain insight into tractography methods as well as to study the sensitivity of structural connectivity measures.

The other chapters deal with neuroimaging and connectivity analyses in epilepsy. In Chapter 3, structural MRI is used to assess cortical morphology in a quantitative fashion. This study demonstrates that rather than being a local (rolandic) impairment, RE is characterized by distributed abnormalities of cortical thickness. The distributed nature of these abnormalities motivates the use of network analysis to study the neuronal dynamics and structural connections involved.

In Chapters 4-6, functional and structural connectivity analyses are applied to establish links between rolandic pathology and language problems. In Chapter 7, functional and structural connectivity are studied in combination by investigation of their correlation. These chapters form the core of this thesis.

Chapter 8 represents are more descriptive work and studies local functional connectivity of FCD lesions.

With respect to the two epilepsy cohorts described, the aim for rolandic epilepsy is to demonstrate its distributed (rather than local) character and to find connectivity abnormalities that link seizures/epileptiform activity originating from the rolandic region to language impairment. For FCD, the goal is to describe the functional connectivity profile of these lesions, which may ultimately lead to a better characterization and delineation of the cortical abnormality and improvements of surgical planning.

The final Chapter 9 combines and discusses the findings, and also deals with a number of methodological considerations.

References

Andersen, S. L. (2003). "Trajectories of brain development: point of vulnerability or window of opportunity?" Neurosci Biobehav Rev **27**(1-2): 3-18.

Axer, M., K. Amunts, et al. (2011). "A novel approach to the human connectome: ultra-high resolution mapping of fiber tracts in the brain." Neuroimage **54**(2): 1091-101.

Baldassano, C., M. C. Iordan, et al. (2012). "Voxel-level functional connectivity using spatial regularization." Neuroimage **63**(3): 1099-106.

Banerjee, P. N., D. Filippi, et al. (2009). "The descriptive epidemiology of epilepsy-a review." Epilepsy Res **85**(1): 31-45.

Basser, P. J., J. Mattiello, et al. (1994). "MR diffusion tensor spectroscopy and imaging." Biophys J **66**(1): 259-67.

Beaulieu, C. (2002). "The basis of anisotropic water diffusion in the nervous system - a technical review." NMR Biomed **15**(7-8): 435-55.

Beckmann, C. F., M. DeLuca, et al. (2005). "Investigations into resting-state connectivity using independent component analysis." Philos Trans R Soc Lond B Biol Sci **360**(1457): 1001-13.

Beckmann, C. F., C. E. Mackay, et al. (2009). Group comparison of resting-state FMRI data using multi-subject ICA and dual regression. OHBM annual meeting, San Francisco.

Berg, A. T., S. F. Berkovic, et al. (2010). "Revised terminology and concepts for organization of seizures and epilepsies: report of the ILAE Commission on Classification and Terminology, 2005-2009." Epilepsia **51**(4): 676-85.

Biswal, B., F. Z. Yetkin, et al. (1995). "Functional connectivity in the motor cortex of resting human brain using echo-planar MRI." Magn Reson Med **34**(4): 537-41.

Blumcke, I., M. Thom, et al. (2011). "The clinicopathologic spectrum of focal cortical dysplasias: a consensus classification proposed by an ad hoc Task Force of the ILAE Diagnostic Methods Commission." Epilepsia **52**(1): 158-74.

Brodmann, K. (1909). "Vergleichende localisationslehre der grosshirnrinde in ihren principien dargestellt auf grund des zellenbaues." Leipzig: Barth.

Brown, R. (1828). "A brief account of microscopical observations made in the months of June, July and August, 1827, on the particles contained in the pollen of plants; and on the general existence of active molecules in organic and inorganic bodies." Phil Mag **4**: 161-173.

Buckner, R. L. and J. L. Vincent (2007). "Unrest at rest: default activity and spontaneous network correlations." Neuroimage **37**(4): 1091-6; discussion 1097-9.

Callaghan, B. C., K. Anand, et al. (2007). "Likelihood of seizure remission in an adult population with refractory epilepsy." Ann Neurol **62**(4): 382-9.

Chang, C. and G. H. Glover (2009). "Effects of model-based physiological noise correction on default mode network anti-correlations and correlations." Neuroimage **47**(4): 1448-59.

Chassoux, F., E. Landre, et al. (2012). "Type II focal cortical dysplasia: electroclinical phenotype and surgical outcome related to imaging." Epilepsia **53**(2): 349-58.

Clarke, T., L. J. Strug, et al. (2007). "High risk of reading disability and speech sound disorder in rolandic epilepsy families: case-control study." Epilepsia **48**(12): 2258-65.

Das, N., M. Dhanawat, et al. (2012). "An overview on antiepileptic drugs." Drug Discov Ther **6**(4): 178-93.

de Lanerolle, N. C., T. S. Lee, et al. (2010). "Astrocytes and epilepsy." Neurotherapeutics **7**(4): 424-38.

Deco, G., V. K. Jirsa, et al. (2008). "The dynamic brain: from spiking neurons to neural masses and cortical fields." PLoS Comput Biol **4**(8): e1000092.

DeFelipe, J., P. Marco, et al. (1999). "Estimation of the number of synapses in the cerebral cortex: methodological considerations." Cereb Cortex **9**(7): 722-32.

Deltour L, Barathon M, et al. (2007). "Children with benign epilepsy with centrotemporal spikes (BECTS) show impaired attentional control: evidence from an attentional capture paradigm." Epileptic Disord. **9**(1): 32-38.

Deltour L, Querné L, et al. (2008). "Deficit of endogenous spatial orienting of attention in children with benign epilepsy with centrotemporal spikes (BECTS)." Epilepsy Res. **79**(2-3): 112-119.

Devinsky, O., A. Vezzani, et al. (2013). "Glia and epilepsy: excitability and inflammation." Trends Neurosci **36**(3): 174-84.

Drachman, D. A. (2005). "Do we have brain to spare?" Neurology **64**(12): 2004-5.

Dubinskaya, V. A., L. Eng, et al. (2007). "Comparative study of the state of water in various human tissues." Bulletin of Experimental Biology and Medicine **144**(3): 294-297.

Engel, J., Jr., P. M. Thompson, et al. (2013). "Connectomics and epilepsy." Curr Opin Neurol **26**(2): 186-94.

Fischl, B., A. van der Kouwe, et al. (2004). "Automatically parcellating the human cerebral cortex." Cereb Cortex **14**(1): 11-22.

Fox, M. D. and M. Greicius (2010). "Clinical applications of resting state functional connectivity." Front Syst Neurosci **4**: 19.

Fox, P. T., M. E. Raichle, et al. (1988). "Nonoxidative glucose consumption during focal physiologic neural activity." Science **241**(4864): 462-4.

Gaël Varoquaux, Alexandre Gramfort, et al. (2010). "Brain covariance selection: better individual functional connectivity models using population prior." arXiv:1008.5071v4 [stat.ML].

Gross, D. W. (2011). "Diffusion tensor imaging in temporal lobe epilepsy." Epilepsia **52 Suppl 4**: 32-4.

Gündüz E, Demirbilek V, et al. (1999). "Benign rolandic epilepsy: neuropsychological findings." Seizure **8**(4): 246-269.

Hauptman, J. S. and G. W. Mathern (2012). "Surgical treatment of epilepsy associated with cortical dysplasia: 2012 update." Epilepsia **53 Suppl 4**: 98-104.

Hauser, W. A. and L. T. Kurland (1975). "The epidemiology of epilepsy in Rochester, Minnesota, 1935 through 1967." Epilepsia **16**(1): 1-66.

Hofman, P. A., G. J. Fitt, et al. (2011). "Bottom-of-sulcus dysplasia: imaging features." AJR Am J Roentgenol **196**(4): 881-5.

Honey, C. J., R. Kotter, et al. (2007). "Network structure of cerebral cortex shapes functional connectivity on multiple time scales." Proc Natl Acad Sci U S A **104**(24): 10240-5.

Honey, C. J., O. Sporns, et al. (2009). "Predicting human resting-state functional connectivity from structural connectivity." Proc Natl Acad Sci U S A **106**(6): 2035-40.

Honey, C. J., J. P. Thivierge, et al. (2010). "Can structure predict function in the human brain?" Neuroimage **52**(3): 766-76.

Hughes, J. R. (2010). "Benign epilepsy of childhood with centrotemporal spikes (BECTS): to treat or not to treat, that is the question." Epilepsy Behav **19**(3): 197-203.

Ijff, D. M. and A. P. Aldenkamp (2013). "Cognitive side-effects of antiepileptic drugs in children." Handb Clin Neurol **111**: 707-18.

J Engel, T. P., J Aicardy, MA Dichter (2007). Epilepsy: a comprehensive textbook.

Jacobs MP, Leblanc GG, et al. (2009). "Curing epilepsy: progress and future directions." Epilepsy Behav. **14**(3): 438-445.

Jocic-Jakubi B and Jovic NJ (2006). "Verbal memory impairment in children with focal epilepsy." Epilepsy Behavior **9**(3): 432-439.

Jones, D. K., T. R. Knosche, et al. (2012). "White matter integrity, fiber count, and other fallacies: The do's and don'ts of diffusion MRI." Neuroimage.

Kasteleijn-Nolst Trenite, D. G., A. de Weerd, et al. (2013). "Chronodependency and provocative factors in juvenile myoclonic epilepsy." Epilepsy Behav **28 Suppl 1**: S25-9.

Kudin, A. P., G. Zsurka, et al. (2009). "Mitochondrial involvement in temporal lobe epilepsy." Exp Neurol **218**(2): 326-32.

Kwan, P. and M. J. Brodie (2000). "Early identification of refractory epilepsy." N Engl J Med **342**(5): 314-9.

Le Bihan, D., E. Breton, et al. (1986). "MR imaging of intravoxel incoherent motions: application to diffusion and perfusion in neurologic disorders." Radiology **161**(2): 401-7.

Liasis A, Bamiou DE, et al. (2006). "Evidence for a neurophysiologic auditory deficit in children with benign epilepsy with centro-temporal spikes." J Neural Transmission **113**(7): 939-949.

Lillywhite, L. M., M. M. Saling, et al. (2009). "Neuropsychological and functional MRI studies provide converging evidence of anterior language dysfunction in BECTS." Epilepsia **50**(10): 2276-84.

Lin, J. J., M. Mula, et al. (2012). "Uncovering the neurobehavioural comorbidities of epilepsy over the lifespan." Lancet **380**(9848): 1180-92.

Loiseau P and Duché B (1989). "Benign childhood epilepsy with centrotemporal spikes." Cleve Clin J Med **56**(Suppl Pt 1): S17-22; discussion S40-2.

Massa R, de Saint-Martin A, et al. (2001). "EEG criteria predictive of complicated evolution in idiopathic rolandic epilepsy." Neurology **57**(6): 1071-1079.

Morimoto, K., M. Fahnestock, et al. (2004). "Kindling and status epilepticus models of epilepsy: rewiring the brain." Prog Neurobiol **73**(1): 1-60.

Morimoto, T., M. Fukuda, et al. (2002). "Sequential changes of brain CT and MRI after febrile status epilepticus in a 6-year-old girl." Brain Dev **24**(3): 190-3.

Naveau, M., G. Doucet, et al. (2012). "A novel group ICA approach based on multi-scale individual component clustering. Application to a large sample of fMRI data." Neuroinformatics **10**(3): 269-85.

Overvliet GM, Aldenkamp AP, et al. (2011). "Correlation between language impairment and problems in motor development in children with Rolandic epilepsy." Epilepsy & Behavior.

Overvliet GM, Aldenkamp AP, et al. (2011). "Impaired language performance as a precursor or consequence of Rolandic epilepsy?" Journal of the Neurological Sciences **304**(1): 71-74.

Overvliet GM, Besseling RM, et al. (2010). "Nocturnal epileptiform EEG discharges, nocturnal epileptic seizures, and language impairments in children: Review of the literature." Epilepsy Behav **19**(4): 550-558.

Overvliet GM, Besseling RMH, et al. (2011). "Association between frequency of nocturnal epilepy and language disturbance in children." Pediatr Neurol **44**(5): 333-339.

Overvliet, G. M., R. M. Besseling, et al. (2013). "Clinical evaluation of language fundamentals in Rolandic epilepsy, an assessment with CELF-4." Eur J Paediatr Neurol.

Palmini, A., I. Najm, et al. (2004). "Terminology and classification of the cortical dysplasias." Neurology **62**(6 Suppl 3): S2-8.

Panayiotopoulos, C. P., M. Michael, et al. (2008). "Benign childhood focal epilepsies: assessment of established and newly recognized syndromes." Brain **131**(Pt 9): 2264-86.

Parker, G. J., H. A. Haroon, et al. (2003). "A framework for a streamline-based probabilistic index of connectivity (PICo) using a structural interpretation of MRI diffusion measurements." J Magn Reson Imaging **18**(2): 242-54.

Patel, M. (2004). "Mitochondrial dysfunction and oxidative stress: cause and consequence of epileptic seizures." Free Radic Biol Med **37**(12): 1951-62.

Pearce, J. M. S. (2005). "Brodmann's cortical maps." J Neurol Neurosurg Psychiatry **76**(259).

R.S.J. Frackowiak, K. J. F., C. Frith, R. Dolan, C.J. Price ,S. Zeki , J. Ashburner, W.D. Penny (2003). Human Brain Function, Academic Press.

Raffelt, D., J. D. Tournier, et al. (2012). "Apparent Fibre Density: a novel measure for the analysis of diffusion-weighted magnetic resonance images." Neuroimage **59**(4): 3976-94.

Raichle, M. E. and D. A. Gusnard (2002). "Appraising the brain's energy budget." Proc Natl Acad Sci U S A **99**(16): 10237-9.

Rubinov, M. and O. Sporns (2010). "Complex network measures of brain connectivity: uses and interpretations." Neuroimage **52**(3): 1059-69.

Rubinov, M., O. Sporns, et al. (2009). "Symbiotic relationship between brain structure and dynamics." BMC Neurosci **10**: 55.

Rudzinski, L. A. and K. J. Meador (2013). "Epilepsy and neuropsychological comorbidities." Continuum (Minneap Minn) **19**(3 Epilepsy): 682-96.

Seri, S., A. Cerquiglini, et al. (1998). "Spike-induced interference in auditory sensory processing in Landau-Kleffner syndrome." Electroencephalogr Clin Neurophysiol **108**(5): 506-10.

Shewmon, D. A. and R. J. Erwin (1988). "The effect of focal interictal spikes on perception and reaction time. II. Neuroanatomic specificity." Electroencephalogr Clin Neurophysiol **69**(4): 338-52.

Shinnar, S. and J. M. Pellock (2002). "Update on the epidemiology and prognosis of pediatric epilepsy." J Child Neurol **17 Suppl 1**: S4-17.

Simonato, M., W. Loscher, et al. (2012). "Finding a better drug for epilepsy: preclinical screening strategies and experimental trial design." Epilepsia **53**(11): 1860-7.

Smith, S. M. (2012). "The future of FMRI connectivity." Neuroimage **62**(2): 1257-66.

Smith, S. M., P. T. Fox, et al. (2009). "Correspondence of the brain's functional architecture during activation and rest." Proc Natl Acad Sci U S A **106**(31): 13040-5.

Smith, S. M., K. L. Miller, et al. (2011). "Network modelling methods for FMRI." Neuroimage **54**(2): 875-91.

Sporns, O. (2013). "The human connectome: origins and challenges." Neuroimage **80**: 53-61.

Sporns, O., G. Tononi, et al. (2005). "The human connectome: A structural description of the human brain." PLoS Comput Biol **1**(4): e42.

Taylor, D. C., M. A. Falconer, et al. (1971). "Focal dysplasia of the cerebral cortex in epilepsy." J Neurol Neurosurg Psychiatry **34**(4): 369-87.

Tomasi, D., G. J. Wang, et al. (2013). "Energetic cost of brain functional connectivity." Proc Natl Acad Sci U S A **110**(33): 13642-7.

Tournier, J. D., C. H. Yeh, et al. (2008). "Resolving crossing fibres using constrained spherical deconvolution: validation using diffusion-weighted imaging phantom data." Neuroimage **42**(2): 617-25.

Tuch, D. S. (2004). "Q-ball imaging." Magn Reson Med **52**(6): 1358-72.

Tzourio-Mazoyer, N., B. Landeau, et al. (2002). "Automated anatomical labeling of activations in SPM using a macroscopic anatomical parcellation of the MNI MRI single-subject brain." Neuroimage **15**(1): 273-89.

van den Heuvel, M. P. and H. E. Hulshoff Pol (2010). "Exploring the brain network: a review on resting-state fMRI functional connectivity." Eur Neuropsychopharmacol **20**(8): 519-34.

van den Heuvel, M. P. and O. Sporns (2011). "Rich-club organization of the human connectome." J Neurosci **31**(44): 15775-86.

van Diessen, E., S. J. Diederen, et al. (2013). "Functional and structural brain networks in epilepsy: What have we learned?" Epilepsia **54**(11): 1855-65.

van Eijsden, P., W. M. Otte, et al. (2011). "In vivo diffusion tensor imaging and ex vivo histologic characterization of white matter pathology in a post-status epilepticus model of temporal lobe epilepsy." Epilepsia **52**(4): 841-5.

Van Essen, D. C., C. H. Anderson, et al. (1992). "Information processing in the primate visual system: an integrated systems perspective." Science **255**(5043): 419-23.

Vos, S. B., D. K. Jones, et al. (2011). "Partial volume effect as a hidden covariate in DTI analyses." Neuroimage **55**(4): 1566-76.

Watts, D. J. and S. H. Strogatz (1998). "Collective dynamics of 'small-world' networks." Nature **393**(6684): 440-2.

WHO (October 2012). Fact sheet N°999 on epilepsy.

Widjaja, E., S. Zarei Mahmoodabadi, et al. (2009). "Subcortical alterations in tissue microstructure adjacent to focal cortical dysplasia: detection at diffusion-tensor MR imaging by using magnetoencephalographic dipole cluster localization." Radiology **251**(1): 206-15.

Witt, J. A. and C. Helmstaedter (2013). "Monitoring the cognitive effects of antiepileptic pharmacotherapy--approaching the individual patient." Epilepsy Behav **26**(3): 450-6.

Zigmond, M. J., F. E. Bloom, et al. (1999). Fundamental Neuroscience, Academic Press.

Zilles, K. and K. Amunts (2009). "Receptor mapping: architecture of the human cerebral cortex." Curr Opin Neurol **22**(4): 331-9.

CHAPTER 2

Tract specific reproducibility of tractography based morphology and diffusion metrics

R.M.H. Besseling, J.F.A. Jansen, G.M. Overvliet, M.J. Vaessen,
H.M.H. Braakman, P.A.M. Hofman, A.P. Aldenkamp, W.H. Backes

PLoS ONE 2012; 7(4): e34125. doi:10.1371/journal.pone.0034125

2.1 Abstract

Introduction The reproducibility of tractography is important to determine its sensitivity to pathological abnormalities. The reproducibility of tract morphology has not yet been systematically studied and the recently developed tractography contrast Tract Density Imaging (TDI) has not yet been assessed at the tract specific level.

Materials and methods Diffusion tensor imaging (DTI) and probabilistic constrained spherical deconvolution (CSD) tractography are performed twice in 9 healthy subjects. Tractography is based on common space seed and target regions and is performed for several major white matter tracts. Tractograms are converted to tract segmentations and inter-session reproducibility of tract morphology is assessed using Dice similarity coefficient (DSC). The coefficient of variation (COV) and intraclass correlation coefficient (ICC) are calculated of the following tract metrics: fractional anisotropy (FA), apparent diffusion coefficient (ADC), volume, and TDI. Analyses are performed both for proximal (deep white matter) and extended (including subcortical white matter) tract segmentations.

Results Proximal DSC values were 0.70-0.92. DSC values were 5-10% lower in extended compared to proximal segmentations. COV/ICC values of FA, ADC, volume and TDI were 1-4%/0.65-0.94, 2-4%/0.62-0.94, 3-22%/0.53-0.96 and 8-31%/0.48-0.70, respectively, with the lower COV and higher ICC values found in the proximal segmentations.

Conclusion For all investigated metrics, reproducibility depended on the segmented tract. FA and ADC had relatively low COV and relatively high ICC, indicating clinical potential. Volume had higher COV but its moderate to high ICC values in most tracts still suggest subject-differentiating power. Tract TDI had high COV and relatively low ICC, which reflects unfavorable reproducibility.

2.2 Introduction

Diffusion weighted MRI (DWI) can be used to probe tissue water diffusion in vivo and thus can provide unique information on tissue microstructure. It is routinely used in the clinic to assess the extent of lesions in cerebral infarction (Davis, Robertson et al. 2006). However, its full potential is in the unveiling of the directional dependence of diffusion in white matter, which is strongest in the direction of the axonal fibers. This anisotropic diffusion process is often modeled using the diffusion tensor (DT, (Basser, Mattiello et al. 1994)) and several clinically relevant metrics can be calculated from it, such as fractional anisotropy (FA), which is a measure for the directional coherence of the tracts, and apparent diffusion coefficient (ADC), which is a measure of water motility.

For a variety of neurological diseases, distributed white matter FA decreases and ADC increases have been reported, both indicative of loss of microstructural integrity. Examples include stroke and multiple sclerosis (Pierpaoli, Barnett et al. 2001) and epilepsy (Eriksson, Rugg-Gunn et al. 2001).

Since diffusion tensor imaging (DTI) provides voxelwise estimates of fiber orientation, a natural extension is to extrapolate the local orientations to continuous streamlines, representing fiber tracts. This technique is called tractography and opens opportunities for interrogating specific white matter tracts. For example, tractography has been used to segment the pyramidal tract in early-stage multiple sclerosis. It was found that only in case of clinical motor symptoms, the fraction of sclerotic lesions was significantly increased in the pyramidal tract compared to the rest of the brain (Pagani, Filippi et al. 2005). Another application is epilepsy, in which tractography of the optic radiation may aid the prediction and prevention of post-operative visual impairment in temporal lobe epilepsy (Clatworthy, Williams et al. 2010).

The tractography pipeline involves many steps, among others data alignment, registration and modeling (fiber orientation and propagation), see Figure 2.1. These steps all have characteristic sources of error, the combination of which leads to a certain amount of variability in the quantitative end results. In line with this, scan-rescan stability and inter-subject variability of tractography are important measures to determine its potential in revealing pathological abnormalities and changes over time. Few studies have investigated the reproducibility of tractography. These studies mainly focus on tract volume and tensor derived metrics (Ciccarelli, Parker et al. 2003; Heiervang, Behrens et al. 2006; Wakana, Caprihan et al. 2007), but investigate morphological reproducibility only to a limited extent (Heiervang, Behrens et al. 2006). Tract morphology involves both tract shape and its embedding within the brain and as such is more descriptive than tract volume. Tract morphology is important in surgical planning,

but also in longitudinal studies of cortical remodeling after stroke or injury, which presently are restricted to dye tracer studies in monkeys (Dancause, Barbay et al. 2005) or gray matter morphological analyses in structural scans (May and Gaser 2006).

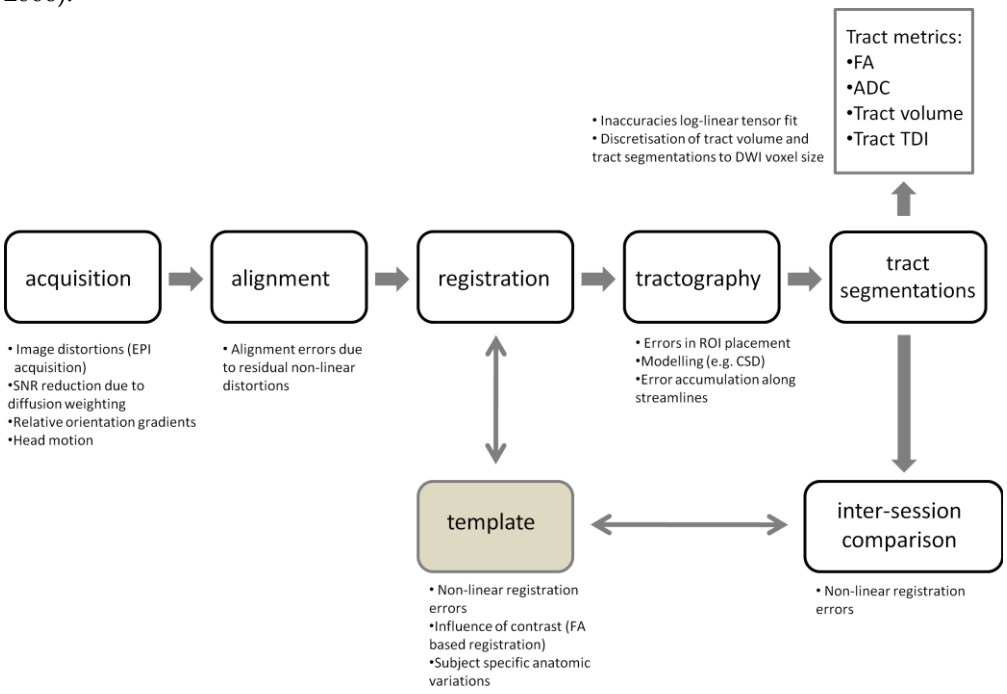

Figure 2.1: The tractography pipeline employed in this paper, from data acquisition to tract segmentations and tract metrics. At each step, several potential error sources are given.

It is known that compared to deep white matter, directly subcortical white matter shows increased bending, fanning and crossing of tracts, which gives rise to partial volume effects. Partial volume effects are inherent to DWI, which assesses microstructure at the meso scale of the imaging voxel, and may compromise tractography accuracy. To address this problem, a multitude of models have been developed which, unlike the diffusion tensor, can represent multiple fiber orientations. These models include q-space imaging (QSI) (Cory and Garroway 1990), Q-ball (Tuch 2004), and constrained spherical deconvolution (CSD) (Tournier, Calamante et al. 2007). However, to our knowledge, the difference in tractography performance for proximal (i.e. deep white matter) and distal (i.e. directly subcortical) parts of tracts has not been investigated yet.

FA and ADC are voxel metrics and as such are restricted to the DWI imaging resolution. Tract density imaging (TDI) has recently been introduced and provides outstanding anatomical contrast in the white matter (Calamante, Tournier

et al. 2010). In TDI, a whole brain tractogram is calculated. This tractogram is converted to a tract density map (by counting the number of streamlines per volume element) on a grid which can be much finer than the acquisition resolution of DWI (super resolution), a concept which previously was not considered (Roberts, Liu et al. 2005). The rationale is that in tractography, directional information is integrated over multiple voxels and the resulting increase in consistency allows for super resolution. Whole brain reproducibility of TDI has recently been addressed (Pannek, Mathias et al. 2011), but not on a tract specific basis.

The purpose of this study is to investigate for several selected well-known tracts both the reproducibility of tract morphology and quantitative metrics. The difference in tractography performance for proximal and distal white matter will also be studied. Tractography will be performed using probabilistic CSD. In addition to conventional tensor metrics (FA and ADC) and tract volume, tract TDI will be investigated as well. The use of non-linear registrations to a common space will be demonstrated for both defining tractography seed and target regions of interest (ROI) and for performing inter-session morphological comparison.

2.3 Materials and methods

2.3.1 Subjects

Nine healthy volunteers (6 male, 3 female, age (mean±SD): 28±6 year) were recruited and scanned at Epilepsy Center Kempenhaeghe. None of the subjects had (a history of) neurological or psychiatric disorders or anatomical abnormalities on structural MRI.

2.3.2 Ethics statement

This study was approved by the local medical ethical committee of Epilepsy Center Kempenhaeghe. All participants gave written informed consent prior to study participation.

2.3.3 Data acquisition

Diffusion weighted MRI (DWI) was performed on a 3 Tesla MRI system (Philips Achieva, maximum gradient strength 40 mT/m, maximum slew rate 200 mT/m/msec) using an 8-element SENSE head coils for parallel imaging (SENSE-factor 2). The imaging resolution was 2x2x2 mm^3 and a b-value of 1200 s/mm^2 was used. An echo planar imaging (EPI) sequence was used with echo time (TE) 72 ms and repetition time (TR) 6965 ms. A set of 128 gradient directions was used, optimized via electrostatic repulsion to ensure homogenous distribution over the

sphere (Jones, Horsfield et al. 1999). A single non-diffusion weighted scan (b0-scan) was obtained. The DWI acquisition time was 15 minutes.

For anatomical reference, a 1x1x1 mm^3 T1-weighted scan was acquired with TR/TE=8.1/3.7 ms, inversion time (TI) 1022 ms (3D TFE acquisition, SENSE-factor 1.5), and an acquisition time of 8.5 minutes.

A complete rescan was performed within a couple of weeks (19±18 days) for inter-session comparison.

2.3.4 Data preprocessing

Each DWI dataset was aligned to its b0-scan (SNR 20.8±2.6) using affine registrations to correct for patient motion and EPI distortions. This alignment was performed in CATNAP (Coregistration, Adjustment, and Tensor-solving, a Nicely Automated Program, version 3.21) and included correction of the gradient table for the rotations (Farrell, Landman et al. 2007; Leemans and Jones 2009). CATNAP makes use of software routines from FSL (FMRIB software library, Oxford).

2.3.5 Tractography

All DT and CSD analyses as well as the tractography and the tract segmentations were performed using the MRtrix software package (Brain Research Institute, Melbourne, Australia, http://www.brain.org.au/software/). Registrations to common space were performed in FSL. Additional analyses were performed in Matlab (The MathWorks, Natick, USA).

DT fits were performed to calculate the FA and ADC maps. In addition, fiber orientation distributions (FODs), representing local fiber orientation, were estimated using CSD. In CSD, the diffusion profile is deconvolved with a so called response function, which is the typical diffusion profile of a voxel containing fibers in a single coherent direction. The resulting initial FOD estimate is constrained to suppress noise-induced negative fiber orientations, which leads to the final FOD (Tournier, Calamante et al. 2007).

For each DWI dataset, the CSD response function was estimated from the data. This was done by taking the signal from high FA voxels (FA>0.7) and aligning them based on their first DT eigenvector. This allows subsequent averaging (noise reduction) so a more robust and representative response function can be estimated than would be possible from a single (arbitrary) high FA voxel.

In CSD, FODs are represented by spherical harmonics, which form a basis for functions over the sphere, much like the Fourier series forms a basis for functions over Cartesian space (Tournier, Calamante et al. 2004). In agreement with (Tournier, Calamante et al. 2009), the spherical harmonics order was taken to be no higher than $\lambda_{max}=8$ to limit overfitting of noise. This corresponds to 45 spherical harmonics.

Probabilistic tractography was performed using FOD sampling (Jeurissen, Leemans et al. 2011). In this method, the tract propagation direction is selected from the FOD using a sample rejection scheme adhering to both a curvature constraint and an amplitude threshold. MRtrix default settings were used, which include a stepsize of 0.2 mm, a maximum curvature radius of 1 mm and an FOD amplitude threshold 0.1. The tractogram of each selected major white matter tract (see below) consisted of 10,000 streamlines.

2.3.6 Selected tracts

Tractography was performed for a number of well known major white matter tracts of various orientations, locations, and size, see Figure 2.2. These tracts provide different tractographical challenges.

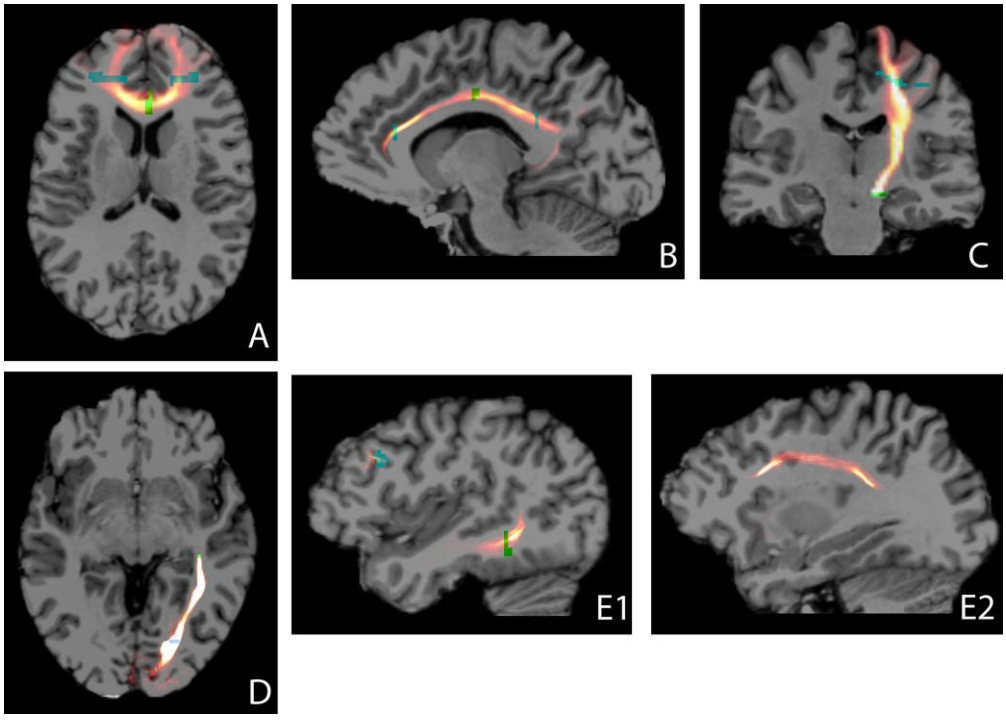

Figure 2.2: Tract density maps of a representative subject. Seed ROIs are given in green, target ROIs in blue. For each subfigure, the tract density windowing (yellow-red) is chosen such that subcortical projections can also be appreciated. The skull-stripped T1 underlay was registered to the diffusion space (b0-scan) using an affine transformation.
A: genu of corpus callosum; B: cingulum; C: pyramidal tract; D: optic radiation; E1, E2: arcuate fasciculus (different sagittal slices).

2.3.6.1 Genu of the corpus callosum

The corpus callosum (CC, Figure 2.2A) is the largest bundle of the brain and forms the major commissure connecting both hemispheres. Because of its commissural nature and the high directional coherence of its medial part, tractography seed regions are easily defined, although it is difficult and somewhat arbitrary to define distal target regions that limit the extent of the tractogram. The genu of the CC connects the prefrontal and orbitofrontal regions (Catani and Thiebaut de Schotten 2008).

2.3.6.2 Cingulum

The cingulum (Ci, Figure 2.2B) is a major associative bundle that is located within the cingulated gyrus. It runs over and around the corpus callosum and below the corona radiata, both of which are likely locations for unwanted spurious streamlines. The Ci contains fibers of different length, the longest of which runs from the anterior temporal gyrus to the orbitofrontal cortex (Catani and Thiebaut de Schotten 2008).

2.3.6.3 Pyramidal tract

The pyramidal tract (PT, Figure 2.2C) is a descending projection bundle of fibers from the motor cortex to the brainstem. The PT crosses the CC and the Ci, among others.

2.3.6.4 Optic radiation

The optic radiations (OR, Figure 2.2D) are large, heavily myelinated projection bundles that consist of fibers primarily between the lateral geniculate nuclei of the thalamus and the primary visual cortices at the bases of the calcarine sulci in the occipital lobe (Clatworthy, Williams et al. 2010). Proper tractographical reconstruction of the OR is complicated by the sharp turn it makes in Meyer's loop (Clatworthy, Williams et al. 2010).

2.3.6.5 Arcuate fasciculus

The arcuate fasciculus (AF, Figures 2.2E1 and E2) is a lateral associative bundle composed of long and short fibers connecting the perisylvian cortex of the frontal, parietal, and temporal lobes. The AF of the left hemisphere is involved in language (Catani and Thiebaut de Schotten 2008). It is one of the four constituents of the superior longitudinal fasciculus (SLF) (Bernal and Ardila 2009) and tractographical delineation is especially challenging.

2.3.7 Tractography ROI placement

Binary tractography ROIs were defined in FSLs 1x1x1 mm^3 average FA space. Tract specific ROIs were defined in single axial, sagittal, or coronal slices, depending on the tract orientation. ROIs were subsequently dilated using a 3x3x3 voxel kernel, giving them a final thickness of 3 mm. Two ROI types were used: seed ROIs, from which streamlines were started, and target ROIs, which streamlines must reach to be included in the final tractogram.

For the genu of the CC, the Ci, the PT, and the OR, the ROI placement guidelines of (Heiervang, Behrens et al. 2006) were followed. For the AF, the guidelines of (Wakana, Caprihan et al. 2007) for SLF delineation were adapted to additionally include the AF-specific temporal projections.

ROIs were registered to each dataset using FSLs non-linear registration and the associated parameter set optimized for alignment to FSL's average FA space (http://www.fmrib.ox.ac.uk/fsl/fnirt/). This scheme ensures objective, operator-independent mapping of the common space ROIs to each dataset. This registration step is given by the vertical double headed arrow in Figure 2.1. After mapping to native space, ROIs were re-binarized using a threshold of 0.01 to correct for interpolation effects.

2.3.8 Proximal and extended tractograms

Tractography was performed both excluding and including cortical projections. In the first case (proximal), streamlines were propagated until they reached the target ROIs (Figure 2.3B). In the second case (extended), streamlines were allowed to propagate beyond the target ROIs until they reach the edge of the brain mask (Figure 2.3C).

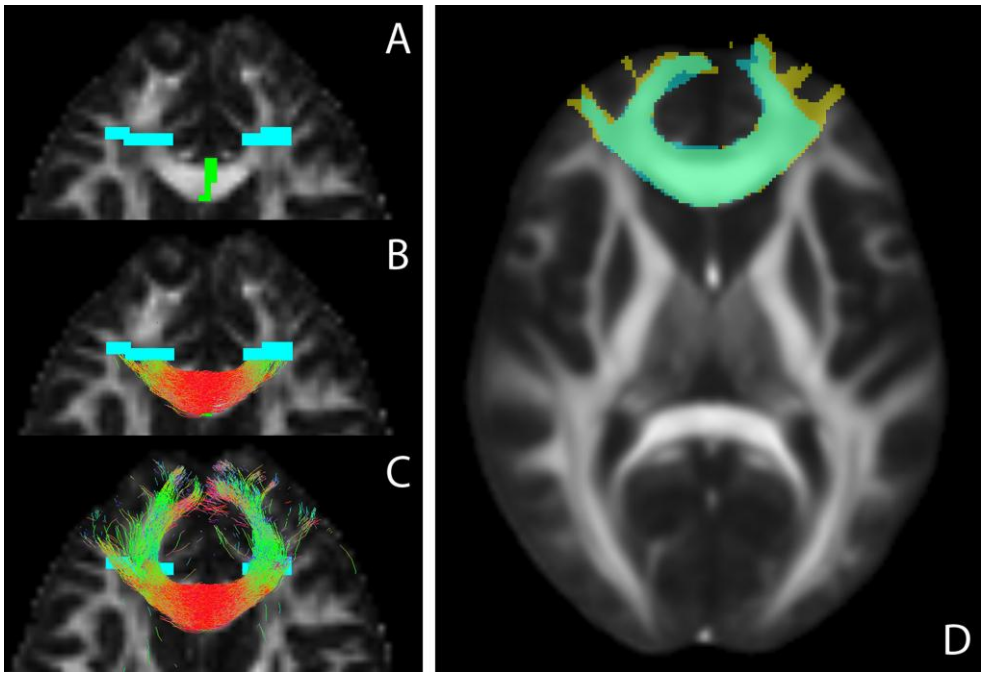

Figure 2.3: Proximal and extended tract segmentations and inter-session comparison
A: ROIs for the genu of the corpus callosum overlaid on the FA map, seed ROI in green, target ROIs in blue; B: proximal tractogram; C: extended tractogram.
D: tract segmentations of both scan sessions of the same subject, registered to the common FA space (underlay). Segmentation 1 in blue, 2 in yellow and segmentation overlap in green.

2.3.9 Registration of tract segmentations

Tractograms were converted to tract density maps at the DWI acquisition resolution by counting the number of streamlines per voxel. These tract density maps were thresholded at 5% of their maximum value to construct binary tract segmentations.

Inter-session morphological comparison of tract segmentations was performed in common space, see the horizontal double headed arrow in Figure 2.1. Also for within-subject comparison, mapping of tract segmentations to a common space is desirable because of scan-specific image distortions inherent to the DWI sequence. FSLs average FA space was used for both subject-independent ROI definition (see above) and as session-independent common space for all diffusion based maps (FA, ADC, TDI), see the vertical and horizontal arrow, respectively, in Figure 2.1. Native space tract segmentations were mapped to the common space by reversing the non-linear deformation field for native space ROI construction, see Figure 2.3D.

After mapping to common space, tract segmentations were re-binarized using a threshold of 0.01.

2.3.10 Tract metrics

The tract segmentations at the DWI resolution were also used to select the relevant voxels for calculating mean tract FA and ADC in the native space. Furthermore, they were used to calculate native space tract volume.

2.3.11 Tract density imaging

Whole brain tractography was performed using 5,000,000 tracts seeded from random locations within the white matter. For each subject, the white matter was segmented from the T1 image and mapped to the diffusion spaces of both sessions via affine registrations to the b0-scans.

Whole brain tractograms were converted to whole brain tract density images (TDIs) by counting the number of streamlines per element on a 1 mm grid. It is emphasized that this is not merely an interpolation step. In TDI, voxel-wise (local) information on fiber orientation is extrapolated to continuous (global) streamlines using tractography. Streamline continuity and smoothness (ensured by tractography constraints such as maximum curvature) are assumed to yield spatial consistency at a higher level of detail. This allows performing TDI at a grid size small than the acquisition resolution. Since the DWI acquisition resolution was 2 mm, performing TDI at 1 mm provides limited super resolution at the benefit of an acceptable number of streamlines (data storage).

Tract TDI was assessed by constructing tract segmentations at the TDI grid size. For each tract, the TDI elements within this segmentation were used to calculate mean tract TDI. Similar to the calculation of tract segmentations at the DWI resolution, a threshold of 5% of the maximum value was used to convert tract probability maps to binary tract segmentations.

In addition to assessing TDI at the tract level, a whole brain TDI atlas was constructed. For this, each whole brain TDI needed to be mapped to the common space, i.e. FSLs average FA space. For each dataset, the coordinates of all the streamlines were mapped to the common space using the nonlinear deformation field obtained in FA normalization (Pannek, Mathias et al. 2011). Subsequently, subject specific normalized TDIs were calculated and combined to construct a whole brain TDI atlas.

2.3.12 Reproducibility measures

2.3.12.1 Dice similarity coefficient

Inter-session morphological agreement of common space tract segmentations was quantified using the Dice similarity coefficient (Dice 1945):

$$DSC = \frac{2N(t_1 \cup t_2)}{N(t_1) + N(t_2)} \quad [1]$$

in which t_1 and t_2 stand for the tract segmentations of session 1 and 2, respectively, and $N(t_i)$ gives the number of voxels. DSC varies between 0 and 1 for no and complete spatial overlap, respectively.

2.3.12.2 Coefficient of variation

The reproducibility of tract metrics was examined using the coefficient of variation (COV), which is defined as

$$COV = \frac{\sigma_{ws}}{\mu} \quad [2]$$

with σ_{ws} the within-subject standard deviation of the measure of interest and μ its population mean (Lachin 2004). The COV is a measure for the precision of a measure and gives an indication of the minimum detectable relative deviation from the mean.

2.3.12.3 Intraclass correlation coefficient

To disentangle the sources of variation, the intraclass correlation coefficient (ICC) was calculated:

$$ICC = \frac{BSMSS - WSMSS}{BSMSS + (k-1)WSMSS} \quad [3]$$

with BSMSS the between-subject mean sum of squares, WSMSS the within-subject mean sum of squares and k the number of scans per subject (Shrout and Fleiss 1979). The ICC ranges from -1 (no reliability, that is, BSMSS=0) to 1 (maximum reliability, achieved in the case of identity between test and retest, that is, WSMSS = 0) (Parsey, Slifstein et al. 2000). The higher a metric's ICC, the better it reflects between-subject differences and the higher its clinical potential.

2.4 Results

2.4.1 Tract segmentation overlap

In Figure 2.4, mean inter-session overlap as quantified by DSC (Equation 1) is shown for both proximal and extended tract segmentations. Compared to proximal

overlap, extended overlap was 5%-10% lower in all cases. Inter-tract differences are clearly visible, with the genu of the CC showing most inter-session overlap and the AF showing least. DSC ICC values were 0.75-0.92 for the proximal segmentations and 0.70-0.84 for the extended segmentations (σ_{bs}=0.007-0.123 and 0.013-0.115, respectively). Complete results are provided in supplementary Table 2.1.

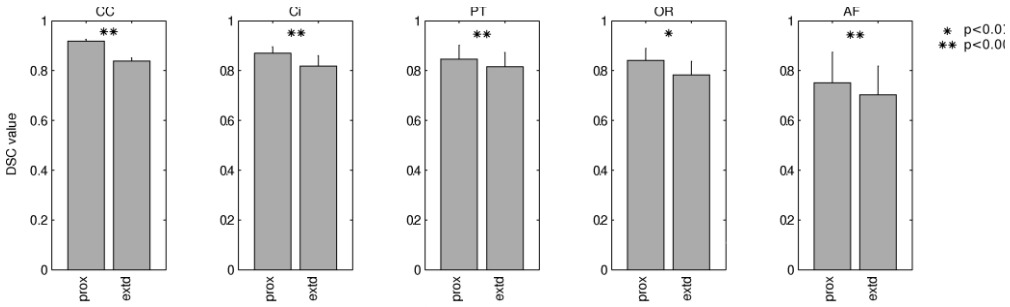

Figure 2.4: Inter-session spatial overlap of tract segmentations, quantified by Dice similarity coefficient (DSC). Results are shown for both proximal (prox) and extended (extd) segmentation. Error bars represent 1 standard deviation.
CC: genu of the corpus callosum; Ci: cingulum; PT: pyramidal tract; OR: optic radiation; AF: arcuate fasciculus.

DSC: between session segmentation overlap	Proximal mean	σ_{bs}	extended mean	σ_{bs}	p-value
corpus callosum	0.92	0.007	0.84	0.013	<0.0005
Cingulum	0.87	0.026	0.82	0.041	<0.0005
pyramidal tract	0.85	0.055	0.82	0.058	<0.0005
optic radiation	0.84	0.048	0.78	0.054	0.002
arcuate fasciculus	0.75	0.123	0.70	0.115	0.001

Table 2.1: Summary statistics for the inter-session overlap of tract segmentations, quantified by DSC. The p-values are of a paired t-test for difference between proximal and extended values. σ_{bs}: between-subject standard deviation.

2.4.2 Tract metrics

The tract metrics are visualized in Figure 2.5. Quantitative results are given in supplementary Table 2.S1. Bland-Altman plots are provided in supplementary Figures 2.S1 and 2.S2 and show that the precision of each metric is independent of the metric value. For the OR, the statistics were based on the data from 8 subjects as for one subject the first session DWI brain coverage was incomplete.

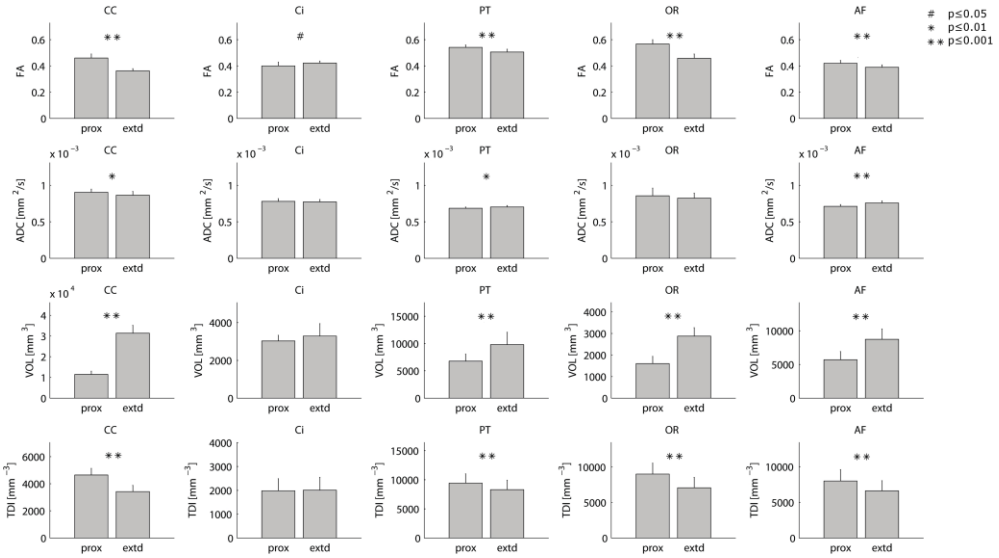

Figure 2.5: Reproducibility of tract metrics for both proximal (prox) and extended (extd) tract segmentations. The p-values are of paired t-tests for difference between proximal and extended values. FA: fractional anisotropy; ADC: apparent diffusion coefficient; VOL: tract volume; TDI: tract density; CC: genu of the corpus callosum; Ci: cingulum; PT: pyramidal tract; OR: optic radiation; AF: arcuate fasciculus.

2.4.2.1 *Fractional anisotropy*

In all tracts except the Ci, the FA values were significantly higher for the proximal tract segmentations. For the Ci, no difference was found. Note that the Ci is the only tract studied that has no extensive cortical projections. Furthermore, for the Ci the volumes of the extended and the proximal segmentations were not significantly different. In the proximal case the FA COV was 2-3%, in the extended case this was 1-4%. The proximal FA ICC value range was 0.65-0.94 and about the same range was found in the extended case, except for a low value in the Ci (0.11).

2.4.2.2 *Apparent diffusion coefficient*

For the ADC, slightly but significantly higher values were found in the proximal segmentations for the genu of the CC. On the other hand, in the PT and the AF, the proximal values were slightly but significantly lower. In the OR and the Ci, no significant differences were found. The following values were found: COV 2-4% (proximal) and 2% (extended), ICC 0.66-0.92 (proximal) and 0.62-0.94 (extended). These values were in the same range as those for FA.

2.4.2.3 Tract volume

In all tracts except the Ci, the volumes of the extended segmentations were significantly larger than those of the proximal segmentations. For the Ci, no difference was found. COVs were 3-22% (proximal) and 5-19% (extended). Highest values were found in the AF, for which also very low ICC values were found, 0.029 (proximal), and -0.054 (extended). For the other tracts, the ICC values ranges were 0.64-0.96 (proximal) and 0.53-0.83 (extended).

2.4.2.4 Tract TDI

The TDI values were significantly higher for the proximal segmentations in all tracts except for the Ci, in which no significant difference was found. COV values were in the range 8-28% (proximal) and 9-31% (extended). No reliable ICC estimates could be found for the Ci and the OR (-0.268 and -0.090, respectively). The ICC values for the other tracts were 0.52-0.70 (proximal) and 0.48-0.65 (extended).

2.4.3 TDI atlas

The TDI atlas is shown in Figure 2.6. For reference, the common space tract segmentations of all subjects were added and overlaid, providing group segmentation probability maps. Figure 2.6 shows that TDI provides clear white matter contrast and is high in large, well-known bundles and low in subcortical regions. These subcortical regions do not necessarily have lower fiber densities, but might exhibit larger within-subject variability and/or lower tractography precision.

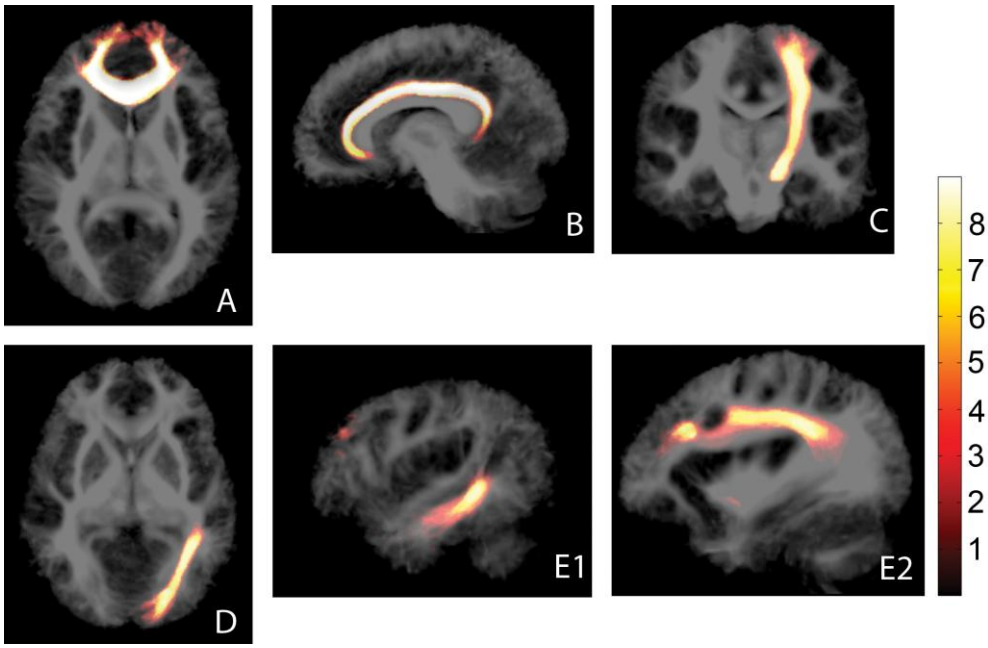

Figure 2.6: Average TDI map, depicted in logarithmic scale to enhance subcortical contrast. Overlaid are the summed common space tract segmentations. Colorbar: number of subjects (1-9). Note that reduced tract density at the subject level (Figure 2) coincides with low between-subject segmentation overlap at the group level (directly subcortical regions).
A: genu of corpus callosum; B: cingulum; C: pyramidal tract; D: optic radiation; E1, E2: arcuate fasciculus (different sagittal slices).

2.5 Discussion

In this paper, we studied reproducibility of tract morphology and of conventional tract tensor metrics FA and ADC, tract volume, and TDI. We used a common space (FSLs 1mm iso FA space) to both define tractography ROIs and to calculate inter-session tract segmentation overlap. We demonstrated that reproducibility of both segmentation overlap and quantitative measures is strongly tract-dependent. We also found lower reproducibility for subcortically extended compared to deep white matter metrics.

2.5.1 Tract segmentation overlap

We have reported inter-session segmentation overlaps of DSC=0.67-0.92. In the study of (Heiervang, Behrens et al. 2006), within-subject reproducibility of tract morphology was investigated over 3 sessions by linear registration to the first session. Only the average DSC value over subjects and tracts was reported (0.81), which falls within the range we found. We also reported that segmentation overlap differs between tracts. Especially in the AF, reduced overlap was observed (DSC=0.67-0.75). We propose that this is related to the complex anatomy of the AF,

which is one of the 4 subcomponents of the SLF (Bernal and Ardila 2009), and for which it difficult to define precluding tractography ROIs. Suboptimal ROI placement in combination with minor registration errors may have led to partial volume effects causing incomplete or non-exclusive segmentation of the AF. Even though guidelines from the literature were followed for common space ROI definition (Wakana, Caprihan et al. 2007), the investigation of inter-operator variability should be a subject of future research. Tractograms can also be improved by using a more sophisticated scheme to construct session-specific ROIs (Clatworthy, Williams et al. 2010), but this is beyond the scope of this paper.

We demonstrated that the inclusion of subcortical regions reduces the segmentation overlap (5-10% lower DSC values in extended segmentations compared to proximal segmentations). This is indicative of reduced tractography performance directly below the cortex, which reveals an important limitation of the technique. Potential causes for sub-optimal performance are increased partial volume effects caused by increased fanning, bending and crossing, and error accumulation because of increased distance from the tractography seed. Both effects cannot be disentangled because of the lack of a golden standard (true tract anatomy). In an attempt to reduce the influence of partial volume effects, we used a model that can deal with multiple fiber orientations per voxel (CSD). Error accumulation along the tract, however, is inherent to any streamline tractography algorithm since streamline propagation is an iterative process. This error accumulation can only be avoided by using algorithms that are not streamline based. Examples of such algorithms include fast marching tractography (Parker, Wheeler-Kingshott et al. 2002) and Bayesian techniques (Behrens, Woolrich et al. 2003). However, streamline tractography is still the method of choice in the majority of DWI studies.

2.5.2 Tract metrics

2.5.2.1 Fractional anisotropy

Significantly decreased FA values were found for the extended segmentations of tracts with cortical projections. A loss of directional coherence (fanning, bending) might explain the trend of decreased FA values in proximity of the cortex. Since tractography was constrained to a brain mask, extended segmentations may contain gray matter, which also decreases mean FA. This effect will be limited because of the FOD amplitude threshold of 0.1, which confines tractography to regions where fiber direction is well-defined (primarily white matter).

The FA COV values found for extended segmentations are comparable to those in (Heiervang, Behrens et al. 2006) and better than those in (Ciccarelli, Parker et al. 2003) (6.2%, 18.6% and 7.1% compared to 2.8%, 2.9% and 1.9% in the current

study for the CC, the PT and the OR, respectively). Possible explanations for the improvement in performance are the higher field strength of 3T (1.5T in (Heiervang, Behrens et al. 2006) and (Ciccarelli, Parker et al. 2003)) and differences in tractography ROI definition. In (Ciccarelli, Parker et al. 2003), manually placed single voxel ROIs were used and in (Heiervang, Behrens et al. 2006), linear (affine) registration was used to map common space ROIs to native space, as opposed to non-linear registration in the current study. Another difference is that both other studies used DT based tractography, whereas we used CSD.

Except for the extended segmentations of the Ci, the low COVs combined with moderate to high ICC values, 0.65-0.94 (proximal) and 0.60-0.93 (extended), which is indicative of the clinical potential of FA in revealing pathological differences. The low ICC values for the extended segmentations of the Ci are caused by relatively large within-subject variability (compared to between-subject variability) since in some subjects the distal streamlines enter into regions of low FA for one session only. Careful tuning of the tractography parameters might circumvent this problem, however, this might lead to suboptimal performance in other tracts. For the sake of consistency, we chose to keep the tractography algorithm and the parameter settings constant. However, we stress that tractography performance can be improved by optimizing tractography parameters to the tract under investigation. For example, the curvature threshold we used yielded good results but was too conservative to reconstruct Myers' loop in the OR, see Figure 2.2D. It is known from the literature that segmentation of Myers' loop is very challenging and requires a dedicated approach (Clatworthy, Williams et al. 2010).

2.5.2.2 Apparent diffusion coefficient

For ADC, the COV and ICC values were in the same range as those for FA. The proximal COV values are 1.5-3.5% and the extended COV values are 1.6-2.1%, which is comparable to 1.49-2.14% as found in (Heiervang, Behrens et al. 2006). The ICC range is 0.66-0.92 (proximal) and 0.62-0.94 (extended). Unlike for FA, for ADC no deviant Ci ICC values were found, probably because ADC displays less contrast than FA in many brain regions. It is known that at the relatively low clinical b-value of b=1200 s/mm^2 we employed, even ADC differences between gray matter and white matter are relatively small (Jones and Cercignani 2010). This reduces the influence of inter-session differences in the extent of distal streamlines.

2.5.2.3 Tract volume

Extended tract segmentations trivially have a larger volume than proximal tract segmentations because of the additional inclusion of cortical projections. Compared to FA and ADC, the COV value of tract volume is relatively high. Proximal values are 3-20% and extended values are 5-19%, which is comparable to

literature values of 8.15-13.03% (Heiervang, Behrens et al. 2006). Except for the AF, the ICC values, on the other hand, indicate moderate to good subject-differentiating power (0.64-0.96 (proximal) and 0.53-0.83 (extended)). This underlines that inter-session reproducibility should be seen relative to between-subject variability. The poor performance in the AF is probably caused by minor scan-specific registration errors combined with suboptimal ROI placement, which leads to relatively large inter-session differences as discussed previously.

2.5.2.4 Tract TDI

We observed decreased TDI values for the extended tract segmentations. This is likely caused by a combination of increased fanning and bending in directly subcortical regions and error accumulation along the streamlines which leads to distal streamline divergence.

The TDI COV can be quite high (9-30% for extended) and is comparable to a literature value of 26% (WM average, (Pannek, Mathias et al. 2011)). In addition, ICC estimates are low (negative in OR and Cing, for both proximal and extended segmentations). This suggests that in the current approach, the between-subject differentiating power of tract TDI is low. It has recently been shown that an extension on TDI, average pathlength mapping (APM), has better COV (WM average of 19%, (Pannek, Mathias et al. 2011)). APM does not only consider the number of streamlines, but also the streamline length, and might have better clinical potential (Pannek, Mathias et al. 2011), although the biological interpretation is different.

2.5.3 Clinical implications

Reproducibility should be seen in the light of pathological abnormalities to make statements about sensitivity. In brain DWI, the literature on pathological differences in FA and ADC is extensive. For example, in epilepsy with malformations of cortical development, local pathological differences in FA and ADC have been reported, both in gray and in white matter. Compared to the values in healthy controls, FA reductions down to 51% and ADC increases up to 119% have been reported (Eriksson, Rugg-Gunn et al. 2001). These differences are large with respect to the COV values we report here, however, this was in patients with active epilepsy and obvious structural lesions. A more subtle example is a study about post-operative seizure-free temporal lobe epilepsy, in which regions of reduced FA were found both within and outside the temporal lobe (Afzali, Soltanian-Zadeh et al. 2011). This study indicates that FA can be used to assess loss of microstructural integrity after seizure remission and also outside the seizure onset zone (temporal lobe), which might be of relevance for follow-up or the unveiling of diseased networks. The average FA reduction of the affected regions

was 0.09 (approximately 15%), which is still relatively large compared to the COV values we report.

Most DWI studies, however, only report the significance of the changes in FA and ADC and do not report the effect size. For this reason, several DWI reproducibility studies reverse the question and provide power analyses that, given a certain effect size, e.g. 10%, provide the number of measurements needed to achieve sufficient statistical power (Heiervang, Behrens et al. 2006; Wakana, Caprihan et al. 2007). In agreement with our results, these studies report comparable sensitivities for FA and ADC (on the order of 10 subjects per group) and a much lower sensitivity for volume (100 subjects per group).

It is important to realize that reproducibility and anatomical plausibility of tractography are mere surrogates for the technique's accuracy since true tract anatomy is unknown at the subject level. The pipeline from data acquisition to tract segmentations is very long in tractography, with many and diverse potential error sources (Figure 2.1). The high DSC values we report suggest that at least the morphology of the structures we reconstruct is reproducible. Since tract tensor metrics and volume are derived from the tract segmentation itself, high morphological reproducibility is assumed to be a prerequisite for high reproducibility of these derived metrics. However, from the relatively low DSC values for the AF it is expected that if the reconstructed morphology does not fully translate to a single anatomical structure, but instead is incomplete or too extensive, reproducibility is reduced.

Finally, the number of subjects in this study (i.e. 9) was limited but comparable to that in other reproducibility studies (Ciccarelli, Parker et al. 2003; Heiervang, Behrens et al. 2006; Wakana, Caprihan et al. 2007). To investigate the effect of group size on reproducibility, we performed bootstrap analysis, taking subsets from our original 9 subject group. This showed that the relative increase in reproducibility achieved by recruiting an additional subject beyond around 10 is relatively low compared to adding a subject at smaller group sizes (results not shown). However, we expect the main source of uncertainty to be within-subject and since within-subject reproducibility is a key issue in individual diagnosis and longitudinal studies, we suggest increasing the number of scans per subject instead of the group size for future research.

2.6 Conclusion

We demonstrated that tractography based tract segmentations can be used to assess tract morphology in a reproducible manner in addition to their more typical use as ROIs to investigate tract metrics such as tract FA, ADC, and volume. We demonstrated that metric reproducibility is strongly tract dependent and also depends on whether or not directly subcortical projections are included (proximal versus extended tract segmentations).

Generally speaking, in our approach FA and ADC both show good COV and good ICC, which indicates good reproducibility and good subject-differentiating power, respectively. For tract volume, higher COV values were found, indicative of lower reproducibility, but since the ICC values were still reasonable, subject differentiation was preserved. For tract TDI, on the other hand, both COV was increased and ICC reduced, indicating both low reproducibility and low subject- differentiating power.

Acknowledgements

We would like to thank Donald Tournier, Alexander Leemans and Ben Jeurissen for useful discussions and Kerstin Pannek for her advice on normalization of the whole brain tractograms. We would like to thank Marc Geerlings for hardware and software support and Remco Berting for data acquisition.

References

Afzali, M., H. Soltanian-Zadeh, et al. (2011). "Tract based spatial statistical analysis and voxel based morphometry of diffusion indices in temporal lobe epilepsy." Comput Biol Med **41**(12): 1082-91.

Basser, P. J., J. Mattiello, et al. (1994). "MR diffusion tensor spectroscopy and imaging." Biophys J **66**(1): 259-67.

Behrens, T. E., M. W. Woolrich, et al. (2003). "Characterization and propagation of uncertainty in diffusion-weighted MR imaging." Magn Reson Med **50**(5): 1077-88.

Bernal and Ardila (2009). "The role of the arcuate fasciculus in conduction aphasia." Brain **132**: 2309-2016.

Calamante, F., J. D. Tournier, et al. (2010). "Track-density imaging (TDI): super-resolution white matter imaging using whole-brain track-density mapping." Neuroimage **53**(4): 1233-43.

Catani, M. and M. Thiebaut de Schotten (2008). "A diffusion tensor imaging tractography atlas for virtual in vivo dissections." Cortex **44**(8): 1105-32.

Ciccarelli, O., G. J. Parker, et al. (2003). "From diffusion tractography to quantitative white matter tract measures: a reproducibility study." Neuroimage **18**(2): 348-59.

Clatworthy, P. L., G. B. Williams, et al. (2010). "Probabilistic tractography of the optic radiations--an automated method and anatomical validation." Neuroimage **49**(3): 2001-12.

Cory, D. G. and A. N. Garroway (1990). "Measurement of translational displacement probabilities by NMR: an indicator of compartmentation." Magn Reson Med **14**(3): 435-44.

Dancause, N., S. Barbay, et al. (2005). "Extensive cortical rewiring after brain injury." J Neurosci **25**(44): 10167-79.

Davis, D. P., T. Robertson, et al. (2006). "Diffusion-weighted magnetic resonance imaging versus computed tomography in the diagnosis of acute ischemic stroke." J Emerg Med **31**(3): 269-77.

Dice, L. R. (1945). "Measures of the Amount of Ecologic Association Between Species." Ecology **26**(3): 297-302.

Eriksson, S. H., F. J. Rugg-Gunn, et al. (2001). "Diffusion tensor imaging in patients with epilepsy and malformations of cortical development." Brain **124**(Pt 3): 617-26.

Farrell, J. A., B. A. Landman, et al. (2007). "Effects of signal-to-noise ratio on the accuracy and reproducibility of diffusion tensor imaging-derived fractional anisotropy, mean diffusivity, and principal eigenvector measurements at 1.5 T." J Magn Reson Imaging **26**(3): 756-67.

Heiervang, E., T. E. Behrens, et al. (2006). "Between session reproducibility and between subject variability of diffusion MR and tractography measures." Neuroimage **33**(3): 867-77.

Jeurissen, B., A. Leemans, et al. (2011). "Probabilistic fiber tracking using the residual bootstrap with constrained spherical deconvolution." Hum Brain Mapp **32**(3): 461-79.

Jones, D. K. and M. Cercignani (2010). "Twenty-five pitfalls in the analysis of diffusion MRI data." NMR Biomed **23**(7): 803-20.

Jones, D. K., M. A. Horsfield, et al. (1999). "Optimal strategies for measuring diffusion in anisotropic systems by magnetic resonance imaging." Magn Reson Med **42**(3): 515-25.

Lachin, J. M. (2004). "The role of measurement reliability in clinical trials." Clin Trials **1**(6): 553-66.

Leemans, A. and D. K. Jones (2009). "The B-matrix must be rotated when correcting for subject motion in DTI data." Magn Reson Med **61**(6): 1336-49.

May, A. and C. Gaser (2006). "Magnetic resonance-based morphometry: a window into structural plasticity of the brain." Curr Opin Neurol **19**(4): 407-11.

Pagani, E., M. Filippi, et al. (2005). "A method for obtaining tract-specific diffusion tensor MRI measurements in the presence of disease: application to patients with clinically isolated syndromes suggestive of multiple sclerosis." Neuroimage **26**(1): 258-65.

Pannek, K., J. L. Mathias, et al. (2011). "The average pathlength map: a diffusion MRI tractography-derived index for studying brain pathology." Neuroimage **55**(1): 133-41.

Parker, G. J., C. A. Wheeler-Kingshott, et al. (2002). "Estimating distributed anatomical connectivity using fast marching methods and diffusion tensor imaging." IEEE Trans Med Imaging **21**(5): 505-12.

Parsey, R. V., M. Slifstein, et al. (2000). "Validation and reproducibility of measurement of 5-HT1A receptor parameters with [carbonyl-11C]WAY-100635 in humans: comparison of arterial and reference tisssue input functions." J Cereb Blood Flow Metab **20**(7): 1111-33.

Pierpaoli, C., A. Barnett, et al. (2001). "Water diffusion changes in Wallerian degeneration and their dependence on white matter architecture." Neuroimage **13**(6 Pt 1): 1174-85.

Roberts, T. P., F. Liu, et al. (2005). "Fiber density index correlates with reduced fractional anisotropy in white matter of patients with glioblastoma." AJNR Am J Neuroradiol **26**(9): 2183-6.

Shrout, P. E. and J. L. Fleiss (1979). "Intraclass correlations: uses in assessing rater reliability." Psychol Bull **86**(2): 420-8.

Tournier, J. D., F. Calamante, et al. (2007). "Robust determination of the fibre orientation distribution in diffusion MRI: non-negativity constrained super-resolved spherical deconvolution." Neuroimage **35**(4): 1459-72.

Tournier, J. D., F. Calamante, et al. (2009). How many diffusion gradient directions are required for HARDI? Proc. Intl. Soc. Mag. Reson. **17**.

Tournier, J. D., F. Calamante, et al. (2004). "Direct estimation of the fiber orientation density function from diffusion-weighted MRI data using spherical deconvolution." Neuroimage **23**(3): 1176-85.

Tuch, D. S. (2004). "Q-ball imaging." Magn Reson Med **52**(6): 1358-72.

Wakana, S., A. Caprihan, et al. (2007). "Reproducibility of quantitative tractography methods applied to cerebral white matter." Neuroimage **36**(3): 630-44.

Supplementary material

A

extended	FA					ADC [x10^{-3} mm^2/s]				
	mean	$\sigma_{\omega\sigma}$	$\sigma_{\beta\sigma}$	COV	ICC	mean	$\sigma_{\omega\sigma}$	$\sigma_{\beta\sigma}$	COV	ICC
CC	0.362	0.01	0.015	0.028	0.635	0.864	0.014	0.052	0.016	0.932
cing	0.421	0.015	0.011	0.035	0.109	0.773	0.016	0.031	0.021	0.754
PT	0.506	0.015	0.021	0.029	0.6	0.703	0.013	0.019	0.018	0.617
OR	0.458	0.009	0.032	0.019	0.926	0.824	0.017	0.068	0.021	0.938
AF	0.389	0.005	0.019	0.014	0.921	0.757	0.015	0.028	0.02	0.754
	Vol [ml]					TDI [x10^3]				
	mean	$\sigma_{\omega\sigma}$	$\sigma_{\beta\sigma}$	COV	ICC	mean	$\sigma_{\omega\sigma}$	$\sigma_{\beta\sigma}$	COV	ICC
	31.364	1.557	3.629	0.05	0.831	3.424	0.296	0.412	0.087	0.589
	3.284	0.391	0.59	0.119	0.641	2.007	0.62	0.333	0.309	-0.268
	9.799	1.573	2.019	0.161	0.534	8.304	1.216	1.447	0.146	0.478
	2.879	0.19	0.379	0.066	0.776	7.070	1.551	1.002	0.219	-0.09
	8.732	1.682	1.127	0.193	-0.054	6.610	0.834	1.286	0.126	0.653

B

proximal	FA					ADC [x10^{-3} mm^2/s]				
	mean	$\sigma_{\omega\sigma}$	$\sigma_{\beta\sigma}$	COV	ICC	mean	$\sigma_{\omega\sigma}$	$\sigma_{\beta\sigma}$	COV	ICC
CC	0.46	0.008	0.031	0.016	0.942	0.906	0.017	0.041	0.018	0.845
cing	0.4	0.011	0.028	0.027	0.866	0.78	0.019	0.037	0.024	0.77
PT	0.541	0.011	0.017	0.021	0.653	0.685	0.01	0.016	0.015	0.659
OR	0.567	0.01	0.032	0.018	0.91	0.855	0.03	0.105	0.035	0.92
AF	0.42	0.01	0.021	0.024	0.786	0.712	0.011	0.022	0.015	0.79
	Vol [ml]					TDI [x10^3]				
	mean	$\sigma_{\omega\sigma}$	$\sigma_{\beta\sigma}$	COV	ICC	mean	$\sigma_{\omega\sigma}$	$\sigma_{\beta\sigma}$	COV	ICC
	11.468	0.313	1.574	0.027	0.961	4.643	0.357	0.449	0.077	0.521
	3.026	0.173	0.276	0.057	0.669	1.982	0.539	0.344	0.272	-0.103
	6.775	0.794	1.192	0.117	0.637	9.421	1.045	1.428	0.111	0.578
	1.603	0.098	0.334	0.061	0.917	9.007	1.705	1.081	0.189	-0.109
	5.704	1.224	0.891	0.215	0.029	7.999	0.873	1.467	0.109	0.699

C

p-value	FA	ADC	Vol	TDI
CC	<0.0005	0.005	<0.0005	<0.0005
cing	0.028	0.113	0.218	0.734
PT	<0.0005	0.006	<0.0005	0.001
OR	<0.0005	0.067	<0.0005	<0.0005
AF	<0.0005	<0.0005	<0.0005	<0.0005

Table 2.S1: Reproducibility of tract metrics for both proximal (A) and extended (B) tract segmentations and paired t-test p-values for comparison of proximal and extended metrics (C). σ_{bs}: between-subject standard deviation; σ_{ws}: within-subject standard deviation; COV: coefficient of variation; ICC: intraclass correlation coefficient.

FA: fractional anisotropy; ADC: apparent diffusion coefficient; VOL: tract volume; TDI: tract density.
CC: genu of the corpus callosum; Ci: cingulum; PT: pyramidal tract; OR: optic radiation; AF: arcuate fasciculus.

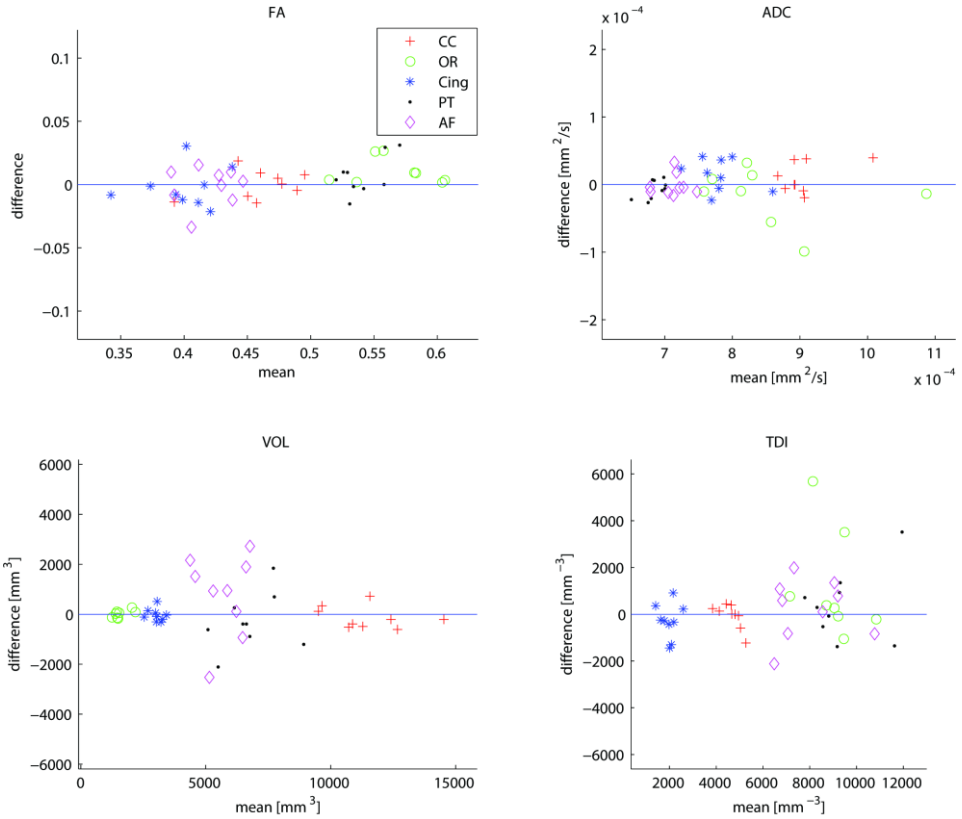

Figure 2.S1: Tract metric Bland-Altman plots for the proximal tract segmentations. The between-session difference of each metric (y-axis) is independent of the between-session mean of the metric. This indicates that in case of a pathological change of the metric (decrease or increase) within the investigate range, this effect is not obscured by change in precision. However, note that there are differences in precision (y-dispersion) between tracts, indicating reproducibility differences between tracts.
FA: fractional anisotropy; ADC: apparent diffusion coefficient; VOL: tract volume; TDI: tract density; CC: genu of the corpus callosum; Ci: cingulum; PT: pyramidal tract; OR: optic radiation; AF: arcuate fasciculus.

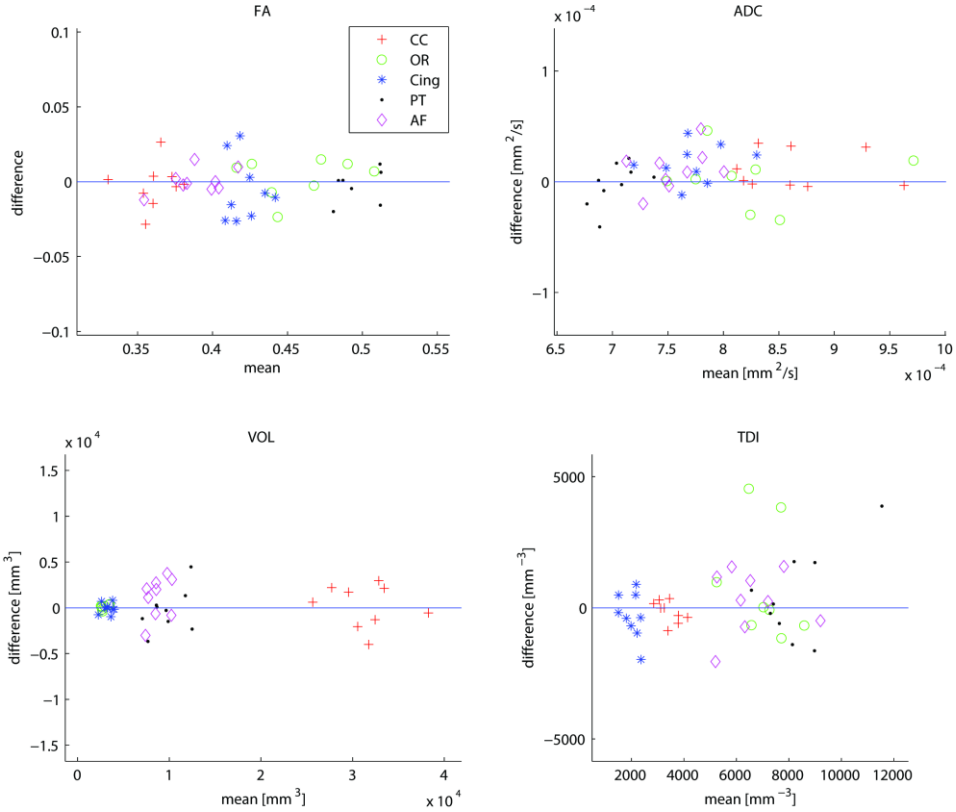

Figure 2.S2: The same as supplementary Figure S1, but now for the metrics of extended tract segmentations.

CHAPTER 3

Early onset of cortical thinning in children with rolandic epilepsy

R.M.H. Besseling*, G.M. Overvliet*, J.F.A. Jansen, S.J.M. van der Kruijs, J.S.H. Vles, P.A.M. Hofman, S.C.M. Ebus, A.J.A. de Louw, A.P. Aldenkamp, W.H. Backes

NeuroImage Clinical 2013; 2: 434–439

*Both authors contributed equally to this study

Abstract

Introduction Rolandic epilepsy, a childhood epilepsy associated with language impairments, was investigated for language-related cortical abnormalities.

Materials and methods Twenty-four children with rolandic epilepsy and 24 controls (age 8-14 years) underwent the Clinical Evaluation of Language Fundamentals test. In addition, structural MRI was performed at 3T (voxel size 1x1x1 mm^3) for fully automated quantitative assessment of cortical thickness. Regression analysis was used to test for differences between patients and controls and to assess the effect of age and language indices on cortical thickness.

Results For patients, the core language score (mean±SD: 92±18) was lower than for controls (106±11, p=0.0026) and below the norm of 100±15 (p=0.047). Patients showed specific impairments in receptive language index (87±19, p=0.002) and language content index (87±18, p=0.0016). Cortical thickness was reduced in patients ($p<0.05$, multiple-comparisons corrected) in left perisylvian regions. Furthermore, extensive cortical thinning with age was found in predominantly left-lateralized frontal, centro-parietal and temporal regions. No associations were found between cortical thickness and language indices in the regions of aberrant cortex.

Conclusion The cortical abnormalities described represent subtle but significant pathomorphology in this critical phase of brain development (8-14 years) and suggest that rolandic epilepsy should not be considered merely a benign condition. Future studies employing longitudinal designs are prompted for further investigations into cerebral abnormalities in RE and associations with cognitive impairment and development.

3.1 Introduction

Rolandic epilepsy (RE) is an idiopathic focal epilepsy with most frequent onset at 7-10 years of age (Gomez & Klass, 1983; Panayiotopoulos, Michael, Sanders, Valeta, & Koutroumanidis, 2008). The epileptic focus is typically located in the lower motor and/or somatosensory cortex (rolandic area) (Koutroumanidis, 2007). RE is also known as Benign (rolandic) Epilepsy (of childhood) with Centro Temporal Spikes (BECTS), which reflects both the typical spontaneous remission of seizures during adolescence and the characteristic location of the epileptiform activity on the electroencephalogram (EEG) (Loiseau P & Duché B, 1989).

Although the seizure semiology of RE is relatively mild (Lerman P & Kivity S, 1975; Loiseau P, Duché B, & Cohadon S, 1992), recent evidence suggests serious comorbidities in selected cases and has put the assumed purely benign nature of RE under debate (Nicolai J, Aldenkamp AP, Arends J, Weber JW, & Vles JSH, 2006; Vinayan KP, Biji V, & Thomas SV, 2005; Völkl-Kernstock S, Bauch-Prater S, Ponocny-Seliger E, & Feucht M, 2009; Weglage J, Demsky A, Pietsch M, & Kurlemann G, 1997). An often reported comorbidity of RE is language impairment (Monjauze C, Tuller L, Hommet C, Barthez MA, & Khomsi A, 2005; Northcott E, et al., 2007; Overvliet GM, et al., 2010; Papavasiliou A, Mattheou D, Bazigou H, Kotsalis C, & Paraskevoulakos E, 2005). It has been suggested that the diagnosis of language impairment may even precede that of RE (Overvliet GM, Aldenkamp AP, Klinkenberg S, Vles JSH, & Hendriksen J, 2011).

Even though the sensorimotor and language system are mutually involved in for instance speech production (in which complex articulatory movement and auditory feedback is required), the link between RE and problems in purely cognitive aspects of language such as reading is less trivial (Carlsson, Igelbrink-Schulze, Neubauer, & Stephani, 2000; Clarke T, et al., 2007). The existence of such an association is suggested by that fact that a significant correlation has been demonstrated between problems in motor and problems in language development (Gündüz E, Demirbilek V, & Korkmaz B, 1999; Overvliet GM, Aldenkamp AP, Klinkenberg S, Nicolai J, et al., 2011). This suggests the existence of a mechanism through which epileptiform activity originating from the sensorimotor cortex might enter and disturb the language system as a whole, the neuronal pathways of which are as yet unknown.

Structural imaging has been used in attempts to identify cerebral abnormalities in RE. Several authors concluded that distributed subtle structural abnormalities on clinical MRI are common in RE (Eeg-Olofsson O, Lundberg S, & Raininko R, 2000; Gelisse P, et al., 2003; Lundberg S, Eeg-Olofsson O, Raininko R, & Eeg-Olofsson KE, 1999), but not specific for this disorder (Boxerman JL, et al., 2007). However, these studies did not include healthy controls, were of qualitative nature, and were not tailored for systematic abnormalities (i.e. consistent over

subjects with respect to location). In this context, quantitative approaches might seem advantageous. In recent years, quantitative techniques to study cortical thickness have been developed (Fischl & Dale, 2000; Kim, et al., 2005). These techniques allow local analysis of the entire cortex and are less influenced by inter-individual gyral variations than traditional voxel-based whole-brain methods, such as voxel-based-morphology (VBM) (Mueller SG, et al., 2009). In a group of children with frontal lobe epilepsy, cortical thickness analysis has been successfully applied; in a study of Widjaja et al (Widjaja E, Mahmoodabadi SZ, Snead OC 3rd, Almehdar A, & Smith ML, 2011), regions of thinner cortex were found both within and beyond the frontal lobe. Also in other types of epilepsy, such as temporal lobe epilepsy in adults, reduced cortical thickness has been reported beyond the lobe of the primary seizure focus (Mueller SG, et al., 2009).

The goal of the current study is to investigate whether abnormalities in cortical thickness can be found in RE, both within and beyond the sensorimotor cortex. Furthermore, we investigated whether such abnormalities are localized in classical left perisylvian language areas and are associated with language impairment as assessed using neuropsychological testing.

3.2 Materials and methods

3.2.1 Study population

A total of 24 children (9 girls) with a clinical diagnosis of RE were selected as recently described (Overvliet, et al., 2013), see also the selection criteria below. The average age at testing was 11.3 years (range: 8-14 years) and the age at epilepsy onset (7.3±2.2 years) was typical (Panayiotopoulos, et al., 2008).

An age and gender-matched healthy control population of 24 children (10 girls) was included. The average age of the controls at testing was 10.6 years (range: 8-14 years; t-test for group age difference: p=0.15).

Of the patients, 20/24 were right handed; of the controls 22/24. For further subject characteristics, see Table 3.1.

Subject characteristics	RE	controls
N	24	24
age [y]	11.3±1.9	10.6±1.8
age at epilepsy onset [y]	7.3±2.2	n.a.
epilepsy duration [y]	2.4±2.0	n.a.
gender (male/female)	15/9	14/10
handedness (r/l/ambidexter)	20/3/1	22/2/0
Number of AEDs (0/1/>1)	8/11/5	n.a.

Table 3.1: Study participant characteri-stics. RE stands for rolandic epilepsy, AED stands for anti epileptic drug. Note that age at onset and epilepsy duration are difficult to accurately establish given the mild and nocturnal nature of RE seizures.

3.2.1.1 Selection criteria

Children with RE were selected based on EEG criteria and seizure semiology (Berroya AM, Bleasel AF, Stevermuer TL, Lawson J, & Bye AM, 2005; Panayiotopoulos, et al., 2008). EEG criteria include the presence of spike and slow wave complexes occurring as individual paroxysms or in repetitive clusters with a maximum in the mid temporal and/or central electrodes and with a temporal-frontal dipole field. Additional independent central, mid temporal, parietal or occipital spike wave foci in the same or other hemisphere were allowed. To exclude severe cases (Landau-Kleffner syndrome (LKS) or LKS-like), interictal epileptiform activity was required to be present <85% of the time during non-REM sleep.

With respect to seizure semiology, seizures with anarthria, hemiclonia involving the face and/or unilateral extremities, or secondarily generalized seizures were considered. In case of poorly observed nocturnal seizures, post-ictal signs of a generalized seizure or confirmation of post-ictal hemiparesis was sufficient for inclusion in case of otherwise typical EEG.

The children with RE were tested by the Wechsler Intelligence Score for Children, third edition (WISC-III), and all had a full-scale IQ >70. None of the healthy controls had (a history of) dyslexia, learning disorders or psychiatric disorders, or attended special education. Children were excluded if they had dental braces (MRI quality) or were somewhat afraid in the scanner. Healthy controls were excluded in case of suspicion of language impairment (see language assessment).

A board certified neuroradiologist specialized in epilepsy (PH) reviewed all scans and no structural abnormalities were found.

All parents (or guardians) and children gave written informed consent prior to study participation. The study was approved by the ethical review boards of both participating institutions and has ClinicalTrials.gov identifier NCT01335425.

3.2.2 Language assessment

To assess language performance, the Clinical Evaluation of Language Fundamentals, Fourth edition (CELF-4), Dutch version, was used (Paslawski C, 2005; Semel E, Wiig EH, & Secord WA, 2010). The CELF-4 is considered the gold standard for the identification of language disorders or delays in children and yields several age-corrected indices. Among these are the core language score (norm value, mean ± standard deviation: 100±15), which is a global measure for language performance and can serve as a screening measure (e.g. exclusion of language impaired controls). More specific language indices were obtained in the group of children with RE only, including receptive language index (listening and

understanding), expressive language index (expressing oneself, speaking), and language content index (semantic development).

3.2.3 MRI acquisition

Structural T1-weighted MRI was performed at 3.0 Tesla (Philips Achieva system; Philips Medical System, Best, the Netherlands) using an eight-element receive-only head coil. Acquisition settings were: 1x1x1 mm^3 voxel size, 3D fast spoiled gradient echo sequence, echo time/repetition time/inversion time 3.8/8.3/1022 ms and acquisition time 8 min.

3.2.4 Cortical thickness analysis

Cortical thickness analysis was performed using the Freesurfer image analysis software package (A. M. Dale, Fischl, & Sereno, 1999; Anders M. Dale & Sereno, 1993; Fischl & Dale, 2000). Freesurfer tessellates the interface between gray and white matter and between gray matter and cerebrospinal fluid (CSF) based on image intensity (gradients) in a highly robust and fully automated fashion. The shortest distance between the two surfaces represents an estimate of the cortical thickness (at approximately 300,000 nodes).

Freesurfer was also used to spatially register the cortical thickness maps to Freesurfer standard space, and to perform general linear model (GLM) analysis for group comparisons and to find predictors for cortical thickness variations. To account for residual registration errors and to strengthen the assumption of Gaussian distribution of the data, the thickness maps were smoothed using a Gaussian kernel (full-with-at-half-maximum 10 mm). As on average males have a somewhat thicker cortex than females (Raznahan A, et al., 2011), all analyses were gender corrected.

Matlab (R2008a, The MathWorks, Natick, MA) was used to perform additional data visualizations. Additionally, Matlab was used to perform robust quadratic fits for cortical thickness – age relationships (Figure 3.2).

3.2.5 Statistical analysis

Group comparisons of core language score and comparisons of patient specific indices to the CELF-4 norm values were performed using two-sided Student's t-tests (SPSS, version 17); p-values below 0.05 were considered significant. The cortical thickness group comparison and associations of cortical thickness with age and language indices were investigated using Freesurfer's build-in GLM tool, Qdec. All Qdec results (at approximately 300,000 nodes) were corrected for multiple comparisons using the built-in tool for assessment of the cluster size p-values. These multiple-comparisons corrected results were considered significant for $p<0.05$.

3.3 Results

3.3.1 Neuropsychological assessment (CELF-4)

The core language score of the patients (92±18) was under the norm score of 100 (p=0.047) and lower than that of the healthy controls (106±10.5, p=0.0026). The patients scored below norm on all subtests. The deficits were significant in receptive language index (87±19, p=0.002) and language content index (87±18, p=.0016) and a trend of reduced expressive language index was found (92±18, p=.054).

3.3.2 Thinner cortex in rolandic epilepsy

In the left hemisphere, a perisylvian region was identified in which patients had a thinner cortex than controls (Figure 3.1A, age corrected). This region was located predominantly in the supramarginal gyrus and partly covered the bank of the superior temporal sulcus, the superior temporal gyrus and the lower postcentral gyrus.

No aberrant regions were found in the right hemisphere and no regions were found in which the patients had a thicker cortex than the controls.

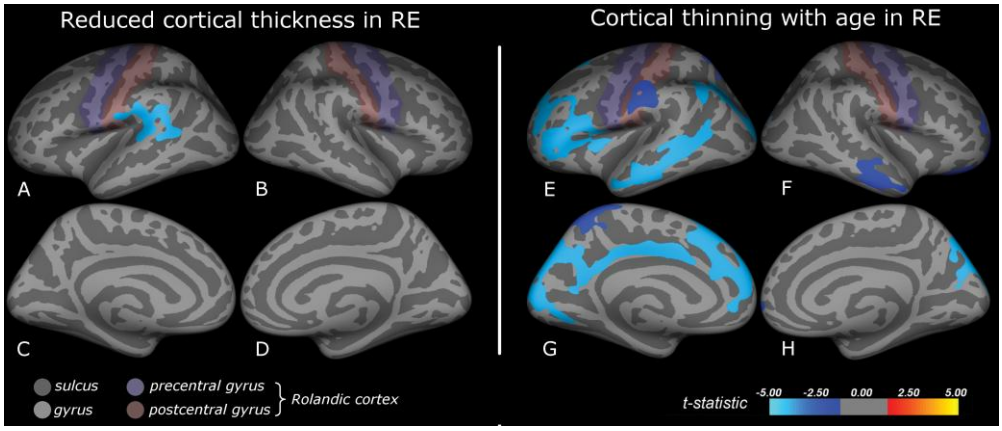

Figure 3.1: Inflated brain visualizations of the regions showing abnormal cortical morphology in RE. Subfigures A-D display reduced cortical thickness in RE (age and gender corrected) , subfigures E-H depict regions showing cortical thinning for increasing age, an effect which was only found in the patients (gender corrected). Reduced cortical thickness was found predominantly in the supramarginal gyrus and partly covered the bank of the superior temporal sulcus, the superior temporal gyrus and the lower postcentral gyrus (A). Cortical thinning with age was predominantly found in the left hemisphere and involved the inferior frontal gyrus, the inferior postcentral and the supramarginal gyrus and the middle temporal gyrus at the lateral side (E), and the cuneus, precuneus and cingulate cortex medially (G).

3.3.3 Cortical thinning with age in rolandic epilepsy

The effect of age on cortical thickness was subsequently investigated for both groups separately. The patients exhibited widespread cortical thinning with age in predominantly the left hemisphere (Figure 3.1E,G). The left frontal region covered superior and rostral middle frontal areas and parts of the pars triangularis and opercularis of the inferior frontal gyrus and the insula (Figure 3.1E). The left parietal region partly covered the supramarginal gyrus and also the lower part of the postcentral gyrus. The left temporal region largely covered the middle temporal gyrus and a part of the bank of the superior temporal sulcus, whereas the posterior region covered parts of the inferior parietal and lateral occipital areas. This region extended medially (Figure 3.1G) to cover parts of the cuneus and precuneus, the pericalcarine and lingual cortex, and the cingulate cortex. In the right hemisphere (Figure 3.1F,H), several smaller regions were found in the rostral middle frontal and lateral orbitofrontal cortex, the lateral temporal, the superior parietal and the lateral occipital cortex.

No regions were found showing cortical thickening with age and also no (linear) age effect was found in the controls. In fact, whereas the patients show consistent cortical thinning, the controls seem to be in the transition from cortical thickening to cortical thinning (Figure 3.2).

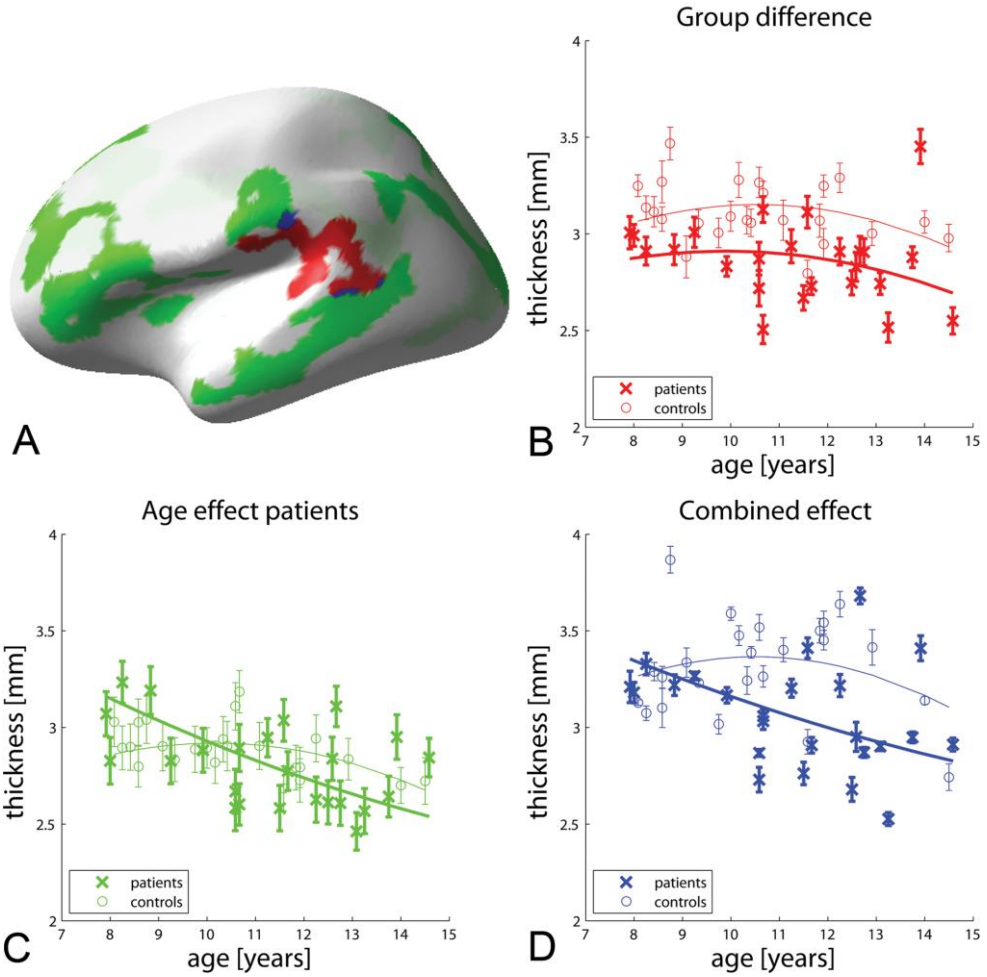

Figure 3.2: A: Colour-coded depiction of abnormalities in cortical thickness in children with rolandic epilepsy. Regions in which patients show reduced cortical thickness are depicted in red, regions in which patients display cortical thinning with age are given in green, and overlap between the two is depicted in blue. For these 3 types of regions, cortical thickness is plotted against age in the same colours in subfigures B, C and D, respectively, for both the patient and the control cohorts. Subfigures C and D reveal linear trends of decreasing cortical thickness with age for the patient group only; the control cohort seems to be in the transition from cortical thickening to cortical thinning . Error bars indicate 1 standard error of spatial variance and for visualization purposes, quadratic fits are provided in addition to the data points.

3.3.4 Correlations between cortical thickness and language indices

The association between cortical thickness and language indices was investigated per group (age corrected). No associations were found within the regions of abnormal cortical thickness and/or aberrant age effect described above. Instead, in the patients, higher core language scores were associated with lower cortical

thickness in the left inferior occipital lobe, more specifically the lingual and lateral occipital cortex (Pearson correlation r=-0.65, p<0.001). Similar effects were found for the receptive language index, the expressive language index and the language content index, while no effects were found in the controls.

3.4 Discussion

In this study, we set out to detect cortical abnormalities in children with RE and potential associations with language (performance).

3.4.1 Main findings

We found reduced cortical thickness in patients compared to controls, not only within the seizure onset zone (rolandic cortex), but also beyond, in perisylvian regions of the left hemisphere. More extensive and distributed cortical abnormalities were observed when taking into account the effect of age, which demonstrated cortical thinning as a function of age, predominantly in the left hemisphere and in patients only. Language impairment in RE was confirmed for multiple language domains, particularly concerning receptive language and language content.

3.4.2 Reduced cortical thickness

Reduced cortical thickness in epilepsy is not specific for RE and has been demonstrated before in both adult and paediatric patients (Mueller SG, et al., 2009; Widjaja E, et al., 2011). In this study, we found reduced cortical thickness not only in the rolandic cortex, but also in the supramarginal and superior temporal gyrus of the left hemisphere. We speculate that this is secondary pathology (i.e. not coinciding with the epileptic zone) and, given its location (Wernicke's area), might be related to language impairment.

To explain reduced cortical thickness outside the seizure onset zone, previously the existence of an underlying network has been suggested that propagates epileptiform activity to other cortical regions and induces distal atrophy (Mueller SG, et al., 2009; Widjaja E, et al., 2011). An alternative explanation is that both cortical abnormalities and seizures are symptoms of an underlying pathology (benign childhood seizure susceptibility syndrome; BCSSS (Panayiotopoulos, 1993; Panayiotopoulos, et al., 2008)).

3.4.3 Cortical thinning with age in RE

Widely distributed morphological abnormalities were found when studying cortical thickness as a function of age. Gradual cortical thinning for increasing age was found in predominantly the left hemisphere in several frontal, centroparietal, temporal, and medial regions in the patients only. Again, not only the laterality of

these abnormalities (left hemisphere) suggests a link with language impairment, but also their specific localization in the left inferior frontal, supramarginal and middle temporal gyrus (Broca's area, Wernicke's area and regions relevant for reading, respectively) (Backes WH, et al., 2005; Deblaere K, et al., 2002).

3.4.4 Abnormal developmental trajectory

Upon further investigation, cortical thickness was also dependent on age in the controls, which showed cortical thickening at the beginning of the study age window and cortical thinning towards the end (Figure 3.2). Cortical thinning is a normal phase of preadolescent brain development and reflects optimization-driven pruning of neurons and synapses in the underlying white matter (Andersen, 2003; Lenroot & Giedd, 2006; Muftuler, et al., 2011). As such, cortical thinning does not reflect pathology per se, but can also be an aspect of normal maturation.

However, the fact that the patients showed consistent cortical thinning over the entire study age window (8-14 years) whereas the controls seemed to be in the transition from cortical thickening to thinning might imply early onset of cortical thinning in the patients, which might represent actual pathomorphology.

During the preadolescent phase of rapid brain development, proper neuronal cues (e.g. hormones, neurotropic factors, environmental demands) are essential for typical differentiation. Especially at the age range under investigation, strong region-specific maturational changes occur in the rolandic gray matter, which present an increased susceptibility to deviations from the normal developmental trajectory by improper signaling (Andersen, 2003; Lenroot & Giedd, 2006). Moreover, during development, preadolescent influences are incorporated into the (further) maturation of anatomy and function as they determine set points for adult function, with possibly lasting effects (Andersen, 2003).

Localized early onset of cortical thinning in RE might represent a deviation from the normal developmental trajectory in the corresponding regions, possibly induced by improper neuronal signaling as a result of the typical preadolescent seizures and/or epileptiform activity.

We combined our findings with information from literature on normal cortical development to construct a hypothetical trajectory for cortical development of aberrant regions in RE (Figure 3.3) (Raznahan A, et al., 2011).

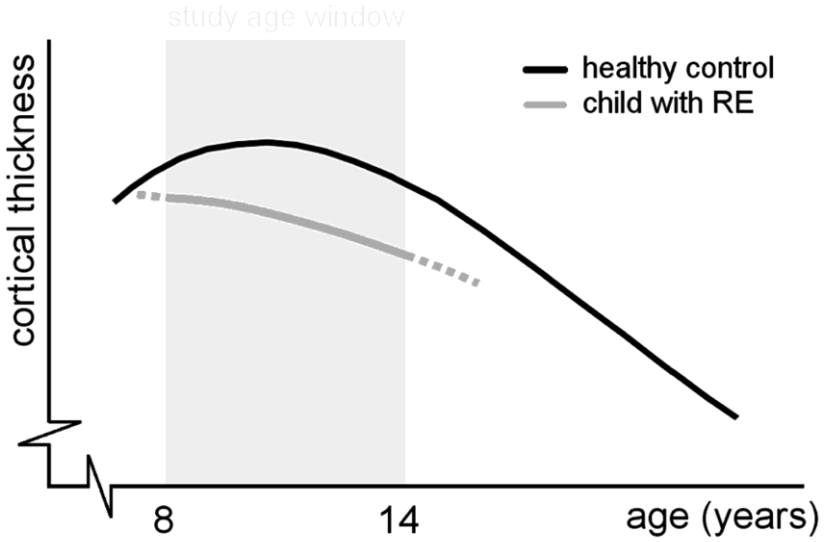

Figure 3.3: Hypothetical cortical thickness developmental trajectory of affected regions in Rolandic epilepsy compared to healthy controls. The normal developmental trajectory follows an inverted U-shaped curve, wherein initial cortical thickening is followed by cortical thinning. In RE, several regions display both reduced cortical thickness and aberrantly early onset of cortical thinning (at or even before 8 years of age), other regions show one of these effects separately, see Fig 2. Normal developmental trajectory adapted from (Raznahan A, et al., 2011).

3.4.5 Mechanisms for impairment

The phase of preadolescent cortical thinning is preceded by a tremendous overshoot of neurons and connections, during which the brain is established as an over-complete network (Andersen, 2003; Lenroot & Giedd, 2006; Muftuler, et al., 2011). The subsequent pruning process removes redundant neurons and connections to optimize the network for environmental needs, the level of redundancy determining the degree of adaptation. In RE, the early onset of cortical thinning in specific regions, alone or in combination with reduced cortical thickness per se, might represent locally suboptimal network formation and/or pruning and might actually be the mechanism behind impaired language function. Dedicated research, i.e. on linking cortical thickness to the integrity of the underlying network, is needed to test this hypothesis, see also the following section.

3.4.6 Lack of association between abnormal cortex and language impairment

The current study did not observe an association between cortical thickness and language performance for regions of aberrant cortex. Possibly this association was not found since it is indirect, i.e. mediated by the underlying network integrity, and might only become apparent in case of severe network breakdown, which is probably not the case in RE. Techniques offering a more direct/closer window on the underlying network, such as diffusion weighted and functional imaging probing functional and structural network integrity, respectively, might prove more sensitive in establishing such associations in future research (Besseling, et al., 2013; D. Jones, 2010; D. K. Jones, Knosche, & Turner, 2012; van den Heuvel & Hulshoff Pol, 2010).

3.4.7 Methodological considerations

In our cross-sectional study, the effect of age could only be assessed by virtue of the variability in age of the subjects included. Our findings suggest (but do not prove) aberrant time courses of cortical development in RE. For future research, longitudinal designs are prompted to further investigate abnormalities in cortical development in individual RE patients.

Furthermore, we can only speculate that abnormal cortical development during preadolescence reflects network impairments in the underlying white matter which may persist into adulthood, however, explicit network assessment and inclusion of adults in remission from RE are needed to validate these claims. For future research, we propose to follow up over many years, from the moment of seizure onset (or even before, e.g. based on the identification of a predictive profile of language impairment (Overvliet GM, Aldenkamp AP, Klinkenberg S, Vles JSH et al., 2011)) until well into adulthood.

In addition to timely inclusion, adequate assessment of characteristics such as seizure frequency is expected to be especially challenging in such longitudinal studies of RE, given its mild and typically nocturnal seizure semiology. We also suggest the acquisition of diffusion weighted or functional imaging to assess structural and functional connectivity, respectively (D. K. Jones, et al., 2012; van den Heuvel & Hulshoff Pol, 2010).

3.4.8 Clinical outlook

RE is commonly regarded as benign and consequently children with RE typically do not receive special care (Lerman P & Kivity S, 1975; Loiseau P, et al., 1992; Loiseau, et al., 1983). Because of the increasing awareness of significant comorbidities in RE, its classification as benign is under debate (Hughes, 2010; Nicolai J, et al., 2006; Vinayan KP, et al., 2005; Völkl-Kernstock S, et al., 2009; Weglage J, et al., 1997). In the current study, we report widespread cortical

abnormalities in language areas in children with RE who were selected based on EEG criteria and seizure semiology and not on language performance.

These findings might signify that language impairment is more general in RE than commonly assumed. Indeed, it has been demonstrated that (seizure free) siblings of children with RE are at increased risk for language disorders (Clarke, et al., 2007), suggesting a shared genetic basis for language impairment and seizures in RE.

When health care professionals are willing to generally regard RE as malign to a certain extent (i.e. not only in atypical cases), they might be more inclined to subject children with RE to treatment instead of the often applied "wait and see" strategy.

Furthermore, the current study demonstrates the relevance of the effect of age in RE and proposes to adopt the view that RE represents a deviation from the normal developmental trajectory of the brain in a critical period of brain maturation. The earlier this deviation occurs, the more severe the consequences, with children of age at seizure onset below 6 years having the lowest language performance (Jurkeviciene, et al., 2012). This warrants further research into whether it is possibly to exploit the increased brain plasticity in this critical period as a window of opportunity to redirect aberrant development onto a normal trajectory (Andersen, 2003). A possible approach is to stimulate language network formation by speech therapy, however this has not systematically been studied yet (Besag, 2006). Alternatively, improper neuronal signaling might be reduced by suppression of seizures and/or epileptiform activity using anti epileptic drugs (Porras-Kattz, et al., 2011), although in clinical practise this is controversial in RE as it is difficult to differentiate adverse effects of medication from disease effects (Hughes, 2010).

3.5 Conclusion

For the first time, specific cortical abnormalities consistent over subjects were observed in children with RE. The abnormalities were localized predominantly in language mediating brain regions of the left hemisphere and involve areas of reduced cortical thickness and of early onset of cortical thinning of patients compared to controls. Future longitudinal research is prompted to further investigate developmental abnormalities in RE, e.g. investigating whether the cortical abnormalities represent a predictive cerebral marker for language impairment risk during and potentially after the active seizure period.

Acknowledgements

This work was supported by the Dutch Epilepsy Foundation (NEF). The author JJ was funded by VENI research grant 916.11.059 from the Netherlands Organization for Scientific Research (NWO) and the Netherlands Organization for Health Research and Development (ZonMw). The funders had no role in study design, data collection and analysis, decision to publish, or preparation of the manuscript.

We would like to thank Esther Peeters for her help with the MRI data acquisitions, Marc Geerlings for continuing ICT back-up and the Dutch Epilepsy Foundation for funding of author AA.

References

Andersen, S. L. (2003). Trajectories of brain development: point of vulnerability or window of opportunity? *Neurosci Biobehav Rev, 27*(1-2), 3-18.

Backes WH, Deblaere K, Vonck K, Kessels AG, Boon P, Hofman P, et al. (2005). Language activation distributions revealed by fMRI in post-operative epilepsy patients: differences between left- and right-sided resections. *Epilepsy Research, 66*(1-3), 1-12.

Berroya AM, Bleasel AF, Stevermuer TL, Lawson J, & Bye AM (2005). Spike morphology, location, and frequency in benign epilepsy with centrotemporal spikes. *J Child Neurol., 20*(3), 188-194.

Besag, F. M. (2006). Cognitive and behavioral outcomes of epileptic syndromes: implications for education and clinical practice. *Epilepsia, 47 Suppl 2*, 119-125.

Besseling, R. M. H., Jansen, J. F., Overvliet, G. M., van der Kruijs, S. J., Vles, J. S., Ebus, S. C. M., et al. (2013). Reduced functional integration of the sensorimotor and language network in rolandic epilepsy. *Neuroimage: Clinical*.

Boxerman JL, Hawash K, Bali B, Clarke T, Rogg J, & Pal DK (2007). Is Rolandic epilepsy associated with abnormal findings on cranial MRI? *Epilepsy Research, 75*(2-3), 180-185.

Carlsson, G., Igelbrink-Schulze, N., Neubauer, B. A., & Stephani, U. (2000). Neuropsychological long-term outcome of rolandic EEG traits. *Epileptic Disord, 2 Suppl 1*, S63-66.

Clarke T, Strug LJ, Murphy PL, Bali B, Carvalho J, Foster S, et al. (2007). High risk of reading disability and speech sound disorder in rolandic epilepsy families: case-control study. *Epilepsia, 48*(12), 2258-2265.

Clarke, T., Strug, L. J., Murphy, P. L., Bali, B., Carvalho, J., Foster, S., et al. (2007). High risk of reading disability and speech sound disorder in rolandic epilepsy families: case-control study. *Epilepsia, 48*(12), 2258-2265.

Dale, A. M., Fischl, B., & Sereno, M. I. (1999). Cortical surface-based analysis. I. Segmentation and surface reconstruction. *Neuroimage, 9*(2), 179-194.

Dale, A. M., & Sereno, M. I. (1993). Improved localization of cortical activity by combining EEG and MEG with mri cortical surface reconstruction: A linear approach. *J. Cognitive Neuroscience, 5*(2), 162-176.

Deblaere K, Backes WH, Hofman P, Vandemaele P, Boon PA, Vonck K, et al. (2002). Developing a comprehensive presurgical functional MRI protocol for patients with intractable temporal lobe epilepsy: a pilot study. *Neuroradiology., 44*(8), 667-673.

Eeg-Olofsson O, Lundberg S, & Raininko R (2000). MRI in rolandic epilepsy. *Epileptic Disorders, 2*(Suppl 1), S51-53.

Fischl, B., & Dale, A. M. (2000). Measuring the thickness of the human cerebral cortex from magnetic resonance images. *Proc Natl Acad Sci U S A, 97*(20), 11050-11055.

Gelisse P, Corda D, Raybaud C, Dravet C, Bureau M, & Genton P (2003). Abnormal neuroimaging in patients with benign epilepsy with centrotemporal spikes. *Epilepsia, 44*(3), 372-378.

Gomez, M. R., & Klass, D. W. (1983). Epilepsies of infancy and childhood. *Ann Neurol, 13*(2), 113-124.

Gündüz E, Demirbilek V, & Korkmaz B (1999). Benign rolandic epilepsy: neuropsychological findings. *Seizure, 8*(4), 246-269.

Hughes, J. R. (2010). Benign epilepsy of childhood with centrotemporal spikes (BECTS): to treat or not to treat, that is the question. *Epilepsy Behav, 19*(3), 197-203.

Jones, D. (2010). Challenges and limitations of quantifying brain connectivity in vivo with diffusion MRI. *Imaging Med, 2*(3), 341-355.

Jones, D. K., Knosche, T. R., & Turner, R. (2012). White matter integrity, fiber count, and other fallacies: The do's and don'ts of diffusion MRI. *Neuroimage*.

Jurkeviciene, G., Endziniene, M., Laukiene, I., Saferis, V., Rastenyte, D., Plioplys, S., et al. (2012). Association of language dysfunction and age of onset of benign epilepsy with centrotemporal spikes in children. *Eur J Paediatr Neurol, 16*(6), 653-661.

Kim, J. S., Singh, V., Lee, J. K., Lerch, J., Ad-Dab'bagh, Y., MacDonald, D., et al. (2005). Automated 3-D extraction and evaluation of the inner and outer cortical surfaces using a Laplacian map and partial volume effect classification. *Neuroimage, 27*(1), 210-221.

Koutroumanidis, M. (2007). Panayiotopoulos syndrome: an important electroclinical example of benign childhood system epilepsy. *Epilepsia, 48*(6), 1044-1053.

Lenroot, R. K., & Giedd, J. N. (2006). Brain development in children and adolescents: insights from anatomical magnetic resonance imaging. *Neurosci Biobehav Rev, 30*(6), 718-729.

Lerman P, & Kivity S (1975). Benign focal epilepsy of childhood. A follow-up study of 100 recovered patients. *Arch Neurology, 32*(4), 261-264.

Loiseau P, & Duché B (1989). Benign childhood epilepsy with centrotemporal spikes. *Cleve Clin J Med, 56*(Suppl Pt 1), S17-22; discussion S40-12.

Loiseau P, Duché B, & Cohadon S (1992). The prognosis of benign localized epilepsy in early childhood. *Epilepsy Res Suppl, 6*, 75-81.

Loiseau, P., Pestre, M., Datigues, J. F., Commenges, D., Barberger-Gateau, C., & Cohadon, S. (1983). Long-term prognosis in two forms of childhood epilepsy: Typical absence seizures and epilepsy with rolandic (centrotemporal) EEG foci. *Annals of Neurology, 13*(6), 642-648.

Lundberg S, Eeg-Olofsson O, Raininko R, & Eeg-Olofsson KE (1999). Hippocampal asymmetries and white matter abnormalities on MRI in benign childhood epilepsy with centrotemporal spikes. *Epilepsia, 40*(12), 1808-1815.

Monjauze C, Tuller L, Hommet C, Barthez MA, & Khomsi A (2005). Language in benign childhood epilepsy with centro-temporal spikes abbreviated form: rolandic epilepsy and language. *Brain and Language, 92*(3), 300-308.

Mueller SG, Laxer KD, Barakos J, Cheong I, Garcia P, & Weiner MW (2009). Widespread neocortical abnormalities in temporal lobe epilepsy with and without mesial sclerosis. *Neuroimage, 46*(2), 353-359.

Muftuler, L. T., Davis, E. P., Buss, C., Head, K., Hasso, A. N., & Sandman, C. A. (2011). Cortical and subcortical changes in typically developing preadolescent children. *Brain Res, 1399*, 15-24.

Nicolai J, Aldenkamp AP, Arends J, Weber JW, & Vles JSH (2006). Cognitive and behavioral effects of nocturnal epileptiform discharges in children with benign childhood epilepsy with centrotemporal spikes. *Epilepsy Behavior, 8*(1), 56-70.

Northcott E, Connolly AM, Berroya A, McIntyre J, Christie J, Taylor A, et al. (2007). Memory and phonological awareness in children with Benign Rolandic Epilepsy compared to a matched control group. *Epilepsy Research, 75*(1), 57-62.

Overvliet GM, Aldenkamp AP, Klinkenberg S, Nicolai J, Vles JS, Besseling RM, et al. (2011). Correlation between language impairment and problems in motor development in children with Rolandic epilepsy. *Epilepsy & Behavior*.

Overvliet GM, Aldenkamp AP, Klinkenberg S, Vles JSH, & Hendriksen J (2011). Impaired language performance as a precursor or consequence of Rolandic epilepsy? *Journal of the Neurological Sciences, 304*(1), 71-74.

Overvliet GM, Besseling RM, Vles JS, Hofman PA, Backes WH, van Hall MH, et al. (2010). Nocturnal epileptiform EEG discharges, nocturnal epileptic seizures, and language impairments in children: Review of the literature. *Epilepsy Behav, 19*(4), 550-558.

Overvliet, G. M., Besseling, R. M., van der Kruijs, S. J., Vles, J. S., Backes, W. H., Hendriksen, J. G., et al. (2013). Clinical evaluation of language fundamentals in Rolandic epilepsy, an assessment with CELF-4. *Eur J Paediatr Neurol*.

Panayiotopoulos, C. P. (1993). Benign childhood partial epilepsies: benign childhood seizure susceptibility syndromes. *J Neurol Neurosurg Psychiatry, 56*(1), 2-5.

Panayiotopoulos, C. P., Michael, M., Sanders, S., Valeta, T., & Koutroumanidis, M. (2008). Benign childhood focal epilepsies: assessment of established and newly recognized syndromes. *Brain, 131*(Pt 9), 2264-2286.

Papavasiliou A, Mattheou D, Bazigou H, Kotsalis C, & Paraskevoulakos E (2005). Written language skills in children with benign childhood epilepsy with centrotemporal spikes. *Epilepsy & Behavior, 6*(1), 50-58.

Paslawski C (2005). The Clinical Evaluation of Language Fundamentals, Fourth Edition (CELF-4): A Review. *Canadian Journal of School Psychology, 20*, 129-134.

Porras-Kattz, E., Harmony, T., Ricardo-Garcell, J., Galan, L., Fernandez, T., Prado-Alcala, R., et al. (2011). Magnesium valproate in learning disabled children with interictal paroxysmal EEG patterns: Preliminary report. *Neurosci Lett, 492*(2), 99-104.

Raznahan A, Shaw P, Lalonde F, Stockman M, Wallace GL, Greenstein D, et al. (2011). How does your cortex grow? *Journal of Neuroscience, 31*(19), 7174-7177.

Semel E, Wiig EH, & Secord WA (2010). *Clinical Evaluation of Language Fundamentals 4, Nederlandse versie* (3 ed.). Amsterdam: Pearson

van den Heuvel, M. P., & Hulshoff Pol, H. E. (2010). Exploring the brain network: a review on resting-state fMRI functional connectivity. *Eur Neuropsychopharmacol, 20*(8), 519-534.

Vinayan KP, Biji V, & Thomas SV (2005). Educational problems with underlying neuropsychological impairment are common in children with Benign Epilepsy of Childhood with Centrotemporal Spikes (BECTS). *Seizure, 14*(3), 207-213.

Völkl-Kernstock S, Bauch-Prater S, Ponocny-Seliger E, & Feucht M (2009). Speech and school performance in children with benign partial epilepsy with centro-temporal spikes (BCECTS). *Seizure, 18*(5), 320-326.

Weglage J, Demsky A, Pietsch M, & Kurlemann G (1997). Neuropsychological, intellectual, and behavioral findings in patients with centrotemporal spikes with and without seizures. *Dev Med Child Neurol, 39*(10), 646-651.

Widjaja E, Mahmoodabadi SZ, Snead OC 3rd, Almehdar A, & Smith ML (2011). Widespread cortical thinning in children with frontal lobe epilepsy. *Epilepsia, 52*(9), 1685-1691.

CHAPTER 4

Aberrant functional connectivity between motor and language networks in rolandic epilepsy

R.M.H. Besseling, G.M. Overvliet, J.F.A. Jansen, S.J.M. van der Kruijs, J.S.H. Vles, S.C.M. Ebus, P.A.M. Hofman, A.J.A. de Louw, A.P. Aldenkamp, W.H. Backes

Epilepsy Research 2013; 107, 253—262

Abstract

Introduction Rolandic epilepsy (RE) is an idiopathic focal childhood epilepsy with a well-established neuropsychological profile of language impairment. The aim of this study is to provide a functional correlate that links rolandic (sensorimotor) pathology to language problems using functional MRI.

Materials and methods Twenty-three children with RE (8-14 years old) and 21 matched controls underwent extensive language assessment (Clinical Evaluation of Language Fundamentals). fMRI was performed at rest and using word generation, reading, and finger tapping paradigms. Since no activation group differences were found, regions of interest (ROIs) were defined at pooled (patients and controls combined) activation maxima and in contralateral homotopic cortex, which were used to assess language lateralization as well as for a resting-state connectivity analysis. Furthermore, the association between connection strength and language performance was investigated.

Results Reduced language performance was found in the children with RE. Bilateral activation was found for both language tasks with some predominance of the left hemisphere in both groups. Compared to controls, patient connectivity was decreased between the left sensorimotor area and right inferior frontal gyrus ($p<0.01$). For this connection, lower connectivity was associated with lower language scores in the patient group ($r=0.49$, $p=0.02$), but not in the controls.

Conclusion Language laterality analysis revealed bilateral language representation in the age range under study (8-14 years). As a consequence, the connection of reduced functional connectivity we found represents an impaired interplay between motor and language networks, and aberrant functional connectivity associated with poorer language performance. These findings provide a first neuronal correlate in terms of aberrant resting-state functional connectivity for language impairment in RE.

4.1 Introduction

Rolandic epilepsy (RE) is an idiopathic focal epilepsy of childhood with typical onset at 7-10 years of age (Panayiotopoulos, Michael et al. 2008). It is also known as benign epilepsy of childhood with centro-temporal spikes (BECTS), which reflects both its mild seizure semiology and the location of the seizure onset zone on EEG (sensorimotor cortex, i.e. rolandic area). Seizures include hemifacial spasms and speech arrest and occur mostly at night (Nayrac P and Beaussart M 1958; Hughes 2010). Furthermore, spontaneous remission of seizures is typically observed during adolescence (Loiseau P and Duché B 1989; Massa R, de Saint-Martin A et al. 2001; Hughes 2010).

Classically, RE is thought to occur in children of normal intellect without neuropsychological problems (Loiseau P and Duché B 1989). In recent years, however, evidence has accumulated that serious co-morbidities may occur, such as behavioral problems, oromotor deficits and language impairment (Monjauze C, Tuller L et al. 2005; Nicolai J, Aldenkamp AP et al. 2006; Northcott E, Connolly AM et al. 2007; Panayiotopoulos, Michael et al. 2008; Kanemura and Aihara 2009; Overvliet GM, Besseling RM et al. 2010). This has put the assumedly benign nature of RE under debate (Weglage J, Demsky A et al. 1997; Vinayan KP, Biji V et al. 2005; Nicolai J, Aldenkamp AP et al. 2006; Völkl-Kernstock S, Bauch-Prater S et al. 2009). This includes a discussion on whether it is clinically desirable and/or beneficial to treat RE, for example by means of anti epileptic drugs (Hughes 2010).

Especially language impairment is increasingly recognized and extensively described with respect to neurocognitive profile (Monjauze C, Tuller L et al. 2005; Northcott E, Connolly AM et al. 2005; Papavasiliou A, Mattheou D et al. 2005; Northcott E, Connolly AM et al. 2006). Interestingly, in RE a significant correlation has been demonstrated between problems in motor and problems in language development, which suggests a common cerebral origin (Gündüz E, Demirbilek V et al. 1999; Overvliet GM, Aldenkamp AP et al. 2011).

Based on EEG, measures have been developed for cognitive impairment risk in RE (Massa R, de Saint-Martin A et al. 2001), and associations have been described between the nature of the language impairments and the laterality of the epileptiform abnormalities (Riva, Vago et al. 2007; Lillywhite, Saling et al. 2009). However, these studies remain inconclusive with respect to the underlying cerebral mechanism. Its unveiling is highly desirable as even though the cognitive deficits in RE are typically deemed reversible (Panayiotopoulos, Michael et al. 2008), it has been suggested that in specific cases they may persist after seizure remission (Kanemura and Aihara 2009; Monjauze C, Broadbent H et al. 2011). Moreover, insight into the pathophysiological mechanism is relevant for the

interpretation of delays in scholar development and to motivate treatment strategies.

The language problems, but also the inattention and impulsivity seen in RE, suggest dysfunction in circuits distant from the rolandic area (Massa R, de Saint-Martin A et al. 2001). In a study of frontal lobe epilepsy in children, it was suggested that abnormalities distal to the seizure onset zone might be involved in the spread of seizure activity or the development of secondary epileptogenic zones (Widjaja E, Mahmoodabadi SZ et al. 2011). These suggestions prompt research employing connectivity analysis to explore potentially aberrant connections in children with RE that could explain the language impairment.

The aim of this study is to investigate whether in RE aberrant functional connectivity can be found between motor and language areas, which might link the location of the epileptic focus (sensorimotor cortex) to the language impairment. Task fMRI is used to identify language and motor networks. Since atypical language lateralization on fMRI has been reported in pediatric epilepsy before (Liegeois, Connelly et al. 2004; Yuan, Szaflarski et al. 2006), the laterality of language activation is also investigated. Resting-state fMRI (rs-fMRI) is employed to determine the functional connectivity within and between the identified functional networks. Language performance is assessed using the Clinical Evaluation of Language Fundamentals (CELF) test for children and the association between connection strength and language performance is studied.

4.2 Materials and methods

4.2.1 Selection criteria

Children with RE were selected at the specialized epilepsy referral centre Kempenhaeghe based on clinical criteria concerning electro encephalography (EEG) and seizure semiology as described in the literature (Berroya AM, Bleasel AF et al. 2005; Panayiotopoulos, Michael et al. 2008). EEG criteria include the presence of spike and slow wave complexes occurring as individual paroxysms or in repetitive clusters with a maximum in mid temporal and/or central electrodes and with a temporal-frontal dipole field. Additional independent central, midtemporal, parietal or occipital spike-wave foci in the same or other hemisphere were allowed. To exclude severe cases (Landau-Kleffner syndrome (LKS) or LKS-like), interictal epileptiform activity was required to be present <85% of the time during non-REM sleep. With respect to seizure semiology, seizures with anarthria, hemiclonia involving the face and/or unilateral extremities, or secondarily generalized seizures were considered. In case of poorly observed nocturnal seizures, post ictal signs of a generalized seizure or confirmation of post ictal hemiparesis were sufficient for inclusion in case of otherwise typical EEG.

4.2.2 Study population

Twenty-three children (7 girls) with RE were selected. The age at epilepsy onset (mean±SD) was 7.5±2.1 and the age at testing 11.4±2.0 years (range: 8-14 years). Nineteen children were right handed, 3 were left handed and 1 child was ambidextrous. As a control group, 21 healthy controls were selected (10 girls, age 10.5±1.6 years, range 8-14 years, 20 right handed and 1 left handed). The age distributions of both groups were comparable (t-test, p=0.11).

As part of their diagnostic workup, the children with RE underwent the Wechsler Intelligence Score for Children, 3rd edition and all had a full-scale IQ >70. None of the healthy controls had (a history of) dyslexia, learning disorders or psychiatric disorders, nor attended special education. Children were excluded if they had dental braces (MRI quality) or were somewhat afraid in the scanner.

A board certified neuroradiologist specialized in epilepsy (PH, 20 years of experience) reviewed all scans and found no structural abnormalities.

The study was approved by the boards of the medical ethical committees of both participating institutions. All parents (or guardians) gave written informed consent prior to study participation.

4.2.3 Language assessment

To assess language performance, the Clinical Evaluation of Language Fundamentals, 4th edition (CELF-4), Dutch version was used (Paslawski C 2005; Semel E, Wiig EH et al. 2010). The CELF-4 is considered the gold standard for language assessment in children and provides several age-corrected metrics. Among these is the core language score, which was assessed in all subjects and is a general language measure that may serve as a screening measure for language impairment. More specific sub metrics were only assessed in the patients to assess which specific language aspects may be impaired. Differences in language performance of the patients with respect to the controls and norm values were assessed using Student's t-tests employing a significance level of $p<0.05$.

4.2.4 MRI acquisition and preprocessing

4.2.4.1 Structural MRI

Structural MRI was performed for anatomical reference at 3.0 Tesla (Philips Achieva system; Philips Medical System, Best, the Netherlands) using an 8-element receive-only head coil. A T1-weighted scan was acquired using the following settings: voxel size 1x1x1 mm^3, field of view (FOV) 240x240x150 mm^3, flip angle 8°, 3D fast spoiled gradient echo sequence, echo time/repetition time/inversion time (TE/TR/TI) 3.8/8.3/1022 ms and acquisition time 8 min. Additionally a T2-weighted scan was acquired (TE/TR 80/3000 ms), as well as a fluid attention inversion

recovery (FLAIR) sequence (TE/TR/TI 125/11000/2800 ms) at voxel size 0.45x0.45x5.5 mm^3, FOV 230x230x143 mm^3, and flip angle 90°.

4.2.4.2 Functional MRI

fMRI was performed both under task and at rest, using identical sequences. A blood oxygenation level dependent (BOLD) echo planar imaging (EPI) sequence (T2*-weighted) was used employing TE/TR 35/2000 ms, 195 dynamic whole cerebrum scans, 2x2 mm^2 in plane resolution, 4 mm thick axial slices (no gap; FOV 256x256x128 mm^3), flip angle 90° and acquisition time 6.5 min.

4.2.4.3 fMRI activation paradigms

For each task, a standard block design was used of 6 task condition blocks interleaved with baseline blocks. Each block lasted 30 s and each paradigm started and ended with a baseline block. Tasks were presented visually.

In the word generation paradigm, the children were asked to covertly generate as many words as possible starting with a certain letter (U-N-K-A-E-P, 1 letter per task block). During baseline, an asterisk (*) was presented for visual fixation (Vlooswijk, Jansen et al. 2010).

During the reading task, text with a semantic meaning was presented (task block) alternated with nonsense text (baseline condition) (Vlooswijk, Jansen et al. 2010). To ensure continuous reading, the text was refreshed 3 times per 30 s block. To minimize the effect of individual differences in reading abilities, each text frame consisted of 4 lines, only the first 2 of which were essential for text continuity.

In the finger tapping task, the children were asked to touch their fingers with their thumb in a consecutive manner. An arrow indicated which hand to use. Right-handed tapping was alternated with left-handed tapping and both were interleaved with the baseline condition (visual fixation).

4.2.4.4 Resting-state fMRI paradigm

For the rs-fMRI scan, the children were asked to clear their mind, lie quietly in the scanner with their eyes closed and to stay awake.

4.2.4.5 Preprocessing of functional images

All fMRI time series were preprocessed using SPM8 (Wellcome Department of Cognitive Neurology, London, UK). First, the images of each dynamic series were realigned to correct for head motion using rigid transformations. Next, the T1-weighted anatomical image was segmented (gray matter, white matter, and cerebrospinal fluid) and transformed to the standardized stereotactic coordinate system of the Montreal Neurological Institute (MNI). This normalization was applied to the realigned dynamic images to generate movement-corrected normalized fMRI data suitable for group analysis. Finally, the task-related

functional images were spatially smoothed using a Gaussian kernel with a full width at half maximum (FWHM) of 6 mm.

4.2.5 Activation analysis

The task-related functional images were analysed using general linear models (GLMs) in SPM8. The task block design was convolved with a standard hemodynamic response function (HRF) to model the BOLD response. For the reading task, reading text with semantic meaning and reading nonsense text were modelled separately. Similarly, left and right handed finger tapping were modelled by 2 independent regressors.

The movement parameters as estimated in the preprocessing were used as confounders to compensate for residual movement.

Significant activation was assessed using t-contrasts of the task regressors. This resulted in activation maps for word generation (task vs baseline), reading (text with semantic meaning vs nonsense text) and left and right handed finger tapping (both vs baseline). A family wise error (FWE) correction for multiple comparisons was applied at p=0.05.

The individual activation maps were combined in a standard random-effects group analysis. For each task, spherical regions of interest (ROIs) were defined at relevant local maxima of the pooled (i.e. patients and controls combined) activation maps. In case of unilateral activation (language tasks), contralateral ROIs were constructed by mirroring with respect to the mid-sagittal plane. This is also motivated by the finding of atypical language lateralization in other types of pediatric epilepsy (Liegeois, Connelly et al. 2004; Yuan, Szaflarski et al. 2006).

4.2.6 Language lateralization

For both language tasks, the laterality index (LI) distribution was assessed following Abbott et al (Abbott, Waites et al. 2010). The LI quantifies the extent to which an activation map is left or right lateralized and is defined as

$$LI=(N_L-N_R)/(N_L+N_R) \quad [1]$$

where N_L and N_R are defined as the number of voxels above a certain activation threshold (t-value) in the left and right hemisphere, respectively. The LI distribution is the LI as a function of the number of activated voxels (for a certain significance level) $N=N_L+N_R$ and is expected to be more sensitive for group differences than assessing LI for a single (fixed) value of N (Abbott, Waites et al. 2010). For both language tasks, only activated voxels within their respective activation ROIs (and the contralateral homologue ROIs) were used.

A norm group LI distribution was constructed based on the data from the controls. Abnormalities in patient LI distribution were defined as being outside the 95% confidence interval of the controls group LI distribution (Abbott, Waites et al. 2010).

4.2.7 Functional connectivity analysis

The ROIs of pooled activation for all tasks were used for a resting-state functional connectivity analysis. First, the registered and normalized resting-state data were spatio-temporally filtered using a high pass filter with a cut-off at 0.01 Hz and a Gaussian spatial filter with a FWHM of 5 mm in FSL (FMRIB's Software Library, Oxford, UK). Next, the data were corrected for the mean brain signal (regressing out the mean brain time series). The average time series of each ROI was calculated, and Pearson's correlation coefficient was used to quantify the functional connectivity between each pair of time series. These correlation coefficients were Fisher-Z transformed to improve normality and compared between patients and controls using permutation tests (Bassett, Bullmore et al. 2008; van den Heuvel, Mandl et al. 2010; Zhang, Liao et al. 2011). For these network investigations, $p<0.01$ was deemed significant.

For the connections that proved aberrant in RE, the association with language performance was assessed by calculating the correlation between connection strength and CELF-4 indices.

4.3 Results

4.3.1 Neuropsychological assessment (CELF-4)

The core language score of the patients (92±18) was only just significantly below the norm of 100 ($p=0.047$) and more importantly was significantly lower than that of the healthy controls (106±11, $p=0.003$). The patients scored below norm on all subtests. These deficits were significant in receptive language (87±19, $p=0.002$) and language content index (87±18, $p=0.002$), and a trend of reduced expressive language index was found (92±18, $p=0.054$).

4.3.2 Activation maps

4.3.2.1 Word generation

The word generation paradigm induced activity in the anterior cingulate cortex (ACC) bilaterally and in the left inferior frontal gyrus (IFG) in both groups. No significant group differences were found ($p>0.05$, FWE corrected), which motivated calculating a pooled activation map, see Figure 4.1A.

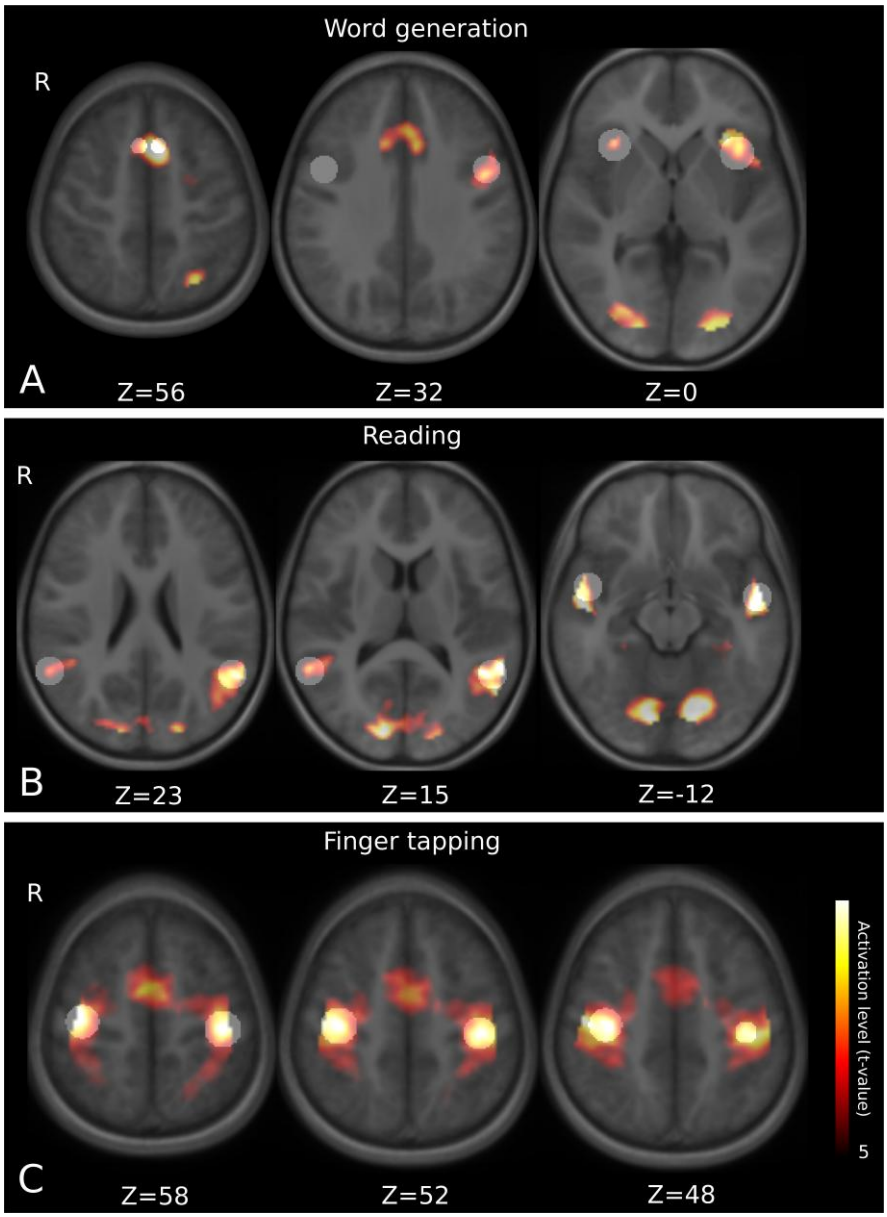

Figure 4.1: Pooled activation maps and spherical regions of interest (transparent white) for (A): word generation; (B): reading and (C): finger tapping. For word generation, regions of interest are defined in the bilateral anterior cingulate (A1), inferior frontal (A2) and insular (A3) cortices. For reading, regions of interest are defined in posterior (B1-2) and anterior (B3) temporal regions. For finger tapping, regions of interest are defined in the bilateral sensorimotor areas (C1-3). In all tasks, activation was also seen in the occipital lobes related to visual task presentation. p=0.05, FWE corrected. The underlay is the averaged MNI-registered structural scan of the controls.

4.3.2.2 *Reading task*

The pooled activation map of the reading task is given in Figure 4.1B. In both patients and controls, activation is seen in the bilateral temporal lobes. In the left temporal lobe, activation appeared more extended and also had an inferior and perisylvian component. No significant group differences were found.

4.3.2.3 *Finger tapping*

Finger tapping related activation was seen in the rolandic areas and the cerebellum. No significant group differences were found and the pooled activation map is given in Figure 4.1C.

4.3.3 Definition of regions of interest in pooled activation maps

Spherical regions of interest (ROIs) were defined at relevant local maxima of the pooled activation maps, as illustrated in Figure 4.1. All ROIs had radius 10 mm, except those in the anterior cingulate cortex (5 mm) to prevent interhemispheric overlap.

4.3.4 Language lateralization

For the word generation and reading tasks, the LI distributions are given in Figure 4.2. Moderately left sided (positive) lateralization is seen for both, but is more pronounced for the word generation task. In word generation, a trend of more pronounced lateralization is seen for patients compared to controls, however the mean patient curve still lies mostly within the 95% confidence interval of the mean controls curve (Figure 4.2A). Also for reading, no aberrant patient lateralization is found (Figure 4.2B).

The limited laterality of the language task activations motivated the inclusion of the contralateral homotopic ROIs in the connectivity analysis.

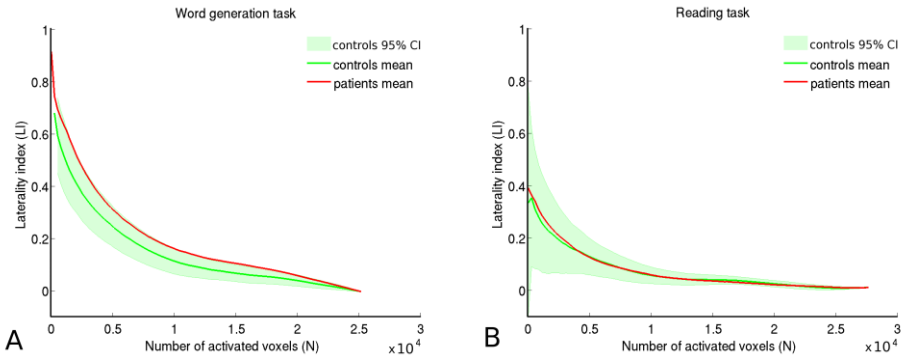

Figure 4.2: Laterality index distributions for (A) word generation and (B) reading. The mean patient and controls curves are given; for the latter, the 95% confidence interval is also shown, see (Abbott, Waites et al. 2010) for details. For both tasks, mostly left sided (positive) lateralization is seen.

4.3.5 Functional connectivity

The group averaged functional connectivity values are visualized as connectivity matrices in Figure 4.3. Note that, first, correlation values are mostly positive, suggestive of co-activation of brain regions. Second, connectivity is strongest for within-task ROIs. This is apparent from the relatively high values within the 3 sub matrices along the diagonal (dashed lines), which indicates that (also) at rest the ROIs representing a separate functional network are strongly interconnected. Third, relatively high connectivity is found for interhemispheric connections of homologue regions, which is reflected by the relatively high values of the corresponding first off-diagonal elements.

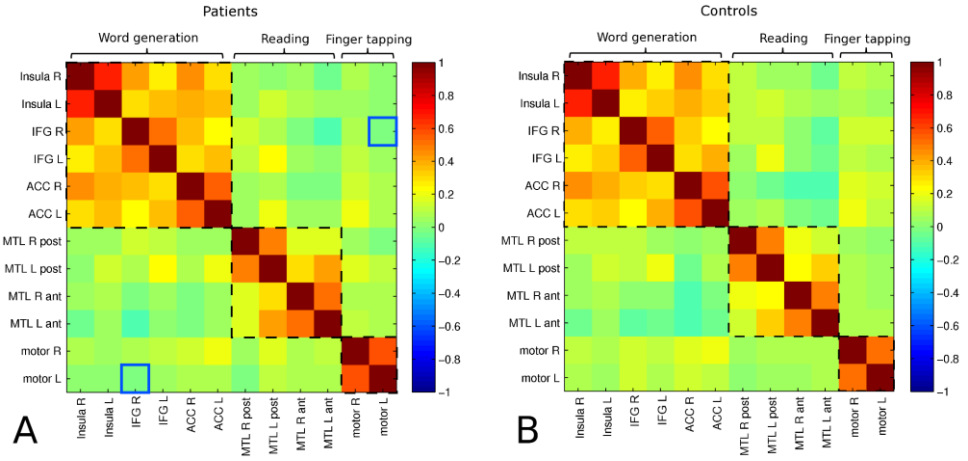

Figure 4.3: Resting-state functional connectivity matrices for (A): patients and (B): controls. Connectivity values are generally positive and highest for contralateral connections (off-diagonals) and for connections within a task network (sub matrices enclosed by dashed lines). The hypo connection in patients compared to controls is indicated by blue boxes in (A).
IFG: inferior frontal gyrus; ACC: anterior cingulated cortex; MTL: mid temporal lobe; L: left; R: right; ant: anterior; post: posterior.

Decreased connectivity in patients compared to controls was found between the left motor ROI and the right IFG (p=0.006; blue boxes in Figure 4.3). This aberrant connection is visualized with respect to anatomy in Figure 4.4. For this connection, the connectivity values were correlated with the CELF-4 language indices; significant positive correlations were found for the core language score (r=0.49, p=0.02), expressive language index (r=0.47, p=0.03), language structure index (r=0.43, p=0.04), and working memory index (r=0.49, p=0.02), see Figure 4.5. Also the data points of the controls are given, as well as the significance level of the individual connections (horizontal lines). Ten controls showed significant positive

connectivity versus 1 showing significant negative connectivity; for the patients this was 4 versus 6, respectively.

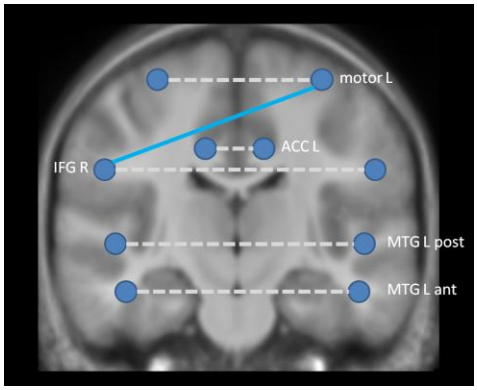

Figure 4.4: Aberrant functional connectivity overlaid on averaged normalized T1 scan of the control group. The blue line represents the significant hypo connection between the left motor ROI and the right inferior frontal gyrus. The dashed lines represent the significant interhemispheric homologue connections.

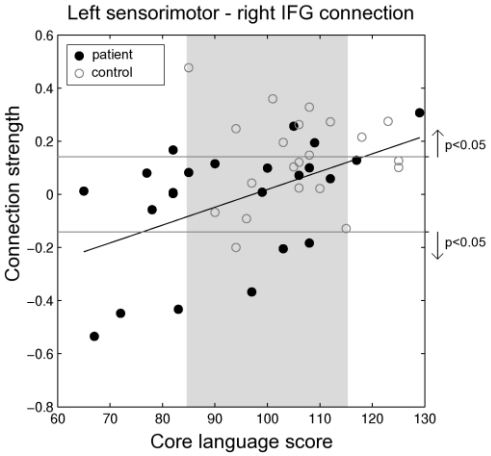

Figure 4.5: Significant positive correlation between core language score and functional connectivity strength in the patient group for the left sensorimotor - right inferior frontal gyrus connection (solid line, r=0.49, p=0.02). In the controls, no significant association was found (r=0.04, p=0.87). The vertical shaded area represent the norm core language score (100±15); multiple patients score below the norm. The vertical lines indicate the range of significantly non-zero connectivity (p<0.05). Note that for most controls displaying significant connectivity, connectivity is positive; for patients, this is negative.
Comparable results were obtained for expressive language, language content and working memory index.

4.4 Discussion

4.4.1 Major findings

In this study, we employed fMRI to find a functional correlate for language impairment in RE. Based on CELF-4 performance, we identified language impairment in a clinical population of children with RE. Activation map analysis of expressive and receptive language tasks revealed no significant differences but an essentially bilateral distribution of activation at the age range under study (8-14 years).

Reduced functional connectivity was found in patients compared to controls for a connection between the motor and the language network. In addition, the strength of this aberrant connection decreased significantly with poorer language performance in children with RE. Both findings indicate that this aberrant connection links rolandic (sensorimotor) pathology to language impairment in RE.

4.4.2 Language impairment profile

The language impairments identified in the children with RE involved both a reduction in core language score and specific impairments in receptive language and language content index. Especially since these impairments were not only found with respect to matched controls but also compared to (global) norm values, these findings imply that in a clinical population of children with RE (i.e. characteristic EEG and seizure semiology), language impairment is detectable at the group level. In earlier work, a strict distinction was made between benign and complicated cases, only the latter showing cognitive impairments (Massa R, de Saint-Martin A et al. 2001). However, in line with our findings, language impairment has recently been described as a general feature of RE (Lillywhite, Saling et al. 2009) and, even more broadly, of nocturnal epileptiform activity in children in general (Overvliet GM, Besseling RM et al. 2010; Overvliet GM, Besseling RMH et al. 2011). Children with RE have been described to underperform especially in sentence production and comprehension (Lillywhite, Saling et al. 2009; Overvliet GM, Aldenkamp AP et al. 2011), which is in analogy with the impaired language content index we report.

4.4.3 Bilateral global language activation

No activation map differences were found. This indicates that in RE, globally the same regions are involved in word generation, reading and finger tapping as in healthy controls. This is in line with the fMRI study of Lillywhite et al (Lillywhite, Saling et al. 2009), which reports typical patterns of language-related activation in both children with RE and controls using a verb-generation task. The absence of abnormalities with respect to activation maps motivated the use of more advanced analyses in finding functional abnormalities in RE. Abnormalities in functional connectivity in combination with normal language activation patterns have been found in epilepsy patients before (Vlooswijk, Jansen et al. 2010).

No differences in language laterality were found and lateralization showed only a slight left predominance in both patients and controls. This is not surprising for this age range (8-14 years) as adult-typical left hemisphere lateralization emerges gradually from an initially bilateral language network (Kadis, Pang et al.

2011). This motivated the inclusion of the contralateral homotopic ROIs of the language tasks in the connectivity analysis.

4.4.4 Abnormal functional connectivity

Functional connectivity analysis revealed a hypo connection in children with RE compared to healthy controls. Previous EEG research has demonstrated that in epileptogenic networks, local increases in synchronization during seizures are associated with decreased functional connectivity in the interictal state (Ponten, Bartolomei et al. 2007; Ponten, Douw et al. 2009; Vlooswijk, Jansen et al. 2010). Therefore, the left motor – right IFG hypo connection might facilitate the ictal spread of seizure activity. A stronger interictal connectivity reduction might be associated with more severe pathology and consequently more pronounced language impairment. In line with this, lower connectivity was associated with reductions of several language scores for this connection. Furthermore, the fact that significant connectivity values were usually positive in controls and negative in patients (Figure 4.5) suggests that the nature of left motor – right IFG connection changes from facilitatory to inhibitory in RE.

Note that given the current findings it is not possible to say whether rolandic epilepsy causes abnormalities in functional connectivity, or whether both are epiphenomena of an underlying epileptogenic process. The interactions between seizures, interictal epileptiform activity, and brain structure and function are highly complex, and their causal relations form an extensive field of research on their own (Jacobs MP, Leblanc GG et al. 2009).

Some light may be shed on this matter by work on EEG data. From EEG literature it has long been known that epileptiform spikes may reduce the amplitude and increase the latency of directly subsequent evoked potentials (Shewmon and Erwin 1988; Seri, Cerquiglini et al. 1998). Especially the inhibitory phase (corresponding to the EEG slow wave) following the spike extensively interferes with neuronal processing, not only locally, but also in distant regions such as contralateral homotopic cortex and the thalamus (Shewmon and Erwin 1988). It is these distal and relatively long lasting (slow wave mediated) effects that may actually be picked up by resting state fMRI analyses of connectivity between distributed regions, such as the work presented here. More specifically, for the role of (nocturnal) epileptiform EEG discharges in language impairment in children, we refer to the review by Overvliet et al (Overvliet GM, Besseling RM et al. 2010).

It has already been mentioned that in RE the language impairments may persist even after (spontaneous) seizure remission (Kanemura and Aihara 2009; Monjauze C, Broadbent H et al. 2011). A mechanism that has been suggested for this in the related Landau-Kleffner syndrome (LKS) is that the epileptiform activity initially may interfere directly with language functionality, and secondarily induces focal atrophy which causes irreversible language impairment which

persists after seizure remission (Bourgeois and Landau 2004; Takeoka, Riviello et al. 2004). More generally, RE (and LKS) may strike the brain at a critical age window of development, and may offset the normal trajectory of functional network formation (Andersen 2003). To gain more insight in this, for future research longitudinal study designs are recommended to investigate how EEG abnormalities, aberrant functional connectivity, and language impairment manifest themselves over time in RE.

For clarity, we repeat that the laterality analysis demonstrated the language network to be essentially bilateral in the age range under study (8-14 years), which is in line with literature on brain development (Kadis, Pang et al. 2011). As a consequence, aberrant connectivity between a motor area and the right hemisphere homologue of Broca's area should still be considered a connectivity abnormality between the motor and the language system. This insight is essential in understanding the aforementioned abnormalities in functional connectivity and their significance with respect to language function.

4.4.5 Methodological issues

Although in the current study expressive and receptive tasks were used to identify the major language networks, this approach does not guarantee inclusion of all possibly relevant language mediating areas. For future research it would be interesting to use specifically tailored tasks to find networks with functional connections related to specific aspects of language impairment in RE.

Alternatively, to avoid the bias caused by the investigation of sparse task networks, resting-state data could be used to define networks based on spatial patterns of similar time series using independent component analysis (Calhoun, Liu et al. 2009; Besseling, Jansen et al. 2013) or by using a large number of anatomical regions of interest (e.g. gyral pattern based, (Dale, Fischl et al. 1999; Fischl and Dale 2000)).

In addition, for the pathophysiological interpretation of the aberrant functional connections identified in this study, we suggest to investigate the integrity of the structural white matter connections involved (Basser, Mattiello et al. 1994; Jones 2010).

Finally, in our connectivity analysis, we employed a relatively strict p-value threshold of $p=0.01$. Future studies employing a more formal correction for the number of connections involved are warranted to validate the robustness of our findings.

4.5 Conclusion

We demonstrated language impairment in children with a clinical diagnosis of RE (seizure semiology and EEG based), which is indicative of language impairment in the general RE population. Connectivity analysis demonstrated abnormalities whereas activation mapping did not, possibly indicating that probing the integrity of and interplay between functional networks is more sensitive than studying their (individual) spatial patterns.

These findings provide a functional correlate for the neuropshychological profile of notably language impairment as previously described in the RE literature. More specificcally, reduced functional connectivity was identified between a language and a sensorimotor region, indicative of a disturbed interplay between language and motor networks in RE. In line with this, lower connectivity values were associated with lower language scores in the patient group.

The exact causal relationship between seizures and/or interictal epileptiform activity and abnormalities in functional connectivity in RE is beyond the scope of this study, and remains an important subject for future research with respect to unveiling the exact pathological mechanism, preferably employing a longitudinal design.

Acknowledgement

We would like to acknowledge Esther Peeters for data acquisition, Marc Geerlings for continuous hardware and software support, and all children and their parents for participating. This project was funded by the Dutch Epilepsy Foundation (NEF). The author JJ was funded by VENI research grant 916.11.059 from the Netherlands Organization for Scientific Research (NWO) and the Netherlands Organization for Health Research and Development (ZonMw).

References

Abbott, D. F., A. B. Waites, et al. (2010). "fMRI assessment of language lateralization: an objective approach." Neuroimage **50**(4): 1446-55.

Andersen, S. L. (2003). "Trajectories of brain development: point of vulnerability or window of opportunity?" Neurosci Biobehav Rev **27**(1-2): 3-18.

Basser, P. J., J. Mattiello, et al. (1994). "MR diffusion tensor spectroscopy and imaging." Biophys J **66**(1): 259-67.

Bassett, D. S., E. Bullmore, et al. (2008). "Hierarchical organization of human cortical networks in health and schizophrenia." J Neurosci **28**(37): 9239-48.

Berroya AM, Bleasel AF, et al. (2005). "Spike morphology, location, and frequency in benign epilepsy with centrotemporal spikes." J Child Neurol. **20**(3): 188-194.

Besseling, R. M. H., J. F. Jansen, et al. (2013). "Reduced functional integration of the sensorimotor and language network in rolandic epilepsy." Neuroimage: Clinical.

Bourgeois, B. F. and W. M. Landau (2004). "Landau-Kleffner syndrome and temporal cortical volume reduction: cause or effect?" Neurology **63**(7): 1152-3.

Calhoun, V. D., J. Liu, et al. (2009). "A review of group ICA for fMRI data and ICA for joint inference of imaging, genetic, and ERP data." Neuroimage **45**(1 Suppl): S163-72.

Dale, A. M., B. Fischl, et al. (1999). "Cortical surface-based analysis. I. Segmentation and surface reconstruction." Neuroimage **9**(2): 179-94.

Fischl, B. and A. M. Dale (2000). "Measuring the thickness of the human cerebral cortex from magnetic resonance images." Proc Natl Acad Sci U S A **97**(20): 11050-5.

Gündüz E, Demirbilek V, et al. (1999). "Benign rolandic epilepsy: neuropsychological findings." Seizure **8**(4): 246-269.

Hughes, J. R. (2010). "Benign epilepsy of childhood with centrotemporal spikes (BECTS): to treat or not to treat, that is the question." Epilepsy Behav **19**(3): 197-203.

Jacobs MP, Leblanc GG, et al. (2009). "Curing epilepsy: progress and future directions." Epilepsy Behav. **14**(3): 438-445.

Jones, D. (2010). "Challenges and limitations of quantifying brain connectivity in vivo with diffusion MRI." Imaging Med **2**(3): 341-55.

Kadis, D. S., E. W. Pang, et al. (2011). "Characterizing the normal developmental trajectory of expressive language lateralization using magnetoencephalography." J Int Neuropsychol Soc **17**(5): 896-904.

Kanemura, H. and M. Aihara (2009). "Growth disturbance of frontal lobe in BCECTS presenting with frontal dysfunction." Brain Dev **31**(10): 771-4.

Liegeois, F., A. Connelly, et al. (2004). "Language reorganization in children with early-onset lesions of the left hemisphere: an fMRI study." Brain **127**(Pt 6): 1229-36.

Lillywhite, L. M., M. M. Saling, et al. (2009). "Neuropsychological and functional MRI studies provide converging evidence of anterior language dysfunction in BECTS." Epilepsia **50**(10): 2276-84.

Loiseau P and Duché B (1989). "Benign childhood epilepsy with centrotemporal spikes." Cleve Clin J Med **56**(Suppl Pt 1): S17-22; discussion S40-2.

Massa R, de Saint-Martin A, et al. (2001). "EEG criteria predictive of complicated evolution in idiopathic rolandic epilepsy." Neurology **57**(6): 1071-1079.

Monjauze C, Broadbent H, et al. (2011). "Language deficits and altered hemispheric lateralization in young people in remission from BECTS." Epilepsia **52**(8): e79-e83.

Monjauze C, Tuller L, et al. (2005). "Language in benign childhood epilepsy with centro-temporal spikes abbreviated form: rolandic epilepsy and language." Brain and Language **92**(3): 300-308.

Nayrac P and Beaussart M (1958). "Pre-rolandic spike-waves: a very peculiar EEG reading; electroclinical study of 21 cases." Rev Neurol (Paris) **99**(1): 201-206.

Nicolai J, Aldenkamp AP, et al. (2006). "Cognitive and behavioral effects of nocturnal epileptiform discharges in children with benign childhood epilepsy with centrotemporal spikes." Epilepsy Behavior **8**(1): 56-70.

Northcott E, Connolly AM, et al. (2007). "Memory and phonological awareness in children with Benign Rolandic Epilepsy compared to a matched control group." Epilepsy Research **75**(1): 57-62.

Northcott E, Connolly AM, et al. (2005). "The neuropsychological and language profile of children with benign rolandic epilepsy." Epilepsia **46**(6): 924-930.

Northcott E, Connolly AM, et al. (2006). "Longitudinal assessment of neuropsychologic and language function in children with benign rolandic epilepsy." J Child Neurology **21**(6): 518-522.

Overvliet GM, Aldenkamp AP, et al. (2011). "Correlation between language impairment and problems in motor development in children with Rolandic epilepsy." Epilepsy & Behavior.

Overvliet GM, Besseling RM, et al. (2010). "Nocturnal epileptiform EEG discharges, nocturnal epileptic seizures, and language impairments in children: Review of the literature." Epilepsy Behav **19**(4): 550-558.

Overvliet GM, Besseling RMH, et al. (2011). "Association between frequency of nocturnal epilepy and language disturbance in children." Pediatr Neurol **44**(5): 333-339.

Panayiotopoulos, C. P., M. Michael, et al. (2008). "Benign childhood focal epilepsies: assessment of established and newly recognized syndromes." Brain **131**(Pt 9): 2264-86.

Papavasiliou A, Mattheou D, et al. (2005). "Written language skills in children with benign childhood epilepsy with centrotemporal spikes." Epilepsy & Behavior **6**(1): 50-58.

Paslawski C (2005). "The Clinical Evaluation of Language Fundamentals, Fourth Edition (CELF-4): A Review." Canadian Journal of School Psychology **20**: 129-134.

Ponten, S. C., F. Bartolomei, et al. (2007). "Small-world networks and epilepsy: Graph theoretical analysis of intracerebrally recorded mesial temporal lobe seizures." Clinical Neurophysiology **118**(4): 918-927.

Ponten, S. C., L. Douw, et al. (2009). "Indications for network regularization during absence seizures: Weighted and unweighted graph theoretical analyses." Experimental Neurology **217**(1): 197-204.

Riva, D., C. Vago, et al. (2007). "Intellectual and language findings and their relationship to EEG characteristics in benign childhood epilepsy with centrotemporal spikes." Epilepsy Behav **10**(2): 278-85.

Semel E, Wiig EH, et al. (2010). Clinical Evaluation of Language Fundamentals 4, Nederlandse versie. Amsterdam, Pearson

Seri, S., A. Cerquiglini, et al. (1998). "Spike-induced interference in auditory sensory processing in Landau-Kleffner syndrome." Electroencephalogr Clin Neurophysiol **108**(5): 506-10.

Shewmon, D. A. and R. J. Erwin (1988). "The effect of focal interictal spikes on perception and reaction time. II. Neuroanatomic specificity." Electroencephalogr Clin Neurophysiol **69**(4): 338-52.

Takeoka, M., J. J. Riviello, Jr., et al. (2004). "Bilateral volume reduction of the superior temporal areas in Landau-Kleffner syndrome." Neurology **63**(7): 1289-92.

van den Heuvel, M. P., R. C. Mandl, et al. (2010). "Aberrant frontal and temporal complex network structure in schizophrenia: a graph theoretical analysis." J Neurosci **30**(47): 15915-26.

Vinayan KP, Biji V, et al. (2005). "Educational problems with underlying neuropsychological impairment are common in children with Benign Epilepsy of Childhood with Centrotemporal Spikes (BECTS)." Seizure **14**(3): 207-213.

Vlooswijk, M. C., J. F. Jansen, et al. (2010). "Functional MRI in chronic epilepsy: associations with cognitive impairment." Lancet Neurol **9**(10): 1018-27.

Vlooswijk, M. C., J. F. Jansen, et al. (2010). "Functional connectivity and language impairment in cryptogenic localization-related epilepsy." Neurology **75**(5): 395-402.

Völkl-Kernstock S, Bauch-Prater S, et al. (2009). "Speech and school performance in children with benign partial epilepsy with centro-temporal spikes (BCECTS)." Seizure **18**(5): 320-326.

Weglage J, Demsky A, et al. (1997). "Neuropsychological, intellectual, and behavioral findings in patients with centrotemporal spikes with and without seizures." Dev Med Child Neurol **39**(10): 646-651.

Widjaja E, Mahmoodabadi SZ, et al. (2011). "Widespread cortical thinning in children with frontal lobe epilepsy." Epilepsia **52**(9): 1685-1691.

Yuan, W., J. P. Szaflarski, et al. (2006). "fMRI shows atypical language lateralization in pediatric epilepsy patients." Epilepsia **47**(3): 593-600.

Zhang, Z., W. Liao, et al. (2011). "Altered functional-structural coupling of large-scale brain networks in idiopathic generalized epilepsy." Brain **134**(Pt 10): 2912-28.

CHAPTER 5

Reduced functional integration of the sensorimotor and language network in rolandic epilepsy

R.M.H. Besseling, J.F.A. Jansen, G.M. Overvliet, S.J.M. van der Kruijs, J.S.H. Vles, S.C.M. Ebus, P.A.M. Hofman, A.J.A. de Louw, A.P. Aldenkamp, W.H. Backes

NeuroImage Clinical 2013; 2: 239–246

Abstract

Introduction Over the last years, evidence has accumulated that rolandic epilepsy (RE) is associated with serious cognitive comorbidities, including language impairment. However, the cerebral mechanism through which epileptiform activity in the rolandic (sensorimotor) areas may affect the language system is unknown. To investigate this, the connectivity between rolandic areas and regions involved in language processing is studied using functional MRI (fMRI).

Materials and methods fMRI data was acquired from 22 children with rolandic epilepsy and 22 age-matched controls (age range: 8-14 years), both at rest and using word-generation and reading tasks. Activation map analysis revealed no group differences (FWE-corrected, $p<0.05$) and was therefore used to define regions of interest for pooled (patients and controls combined) language activation. Independent component analysis with dual regression was used to identify the sensorimotor resting-state network in all subjects. The associated functional connectivity maps were compared between groups at the regions of interest for language activation identified from the task data. In addition, neuropsychological language testing (Clinical Evaluation of Language Fundamentals, 4th edition) was performed.

Results Functional connectivity with the sensorimotor network was reduced in patients compared to controls ($p=0.011$) in the left inferior frontal gyrus, i.e. Broca's area as identified by the word-generation task. No aberrant functional connectivity values were found in the other regions of interest, nor were any associations found between functional connectivity and language performance. Neuropsychological testing confirmed language impairment in patients relative to controls (reductions in core language score, $p=0.03$; language content index, $p=0.01$; receptive language index, $p=0.005$).

Conclusion Reduced functional connectivity was demonstrated between the sensorimotor network and the left inferior frontal gyrus (Broca's area) in children with RE, which might link epileptiform activity/seizures originating from the sensorimotor cortex to language impairment, and is in line with the identified neuropsychological profile of anterior language dysfunction.

5.1 Introduction

Rolandic epilepsy (RE) is an idiopathic focal epilepsy of childhood with typical onset at age 7-10 years (Loiseau P & Duché B, 1989; Panayiotopoulos, Michael, Sanders, Valeta, & Koutroumanidis, 2008). The epileptic focus is mostly located in the inferior part of the rolandic area (i.e. the pre- and postcentral gyri), seizures are relatively mild and typically nocturnal, and involve hemifacial spasms and speech arrest (Loiseau P & Duché B, 1989; Panayiotopoulos, et al., 2008). Furthermore, spontaneous remission of seizures is typically seen during adolescence. Given these characteristics, RE is classically considered a benign condition and is also known as benign (rolandic) epilepsy (of childhood) with centro-temporal spikes (BECTS), which is, however, insensitive to the distress inflicted on the children and their families by these events.

Recently RE has been associated with a variety of visuomotor, neuropsychological and cognitive comorbidities (Deltour L, et al., 2007; Deltour L, Querné L, Vernier-Hauvette MP, & Berquin P, 2008; Kavros PM, et al., 2008), of which language impairment is one of the most prominent (Clarke, et al., 2007; Jocic-Jakubi B & Jovic NJ, 2006; Liasis A, Bamiou DE, Boyd S, & Towell A, 2006; Lillywhite, et al., 2009; Lundberg S, Frylmark A, & Eeg-Olofsson O, 2005; Monjauze C, Tuller L, Hommet C, Barthez MA, & Khomsi A, 2005). It was recently suggested that the language impairments may be present before the onset of seizures (Overvliet GM, Aldenkamp AP, Klinkenberg S, Vles JSH, & Hendriksen J, 2011) and may persist after seizure remission (Kanemura & Aihara, 2009; Monjauze C, Broadbent H, Boyd SG, Neville BG, & Baldeweg T, 2011). In this light, in RE, the prevention of language impairment might be considered of higher priority than seizure control.

Cognitive impairment risk has been associated with interictal epileptiform discharges in pediatric epilepsy including RE (Massa R, et al., 2001; Nicolai, et al., 2007; Overvliet GM, et al., 2010), but the underlying mechanism remains to be elucidated. Neuropsychological testing and functional MRI (fMRI) suggest anterior language dysfunction in RE (Lillywhite, et al., 2009; Yuan, et al., 2006), however a better understanding of the functional circuits linking (epileptiform activity in) the rolandic areas with language areas/dysfunction seems of major importance in this context.

In the current study, we aim to link epileptiform activity/seizures originating from the rolandic cortex with language impairment in children with RE using fMRI. We employed independent component analysis (ICA) to segment resting-state fMRI data from a group of children with RE and age-matched controls into distinct functional networks (Beckmann, DeLuca, Devlin, & Smith, 2005; Calhoun, Liu, & Adali, 2009). ICA is a robust data-driven method, allows the study

of functional organization on the whole brain level, and precludes the a priori definition of (a sparse set of) regions on interest (Cole, Smith, & Beckmann, 2010). From the ICA output, we selected the network with maximum involvement of the bilateral pre- and postcentral gyri and, given the location of the epileptic focus, hypothesize that this rolandic network is impaired in RE. To infer on abnormalities associated with language impairment, we investigated rolandic network functional connectivity in language-mediating regions of interest derived from task fMRI (word-generation and reading tasks). To relate our findings to language performance, neuropsychological language testing was performed (Clinical Evaluation of Language Fundamentals, 4th edition).

5.2 Methods

5.2.1 Study population

Twenty-two children with a clinical diagnosis of RE (6 girls) were selected at our specialized epilepsy referral center (see selection criteria below). The age at seizure onset was (mean±SD) 7.5±2.3 years and the age at testing 11.4±1.8 years, half of the subjects (11/22) had ongoing seizures (at least 1 seizure over the 6 months prior to scanning). Two children were left handed and 1 was ambidextrous. For comparison, 22 age-matched controls were included (11 girls, age 10.3±1.7 years, 2 left handed). For further characteristics, see Table 5.1.

The study was approved by the medical ethics committees of both participating institutions and written informed consent was obtained from the participating children's parents and/or care-givers.

Subject characteristics	**RE**	**controls**
N	22	22
age [y]	11.4±1.8	10.3±1.7
age at epilepsy onset [y]	7.5±2.3	n.a.
epilepsy duration [y]	2.4±2.0	n.a.
seizure frequency [per y]	2.3±1.6	n.a.
gender (male/female)	16/6	11/11
handedness (r/l/ambidexter)	19/2/1	20/2/0
Number of AEDs (0/1/>1)	12/5/5	n.a.

Table 5.1: Subject characteristics. Note that age at epilepsy onset, epilepsy duration, and seizure frequency are difficult to accurately establish given the mild and typically nocturnal nature of the seizures, which may lead to delayed diagnosis and underestimation of the number of seizures.
N, number; AED, anti epileptic drug; n.a., not applicable. Notation: mean±SD.

5.2.2 Selection criteria

Patient selection was based on criteria concerning seizure semiology and EEG as described in the literature (Berroya AM, Bleasel AF, Stevermuer TL, Lawson J, & Bye AM, 2005; Panayiotopoulos, et al., 2008). EEG criteria include the presence of spike and slow wave complexes occurring as individual paroxysms or in repetitive clusters with a maximum in the mid temporal and/or central electrodes and with a temporal-frontal dipole field. Additional independent central, mid temporal, parietal or occipital spike wave foci in the same or other hemisphere were allowed. To exclude severe cases (Landau-Kleffner syndrome (LKS) or LKS-like), interictal epileptiform activity was required to be present <85% of the time during non-REM sleep. With respect to seizure semiology, seizures with anarthria, hemiclonia involving the face and/or unilateral extremities, or secondarily generalized seizures were considered. In case of poorly observed nocturnal seizures (3 cases), post ictal signs of a generalized seizure or confirmation of post-ictal hemiparesis were sufficient for inclusion in case of otherwise typical EEG.

The children with RE underwent neuropsychological testing using the Wechsler Intelligence Score for Children, third edition, Dutch version (WISC-III, http://www.pearsonclinical.nl/tests), and all had a full-scale IQ >70. None of the healthy controls had (a history of) dyslexia, learning disorders or neurological/psychiatric disorders, or attended special education. Children were excluded if they had dental braces (MRI quality), were somewhat afraid in the scanner, or had structural brain abnormalities on conventional MRI.

5.2.3 Magnetic resonance imaging

Imaging was performed on a 3T MRI systems (Philips Achieva, Best, the Netherlands) using an 8-element receive-only head coil. Both resting-state and task fMRI data was acquired; resting-state data was acquired before task data. In addition, structural MRI was performed for anatomical reference and involved a T1-weighted scan with the following settings: 3D fast spoiled gradient echo sequence, echo time/repetition time/inversion time (TE/TR/TI) 3.8/8.3/1022 ms, 1x1x1 mm^3 resolution, and acquisition time 8 min.

Functional MRI involved a T2*-weighted blood oxygen level dependent (BOLD) sequence comprising 195 dynamic acquisitions at TR 2s, resulting in a total dynamic acquisition time of 6.5 min. Other settings included: single-shot echo planar imaging (EPI) sequence, TE 35 ms, 2x2 mm^2 in plane resolution, and 4 mm axial slices.

Task fMRI involved a word-generation and a reading task. A standard block design was used and comprised six 30 s task blocks interleaved with 30 s baseline blocks. Each paradigm started and ended with a baseline block.

The word-generation task involved visual presentation of a letter (U-N-K-A-E-P) interleaved with presentation of an asterisk for visual fixation. Subjects were instructed to covertly generate as many words as possible starting with the presented letter.

In the reading task, text with semantic meaning (task block) was interleaved with nonsense text (baseline). To ensure continuous reading, the text was refreshed 3 times per block (i.e. every 10 s). Each text frame consisted of 4 lines and for the meaningful text, only the first 2 lines of each frame were essential for text continuity (short story).

5.2.4 fMRI preprocessing

fMRI preprocessing was performed using SPM8 (Welcome Department of Cognitive Neurology, London, UK, http://www.fil.ion.ucl.ac.uk/spm/). First, the dynamic series were realigned to correct for head movement using rigid body transformations (rotation and translation) and aligned to the structural scan. Next, the structural scan was segmented into gray matter, white matter, and cerebrospinal fluid, and registered into Montreal Neurological Institute (MNI) standard space. This normalization was subsequently also applied to the realigned dynamic series to generate movement corrected normalized fMRI data suitable for group analysis.

5.2.5 Activation mapping

Task-related dynamic series were smoothed using a Gaussian kernel of full width at half maximum (FWHM) 6 mm and analyzed using general linear models (GLMs) in SPM8. The task block design was convolved with a canonical hemodynamic response function (HRF) to model the task-related BOLD response. In addition, the movement parameters from the realignment step were used as regressors of no interest to model residual movement.

Significant activations were assessed using t-contrasts of task regressors; word-generation was contrasted versus baseline and meaningful text versus nonsense text. Voxel-wise effects were corrected for multiple comparisons using family wise error (FWE) p-value adjustment at $p<0.05$.

A standard random-effects analysis was used for group analysis. As no significant group differences were found ($p>0.05$, FWE corrected), pooled activation maps (patients and controls combined) were generated. Spherical regions of interest (ROIs) of language activation with a radius of 10 mm were defined at local maxima of pooled activation. In case of unilateral activation, a contralateral homotopic ROI was defined by mirroring with respect to the median plane.

5.2.6 Resting-state independent component analysis

Preprocessed resting-state dynamic series were spatio-temporally filtered and subjected to group ICA using FSL's MELODIC (Multivariate Exploratory Linear Optimized Decomposition into Independent Components, v3.10, FMRIB's Software Library, Oxford, UK; http://fsl.fmrib.ox.ac.uk/fsl/fslwiki/MELODIC). Filtering involved Gaussian smoothing (FWHM 5 mm) and temporal filtering at a 100 s (0.01 Hz) high pass filter cut off. Group ICA involved temporal concatenation of all resting-state datasets (patients as well as controls) and assessment of independent time series and associated spatial maps (BOLD related resting-state networks and noise induced artifactual maps). The number of components was estimated from the data using the build-in Bayesian approach.

Since resting-state networks represent distributed synchronization of spontaneous fluctuations in neuronal activity, they represent across subjects as similar spatial patterns (comparable neuronal circuits), but different time series. FSLs' dual regression was used, which employs this observation to map pooled independent component (IC) maps to the individual subject level in a two step approach (Beckmann, Mackay, Filippini, & Smith, 2009; Filippini, et al., 2009); see http://fsl.fmrib.ox.ac.uk/fsl/fslwiki/DualRegression. First, for each subject, the resting-state data was regressed against the pooled IC maps for each dynamic scan (spatial regression) to obtain subject specific time series. Second, these IC time series were used to calculate subject specific spatial maps (temporal regression), which were normalized by the residual noise to represents the functional connectivity with the corresponding network (Z-statistic).

The IC maps were visually inspected to select the network of maximum overlap with the bilateral pre- and postcentral gyri (i.e. the rolandic areas). A GLM framework using FSLs randomize (v2.8) and 5000 permutations was used to calculate the corresponding group networks ($p<0.05$, cluster corrected). Furthermore, for each subject the functional connectivity with this network (Z-statistic) was assessed for each language ROI (see Figure 5.1) and compared between patients and controls using two-tailed Student's t-tests; results were corrected for multiple comparisons using a false discovery rate (FDR) of 10%. Following Voets et all (Voets, et al., 2012), this analysis was not confined to ROIs within the rolandic network to allow the detection of connectivity abnormalities beyond the network boundaries.

For completeness and consistency, the same approach was applied to the task data to check for activation differences on the ROI level.

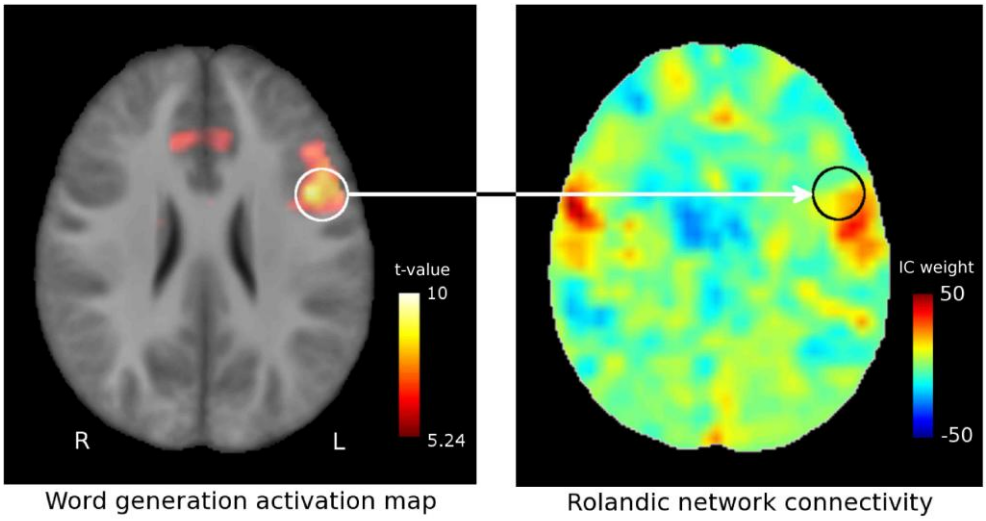

Figure 5.1: Region of interest rolandic network connectivity: the left inferior frontal gyrus is selected as a region of interest from the pooled word-generation activation map (left) and used to extract subject-specific values from the rolandic connectivity map (right), which represents the degree of similarity between the voxel time series and the rolandic independent component (weight of the rolandic independent component in a full independent component fit to the data).
Color bars represent pooled activation level (t-contrast, corrected for family-wise error (FWE) at p<0.05) and rolandic connectivity for a representative subject, respectively. Images are normalized to MNI-space.

5.2.7 Language assessment

All children underwent the Clinical Evaluation of Language Fundamentals, fourth version (CELF-4), Dutch edition (Semel E, Wiig EH, & Secord WA, 2010). The CELF-4 is the gold standard for language assessment in children and provides several age-corrected measures for language performance (Paslawski C, 2005). The core language score was assessed in all subjects to check for language impairment. To infer the specific impairment profile, in the patient group specific metrics such as expressive and receptive language index were also assessed.

Outcomes were compared between groups and to norm scores (mean±SD: 100±15) using 2-tailed Student's t-tests ($p<0.05$). Furthermore, within all language ROIs it was tested for associations between rolandic network connectivity and language metrics using Spearman's correlation ($p<0.05$).

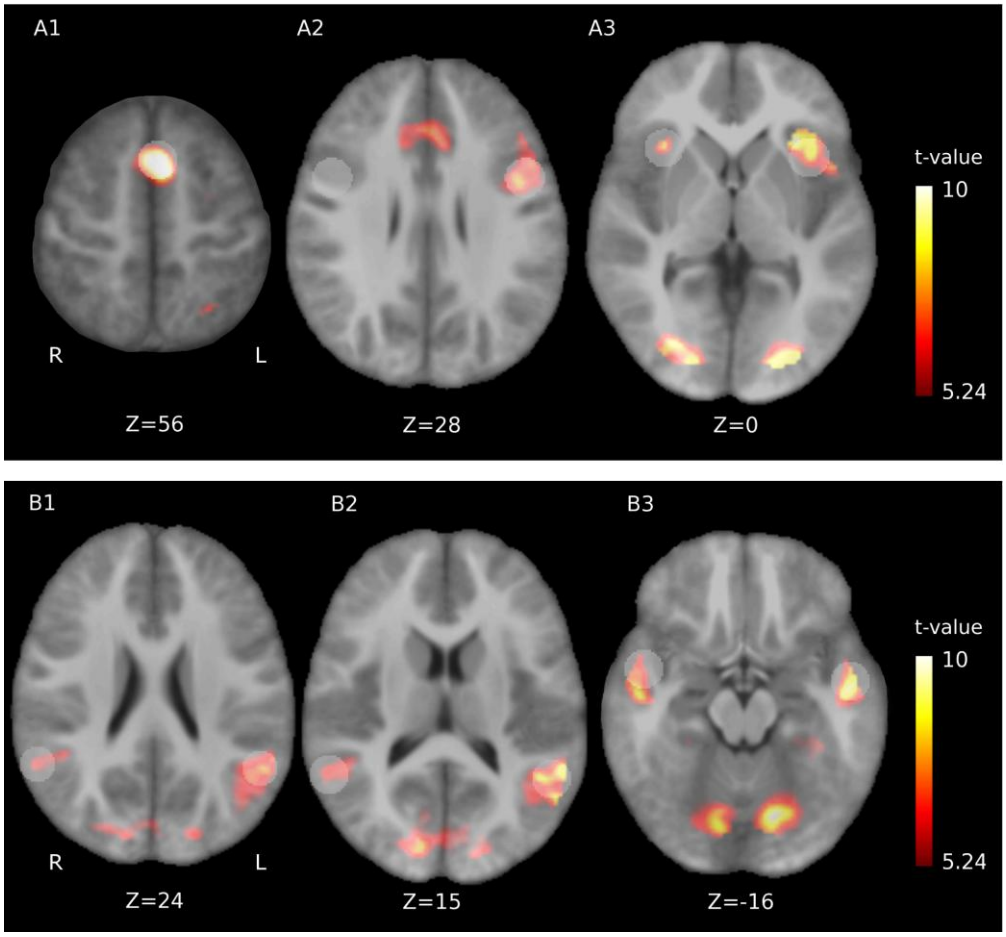

Figure 5.2: Pooled activation maps (i.e. patients and controls combined) for A: word-generation and B: reading. In word-generation, the anterior cingulate cortex (A1), left inferior prefrontal cortex (A2) and bilateral insular regions (A3) were activated. Reading induced activity in posterior (B1-2) and anterior (B3) bilateral mid temporal regions. Z-values indicate MNI slice coordinates, the colorbar gives the activation t-statistic and activation maps are given for p<0.05 (family-wise error (FWE) corrected). Regions of interest are overlaid in transparent white, the one in the right inferior prefrontal cortex (A2) was constructed by mirroring with respect to the median plane. Z-values indicate axial MNI coordinates.

5.3 Results

5.3.1 Activation mapping

Pooled (patients and controls combined) activation maps for the word-generation and reading tasks and associated ROIs are given in Figure 5.2. Task-related BOLD signal fluctuations (i.e. activation) were found in the anterior cingulate cortex,

bilateral insular regions, and the left inferior prefrontal cortex. Reading task activation was seen in the bilateral mid temporal gyri and posteriorly displayed a left predominance. See Table 5.2 for more information on these 9 language-mediating regions of interest.

In both tasks, activation was also found in the occipital lobes, due to the visual task presentation.

Task ROIs	Description	MNI-coordinate [mm]	t-value (ROI mean)
Word gen	ACC	(-2,14,54)	8.7
	IFG L	(-48,7,26)	6.8
	IFG R	(48,7,26)*	1.0
	Insula L	(-38,15,0)	4.8
	Insula R	(34,20,3)	2.5
Reading	MTG R ant	(50,0,-18)	2.6
	MTG R post	(58,-50,18)	3.9
	MTG L ant	(-52,-6,-18)	3.8
	MTG L post	(-52,-52,18)	6.2

*Table 5.2: Regions of interest (ROIs) for activation in reading and word-generation. MTG: mid temporal gyrus; ant: anterior; post: posterior; R: right; L: left; ACC: anterior cingulate cortex; IFG: inferior frontal gyrus. *Constructed from the contralateral (activation-based) ROI by mirroring with respect to the median plane.*

5.3.2 Rolandic network differences

Pooled probabilistic group ICA identified 34 independent components; the component identified as the rolandic network is depicted in Figure 5.3 ($p<0.05$, uncorrected). This network covered bilateral pre- and postcentral gyri (sensorimotor areas), but in addition included perisylvian (among which superior temporal) regions, as well as bilateral cerebellar and medial regions. Furthermore, the involvement of a left prefrontal region is suggested (see arrowheads), which was absent at the right.

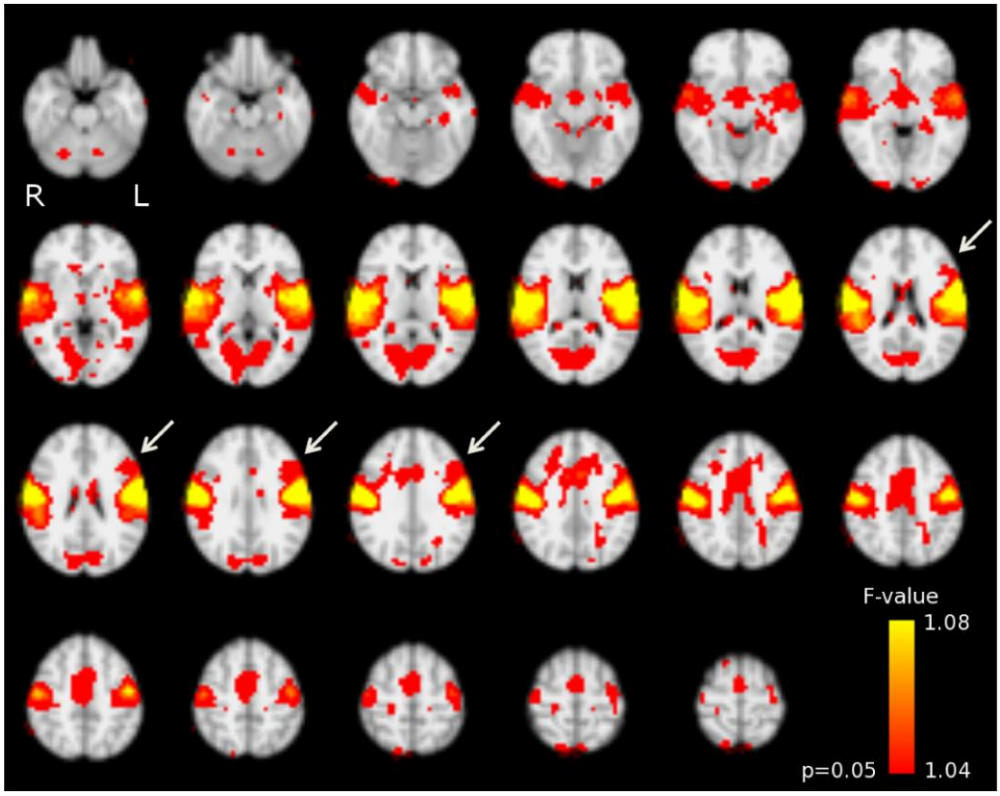

Figure 5.3: Rolandic resting-state network as identified using pooled group independent component analysis. This involves the bilateral sensorimotor areas (pre- and postcentral gyrus), superior temporal, cerebellar, and medial regions. Note the involvement of a left inferior prefrontal region (arrowheads), which is absent at the right
Colorbar: voxel-wise F-value for the test on the relevance of the rolandic independent component (IC) to the full-IC fit of the pooled data concatenated over time. Results are normalized to MNI-space.

Upon further investigation, this region corresponded to the left inferior frontal gyrus showing activation for the word-generation task, and had significantly reduced rolandic network connectivity in patients compared to controls (ROI centered at MNI coordinate -48,7,26 mm; p=0.011, FDR corrected), see Figure 5.4.

No other ROI-wise reductions in rolandic network connectivity were found, nor were any ROIs identified in which rolandic network connectivity was increased.

Also with respect to the activation maps, no ROI-wise differences were found in the respective ROIs for neither the word-generation nor the reading task.

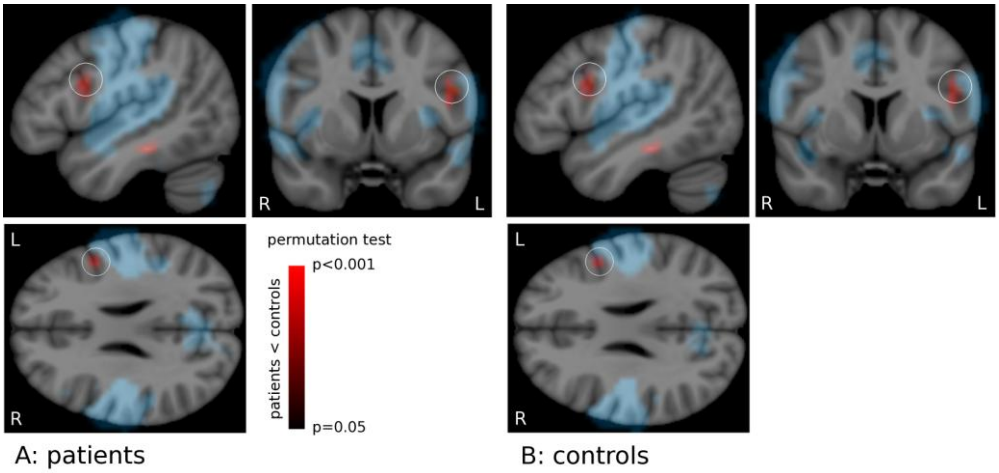

Figure 5.4: Local reduction of rolandic network connectivity. The rolandic network of A) controls and B) patients (blue). Rolandic network functional connectivity is reduced in patients compared to controls (red colorbar; identical overlay in A and B) outside (but directly adjacent to) the network itself. This local reduction of connectivity coincides with a region of activation for word-generation (white circle; p=0.011). See text for details.
Maps generated by permutation testing (N=5000, p<0.05); rolandic network cluster corrected. Colorbar: p-value for the group difference. Results are normalized to MNI-space.

5.3.3 Language assessment

As expected, patients had lower core language scores than controls (95±18 vs 105±11, respectively; p=0.03). Furthermore, patients scored below the norm (100±15) on language content index (88±18; p=0.01) and receptive language index (86±19; p=0.005). Also a trend of reduced language working memory was found (92±18; p=0.09).

5.3.4 Association between connectivity and language metrics

No associations were found between language metrics and functional connectivity for any of the language ROIs.

5.4 Discussion

In this study, we attempted to link the rolandic nature of RE (given the location of the epileptic focus) with the growing insight that language impairment may be an inherent trait of this type of epilepsy. We used functional MRI to study the rolandic network in association with language areas in children with RE employing resting-state and language task fMRI in a task-informed resting-state analysis. We hypothesized that the rolandic network is disturbed in RE and investigated whether the aberrant regions co-localize with well-known language areas as

identified by task fMRI. Furthermore, we correlated rolandic network connectivity within these language areas with language metrics as assessed by neuropsychological testing.

5.4.1 Major findings

The rolandic network was successfully identified from resting state data using group ICA. This network extended beyond the sensorimotor cortex to include superior temporal regions and also seemed to involve a left inferior prefrontal region. This region was identified as Broca's area using activation maps of a word generation task, and displayed significantly reduced rolandic network connectivity in patients compared to controls. No associations were found between rolandic network connectivity and neuropsychological metrics of language performance in any of the language task ROIs (reading and word generation).

5.4.2 Functional (sub)networks

The network we refer to as "rolandic" resembles one of a limited set of canonical resting-state networks typically referred to as the sensorimotor network (Beckmann, et al., 2005; Cole, et al., 2010). However, this naming conveys a functional interpretation, which we deemed inappropriate in the current context since it was selected based purely on involvement of the rolandic areas, but actually was more extensive. Generally, even though close similarities exist between resting-state networks and task-derived activation patterns, their correspondence is not one-to-one, which complicates comprehensive and complete functional descriptions of resting-state networks (Smith, et al., 2009). For this reason, we found it more adequate to adopt an anatomical-descriptive naming interpretable in the context of the pathology under study (rolandic network and RE, respectively).

Indeed, the rolandic network as identified in this study was demonstrated to be not purely of primary sensorimotor nature, but included perisylvian regions and also seemed to extend into the left inferior frontal gyrus (Broca's area). Similarly, in recent work on hierarchical clustering of resting state networks based on similarity of characteristic time series, the rolandic and superior temporal regions were clustered into a so-called centro-temporal module (Doucet, et al., 2011; Doucet, et al., 2012).

In general, separation or merging of functional networks not only depends on intrinsic functional architecture, but is also determined by the dimensionality of the IC decomposition. More fine-grained functional parcellations can be constructed by increasing the number of components, but this will put additional demands on data quality (Cole, et al., 2010). The Bayesian dimensionality estimation we employed indicated 34 components to be supported by our data

(resting-state acquisitions of 6.5 min at TR=2s), which is a typical order for the relatively short resting-state acquisitions (5-10 min) presently reported in literature (Doucet, et al., 2011; Greicius, Krasnow, Reiss, & Menon, 2003; Voets, et al., 2012).

Our results indicate that at this level of detail, superior temporal, rolandic and possibly left inferior frontal regions cluster within the same functional network, although this finding does not preclude their separation into more specific sub-networks at higher-dimensional analysis. Furthermore, it is known that functional specialization of neuronal networks is progressively established during maturation and is not yet completed at the age range under study (8-14 years; (Joseph, et al., 2012; Rubia, 2012)).

5.4.3 Connectivity differences beyond functional networks

Note that although the involvement of the left inferior frontal gyrus in the rolandic network was suggested by the uncorrected pooled results (Figure 5.3), this was not confirmed by the (cluster-corrected) group maps (Figure 5.4, in blue). Indeed, Tomasi et al performed a resting-state study of the language network in adults (970 subjects), in which involvement of the rolandic areas could not be demonstrated (Tomasi & Volkow, 2012).

However, we were able to demonstrate significantly reduced connectivity with the rolandic network in patients compared to controls in the left inferior frontal gyrus on the ROI level, i.e. outside (but directly adjacent to) the rolandic network. The finding of aberrant connectivity beyond the functional network under investigation is not uncommon; for example the recruitment of the right frontal lobe into the left-lateralized language network has been described in left-sided temporal lobe epilepsy (Waites, Briellmann, Saling, Abbott, & Jackson, 2006). Recently Voets et al also reported connectivity abnormalities in temporal lobe epilepsy beyond the resting-state networks under investigation, among others in an "extended sensorimotor network", incidentally also involving temporal regions (Voets, et al., 2012).

5.4.4 Functional integration of motor and language networks

The reduced integration of Broca's area into the rolandic network might be of relevance for understanding language impairment in RE. Indeed, an extensive body of literature exists on the relevance of the motor system for language (Cappa & Pulvermuller, 2012; Meister IG, et al., 2003; Pulvermuller, et al., 2006).

Remarkably, this integration goes beyond the (somewhat trivial) relevance of the (pre)motor cortex in the coordination of complex articulatory movement. For example, using fMRI it has been shown that the perception of speech sounds most strongly activates the superior temporoparietal cortex (Wernicke's area), but shows differential activation dependent on the specific articulator involved in the motor cortex (lips and tongue area, respectively) (Pulvermuller, et al., 2006). Thus, a

shared neuronal substrate was demonstrated for speech production (motor system) and comprehension (language system). Furthermore, motor neuron disease (MND) has been associated with a specific deficit in the processing of verbs, suggesting that the motor and language symptoms are due to the same selective neurodegenerative process, spreading along functionally integrated networks (Bak & Chandran, 2012).

In completely different fields of research (linguistics), the motor theory of speech perception and theories on the gestural origin of language are well established (Galantucci, Fowler, & Turvey, 2006; Johannesson, 1950). In line with this, the relevance of gestures in speech perception has recently been demonstrated using EEG (Obermeier, Dolk, & Gunter, 2012).

Taken together, the concept of moto-lingual integration seems key in explaining language impairment in RE.

5.4.5 Relation with language performance

No associations were found between rolandic network connectivity and neuropsychological metrics of language performance in any of the language ROIs. Possibly reduced functional connectivity between Broca's area and the rolandic network is not very sensitive to dysfunction within the language system itself.

Another possible explanation is that as the CELF-4 assesses the language profile as a whole, its specificity to impairments in Broca's area might have been insufficient. We employed the CELF-4 since it is one of the few tests that is developed for and well-validated in children (Paslawski C, 2005). Furthermore, the impaired language content index found in RE signifies problems in semantic development and sentence formulation and construction, which have been linked to the inferior prefrontal cortex (Broca's expressive language area) (Rogalsky & Hickok, 2011). In addition, the left inferior frontal gyrus has been associated with working memory, which is in line with the trend of reduced language working memory we found in RE (Rogalsky & Hickok, 2011).

The impairment with respect to receptive language index hints at problems in posterior language function (Wernicke's receptive language area). However, the view that the language network can be strictly segregated in expressive anterior and receptive posterior regions is difficult to maintain given recent evidence (D'Ausilio, Bufalari, Salmas, & Fadiga, 2012; Pulvermuller, et al., 2006). For example, the inferior prefrontal cortex has also been associated with language comprehension (Pulvermuller, et al., 2006).

Hence, the CELF-4 results are consistent with anterior language dysfunction, which has been described in RE before (Lillywhite, et al., 2009).

5.4.6 Future research

Future studies would benefit from the inclusion of more precisely characterized patients. For example, in the present cohort the duration of epilepsy was quite variable (SD of 2.4 years on a mean of 2). Narrowing our inclusion based on such measures, however, would not have made much sense because they are difficult to accurately estimate. Due to the mild and typically nocturnal nature of RE, there might be a considerable (and variable) lag between the diagnosis and the first occurrence of seizures (Overvliet GM, et al., 2011). To our knowledge, there is no accurate alternative for the child's or parents' report to determine the actual age at onset, which makes adequate patient characterization especially challenging.

Furthermore, the onset of (subclinical) epileptiform activity rather than full-blown seizures might actually be a more relevant in the context of language impairment in RE. This is supported by the finding that in RE families, seizure-free siblings of children with RE are at increased risk for language impairment (Clarke, et al., 2007), and also compromises timely inclusion in scientific studies.

Related to this is the question whether the language impairments may persist after spontaneous seizure remission. Recent findings suggest that this is the case, however, this matter deserves further research (Monjauze C, et al., 2011).

Finally, in our experience, it is hard to recruit large cohorts of RE patients, even at a specialized epilepsy referral center, compromising statistical power of the analyses. We expect this is caused by the fact that an important fraction of children with RE only receives primary care. Our study adds to the growing body of evidence that RE is not merely a benign condition. In line with this, we hope that primary caregivers will become more readily inclined to refer a child under suspicion of epilepsy to specialized care. Especially in the case of RE this might too often still not be the case (Hughes, 2010).

5.5 Conclusion

The functional connectivity between the resting-state network involving the rolandic regions and the left inferior frontal gyrus (Broca's area) was reduced in RE. This functional decoupling might be key in understanding RE-typical language impairment, and is in line with the identified neuropsychological profile of anterior language dysfunction.

Acknowledgements

We would like to acknowledge Esther Peeters for data acquisition, Marc Geerlings for continuous hardware and software support, and all children and their parents for participating.

References

Bak, T. H., & Chandran, S. (2012). What wires together dies together: verbs, actions and neurodegeneration in motor neuron disease. *Cortex, 48*(7), 936-944.

Beckmann, C. F., DeLuca, M., Devlin, J. T., & Smith, S. M. (2005). Investigations into resting-state connectivity using independent component analysis. *Philos Trans R Soc Lond B Biol Sci, 360*(1457), 1001-1013.

Beckmann, C. F., Mackay, C. E., Filippini, N., & Smith, S. (2009). *Group comparison of resting-state FMRI data using multi-subject ICA and dual regression.* Paper presented at the OHBM annual meeting, San Francisco.

Berroya AM, Bleasel AF, Stevermuer TL, Lawson J, & Bye AM (2005). Spike morphology, location, and frequency in benign epilepsy with centrotemporal spikes. *J Child Neurol., 20*(3), 188-194.

Calhoun, V. D., Liu, J., & Adali, T. (2009). A review of group ICA for fMRI data and ICA for joint inference of imaging, genetic, and ERP data. *Neuroimage, 45*(1 Suppl), S163-172.

Cappa, S. F., & Pulvermuller, F. (2012). Cortex special issue: language and the motor system. *Cortex, 48*(7), 785-787.

Clarke, T., Strug, L. J., Murphy, P. L., Bali, B., Carvalho, J., Foster, S., et al. (2007). High risk of reading disability and speech sound disorder in rolandic epilepsy families: case-control study. *Epilepsia, 48*(12), 2258-2265.

Cole, D. M., Smith, S. M., & Beckmann, C. F. (2010). Advances and pitfalls in the analysis and interpretation of resting-state FMRI data. *Front Syst Neurosci, 4*, 8.

D'Ausilio, A., Bufalari, I., Salmas, P., & Fadiga, L. (2012). The role of the motor system in discriminating normal and degraded speech sounds. *Cortex, 48*(7), 882-887.

Deltour L, Barathon M, Quaglino V, Vernier MP, Despretz P, Boucart M, et al. (2007). Children with benign epilepsy with centrotemporal spikes (BECTS) show impaired attentional control: evidence from an attentional capture paradigm. *Epileptic Disord., 9*(1), 32-38.

Deltour L, Querné L, Vernier-Hauvette MP, & Berquin P (2008). Deficit of endogenous spatial orienting of attention in children with benign epilepsy with centrotemporal spikes (BECTS). *Epilepsy Res. , 79*(2-3), 112-119.

Doucet, G., Naveau, M., Petit, L., Delcroix, N., Zago, L., Crivello, F., et al. (2011). Brain activity at rest: a multiscale hierarchical functional organization. *J Neurophysiol, 105*(6), 2753-2763.

Doucet, G., Naveau, M., Petit, L., Zago, L., Crivello, F., Jobard, G., et al. (2012). Patterns of hemodynamic low-frequency oscillations in the brain are modulated by the nature of free thought during rest. *Neuroimage, 59*(4), 3194-3200.

Filippini, N., MacIntosh, B. J., Hough, M. G., Goodwin, G. M., Frisoni, G. B., Smith, S. M., et al. (2009). Distinct patterns of brain activity in young carriers of the APOE-epsilon4 allele. *Proc Natl Acad Sci U S A, 106*(17), 7209-7214.

Galantucci, B., Fowler, C. A., & Turvey, M. T. (2006). The motor theory of speech perception reviewed. *Psychon Bull Rev, 13*(3), 361-377.

Greicius, M. D., Krasnow, B., Reiss, A. L., & Menon, V. (2003). Functional connectivity in the resting brain: a network analysis of the default mode hypothesis. *Proc Natl Acad Sci U S A, 100*(1), 253-258.

Hughes, J. R. (2010). Benign epilepsy of childhood with centrotemporal spikes (BECTS): to treat or not to treat, that is the question. *Epilepsy Behav, 19*(3), 197-203.

Jocic-Jakubi B, & Jovic NJ (2006). Verbal memory impairment in children with focal epilepsy. *Epilepsy Behavior, 9*(3), 432-439.

Johannesson, A. (1950). The gestural origin of language; evidence from six 'unrelated' languages. *Nature, 166*(4210), 60-61.

Joseph, J. E., Swearingen, J. E., Clark, J. D., Benca, C. E., Collins, H. R., Corbly, C. R., et al. (2012). The changing landscape of functional brain networks for face processing in typical development. *Neuroimage, 63*(3), 1223-1236.

Kanemura, H., & Aihara, M. (2009). Growth disturbance of frontal lobe in BCECTS presenting with frontal dysfunction. *Brain Dev, 31*(10), 771-774.

Kavros PM, Clarke T, Strug LJ, Halperin JM, Dorta NJ, & Pal DK (2008). Attention impairment in rolandic epilepsy: systematic review. *Epilepsia, 49*(9), 1570-1580.

Liasis A, Bamiou DE, Boyd S, & Towell A (2006). Evidence for a neurophysiologic auditory deficit in children with benign epilepsy with centro-temporal spikes. *J Neural Transmission, 113*(7), 939-949.

Lillywhite, L. M., Saling, M. M., Harvey, A. S., Abbott, D. F., Archer, J. S., Vears, D. F., et al. (2009). Neuropsychological and functional MRI studies provide converging evidence of anterior language dysfunction in BECTS. *Epilepsia, 50*(10), 2276-2284.

Loiseau P, & Duché B (1989). Benign childhood epilepsy with centrotemporal spikes. *Cleve Clin J Med, 56*(Suppl Pt 1), S17-22; discussion S40-12.

Lundberg S, Frylmark A, & Eeg-Olofsson O (2005). Children with rolandic epilepsy have abnormalities of oromotor and dichotic listening performance. *Dev Med Child Neurol, 47*(9), 603-608.

Massa R, de Saint-Martin A, Carcangiu R, Rudolf G, Seegmuller C, Kleitz C, et al. (2001). EEG criteria predictive of complicated evolution in idiopathic rolandic epilepsy. *Neurology, 57*(6), 1071-1079.

Meister IG, Boroojerdi B, Foltys H, Sparing R, Huber W, & Töpper R (2003). Motor cortex hand area and speech: implications for the development of language. *Neuropsychologia, 41*(4), 401-406.

Monjauze C, Broadbent H, Boyd SG, Neville BG, & Baldeweg T (2011). Language deficits and altered hemispheric lateralization in young people in remission from BECTS. *Epilepsia, 52*(8), e79-e83.

Monjauze C, Tuller L, Hommet C, Barthez MA, & Khomsi A (2005). Language in benign childhood epilepsy with centro-temporal spikes abbreviated form: rolandic epilepsy and language. *Brain and Language, 92*(3), 300-308.

Nicolai, J., van der Linden, I., Arends, J. B., van Mil, S. G., Weber, J. W., Vles, J. S., et al. (2007). EEG characteristics related to educational impairments in children with benign childhood epilepsy with centrotemporal spikes. *Epilepsia, 48*(11), 2093-2100.

Obermeier, C., Dolk, T., & Gunter, T. C. (2012). The benefit of gestures during communication: evidence from hearing and hearing-impaired individuals. *Cortex, 48*(7), 857-870.

Overvliet GM, Aldenkamp AP, Klinkenberg S, Vles JSH, & Hendriksen J (2011). Impaired language performance as a precursor or consequence of Rolandic epilepsy? *Journal of the Neurological Sciences, 304*(1), 71-74.

Overvliet GM, Besseling RM, Vles JS, Hofman PA, Backes WH, van Hall MH, et al. (2010). Nocturnal epileptiform EEG discharges, nocturnal epileptic seizures, and language impairments in children: Review of the literature. *Epilepsy Behav, 19*(4), 550-558.

Panayiotopoulos, C. P., Michael, M., Sanders, S., Valeta, T., & Koutroumanidis, M. (2008). Benign childhood focal epilepsies: assessment of established and newly recognized syndromes. *Brain, 131*(Pt 9), 2264-2286.

Paslawski C (2005). The Clinical Evaluation of Language Fundamentals, Fourth Edition (CELF-4): A Review. *Canadian Journal of School Psychology, 20*, 129-134.

Pulvermuller, F., Huss, M., Kherif, F., Moscoso del Prado Martin, F., Hauk, O., & Shtyrov, Y. (2006). Motor cortex maps articulatory features of speech sounds. *Proc Natl Acad Sci U S A, 103*(20), 7865-7870.

Rogalsky, C., & Hickok, G. (2011). The role of Broca's area in sentence comprehension. *J Cogn Neurosci, 23*(7), 1664-1680.

Rubia, K. (2012). Functional brain imaging across development. *Eur Child Adolesc Psychiatry*.

Semel E, Wiig EH, & Secord WA (2010). *Clinical Evaluation of Language Fundamentals 4, Nederlandse versie* (3 ed.). Amsterdam: Pearson

Smith, S. M., Fox, P. T., Miller, K. L., Glahn, D. C., Fox, P. M., Mackay, C. E., et al. (2009). Correspondence of the brain's functional architecture during activation and rest. *Proc Natl Acad Sci U S A, 106*(31), 13040-13045.

Tomasi, D., & Volkow, N. D. (2012). Resting functional connectivity of language networks: characterization and reproducibility. *Mol Psychiatry, 17*(8), 841-854.

Voets, N. L., Beckmann, C. F., Cole, D. M., Hong, S., Bernasconi, A., & Bernasconi, N. (2012). Structural substrates for resting network disruption in temporal lobe epilepsy. *Brain, 135*(Pt 8), 2350-2357.

Waites, A. B., Briellmann, R. S., Saling, M. M., Abbott, D. F., & Jackson, G. D. (2006). Functional connectivity networks are disrupted in left temporal lobe epilepsy. *Ann Neurol, 59*(2), 335-343.

Yuan, W., Szaflarski, J. P., Schmithorst, V. J., Schapiro, M., Byars, A. W., Strawsburg, R. H., et al. (2006). fMRI shows atypical language lateralization in pediatric epilepsy patients. *Epilepsia, 47*(3), 593-600.

CHAPTER 6

Reduced structural connectivity between sensorimotor and language areas in rolandic epilepsy

R.M.H. Besseling, J.F.A. Jansen, G.M. Overvliet, S.J.M van der Kruijs, S.C.M. Ebus, A.J.A. de Louw, P.A.M. Hofman, J.S.H. Vles, A.P. Aldenkamp, W.H. Backes

PLoS ONE 2013; 8(12): e83568. doi: 10.1371 /journal.pone.0083568

Abstract

Introduction Rolandic epilepsy (RE) is a childhood epilepsy with centrotemporal (rolandic) spikes, that is increasingly associated with language impairment. In this study, we tested for a white matter (connectivity) correlate, employing diffusion weighted MRI and language testing.

Methods Twenty-three children with RE and 23 matched controls (age: 8-14 years) underwent structural (T1-weighted) and diffusion-weighted MRI (b=1200 s/mm^2, 66 gradient directions) at 3T, as well as neuropsychological language testing. Combining tractography and a cortical segmentation derived from the T1-scan, the rolandic tract were reconstructed (pre- and postcentral gyri), and tract fractional anisotropy (FA) values were compared between patients and controls. Aberrant tracts were tested for correlations with language performance.

Results Several reductions of tract FA were found in patients compared to controls, mostly in the left hemisphere; the most significant effects involved the left inferior frontal (p=0.005) and supramarginal (p=0.004) gyrus. In the patient group, lower tract FA values were correlated with lower language performance, among others for the connection between the left postcentral and inferior frontal gyrus (p=0.043, R=0.43).

Conclusion In RE, structural connectivity is reduced for several connections involving the rolandic regions, from which the epileptiform activity originates. Most of these aberrant tracts involve the left (typically language mediating) hemisphere, notably the pars opercularis of the inferior frontal gyrus (Broca's area) and the supramarginal gyrus (Wernicke's area). For the former, reduced language performance for lower tract FA was found in the patients. These findings provide a first microstructural white matter correlate for language impairment in RE.

6.1 Introduction

Rolandic epilepsy (RE) is an idiopathic localization-related epilepsy of childhood characterized by centro-temporal spikes on EEG, i.e. originating from the rolandic (sensorimotor) cortex. Seizures are usually mild and nocturnal, and involve hemifacial spasms and speech arrest (Loiseau P and Duché B 1989; Panayiotopoulos, Michael et al. 2008). The typical age at seizure onset is 7-10 years and spontaneous remission of seizures is observed during adolescence, usually before the age of 16 years (Panayiotopoulos, Michael et al. 2008). RE is classically considered a benign condition, and is therefore also known as benign epilepsy of childhood with centro-temporal spikes (BECTS).

However, over the last years RE has been associated with visuomotor impairments and problems in spatial perception and orientation, but also with psychiatric disorders, lower IQ, dyscalculia and dyslexia (Hughes 2010). Not only has the presence and severity of these comorbidities put the assumed benign character of RE under debate (Hughes 2010); more importantly, their nature hints at dysfunction in neuronal circuits distant from the rolandic focus, rather than purely sensorimotor pathology (Massa R, de Saint-Martin A et al. 2001).

Despite the wide range of associated cognitive impairments, especially impairments of the language system have frequently been reported. These vary from verbal memory impairment and auditory deficits to reading disability and speech sound disorder (Jocic-Jakubi B and Jovic NJ 2006; Liasis A, Bamiou DE et al. 2006; Clarke, Strug et al. 2007; Overvliet GM, Besseling RM et al. 2010). Functional imaging, combined with neuropsychological testing, suggests that especially anterior language areas are affected (Lillywhite, Saling et al. 2009; Besseling, Jansen et al. 2013). Abnormalities in functional as well as structural connectivity have been found in other types of childhood epilepsy (Braakman, Vaessen et al. 2012). Moreover, investigations of conventional MRI scans have revealed structural abnormalities in RE (Kanemura and Aihara 2009), including white matter hyper-intensities (Lundberg S, Eeg-Olofsson O et al. 1999). Also, patterns of subtle cortical thickness abnormalities have been described (Overvliet, Besseling et al. 2013). These findings prompt for an investigation into the underlying white matter connections (and the association with language impairment) in RE.

Given the origin of the epileptiform activity in the rolandic regions, we hypothesize that the white matter tracts connecting to these regions may be compromised, and that these abnormalities may be related to the language impairments. We employ diffusion-weighted MRI to reconstruct these tracts (tractography) and to quantify their microstructural integrity in a group of children with RE and a cohort of age-matched controls. Potentially aberrant tracts are interpreted in the light of language impairment based on their topology and

possible associations with a neuropsychological measure for language performance. In addition and for completeness, we tested for voxel-wise abnormalities in white matter integrity using a robust and well-established technique (tract based spatial statistics; TBSS).

6.2 Materials and methods

6.2.1 Ethics statement

Written informed consent was obtained from all parents or guardians and the study was approved by the review boards of both Maastricht University Medical Center and epilepsy center Kempenhaeghe. The study is registered at www.clinicaltrials.gov under number NCT01335425.

6.2.2 Subjects

A clinical cohort of 23 children with RE (11.4±2 years; range: 8.0-14.6 years; 9 girls) were recruited at the specialized epilepsy referral centre Kempenhaeghe; for inclusion criteria, see below. An age- and gender-matched healthy control cohort was also included (N=23; 10.4±1.6 years; range 8.1-14.0 years; 11 girls). For further subject characteristics, see Table 6.1.

Subject characteristics	Patients	Controls
N (m/f)	14/9	12/11
Age [y]	10.4±1.6	11.4±2.0
Age at epilepsy onset [y]	7.5±2.1	n.a.
Epilepsy duration [y]	3.9±2.1	n.a.
Handedness (r/l/ambi)	19/3/1	21/2/0
Number of AEDs (0/1/>1)	13/6/4	n.a.

Table 6.1: Subject characteristics, if applicable mean±SD.
AED stands for anti-epileptic drug; n.a. for not applicable.

6.2.3 Inclusion criteria

Patient selection was based on seizure semiology and electrophysiological (EEG) data as acquired during the diagnostic work-up. For this, criteria from literature were used (Berroya AM, Bleasel AF et al. 2005; Panayiotopoulos, Michael et al. 2008). EEG criteria included the presence of spike and slow wave complexes occurring as individual paroxysms or in repetitive clusters with a maximum in the mid temporal and/or central electrodes and with a temporal-frontal dipole field. Additional independent central, mid temporal, parietal or occipital spike wave foci in the same or other hemisphere were allowed. To exclude severe cases (Landau-Kleffner syndrome (LKS) or LKS-like), interictal epileptiform activity was required to be present <85% of the time during non-REM sleep. With respect to seizure semiology, seizures with anarthria, hemiclonia involving the face and/or unilateral extremities, or secondarily generalized seizures were considered. In case of poorly observed nocturnal seizures (3 cases), post-ictal signs of a generalized seizure or confirmation of post-ictal hemiparesis were sufficient for inclusion in case of otherwise typical EEG.

The children with RE were tested using the Wechsler Intelligence Scale for Children, third revised edition, Dutch version (WISC-3), and all had a full-scale IQ >70. None of the healthy controls had (a history of) dyslexia, learning and/or psychiatric disorders, nor attended special education. Children were excluded if they had dental braces (MRI quality) or were somewhat afraid in the scanner.

6.2.4 Language assessment

All children were subjected to the Clinical Evaluation of Language Fundamentals test, 4th edition (CELF-4), Dutch version (Paslawski C 2005; Semel E, Wiig EH et al. 2010). The CELF is a verbally presented language test, which is the gold standard for language assessment in children and adolescents (5-21 years). It was used to

assess the core language score, which is a global measure for overall language performance.

6.2.5 MR imaging

Structural T1-weighted imaging was performed at 3T (Philips Achieva, Best, the Netherlands) using a receive-only SENSE head-coil. A 3D fast-spoiled gradient echo sequence was used employing echo time/repetition time/inversion time (TE/TR/TI) 3.8/8.3/1022 ms at a resolution of 1x1x1 mm^3. The acquisition time was 8 min.

The T1-weighted scans were reviewed by a board certified neuroradiologist with >20 years of experience (PH). No relevant structural abnormalities were found.

High angular resolution diffusion-weighted imaging (HARDI) was performed using a set of 66 gradient directions distributed evenly over the sphere (Jones, Horsfield et al. 1999), employing a diffusion-sensitizing b-value of 1200 s/mm^2. In addition, a single minimally diffusion-weighted image (b0-scan) was acquired. Other settings were: TE/TR 72/6600 ms, resolution 2x2x2 mm^3, and acquisition time 9 min.

6.2.6 Cortical parcellation

The T1-weighted structural image was parcellated into 35 cortical regions per hemisphere using the Freesurfer software package as available at http://surfer.nmr.mgh.harvard.edu/. The steps involved are brain extraction, tissue segmentation, and cortical parcellation based on image intensity (gradients) in a template-driven, fully automated and highly robust way (Fischl, van der Kouwe et al. 2004; Desikan, Segonne et al. 2006; Fischl, Rajendran et al. 2008). The resulting cortical parcellation of in total 70 regions is gyral pattern based and includes, among others, the left and right pre- and postcental gyrus (henceforth referred to as the 4 rolandic regions).

The cortical parcellation was transformed into diffusion space by affine registration to the b0-scan using FSL routines (FMRIB's Software Library, Oxford, UK).

6.2.7 Tractography

6.2.7.1 Preprocessing

Preprocessing and tractography were performed as described previously (Besseling, Jansen et al. 2012). Diffusion-weighted sequences were movement-corrected by affine registration to the b0-scan using CATNAP (Coregistration, Adjustment, and Tensor-solving: a Nicely Automated Program, 2008). This

included correction of the gradient directions for the corresponding rotations (Landman, Farrell et al. 2007; Leemans and Jones 2009).

6.2.7.2 Constrained spherical deconvolution

Voxel-wise fiber orientation distributions (FODs) were estimated using constrained spherical deconvolution (CSD, (Tournier, Calamante et al. 2004; Tournier, Calamante et al. 2007)) as implemented in the MRtrix software package, see http://www.nitrc.org/projects/mrtrix/. As opposed to the conventional diffusion tensor (DT), CSD FODs can represent *multiple* fiber orientations per voxel and as such account for partial volume effects induced by within-voxel fiber crossing, kissing, bending and fanning (Tournier, Yeh et al. 2008).

Diffusion tensor imaging (DTI) was employed to calculate fractional anisotropy (FA) maps (Basser, Mattiello et al. 1994). For each subject, the response function needed for CSD was estimated from the data by averaging the diffusion profiles of high FA voxels (FA>0.7), aligned along the direction of their principal eigenvector. To ensure that the selected voxels represent (deep) white matter, an eroded brain mask was applied (5 single voxel erosion iterations). For more information on the CSD methodology, we refer to our previous work (Besseling, Jansen et al. 2012).

CSD FODs are expressed in spherical harmonics, much as (periodic) time signals can be expressed as Fourier series (Tournier, Calamante et al. 2004). Higher orders can represent better resolved FODs, with sharper lobes. A spherical harmonic order l_{max} of 8 was used (corresponding to 45 spherical harmonics), which is assumed to adequately resolve crossings without over-fitting the data (Tournier, Yeh et al. 2008).

6.2.7.3 Whole brain tracking and investigated pathways

For each subject, a whole-brain tractogram was constructed, consisting of 5.000.000 streamlines seeded randomly throughout the brain. Probabilistic CSD tractography was used as implemented in MRtrix. This implies that streamline propagation is allowed in any FOD direction above a certain amplitude threshold, rather than only in the direction of FOD maxima. This allows the streamlines to disperse (to a limited extent) over the width of the FOD lobes, exploring connectivity over a certain angular range. The tractography settings included an FOD amplitude threshold of 0.1, a propagation step size of 0.2 mm, a minimum curvature radius of 1 mm and minimum/maximum streamline lengths of 10/200 mm, respectively.

In an approach similar to Rose et al. (Rose, Pannek et al. 2012), for each of the 4 rolandic areas as obtained from the (b0-registered) Freesurfer parcellation, the connectivity to the 69 other cortical regions (both ipsi- and contralateral) was investigated by iteratively selecting those streamlines from the whole-brain

tractogram that passed through both the rolandic (seed) and the target region, leading to a total of 270 potential (unique) connections. Since the number of streamlines depends on the size of the seed and/or target region, the number of streamlines of each connection was normalized by its respective number of seed and target voxels (van den Heuvel and Sporns 2011). To discard noise-dominated connections, only those for which this ratio exceeded 5 were selected. This corresponds to approximately 10% of the maximum value of this ratio, and led to a limited number of 30 connections being taken forward for further analysis, see below.

6.2.7.4 Connectivity metrics

For each connection, structural connectivity was quantified by tract FA, which was calculated by constructing a map of the number of streamlines passing through each voxel (tract density imaging (TDI, (Calamante, Tournier et al. 2010)) and employing this to calculate a weighted average. This method gives more weight to FA values in regions where streamline packing is high.

Since FA is age dependent (Bonekamp, Nagae et al. 2007; Taki, Thyreau et al. 2012), tract FA values were group-wise corrected for age using linear regression. Group differences in (age-corrected) tract FA values were inferred on using permutation testing (N=100.000). Results were corrected for multiple comparisons employing false discovery rate (FDR) control at q<10% (Rose, Pannek et al. 2012). For the aberrant connections, the (age corrected) tract FA values were correlated with core language scores to test for associations between structural connectivity and language performance.

6.2.8 Tract-based spatial statistics

To detect possible voxel-wise FA abnormalities, patients were compared to controls employing tract-based spatial statistics (TBSS, (Smith, Jenkinson et al. 2006)) as implemented in FSL. This involves spatial normalization of the individual FA maps and the subsequent construction of a mean (common) FA skeleton. Next, all subjects' FA data are projected onto this skeleton and voxel-wise cross-subjects statistics is applied to test for group differences (permutation testing, N=5000). TBSS is assumed to have higher sensitivity than conventional voxel-wise comparison of DT metrics, among others by improved spatial normalization. Since its introduction, TBSS has rapidly become accepted in the field, and has been repeatedly applied to a range of neurological diseases including epilepsy (Smith, Jenkinson et al. 2006; Schoene-Bake, Faber et al. 2009; Nguyen, Vargas et al. 2011; Fonseca Vde, Yasuda et al. 2012; Miao, Li et al. 2012; Rose, Pannek et al. 2012).
Results were enhanced for clustered effects using threshold-free cluster enhancement (TFCE, (Smith and Nichols 2009)) and corrected for multiple

comparisons at p<0.05 within the TBSS tool. In line with the tract-wise approach, the TBSS analysis was also corrected for age using group-wise linear regression.

6.3 Results

6.3.1 Language performance

The core language score of the patients was 94±17, which is significantly reduced compared to the controls (106±11; p=0.007, Student's t-test).

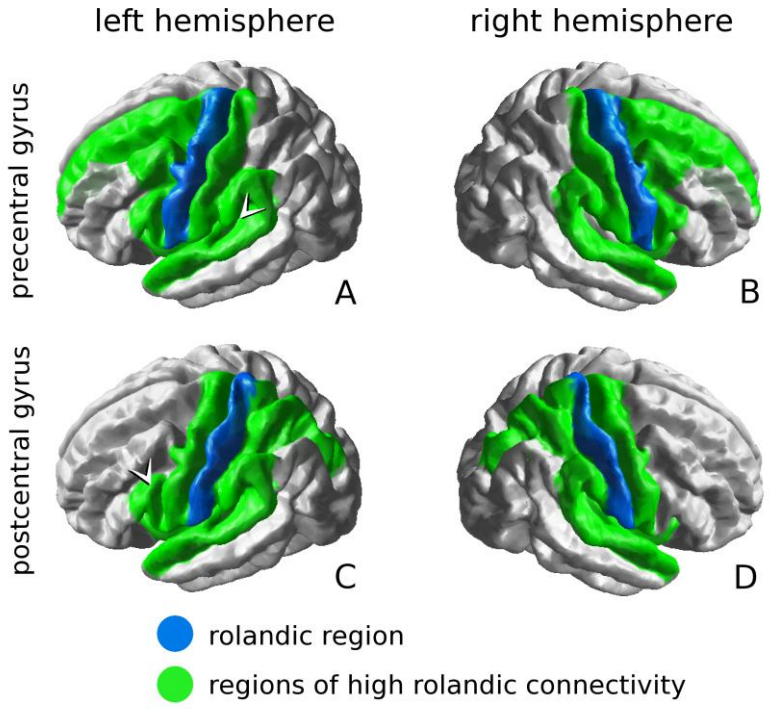

Figure 6.1: The 10% most robust rolandic connections, for which the number of streamlines/voxel >5. Averaged over all subjects, all 4 rolandic regions show high perisylvian connectivity, connecting strongly to the supramarginal and superior temporal gyri. Furthermore, the precentral gyri also strongly connect to prefrontal regions (A, B), whereas the postcentral gyri show strong connectivity with the superior parietal cortex. For the precentral gyri, the interhemispheric difference lies in the transverse temporal gyrus (arrowhead in A); for the postcentral gyri, the differences in connectivity lies in the pars opercularis of the inferior frontal gyrus (arrowhead in C).

6.3.2 Rolandic connectivity

For each of the 4 rolandic regions, the robust connectivity patterns for the pooled subjects (patients and controls combined) are given in Figure 6.1. These prominent connections were confined to the ipsilateral hemisphere and had several features in common. In both hemispheres, the pre- and postcentral gyrus showed strong mutual connectivity, and each rolandic region was strongly connected with the superior temporal and supramarginal gyrus (i.e. perisylvian cortex). Also the insula and the paracentral gyrus (adjacent to the rolandic cortex, in the medial plane) were among the regions of prominent connectivity for all 4 rolandic regions.

Specific for the bilateral precentral gyri was high connectivity to several (pre)frontal regions, i.e. the superior and caudal middle frontal cortex, and the pars opercularis of the inferior frontal gyrus (IFG), see Figure 6.1A, B. Furthermore, high connectivity was found with the transverse temporal gyrus (adjacent to the insula), but only in the left hemisphere (arrowhead in Figure 6.1A).

Furthermore, both postcentral gyri specifically showed strong connectivity with the superior parietal and the transverse temporal gyri, see Figure 6.1C, D. Only for the left postcentral gyrus, strong connectivity was found with the pars opercularis of the IFG (arrowhead in Figure 6.1C).

6.3.3 Aberrant tract fractional anisotropy

Several significant reductions in tract FA were found in patients compared to controls, see Figure 6.2. No connections were found for which FA values were higher in patients than in controls.

General features are reduced tract FA for the connections between the pre- and postcentral gyri in both hemispheres, as well as reduced tract FA for the connections between each of the 4 rolandic regions and the ipsilateral insula and superior temporal gyrus.

For the precentral gyri, additional reductions in tract FA were found for the connections with the superior frontal cortex and the pars opercularis of the IFG. Specific for the left precentral gyrus was a reduction in tract FA for the connection with the caudal middle frontal cortex ($p=0.03$), which was not found at the right.

For the postcentral gyri, additional reductions in tract FA were found for the connections with the supramarginal gyri. This effect was more pronounced in the left than in the right hemisphere ($p=0.005$ compared to $p=0.03$, respectively), see the black arrow in Figure 6.2C. Furthermore, for the left precental gyrus, tract FA was reduced for the connection with the pars opercularis of the IFG ($p=0.006$), see the white arrow in Figure 6.2C. Again, a comparable effect in the right hemisphere was absent.

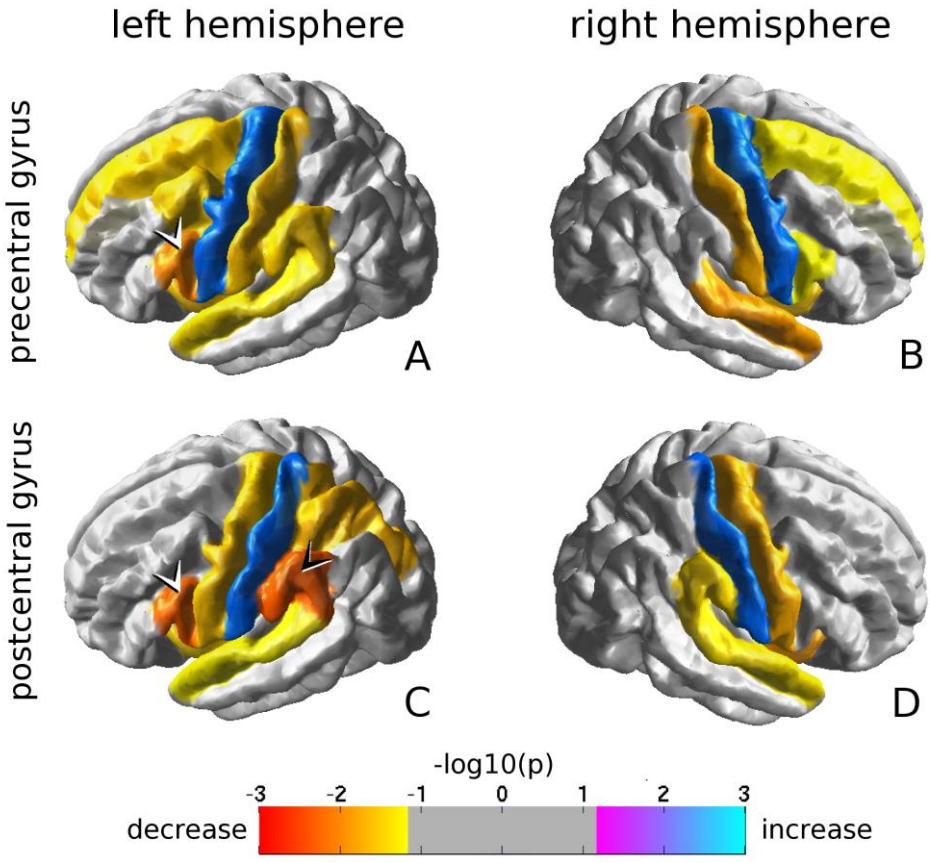

Figure 6.2: Only reductions in tract FA were found for patients compared to controls, the most extensive and significant of which were located in the left hemisphere. Especially notice the FA reduction for the rolandic connections with the pars opercularis of the inferior frontal gyrus (white arrowheads in A and C), and the postcentral connection with the supramarginal gyrus (black arrowhead in C).

6.3.4 Associations with language performance

For several of the aberrant connections, significant correlations were found between core language score and (age corrected) tract FA. In the patients, lower core language scores were associated with lower tract FA for the connection between the left postcentral gyrus and the pars opercularis of the left IFG (p=0.043, Pearson's R=0.43), see Figure 6.3. Similar effects were found for three connections involving the right precentral gyrus, i.e. the connection with the right postcentral gyrus (p=0.030, R=0.45), the connection with the right paracentral gyrus (p=0.016, R=0.50), and the connection with the right superior frontal cortex (p=0.023, R=0.47).

No significant correlations were found in the controls.

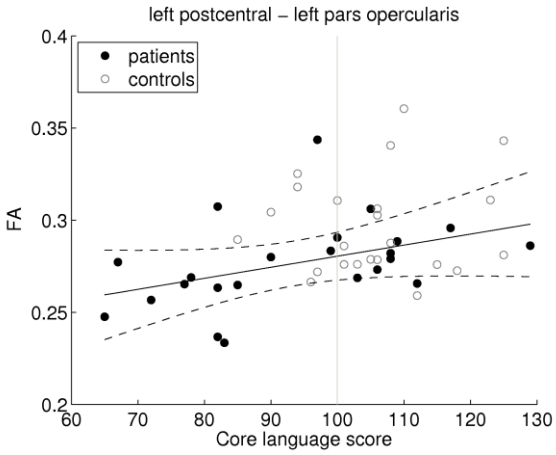

Figure 6.3: In the children with RE, lower tract FA values were significantly correlated with lower core language scores for the connection between the left postcentral gyrus and the pars opercularis of the left inferior frontal gyrus (p=0.043, Pearson's R=0.43).
Regression line (solid) and 95% confidence interval (dashed) in black; norm core language score (100) indicated by vertical gray line. FA values were age-corrected.

6.3.5 Tract-based spatial statistics

TBSS revealed no significant FA differences between patients and controls.

6.4 Discussion

This study was set out to find white matter abnormalities involving the rolandic (sensorimotor) cortex in children with RE. We hypothesized rolandic connections to be disturbed in this type of epilepsy since it is characterized by rolandic epileptic foci. Moreover, since RE is associated with language problems, we explored whether potential connectivity abnormalities might be linked to language impairment.

6.4.1 Major findings

We identified anatomically plausible patterns of connectivity for the rolandic regions, generally displaying high centro-temporal connectivity, and specific additional frontal and parietal connections for the precentral and the postcentral gyri, respectively. With respect to connectivity abnormalities, our main findings are:

1) Significant reductions in tract FA were found in patients compared to controls, indicative of reduced structural connectivity;
2) More connectivity reductions were found in the left (typically language dominant) hemisphere than in the right;
3) Several of these abnormalities were more pronounced in the left hemisphere (i.e. higher significance) than in the right;

4) For the connection between the left postcentral gyrus and the pars opercularis of the left IFG, lower tract FA was associated with lower core language scores in the patients.

6.4.2 Patterns of connectivity

The patterns of rolandic connectivity are given in Figure 6.1. The connectivity patterns are highly symmetric, with the exception of 2 connections that are specific for the left hemisphere, i.e. the connection between the precentral gyrus and the transverse temporal gyrus, and that between the postcentral gyrus and the pars opercularis (arrowheads in Figure 6.1). Note that generally, the left hemisphere is language dominant; more specifically the left pars opercularis (or rather, the left IFG as a whole) is considered important for expressive language (Broca's area) (Catani, Jones et al. 2005; Price CJ 2010). Our findings suggest that specifically the left pars opercularis is structurally integrated with the rolandic regions, which implies it might inherently be affected by rolandic neuropathology, such as epileptiform activity in RE. In line with this, we observed that for all 4 rolandic regions, the superior temporal and supramarginal gyrus of the perisylvian cortex are among the important connections. The perisylvian cortex of the left hemisphere is associated with language, covering Broca's area in the inferior frontal gyrus, Wernicke's area in the supramarginal gyrus, and areas relevant for reading in the temporal lobe (Deblaere K, Backes WH et al. 2002; Backes WH, Deblaere K et al. 2005).

6.4.3 Reductions in tract fractional anisotropy

The investigation of tract FA demonstrated reduced rolandic connectivity in patients compared to controls, predominantly in the left hemisphere. The most significant effects involved tracts connecting the rolandic cortex to the pars opercularis and supramarginal gyrus of the left hemisphere (arrowheads in Figure 6.2). Since both represent language-mediating regions, the reductions in structural connectivity might be relevant in the context of language impairment.

On the other hand, reduced language lateralization and/or reorganization of language to the right hemisphere have recently been described in RE (Vannest, Karunanayaka et al. 2009; Besseling, Overvliet et al. 2013; Datta, Oser et al. 2013). This relative increase of right-hemispheric involvement in language may (partly) compensate for the reported abnormalities in structural connectivity of left-lateralized language connections.

6.4.4 Associations with language performance

We further investigated the relevance of the aberrant connections for language impairment by correlating their connection strength with language performance.

Significant effects were found for the patients only, in which lower tract FA values were associated with lower core language scores. Among others, this was the case for 2 central connections, i.e. those between the right precentral gyrus and the right postcentral and paracentral gyri, respectively. Because of the proximity of these connections to the epileptic focus, we assume these associations merely imply that more severe primary (rolandic) pathology is (indirectly) related to more pronounced cognitive impairment, among others lower language performance. Similarly, the association between lower tract FA values and lower core language scores for the connection between the right precentral gyrus and the right superior frontal cortex may also just provide an indirect window on general cognitive impairment, given the importance of the frontal lobe in cognitive processing. In fact, reduced connectivity of the frontal lobe has been related to reduced cognitive performance in childhood epilepsy before (Braakman, Vaessen et al. 2012).

On the other hand, the association between lower tract FA values and lower core language scores for the connection between the left postcentral gyrus and the pars opercularis of the left IFG is expected to be specifically related to language impairment, since this connection provides a link between a rolandic region and a language area (Broca's). Note that in language mediating connections such as this, a positive correlation between FA and language performance is also expected in the controls, as increased structural integrity may lead to improved cognitive performance. Possibly this lack of association in the controls is due to the narrower range of core language scores. This suggestion was also made concerning comparable findings with respect to functional connectivity in patients with cryptogenic localization-related epilepsy by our group (Vlooswijk, Jansen et al. 2010).

6.4.5 Integration of the motor and language system

The question why loss of structural connectivity *between* the rolandic (sensorimotor) regions and the language system (left pars opercularis and supramarginal gyrus) might impact functionality *within* the language system needs to be addressed.

The relevance of Broca's area for expressive language has long been established, and might hinge on the relevance of this region as (pre)motor area relevant for the coordination of complex articulatory movement. However, several recent studies have demonstrated that the motor and the language system are more fundamentally integrated (Meister IG, Boroojerdi B et al. 2003; Galantucci, Fowler et al. 2006; Pulvermuller, Huss et al. 2006; Cappa and Pulvermuller 2012; D'Ausilio, Bufalari et al. 2012). For example, it has been demonstrated that speech sounds predominantly activate the left supramarginal gyrus (Wernicke's area) but, depending on the articulator involved (lips or tongue), differently activate the associated regions in the motor cortex (Pulvermuller, Huss et al. 2006). This implies

language functionality within the motor cortex, in other words: the motor and the language system have an (at least partly) shared neuronal substrate, and in that sense cannot be viewed as separate entities (Pulvermuller, Huss et al. 2006). For an overview, see Cappa et al. (Cappa and Pulvermuller 2012), and the references therein.

The rolandic connectivity patterns we identified are in line with this view as they demonstrate strong connectivity between the (in the left hemisphere language-mediating) supramarginal cortex and the rolandic regions. From this, it can be speculated that rolandic neuropathology might inherently influence the language system, as is consistent with our findings of reduced structural integrity of these connections.

Furthermore, if the role of Broca's area in the language network is not purely expressive, impairments within this region might cause a range of language problems. A number of studies exist on the role of Broca's area beyond expressive language (Rogalsky, Matchin et al. 2008; Rogalsky and Hickok 2011), for an overview we refer to Burns et al. (Burns and Fahy 2010). These findings fits to the broad profile of language impairment as found in RE, including reading disability, speech sound disorder, verbal memory impairment, neurophysiologic auditory deficit and abnormalities in oromotor and dichotic listening performance (Lundberg S, Frylmark A et al. 2005; Jocic-Jakubi B and Jovic NJ 2006; Liasis A, Bamiou DE et al. 2006; Clarke, Strug et al. 2007; Overvliet GM, Besseling RM et al. 2010).

All this is in line with our finding of reduced tract FA (and core language score) in the connection between the left postcentral gyrus and the pars opercularis of the left IFG.

6.4.6 No voxel-wise FA abnormalities

TBSS revealed no abnormalities, which might imply higher sensitivity of analysis on the tract level rather than voxel-wise inference, at least in the case of a clearly localized hypothesis, such as our case of aberrant rolandic connectivity in RE. This might (partly) be related to group-wise overlap of abnormalities on the tract level, but not on the (more local) voxel level. Note that TBSS projects subject-specific FA values onto a common (group-specific) FA skeleton, already improving spatial regularization with respect to conventional (whole-brain) voxel-wise techniques.

6.4.7 Methodological considerations and outlook

In this study, we investigated connectivity between relatively large cortical regions as defined by an automated, gyral pattern based cortical parcellation (Freesurfer). These regions might not have been optimal to fully and unambiguously segment the underlying major white matter tracts, but allowed us to investigate the

connectivity of specific gyral features of interest, i.e. the pre- and postcentral gyri (rolandic regions). The Freesurfer parcellation has been shown to be robust (Desikan et al., 2006), and ensured objectivity and consistency over subjects. Furthermore, it has been successfully applied for investigations of structural connectivity before (van den Heuvel, Mandl et al. 2010; Rose, Pannek et al. 2012).

Our aim was to examine aberrant rolandic connectivity in RE. Although our interest was in language impairment, this methodology was not biased towards finding aberrant connectivity with classical language mediating areas. Nonetheless, the most pronounced impairments in structural connectivity were found in the left hemisphere, more specifically in the left supramarginal gyrus (Wernicke's area) and the pars opercularis of the left IFG (Broca's area). What is more, for the latter it was demonstrated that lower tract FA values were associated with lower language performance.

These findings are in line with the view that language impairment is a prominent aspect of the cognitive problems seen in RE. For future research, it would be interesting to study structural connectivity abnormalities in RE in classical language-mediating white matter bundles such as the arcuate fasciculus (Catani, Jones et al. 2005; Bernal and Ardila 2009). However, such analyses required dedicated approaches (Catani and Thiebaut de Schotten 2008), and are beyond the methodological scope of this study.

In this work, we quantified structural connectivity using FA. FA is at best an indirect measure for white matter integrity, and its accuracy is compromised at regions of fiber crossing, kissing, bending and fanning (Jones, Knosche et al. 2012; Reijmer, Leemans et al. 2012). However, in our experience FA has good reproducibility and subject-differentiating power on the tract level (Besseling, Jansen et al. 2012). Indeed, at present FA is still the measure of choice in most investigations of structural connectivity (Rose, Pannek et al. 2012), whereas other measures for white matter integrity may also be used, such as apparent diffusion coefficient (ADC), number of streamlines per seed/target voxel, tract volume, or the recently introduced apparent fiber density (AFD; (Raffelt, Tournier et al. 2012)). Each of these measures has a different interpretation and they also vary in reproducibility (and therefore in sensitivity for abnormalities) (Besseling, Jansen et al. 2012). In our view, the field of tract connectivity measures other than FA is underexplored and forms an interesting subject for future research. The use of measures not derived from the diffusion-weighted data itself, such as magnetization transfer ratio (MTR) imaging to obtain estimates for the degree of myelination (van den Heuvel, Mandl et al. 2010), even further broadens the scope of possibilities.

Finally, our results were robust with respect to FDR correction for multiple comparisons at q=10%. In a methodologically similar approach, the same q-value was applied (Rose, Pannek et al. 2012). For future studies it remains to be

investigated whether our results are robust with respect to more stringent statistical correction employing larger numbers of subjects.

In conclusion, in RE abnormalities in structural connectivity can be found for specific white matter tracts involving the rolandic regions, where the epileptic focus is located. Most of these aberrant tracts involve the left hemisphere, notably the pars opercularis of the inferior frontal gyrus (Broca's area) and the supramarginal gyrus (Wernicke's area). For the former, lower structural connectivity was significantly correlated with reduced language performance in the patients. The fundamental integration of the motor and the language system as described in recent literature might explain why impairment of these moto-lingual connections impacts language performance, and might be a key concept in understanding language impairment in RE.

6.5 Acknowledgements

We would like to acknowledge Esther Peeters for data acquisition, Marc Geerlings and Jos Slenter for continuous hard- and software support, and all children and their parents for participating in this study.

6.6 References

Backes WH, Deblaere K, et al. (2005). "Language activation distributions revealed by fMRI in post-operative epilepsy patients: differences between left- and right-sided resections." Epilepsy Research **66**(1-3): 1-12.

Basser, P. J., J. Mattiello, et al. (1994). "MR diffusion tensor spectroscopy and imaging." Biophys J **66**(1): 259-67.

Bernal and Ardila (2009). "The role of the arcuate fasciculus in conduction aphasia." Brain **132**: 2309-2016.

Berroya AM, Bleasel AF, et al. (2005). "Spike morphology, location, and frequency in benign epilepsy with centrotemporal spikes." J Child Neurol. **20**(3): 188-194.

Besseling, R., G. Overvliet, et al. (2013). "Aberrant functional connectivity between motor and language networks in rolandic epilepsy." Epilepsy Res **in press**.

Besseling, R. M., J. F. Jansen, et al. (2012). "Tract specific reproducibility of tractography based morphology and diffusion metrics." PLoS One **7**(4): e34125.

Besseling, R. M. H., J. F. Jansen, et al. (2013). "Reduced functional integration of the sensorimotor and language network in rolandic epilepsy." Neuroimage: Clinical.

Bonekamp, D., L. M. Nagae, et al. (2007). "Diffusion tensor imaging in children and adolescents: reproducibility, hemispheric, and age-related differences." Neuroimage **34**(2): 733-42.

Braakman, H. M., M. J. Vaessen, et al. (2012). "Frontal lobe connectivity and cognitive impairment in pediatric frontal lobe epilepsy." Epilepsia.

Burns, M. S. and J. Fahy (2010). "Broca's area: rethinking classical concepts from a neuroscience perspective." Top Stroke Rehabil **17**(6): 401-10.

Calamante, F., J. D. Tournier, et al. (2010). "Track-density imaging (TDI): super-resolution white matter imaging using whole-brain track-density mapping." Neuroimage **53**(4): 1233-43.

Cappa, S. F. and F. Pulvermuller (2012). "Cortex special issue: Language and the motor system." Cortex.

Cappa, S. F. and F. Pulvermuller (2012). "Cortex special issue: language and the motor system." Cortex **48**(7): 785-7.

Catani, M., D. K. Jones, et al. (2005). "Perisylvian language networks of the human brain." Ann Neurol **57**(1): 8-16.

Catani, M. and M. Thiebaut de Schotten (2008). "A diffusion tensor imaging tractography atlas for virtual in vivo dissections." Cortex **44**(8): 1105-32.

Clarke, T., L. J. Strug, et al. (2007). "High risk of reading disability and speech sound disorder in rolandic epilepsy families: case-control study." Epilepsia **48**(12): 2258-65.

D'Ausilio, A., I. Bufalari, et al. (2012). "The role of the motor system in discriminating normal and degraded speech sounds." Cortex **48**(7): 882-7.

Datta, A. N., N. Oser, et al. (2013). "Cognitive impairment and cortical reorganization in children with benign epilepsy with centrotemporal spikes." Epilepsia **54**(3): 487-94.

Deblaere K, Backes WH, et al. (2002). "Developing a comprehensive presurgical functional MRI protocol for patients with intractable temporal lobe epilepsy: a pilot study." Neuroradiology. **44**(8): 667-673.

Desikan, R. S., F. Segonne, et al. (2006). "An automated labeling system for subdividing the human cerebral cortex on MRI scans into gyral based regions of interest." Neuroimage **31**(3): 968-80.

Fischl, B., N. Rajendran, et al. (2008). "Cortical folding patterns and predicting cytoarchitecture." Cereb Cortex **18**(8): 1973-80.

Fischl, B., A. van der Kouwe, et al. (2004). "Automatically parcellating the human cerebral cortex." Cereb Cortex **14**(1): 11-22.

Fonseca Vde, C., C. L. Yasuda, et al. (2012). "White matter abnormalities in patients with focal cortical dysplasia revealed by diffusion tensor imaging analysis in a voxelwise approach." Front Neurol **3**: 121.

Galantucci, B., C. A. Fowler, et al. (2006). "The motor theory of speech perception reviewed." Psychon Bull Rev **13**(3): 361-77.

Hughes, J. R. (2010). "Benign epilepsy of childhood with centrotemporal spikes (BECTS): to treat or not to treat, that is the question." Epilepsy Behav **19**(3): 197-203.

Jocic-Jakubi B and Jovic NJ (2006). "Verbal memory impairment in children with focal epilepsy." Epilepsy Behavior **9**(3): 432-439.

Jones, D. K., M. A. Horsfield, et al. (1999). "Optimal strategies for measuring diffusion in anisotropic systems by magnetic resonance imaging." Magn Reson Med **42**(3): 515-25.

Jones, D. K., T. R. Knosche, et al. (2012). "White matter integrity, fiber count, and other fallacies: The do's and don'ts of diffusion MRI." Neuroimage.

Kanemura, H. and M. Aihara (2009). "Growth disturbance of frontal lobe in BCECTS presenting with frontal dysfunction." Brain Dev **31**(10): 771-4.

Landman, B. A., J. A. Farrell, et al. (2007). "Effects of diffusion weighting schemes on the reproducibility of DTI-derived fractional anisotropy, mean diffusivity, and principal eigenvector measurements at 1.5T." Neuroimage **36**(4): 1123-38.

Leemans, A. and D. K. Jones (2009). "The B-matrix must be rotated when correcting for subject motion in DTI data." Magn Reson Med **61**(6): 1336-49.

Liasis A, Bamiou DE, et al. (2006). "Evidence for a neurophysiologic auditory deficit in children with benign epilepsy with centro-temporal spikes." J Neural Transmission **113**(7): 939-949.

Lillywhite, L. M., M. M. Saling, et al. (2009). "Neuropsychological and functional MRI studies provide converging evidence of anterior language dysfunction in BECTS." Epilepsia **50**(10): 2276-84.

Loiseau P and Duché B (1989). "Benign childhood epilepsy with centrotemporal spikes." Cleve Clin J Med **56**(Suppl Pt 1): S17-22; discussion S40-2.

Lundberg S, Eeg-Olofsson O, et al. (1999). "Hippocampal asymmetries and white matter abnormalities on MRI in benign childhood epilepsy with centrotemporal spikes." Epilepsia **40**(12): 1808-1815.

Lundberg S, Frylmark A, et al. (2005). "Children with rolandic epilepsy have abnormalities of oromotor and dichotic listening performance." Dev Med Child Neurol **47**(9): 603-608.

Massa R, de Saint-Martin A, et al. (2001). "EEG criteria predictive of complicated evolution in idiopathic rolandic epilepsy." Neurology **57**(6): 1071-1079.

Meister IG, Boroojerdi B, et al. (2003). "Motor cortex hand area and speech: implications for the development of language." Neuropsychologia **41**(4): 401-406.

Miao, W., J. Li, et al. (2012). "Altered White Matter Integrity in Adolescents with Prelingual Deafness: A High-Resolution Tract-Based Spatial Statistics Imaging Study." AJNR Am J Neuroradiol.

Nguyen, D., M. I. Vargas, et al. (2011). "Diffusion tensor imaging analysis with tract-based spatial statistics of the white matter abnormalities after epilepsy surgery." Epilepsy Res.

Overvliet GM, Besseling RM, et al. (2010). "Nocturnal epileptiform EEG discharges, nocturnal epileptic seizures, and language impairments in children: Review of the literature." Epilepsy Behav **19**(4): 550-558.

Overvliet, G. M., R. M. H. Besseling, et al. (2013). "Early onset of cortical thinning in children with rolandic epilepsy." Neuroimage: Clinical **2**(0): 434-439.

Panayiotopoulos, C. P., M. Michael, et al. (2008). "Benign childhood focal epilepsies: assessment of established and newly recognized syndromes." Brain **131**(Pt 9): 2264-86.

Paslawski C (2005). "The Clinical Evaluation of Language Fundamentals, Fourth Edition (CELF-4): A Review." Canadian Journal of School Psychology **20**: 129-134.

Price CJ (2010). "The anatomy of language: a review of 100 fMRI studies published in 2009." Ann N Y Acad Science **1191**: 62-88.

Pulvermuller, F., M. Huss, et al. (2006). "Motor cortex maps articulatory features of speech sounds." Proc Natl Acad Sci U S A **103**(20): 7865-70.

Raffelt, D., J. D. Tournier, et al. (2012). "Apparent Fibre Density: a novel measure for the analysis of diffusion-weighted magnetic resonance images." Neuroimage **59**(4): 3976-94.

Reijmer, Y. D., A. Leemans, et al. (2012). "Improved sensitivity to cerebral white matter abnormalities in Alzheimer's disease with spherical deconvolution based tractography." PLoS One **7**(8): e44074.

Rogalsky, C. and G. Hickok (2011). "The role of Broca's area in sentence comprehension." J Cogn Neurosci **23**(7): 1664-80.

Rogalsky, C., W. Matchin, et al. (2008). "Broca's area, sentence comprehension, and working memory: an fMRI Study." Front Hum Neurosci **2**: 14.

Rose, S., K. Pannek, et al. (2012). "Direct evidence of intra- and interhemispheric corticomotor network degeneration in amyotrophic lateral sclerosis: an automated MRI structural connectivity study." Neuroimage **59**(3): 2661-9.

Schoene-Bake, J. C., J. Faber, et al. (2009). "Widespread affections of large fiber tracts in postoperative temporal lobe epilepsy." Neuroimage **46**(3): 569-76.

Semel E, Wiig EH, et al. (2010). Clinical Evaluation of Language Fundamentals 4, Nederlandse versie. Amsterdam, Pearson

Smith, S. M., M. Jenkinson, et al. (2006). "Tract-based spatial statistics: voxelwise analysis of multi-subject diffusion data." Neuroimage **31**(4): 1487-505.

Smith, S. M. and T. E. Nichols (2009). "Threshold-free cluster enhancement: addressing problems of smoothing, threshold dependence and localisation in cluster inference." Neuroimage **44**(1): 83-98.

Taki, Y., B. Thyreau, et al. (2012). "Linear and curvilinear correlations of brain white matter volume, fractional anisotropy, and mean diffusivity with age using voxel-based and region-of-interest analyses in 246 healthy children." Hum Brain Mapp.

Tournier, J. D., F. Calamante, et al. (2007). "Robust determination of the fibre orientation distribution in diffusion MRI: non-negativity constrained super-resolved spherical deconvolution." Neuroimage **35**(4): 1459-72.

Tournier, J. D., F. Calamante, et al. (2004). "Direct estimation of the fiber orientation density function from diffusion-weighted MRI data using spherical deconvolution." Neuroimage **23**(3): 1176-85.

Tournier, J. D., C. H. Yeh, et al. (2008). "Resolving crossing fibres using constrained spherical deconvolution: validation using diffusion-weighted imaging phantom data." Neuroimage **42**(2): 617-25.

van den Heuvel, M. P., R. C. Mandl, et al. (2010). "Aberrant frontal and temporal complex network structure in schizophrenia: a graph theoretical analysis." J Neurosci **30**(47): 15915-26.

van den Heuvel, M. P. and O. Sporns (2011). "Rich-club organization of the human connectome." J Neurosci **31**(44): 15775-86.

Vannest, J., P. R. Karunanayaka, et al. (2009). "Language networks in children: evidence from functional MRI studies." AJR Am J Roentgenol **192**(5): 1190-6.

Vlooswijk, M. C., J. F. Jansen, et al. (2010). "Functional connectivity and language impairment in cryptogenic localization-related epilepsy." Neurology **75**(5): 395-402.

CHAPTER 7

Delayed convergence between brain network structure and function in rolandic epilepsy

R.M.H. Besseling, J.F.A. Jansen, G.M. Overvliet, S.J.M. van der Kruijs, S.C.M. Ebus, A.J.A. de Louw, P.A.M. Hofman, A.P. Aldenkamp, W.H. Backes

In submission

Abstract

Introduction Rolandic epilepsy (RE) of childhood occurs during a critical phase of brain development, and has been associated with language problems. Concordant abnormalities in both structural and functional connectivity (SC and FC, respectively) have been reported before. However, brain development is characterized by continuous interactions between developing structural and functional circuits, and this interaction may be disturbed as well. The SC-FC correlation is studied as a function of age in children with RE compared to healthy controls.

Materials and methods Twenty-two children with RE and 22 healthy controls underwent structural MRI, as well as functional and diffusion weighted imaging. The anatomical landmarks atlas (137 regions) was used to define network nodes. Correlation of time series was used to determine FC, and tractography streamlines were counted to quantify SC. The SC-FC correlation was investigated over a range of sparsity values (0.01-0.75; based on SC) and compared between groups. The normalized clustering coefficient and path length of both SC and FC were assessed as well. These analyses were also performed for sub-networks as derived from a modularity analysis of the average SC network of the controls.

Results The SC-FC correlation was reduced in patients compared to controls, whereas no consistent abnormalities in structural or functional network organization were found. The SC-FC correlation progressively increased with age in the patients, but not in the controls. At the module level, similar effects were found in a left and a right centro-temporal sub-network, and even more so in a medial parietal module.

Conclusion The developmental integration between SC and FC appears to be disturbed in children with RE. The abnormalities in SC-FC correlation in notably centro-temporal and medial parietal cortex may reflect a maturational delay in the convergence between SC and FC in or near epileptogenic cortex.

7.1 Introduction

Although rolandic epilepsy (RE) is classically considered a benign epilepsy of childhood, over the last decade it has been associated with inattention, impulsivity, and cognitive complaints (Loiseau P and Duché B 1989; Massa R, de Saint-Martin A et al. 2001). The latter notably involves a range of impaired language abilities, such as oromotor deficits, problems in phonological awareness, compromised written language skills, reading disability, and speech sound disorder (Lundberg S, Frylmark A et al. 2005; Papavasiliou A, Mattheou D et al. 2005; Clarke, Strug et al. 2007; Northcott E, Connolly AM et al. 2007; Overvliet GM, Aldenkamp AP et al. 2011). These language impairments can clinically be of greater concern than the seizures, especially since they may persist after spontaneous seizure remission, which in RE is typically seen before the age of 16 years (Hommet C, Billard C et al. 2001; Panayiotopoulos, Michael et al. 2008; Monjauze C, Broadbent H et al. 2011).

In neuroimaging, there has recently been a renewed interest in the integration of the motor and the language system. Several studies have demonstrated that the motor system is not only relevant for language in a straightforward way such as coordination of articulatory movement, but is also involved in purely cognitive aspects of language, such as speech comprehension (Pulvermuller, Huss et al. 2006). For an overview, we refer to the recent work by Cappa and Pulvermuller and the references therein (Cappa and Pulvermuller 2012).

In RE, this moto-lingual integration may be key in linking the epileptic focus in the sensorimotor (i.e. rolandic) cortex to the broad range of associated language impairments. Indeed, using functional MRI it has recently been demonstrated that the integration between the motor and the language system is compromised in RE compared to healthy controls (Besseling, Overvliet et al. 2013; Besseling, Jansen et al. 2013). Concordant abnormalities in structural connectivity have also recently been described (Besseling, Jansen et al. 2013). However, how these functional and structural abnormalities relate to each other remains to be investigated.

It should be noted that RE manifests during a critical and vulnerable phase of brain maturation. The networks that are formed during this period actually are the result of continuous interactions between the developing structural and functional circuits, among other factors (Andersen 2003). Neuropathological cues, such as epileptiform discharges, may offset normal developmental trajectories and compromise the final adult network organization (Andersen 2003). In other words, abnormalities in either structural or functional connectivity (SC and FC, respectively) or their interaction may explain behavioral and cognitive problems in children with RE, as well as their persistence in those that are in seizure remission

(Hommet C, Billard C et al. 2001; Panayiotopoulos, Michael et al. 2008; Monjauze C, Broadbent H et al. 2011).

The study of the association between SC and FC is an emerging field of research, which is rapidly gaining interest (Sporns 2013). Several studies have demonstrated that FC is determined (and constrained) by structural white matter connections (Honey, Kotter et al. 2007; Greicius, Supekar et al. 2009; Honey, Sporns et al. 2009; Honey, Thivierge et al. 2010). Vice versa, simulation studies have shown that functional dynamics are spontaneously self-structuring, and in turn may help to sculpt SC as well (Rubinov, Sporns et al. 2009). It has been suggested that during normal brain development, the SC-FC correlation increases as white matter connections and network dynamics converge under influence of a common optimization process to improve both network efficiency and efficacy (Hagmann, Sporns et al. 2010; Supekar, Uddin et al. 2010).

In epilepsy, abnormalities in either SC or FC have extensively been described, as recently reviewed by Van Diessen et al. (van Diessen, Diederen et al. 2013). However, abnormalities in the SC-FC correlation have hardly been investigated, and to our knowledge not yet in the developing epileptic child.

In the current work, the SC-FC correlation is investigated as a function of age in children with RE compared to healthy controls. A modularity analysis is employed to investigate whether potential abnormalities can be localized to certain sub-network, and graph-theoretical measures are employed to check for underlying aberrant SC and/or FC network organization.

7.2 Materials and methods

7.2.1 Patient selection

Twenty-two children with RE (8 girls; age, mean±SD: 11.3±2.0 years) were selected at our specialized epilepsy referral center. Selection criteria included centro-temporal spikes on EEG and concordant seizure semiology, representing anarthria, hemiclonia involving the face and/or unilateral extremities, or secondarily generalized seizures. In case of poorly observed nocturnal seizures, post-ictal signs of a generalized seizure or confirmation of post-ictal hemiparesis was sufficient for inclusion in case of otherwise typical EEG. Further details were described previously (Overvliet, Besseling et al. 2013).

In addition, 22 healthy controls were enrolled in the study (11 girls, age 10.5±1.6 years). All patients had an IQ>70 and all controls attended regular education, and had neither (a history of) neurological disorders, nor learning problems. The parents or guardians of all children gave written informed consent for study participation, and the study was approved by the ethical review boards of both participating institutions.

7.2.2 Magnetic Resonance Imaging

Conventional structural magnetic resonance imaging (MRI) was applied, as well as diffusion weighted imaging (DWI) and functional MRI (fMRI). Structural imaging included a T1-weigthed sequence. A 3D fast-spoiled gradient echo sequence was used, employing echo time/repetition time/inversion time (TE/TR/TI) 3.8/8.3/1022 ms, and at a resolution of 1x1x1 mm^3. The acquisition time was 8 min.

Also high angular resolution diffusion weighted imaging (HARDI) was performed, employing 66 non-colinear gradient directions (Jones, Horsfield et al. 1999), and a diffusion-sensitizing b-value of 1200 s/mm^2. In addition, a single minimally diffusion-weighted image (b0-scan) was acquired. Other settings were: echo planar imaging (EPI) sequence, TE/TR 72/6600 ms, resolution 2x2x2 mm^3, and acquisition time 9 min.

Functional MRI involved a task-free T2*-weighted blood oxygen level dependent (BOLD) sequence of 195 dynamic image volumes at a TR of 2s, resulting in an acquisition time of 6.5 min. Further settings included: EPI sequence, TE 35 ms, 2x2 mm^2 in plane resolution, and 4 mm thick axial slices.

7.2.3 Cortical parcellation

The probabilistic anatomical landmark atlas of gyri, sulci, and basal ganglia was used to parcellate the cortical and subcortical gray matter (Perrot, Riviere et al. 2009; Gaël Varoquaux, Alexandre Gramfort et al. 2010). The anatomical landmark atlas consists of N=137 volumes, each representing a probabilistic map for a certain brain region. To map this atlas to native T1 space, affine registrations were implemented using SPM (version 8). In addition, deterministic node labels were constructed by assigning each voxel to its region of maximum probability.

7.2.4 Structural connectivity

The diffusion-weighted data were preprocessed and tractography was performed as previously described (Besseling, Jansen et al. 2012). Briefly, this involves that the diffusion-weighted volumes were registered to the b0-scan to correct for head motion and EPI distortions using affine registrations as implemented in CATNAP (Coregistration, Adjustment, and Tensor-solving: a Nicely Automated Program). CATNAP is based on FSL routines (FMRIB Software Library) and includes correction of the gradient directions for rotations (Landman, Farrell et al. 2007; Leemans and Jones 2009).

Next, constrained spherical deconvolution (CSD) was used to estimate voxel-wise fiber orientation distributions (FODs). CSD FODs can represent multiple fiber orientation per voxel, and thus account for partial volume effects such as within-voxel fiber kissing, crossing and bending (Tournier, Calamante et al. 2007; Tournier, Yeh et al. 2008; Tournier, Calamante et al. 2012). The CSD

response function was estimated from the data employing high fractional anisotropy voxels (FA>0.7) and a CSD order of l_{max}=8 (i.e. 45 spherical harmonics) was used; for details, see (Tournier, Calamante et al. 2009; Besseling, Jansen et al. 2012).

Probabilistic tractography was performed employing MRtrix to extrapolate voxel-wise FODs to global (semi)continuous streamlines (Tournier, Calamante et al. 2012). Per subject, 50.000 streamlines were seeded from the gray matter (FSL based tissue segmentation of the T1 scan), and propagated over the brain to represent the overall topology of the global white matter network. Standard MRtrix tractography settings were used, which includes a streamline propagation step size of 0.2 mm, a minimum radius of curvature of 1 mm, and an FOD amplitude threshold >0.1.

Structural connectivity (SC) was investigated for the deterministic node labels. For this, first the streamlines were mapped to the T1-space based on an affine registration of the b0-scan to the T1-scan using FSL (Pannek, Mathias et al. 2011). Next, for each pair of nodes, the interconnecting streamlines were assessed. As larger nodes typically contain more streamlines, connection strength was quantified as the number of streamlines normalized for the number of voxels per node pair (van den Heuvel and Sporns 2011; Zhang, Liao et al. 2011).

7.2.5 Functional connectivity

Preprocessing of the functional data included registration of all fMRI volumes to the first dynamic to correct for head motion employing SPM8. Subsequently, the mean fMRI image volume was calculated and used to affinely register the fMRI data to the native T1-space.

The T1 tissue segmentation was downsampled to the fMRI resolution to calculate averaged time series for the white matter and the CSF. These time series, combined with the movement parameters of the previous step, were used as nuisance regressors to deconfound the fMRI data employing linear regression. This procedure is assumed to provide a more specific and robust correction for non-neuronal signal fluctuations such as scanner drift or physiological noise (cardioballistics and breathing) than whole-brain signal regression (Smith, Miller et al. 2011).

Finally, the fMRI data were smoothed using a Gaussian kernel of full-width-at-half-maximum 10 mm, and band-pass filtered to confine the signal to the range of 0.01-0.1 Hz typically used in resting-state fMRI analyses (Zalesky, Fornito et al. 2010; Cocchi, Bramati et al. 2012; Hong, Zalesky et al. 2013).

Functional connectivity (FC) was assessed using correlation of node pair time series. The probabilistic atlas maps were used to calculate these node time series as a weighted average, effectively assigning more weight to the core and less weight to the border of each node.

7.2.6 Correlation between structural and functional connectivity

To assess the SC-FC correlation, the SC values were resampled to a normal distribution of mean 0.5 and SD 0.1 following previous work (Honey, Sporns et al. 2009; Zhang, Liao et al. 2011). Furthermore, negative FC values were set to zero (Smith, Miller et al. 2011).

For each subject, the SC-FC association was calculated by appending the SC and FC values of the non-zero structural connections in two separate vectors, which were subsequently correlated. To assess the robustness of the above analysis, it was applied over a range of sparsity values. This means that not all structural connections were included in the correlation analysis, but only a certain top percentage.

The sparsity structure (i.e. which connections were included) was based on the mean SC matrix of the controls, see Figure 7.1. Since the mean sparsity of the SC of the controls was 0.75, a sparsity range of 0.01-0.75 was chosen, corresponding to 93-6987 connections. Sparsity values were incremented at a step size of 0.01.

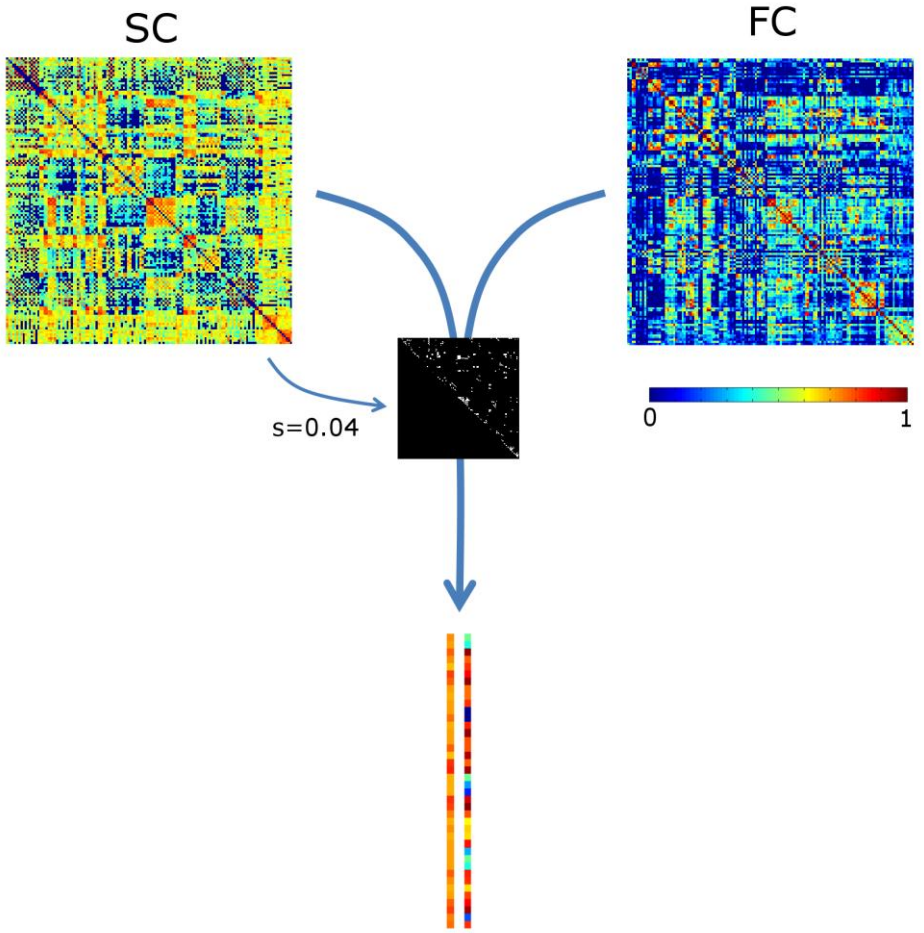

Figure 7.1: Assessing the correlation between structural and functional connectivity (SC and FC, respectively). The most prominent structural connections (here at sparsity s=0.04) are selected. The SC and FC values of these are appended in 2 vectors, which are subsequently correlated.
For visualization purposes, the vectors are not visualized in full length. SC values were scaled to a Gaussian distribution (mean,SD: 0.5,0.1); negative FC values were set to 0.

7.2.7 Modularity analysis

To investigate whether potential abnormalities in SC-FC correlation may be contributed to specific brain sub-networks, a modularity analysis was applied to the average SC network of the controls using the Brain Connectivity Toolbox (BCT; (Rubinov and Sporns 2010)). This analysis clusters nodes into modules, based on relatively high within-module and low between-module connectivity (Newman 2006). Because of heuristics in the algorithm, the modularity analysis was repeated 100 times, and the most robust modularity structure (of highest occurrence) was retained.

7.2.8 Assessing differences in structure-function correlation

Abnormalities in SC-FC correlation in patients compared to controls were inferred upon using a general linear model (GLM), in which also the effect of age was incorporated. Group differences with respect to SC-FC correlation were deemed significant on the whole-brain level for $p<0.05$. If such a significant group difference was found, it was investigated whether it could be attributed to one (or multiple) of the sub-networks, employing Bonferroni multiple comparisons correction for the number of sub-networks under investigation.

7.2.9 Measures of network organization

To investigate whether SC and/or FC as such were abnormal, graph theoretical measures of network integrity were calculated. For each subject, structural and functional network organization were quantified by average path length and clustering coefficient as assessed using the BCT. Individual SC and FC connectivity matrices were scaled with respect to their total connectivity weight to normalize the "wiring cost" over subjects (Zhang, Liao et al. 2011). Potential differences in graph measures thus only reflect differences in the distribution of connectivity values, similar to the SC-FC correlation analysis which also only takes the distribution of the connectivity values into account (and not their amplitude). Furthermore, for each subject the graph measures were normalized with respect to comparable random graphs (N=20) (van den Heuvel and Sporns 2011). The comparisons between patients and controls were performed using the same GLM as described above.

7.3 Results

The modularity analysis revealed 5 clusters: a prefrontal cluster, a medial parietal cluster, an inferior temporo-occipital cluster, and left and right centro-temporal clusters, see Figure 7.2.

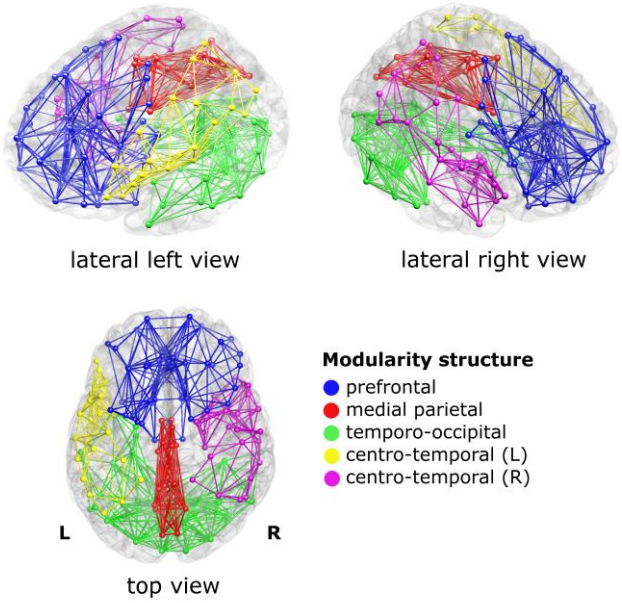

Figure 7.2: Sub-networks as derived from a modularity analysis of the mean structural connectivity (SC) network of the controls. Five sub-networks (i.e. modules) were found; a prefrontal cluster (blue), a medial parietal cluster (red), an inferior temporo-occipital cluster (green), and a left and a right centro-temporal cluster (yellow and magenta, respectively).
For visualization purposes, only the within-module connections were visualized, at sparsity level 0.1.

At the whole-brain level, significant reductions in SC-FC correlation were found in the patients for the most prominent brain connections (sparsity range 0.01-0.11; Figure 7.3A, top row). Within this sparsity range, the SC-FC correlation was also consistently reduced within all 5 modules. Significant effects were found in the medial parietal cluster, and also in the bilateral centro-temporal clusters. Within the medial parietal cluster, the reduction in SC-FC correlation was most robust over the sparsity range, and also most pronounced (Figure 7.3A; $p<0.01$).

For a representative sparsity value of 0.04, the connections under investigation and the regression lines are given for the whole brain and the medial parietal cluster in Figure 7.3B and C, respectively. Note the significant progressive increase in SC-FC correlation in the patients; no such age effect was found in the controls. This implies that the group differences were strongest for the youngest participants and diminished towards the end of the age window under investigation (8-14 years).

Concerning graph analysis, no clear differences in either SC or FC network organization were found between patients and controls. For single sparsity values,

a decrease in SC clustering coefficient and an increase in FC path length were found (sparsity 0.04 and 0.08, respectively), see Figure 7.4. No consistent effects were found over any of the modules under investigation.

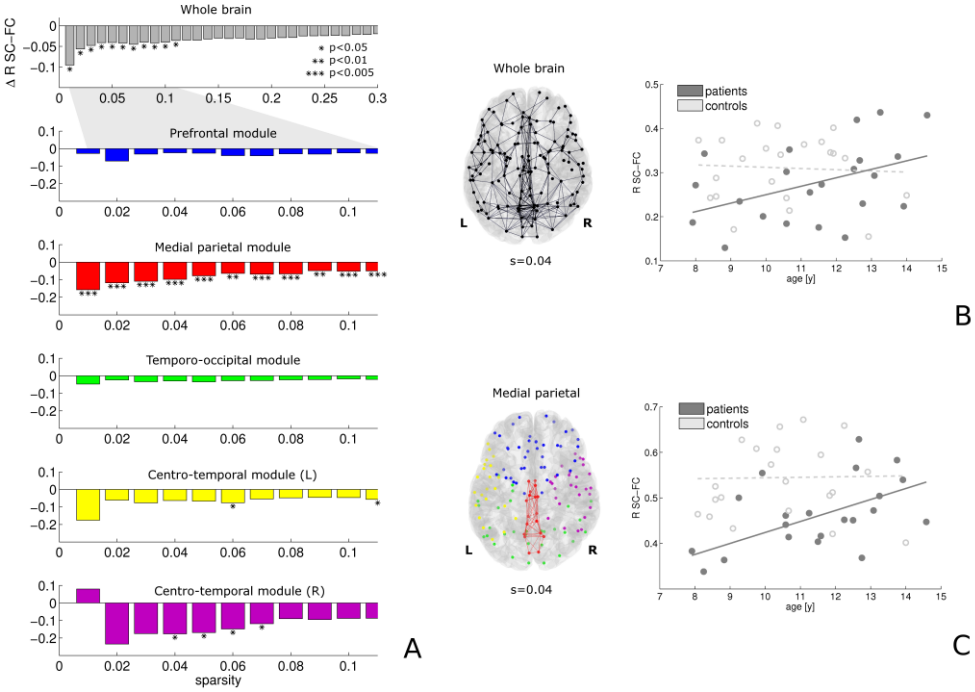

Figure 7.3: At the whole-brain level, the correlation between structural and functional connectivity is reduced in patients versus controls for the sparsity range 0.01-0.11 (A, top). Within this sparsity range, similar effects were found in all modules; effects of highest significance were found within the medial parietal module (A, third plot from above). For sparsity value 0.04, the connections investigated and the regression lines are given in B and C for the whole brain and the medial parietal module, respectively. Note that the reduction is SC-FC correlation is more pronounced in the medial parietal module. Furthermore, significant increases in SC-FC correlation with age were found in the patients only (solid lines).

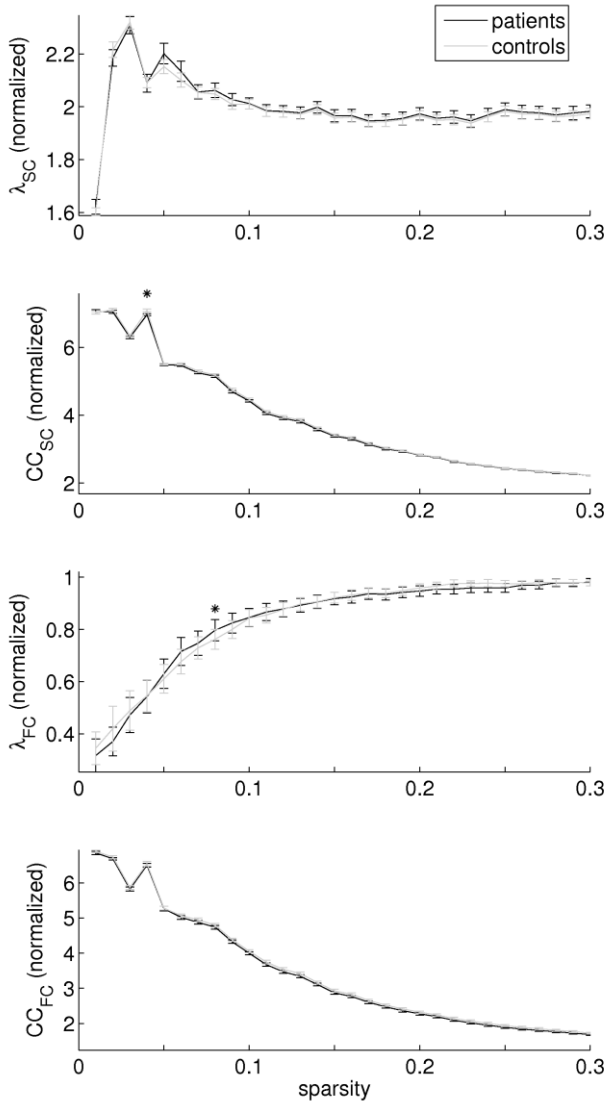

Figure 7.4: Structural and functional connectivity (SC and FC, respectively) were investigated separately by assessing the normalized path length (λ) and clustering coefficient (CC). Effects were limited to a decrease in SC clustering coefficient for sparsity value 0.04, and an increase in FC path length for sparsity value 0.08.

7.4 Discussion

In this study, we investigated the correlation between SC and FC as a function of age in children with RE compared to healthy controls. We employed a modularity analysis to investigate whether potential effects on the whole-brain level may be attributed to certain sub-networks. Additionally, graph theoretical measures of network organization were used to assess SC and FC separately, both at the global level and concerning the identified modules.

7.4.1 Major findings

Our main results are:

1) In children with RE, the SC-FC correlation is reduced compared to healthy controls at the whole-brain level;
2) The SC-FC correlation increases with age in the children with RE, implying that the reduction in SC-FC correlation is less pronounced towards the end of the age window under investigation (8-14 years);
3) Similar effects were found at the module level, i.e. for the bilateral centro-temporal clusters and most notably for the medial parietal cluster, in which the reduction in SC-FC correlation was more pronounced than at the whole-brain level;
4) Employing graph analysis, no prominent abnormalities of SC nor FC network organization were found.

7.4.2 Interpretation of differences in SC-FC correlation

During normal brain maturation, network structure and function gradually adapt to each other, leading to an increase in the SC-FC correlation (Hagmann, Sporns et al. 2010; Supekar, Uddin et al. 2010). In adults with idiopathic generalized epilepsy, reductions in SC-FC correlation have been described which are more pronounced for increased disease duration (Zhang, Liao et al. 2011). From these findings, one may deduce that an increase in SC-FC correlation signifies an improvement of network organization, and vice versa. In contrast, increased SC-FC correlation has recently been reported in idiopathic generalized epilepsy as well (Liao, Zhang et al. 2013).

To understand these seemingly contradictory results, note that the correlation between SC and FC only quantifies how well brain structure and function match, but conveys no direct information on structural or functional network integrity as such. During normal brain development, SC and FC may converge driven by a common optimization process to improve network efficiency and efficacy (Andersen 2003). In epilepsy, on the other hand, various scenarios may apply. If brain structure and function are differentially affected by the

epilepsy, SC and FC may diverge and the SC-FC correlation decreases. However, if both SC and FC strongly reflect epileptic remodeling, this may actually increase the SC-FC correlation. To which extent either of these scenarios applies may depend on the type of epilepsy, the disease duration, the seizure frequency, and anti-epileptic drug use, among other factors (van Diessen, Diederen et al. 2013).

7.4.3 Measures of network organization

To interpret the current finding of reduced SC-FC correlation in children with RE compared to healthy controls, we assessed potential abnormalities in structural and functional network integrity separately employing graph theoretical measures. A decrease in SC clustering coefficient and an increase in FC path length were found. Both findings may represent reduced network integrity, and similar findings have been reported in epilepsy before (van Diessen, Diederen et al. 2013). However, although these effects were within the sparsity range of global SC-FC correlation effect (0.01-0.11), they were only found for single sparsity values, and within this sparsity range, also no consistent module effects were found. These findings suggest that in RE, gross abnormalities in structural and/or functional network organization are not the case. Indeed, RE is a relatively mild disorder compared to other epilepsy syndromes within the same spectrum, such as Landau Kleffner Syndrome (Hughes 2010; Overvliet GM, Besseling RM et al. 2010). Our finding of reduced SC-FC correlation should thereby be interpreted in the context of aberrant brain maturation, and reflects a reduced convergence between network structure and function. In agreement, cortical abnormalities, reflective of impaired development of the underlying network, have been reported in RE before (Overvliet, Besseling et al. 2013).

7.4.4 Effect of age

Note that the SC-FC correlation actually progressively increased with age in the patients, whereas no age effect was found in the controls. This suggests that the maturational convergence of SC and FC is merely delayed in RE. Potentially, for the age range under investigation (8-14 years), network structure and function are already to a certain extent matched for the controls, whereas in the children with RE, this optimization process is still ongoing. However, given the persistence of cognitive complaints, a full recovery of the SC-FC correlation is not expected (Hommet C, Billard C et al. 2001; Andersen 2003; Monjauze C, Broadbent H et al. 2011).

7.4.5 Localization to sub-networks

Concerning the localization of effects, the overall reduction in SC-FC correlation seems to be particularly attributable to a medial parietal network, where the effect was actually more pronounced than at the whole-brain level. Note that the parietal

lobe has been associated with visuo-spatial skills, which may indeed be impaired in RE (Pinton, Ducot et al. 2006; Volkl-Kernstock, Willinger et al. 2006).

More importantly, the medial parietal module provides an interface between the bilateral centro-temporal modules, from which the epileptiform activity originates (i.e. RE typical centro-temporal spikes). The SC-FC correlation appeared (to a lesser extent) compromised within these centro-temporal modules themselves as well. Abnormalities in the left centro-temporal module may translate to the prominent language impairments in RE, as this module roughly covers classical inferior frontal and supramarginal language areas (Broca's and Wernicke's, respectively). Furthermore, since language lateralization is limited in children in general (Kadis, Pang et al. 2011) and in RE in particular (Besseling, Overvliet et al. 2013), impairments of contralateral (right hemisphere) homotopic cortex may also relate to compromised language skills.

The module effect was more robust for the medial parietal module than for the centro-temporal modules, which might be due to variations in the laterality of EEG abnormalities. Defining a homogeneous RE cohort with respect to electrophysiology is very challenging as the laterality (and extent) of the EEG abnormalities may dramatically change over time (Riva, Vago et al. 2007). Actually this is considered a general confound for epilepsy connectivity studies (van Diessen, Diederen et al. 2013). Since in our clinical cohort electrophysiology was assessed during the diagnostic work-up and not at the time of scanning, the patients can be assumed to be somewhat heterogenous with respect to EEG characteristics. On the group level, an un-lateralized module effect may therefore be the most robust.

7.4.6 Methodological consideration and directions for future research

Concerning the localization of the network impairments, it is unclear whether the modularity structure employed in this study was optimal to detect aberrant sub-networks in RE. The sub-networks we investigated were derived from an unbiased graph theoretical modularity analysis. For the atlas we employed, this yielded a robust set of 5 compact clusters with a relatively straightforward anatomical description and interpretation.

Note that specific investigations of e.g. the language network may have yielded more illustrative results in the context of the RE-typical neuropsychological profile of language impairment (Overvliet GM, Besseling RM et al. 2010). However, this would be at the cost of subjective choices, since at present the language network cannot unambiguously be identified from e.g. functional connectivity patterns (Beckmann, DeLuca et al. 2005; Besseling, Overvliet et al. 2013).

In any case, our findings illustrate that investigations into the SC-FC correlation can be used to infer where in the brain neuronal network formation is impaired, and as such our study extends the work by Zhang et al on generalized epilepsy to localization-related epilepsies such as RE (Zhang, Liao et al. 2011).

In our cross-sectional study, the effect of age could only be assessed by virtue of the variability in age of the subjects included. Longitudinal studies are called for to verify the robustness of our findings. Follow-up until after seizure remission is proposed to investigate to what extent the reported abnormalities may eventually normalize.

7.5 Conclusion

In children with RE, the correlation between SC and FC is reduced compared to healthy controls. As structural nor functional network organization seems much affected, this is interpreted as reduced matching of SC and FC due to aberrant brain maturation. Since the reduction is SC-FC correlation diminishes as a function of age, these findings may actually represent a maturational delay. Concerning the localization of brain network abnormalities, the observed effects seem especially attributable to medial parietal connections, which form an intermediate between the bilateral centro-temporal modules of epileptiform activity.

Acknowledgements

We would like to acknowledge Esther Peeters for data acquisitions and Marc Geerlings and Jos Slenter for continuous hardware and software support. The Dutch Epilepsy Foundation we thank for research funding, and the participating children and their families for their time and commitment, and their interest in our work.

References

Andersen, S. L. (2003). "Trajectories of brain development: point of vulnerability or window of opportunity?" Neurosci Biobehav Rev ***27****(1-2): 3-18.*

Beckmann, C. F., M. DeLuca, et al. (2005). "Investigations into resting-state connectivity using independent component analysis." Philos Trans R Soc Lond B Biol Sci ***360****(1457): 1001-13.*

Besseling, R., J. Jansen, et al. (2013). "Reduced structural connectivity between sensorimotor and language areas in rolandic epilepsy." PloS One ***in press****.*

Besseling, R., G. Overvliet, et al. (2013). "Aberrant functional connectivity between motor and language networks in rolandic epilepsy." Epilepsy Res ***in press****.*

Besseling, R. M., J. F. Jansen, et al. (2012). "Tract specific reproducibility of tractography based morphology and diffusion metrics." PLoS One ***7****(4): e34125.*

Besseling, R. M. H., J. F. Jansen, et al. (2013). "Reduced functional integration of the sensorimotor and language network in rolandic epilepsy." Neuroimage: Clinical.

Cappa, S. F. and F. Pulvermuller (2012). "Cortex special issue: language and the motor system." Cortex ***48****(7): 785-7.*

Clarke, T., L. J. Strug, et al. (2007). "High risk of reading disability and speech sound disorder in rolandic epilepsy families: case-control study." Epilepsia ***48****(12): 2258-65.*

Cocchi, L., I. E. Bramati, et al. (2012). "Altered functional brain connectivity in a non-clinical sample of young adults with attention-deficit/hyperactivity disorder." J Neurosci ***32****(49): 17753-61.*

Gaël Varoquaux, Alexandre Gramfort, et al. (2010). "Brain covariance selection: better individual functional connectivity models using population prior." arXiv:1008.5071v4 [stat.ML].

Greicius, M. D., K. Supekar, et al. (2009). "Resting-state functional connectivity reflects structural connectivity in the default mode network." Cereb Cortex ***19****(1): 72-8.*

Hagmann, P., O. Sporns, et al. (2010). "White matter maturation reshapes structural connectivity in the late developing human brain." Proc Natl Acad Sci U S A ***107****(44): 19067-72.*

Hommet C, Billard C, et al. (2001). "Cognitive function in adolescents and young adults in complete remission from benign childhood epilepsy with centro-temporal spikes." Epileptic Disord. ***3****(4): 207-216.*

Honey, C. J., R. Kotter, et al. (2007). "Network structure of cerebral cortex shapes functional connectivity on multiple time scales." Proc Natl Acad Sci U S A ***104****(24): 10240-5.*

Honey, C. J., O. Sporns, et al. (2009). "Predicting human resting-state functional connectivity from structural connectivity." Proc Natl Acad Sci U S A ***106****(6): 2035-40.*

Honey, C. J., J. P. Thivierge, et al. (2010). "Can structure predict function in the human brain?" Neuroimage ***52****(3): 766-76.*

Hong, S. B., A. Zalesky, et al. (2013). "Decreased functional brain connectivity in adolescents with internet addiction." PLoS One ***8****(2): e57831.*

Hughes, J. R. (2010). "Benign epilepsy of childhood with centrotemporal spikes (BECTS): to treat or not to treat, that is the question." Epilepsy Behav ***19****(3): 197-203.*

*Jones, D. K., M. A. Horsfield, et al. (1999). "Optimal strategies for measuring diffusion in anisotropic systems by magnetic resonance imaging." Magn Reson Med **42**(3): 515-25.*

*Kadis, D. S., E. W. Pang, et al. (2011). "Characterizing the normal developmental trajectory of expressive language lateralization using magnetoencephalography." J Int Neuropsychol Soc **17**(5): 896-904.*

*Landman, B. A., J. A. Farrell, et al. (2007). "Effects of diffusion weighting schemes on the reproducibility of DTI-derived fractional anisotropy, mean diffusivity, and principal eigenvector measurements at 1.5T." Neuroimage **36**(4): 1123-38.*

*Leemans, A. and D. K. Jones (2009). "The B-matrix must be rotated when correcting for subject motion in DTI data." Magn Reson Med **61**(6): 1336-49.*

*Liao, W., Z. Zhang, et al. (2013). "Relationship between large-scale functional and structural covariance networks in idiopathic generalized epilepsy." Brain Connect **3**(3): 240-54.*

*Loiseau P and Duché B (1989). "Benign childhood epilepsy with centrotemporal spikes." Cleve Clin J Med **56**(Suppl Pt 1): S17-22; discussion S40-2.*

*Lundberg S, Frylmark A, et al. (2005). "Children with rolandic epilepsy have abnormalities of oromotor and dichotic listening performance." Dev Med Child Neurol **47**(9): 603-608.*

*Massa R, de Saint-Martin A, et al. (2001). "EEG criteria predictive of complicated evolution in idiopathic rolandic epilepsy." Neurology **57**(6): 1071-1079.*

*Monjauze C, Broadbent H, et al. (2011). "Language deficits and altered hemispheric lateralization in young people in remission from BECTS." Epilepsia **52**(8): e79-e83.*

*Newman, M. E. (2006). "Modularity and community structure in networks." Proc Natl Acad Sci U S A **103**(23): 8577-82.*

*Northcott E, Connolly AM, et al. (2007). "Memory and phonological awareness in children with Benign Rolandic Epilepsy compared to a matched control group." Epilepsy Research **75**(1): 57-62.*

*Overvliet GM, Aldenkamp AP, et al. (2011). "Impaired language performance as a precursor or consequence of Rolandic epilepsy?" Journal of the Neurological Sciences **304**(1): 71-74.*

*Overvliet GM, Besseling RM, et al. (2010). "Nocturnal epileptiform EEG discharges, nocturnal epileptic seizures, and language impairments in children: Review of the literature." Epilepsy Behav **19**(4): 550-558.*

*Overvliet, G. M., R. M. H. Besseling, et al. (2013). "Early onset of cortical thinning in children with rolandic epilepsy." Neuroimage: Clinical **2**(0): 434-439.*

*Panayiotopoulos, C. P., M. Michael, et al. (2008). "Benign childhood focal epilepsies: assessment of established and newly recognized syndromes." Brain **131**(Pt 9): 2264-86.*

*Pannek, K., J. L. Mathias, et al. (2011). "The average pathlength map: a diffusion MRI tractography-derived index for studying brain pathology." Neuroimage **55**(1): 133-41.*

*Papavasiliou A, Mattheou D, et al. (2005). "Written language skills in children with benign childhood epilepsy with centrotemporal spikes." Epilepsy & Behavior **6**(1): 50-58.*

*Perrot, M., D. Riviere, et al. (2009). "Joint Bayesian cortical sulci recognition and spatial normalization." Inf Process Med Imaging **21**: 176-87.*

*Pinton, F., B. Ducot, et al. (2006). "Cognitive functions in children with benign childhood epilepsy with centrotemporal spikes (BECTS)." Epileptic Disord **8**(1): 11-23.*

*Pulvermuller, F., M. Huss, et al. (2006). "Motor cortex maps articulatory features of speech sounds." Proc Natl Acad Sci U S A **103**(20): 7865-70.*

*Riva, D., C. Vago, et al. (2007). "Intellectual and language findings and their relationship to EEG characteristics in benign childhood epilepsy with centrotemporal spikes." Epilepsy Behav **10**(2): 278-85.*

*Rubinov, M. and O. Sporns (2010). "Complex network measures of brain connectivity: uses and interpretations." Neuroimage **52**(3): 1059-69.*

*Rubinov, M., O. Sporns, et al. (2009). "Symbiotic relationship between brain structure and dynamics." BMC Neurosci **10**: 55.*

*Smith, S. M., K. L. Miller, et al. (2011). "Network modelling methods for FMRI." Neuroimage **54**(2): 875-91.*

*Sporns, O. (2013). "The human connectome: origins and challenges." Neuroimage **80**: 53-61.*

*Supekar, K., L. Q. Uddin, et al. (2010). "Development of functional and structural connectivity within the default mode network in young children." Neuroimage **52**(1): 290-301.*

Tournier, J. D., F. Calamante, et al. (2007). "Robust determination of the fibre orientation distribution in diffusion MRI: non-negativity constrained super-resolved spherical deconvolution." Neuroimage ***35****(4): 1459-72.*

Tournier, J. D., F. Calamante, et al. (2009). How many diffusion gradient directions are required for HARDI? Proc. Intl. Soc. Mag. Reson. ***17****.*

Tournier, J. D., F. Calamante, et al. (2012). "MRtrix: Diffusion tractography in crossing fiber regions." International Journal of Imaging Systems and Technology ***22****(1): 53-66.*

Tournier, J. D., C. H. Yeh, et al. (2008). "Resolving crossing fibres using constrained spherical deconvolution: validation using diffusion-weighted imaging phantom data." Neuroimage ***42****(2): 617-25.*

van den Heuvel, M. P. and O. Sporns (2011). "Rich-club organization of the human connectome." J Neurosci ***31****(44): 15775-86.*

van Diessen, E., S. J. Diederen, et al. (2013). "Functional and structural brain networks in epilepsy: What have we learned?" Epilepsia ***54****(11): 1855-65.*

Volkl-Kernstock, S., U. Willinger, et al. (2006). "Spacial perception and spatial memory in children with benign childhood epilepsy with centro-temporal spikes (BCECTS)." Epilepsy Res ***72****(1): 39-48.*

Zalesky, A., A. Fornito, et al. (2010). "Network-based statistic: identifying differences in brain networks." Neuroimage ***53****(4): 1197-207.*

Zhang, Z., W. Liao, et al. (2011). "Altered functional-structural coupling of large-scale brain networks in idiopathic generalized epilepsy." Brain ***134****(Pt 10): 2912-28.*

CHAPTER 8

Abnormal profiles of local functional connectivity proximal to focal cortical dysplasias

R.M.H. Besseling, J.F.A. Jansen, A.J.A. de Louw, M.C.G. Vlooswijk,
M.C. Hoeberigs, A.P. Aldenkamp, W.H. Backes, P.A.M. Hofman

In submission

Abstract

Purpose Focal cortical dysplasia (FCD) is a congenital malformation of cortical development that often leads to medically refractory epilepsy. Focal resection can be an effective treatment, but is challenging as the surgically relevant abnormality may exceed the MRI-visible lesion. The aim of the current study is to describe the profile of functional connectivity around FCDs using resting-state functional MRI. The detection of aberrant connectivity may provide a means to more completely delineate the clinically relevant lesion.

Materials and methods Fifteen FCD patient and 16 matched healthy controls underwent structural and functional imaging at 3 Tesla. The cortical surface was reconstructed from the T1-weighted scan and the registered functional MRI data was spatially normalized to a common anatomical standard space employing the gyral pattern. Seed-based functional connectivity was determined in all subjects for all dysplasia locations. A single patient was excluded based on an aberrant FCD seed time series.
Functional connectivity as a function of geodesic distance (along the cortical surface) was compared between the individual patients and homotopic normative connectivity profiles derived from the controls.

Results In 13/15 patients, aberrant profiles of functional connectivity were found, which demonstrated both hyper- and hypoconnectivity as well as combinations. Abnormal functional connectivity was typically found (also) beyond the lesion visible on structural MRI.

Conclusion This novel functional MRI technique might be of value for delineating clinically relevant aberrant cortex beyond the structural lesion in FCD.

8.1 Introduction

Focal cortical dysplasias (FCDs) are congenital malformations of cortical development that are highly epileptogenic, and often give rise to medically refractory epilepsy (Taylor, Falconer et al. 1971; Blumcke, Thom et al. 2011). Resection of the dysplasia can be an effective treatment, and FCD is the most common etiology in children and the third most frequent finding in adults undergoing epilepsy neurosurgery (Hauptman and Mathern 2012).

Accurate visualization through neuroimaging is crucial for surgical planning and outcome. Histopathological examination of surgical specimens has demonstrated that 80% of patients who had a complete resection become seizure free, compared to only 20% for incomplete resections (Hauptman and Mathern 2012). Advances in MR technology such as higher field strengths and improved head coils have significantly increased the diagnostic yield, and allow the detection and demarcation of smaller and more subtle lesions (Winston, Micallef et al. 2013).

Semi-automatic approaches that enhance morphological characteristics of FCD such as cortical thickening and blurring of the gray matter- white matter interface may aid lesion detection (Yagishita, Arai et al. 1997; Kassubek, Huppertz et al. 2002; Hofman, Fitt et al. 2011). The presence of underlying white matter abnormalities may also help to more completely delineate the region of aberrant cortex. For example, it has recently been reported that postsurgical outcome is significantly better in patients with an FCD-typical white matter transmantle sign compared to those without (Wang, Deans et al. 2013).

In an attempt to improve sensitivity for white matter abnormalities compared to conventional structural imaging, diffusion weighted imaging (DWI) has been used to study white matter microstructure and structural connectivity. Compared to the contralateral hemisphere, lower fractional anisotropy (FA) was found in directly adjacent white matter, indicative of reduced microstructural tissue integrity, as well as reduced volume of nearby major white matter tracts (Lee, Kim et al. 2004; Widjaja, Blaser et al. 2007). Also distal effects of reduced FA have been found, in major white matter tracts projecting to or from the FCD (Widjaja, Zarei Mahmoodabadi et al. 2009).

Alternatively, the functional connectivity of FCDs may be investigated. Since functional connectivity analysis assesses similarities in gray matter time series, this may provide a more direct way to demarcate aberrant cortex. Furthermore, since functional and structural connectivity are mutually dependent, functional remodeling is to be expected in relation to the already described (micro)structural changes (Widjaja, Blaser et al. 2007; Widjaja, Zarei Mahmoodabadi et al. 2009; Fonseca Vde, Yasuda et al. 2012; Wang, Deans et al. 2013).

In this study, we investigate functional connectivity as a function of distance from the MR-visible structural lesion in a cohort of patients with FCD. Distance is defined as the geodesic distance (along the cortical surface), as an approximation to the distance of information flow along juxtacortical short association fibers, in order to study local connectivity. FCD connectivity profiles are compared to normative profiles derived from homotopic cortex in matched healthy controls. The aim is to detect local abnormalities in functional connectivity, reflecting the broader focal abnormality of the underlying tissue.

8.2 Materials and methods

8.2.1 Subjects

Fifteen patients with FCD-related epilepsy were recruited at our specialized epilepsy referral center (age, mean±SD: 31±11 years; 11 males), as well as 16 age and gender matched healthy controls (35±9 years, 7 males).

The clinical diagnosis was based on concordance between seizure semiology, EEG findings, and neuroimaging (Taylor, Falconer et al. 1971; Palmini, Najm et al. 2004; Blumcke, Thom et al. 2011). Briefly, this involved recurrent stereotyped seizures and focal interictal and/or ictal EEG abnormalities that coincided with an FCD-concordant lesion on MRI (Chassoux, Landre et al. 2012). Relevant imaging features included, among others, abnormal gyral pattern, increased cortical thickness, transmantle sign, and blurring of the gray matter-white matter interface (Yagishita, Arai et al. 1997; Rastogi, Lee et al. 2008; Blumcke, Thom et al. 2011), for an example, see Figure 8.1. Information on individual dysplasia locations and EEG findings are given in Table 8.1.

All subjects underwent structural as well as functional MRI at 3T (Philips Achieva, Best, the Netherlands) using an 8-element receive-only SENSE head-coil.

Informed written consent was acquired from all subjects, and the study was approved by the ethics committees of both participating institutions.

8.2.2 MR imaging

Structural imaging involved a T1-weighted scan employing the following settings: 3D fast spoiled gradient echo sequence; echo time/repetition time/inversion time (TE/TR/TI) 3.8/8.3/1022 ms; voxel size 1x1x1 mm^3; and acquisition time 7.5 min. In addition, a fluid attenuated inversion recovery (FLAIR) sequence was used (3D turbo spin echo; TE/TR/TI 330/8000/2400 ms; 0.4x0.4x mm^2 in plane resolution, 0.6 mm axial slices; and acquisition time 8 min).

Functional MRI involved a blood oxygen level dependent (BOLD) T2*-weighted task-free scan, for which the participants were instructed to close their eyes, lie still, and think of nothing in particular. The settings were: single-shot echo

planar imaging (EPI) sequence; TE/TR 35/2000 ms; 2x2 mm^2 in plane resolution, 4 mm axial slices; 195 dynamics; and acquisition time 6.5 min.

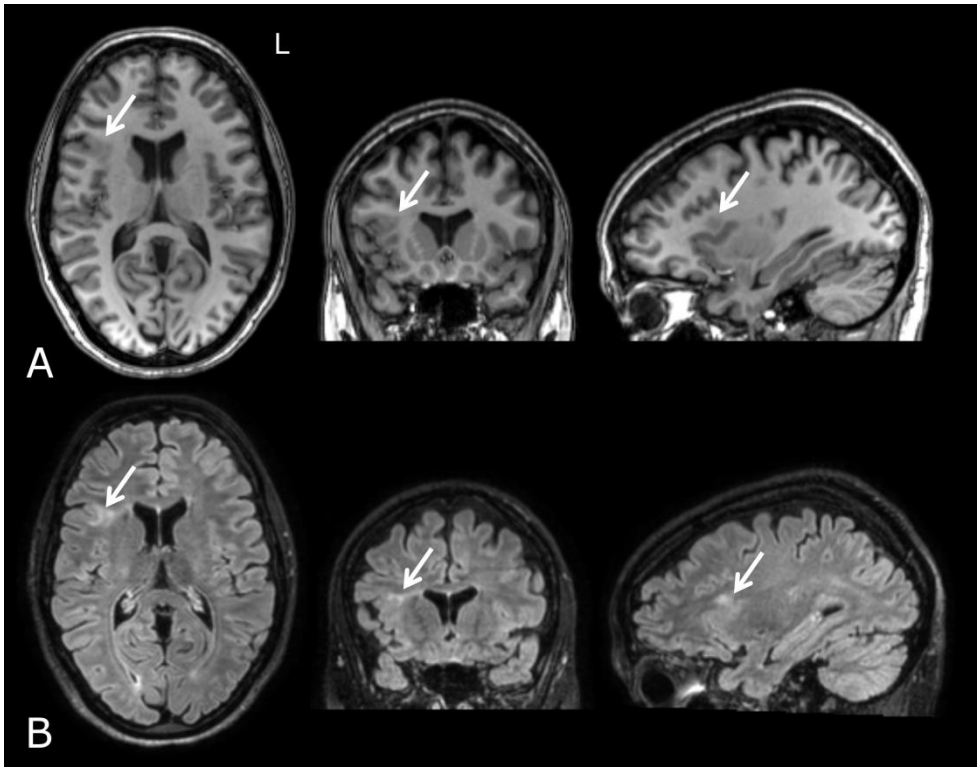

Figure 8.1: Conventional structural MRI features of focal cortical dysplasia in a representative subject (patient 1) for 3 orthogonal slices. The abnormalities are indicates by arrows; in the T1-weighted images (A) these are cortical thickening and blurring of the gray matter-white matter interface; in the FLAIR-weighted images (B), hyperintensities in the underlying white matter can be observed.

ID	age [y]	gender	SF	IISS	FCD location	Aberrant connectivity profile	Relation to structural lesion
1	30	f	high	high	right insula	hypo	both within and beyond
2	29	f	high	n.d.	right superior frontal	distal transient hypo	only beyond
3	33	m	low	none	right inferior frontal	distal hyper	only beyond
4	47	f	high	none	right precentral	n.a.	n.a.
5	21	m	low	high	left postcentral	distal hyper	both within and beyond
6	47	m	high	low	left posterior cingulate	n.a.	n.a.
7	43	m	high	low	left caudal middle frontal	distal transient hypo	both within and beyond
8	26	m	low	none	left rostral middle frontal	distal transient hypo	only beyond
9	21	f	low	n.d.	caudal anterior cingulate	hyper	both within and beyond
10	21	m	high	n.d.	left medial occipital	hypo	both within and beyond
11	21	m	high	none	right supramarginal	proximal hyper, distal hypo	both within and beyond
12	21	m	low	n.d.	right insular	proximal hyper	only within
13	27	m	moderate	none	left precentral	transient hyper	both within and beyond
14	54	m	high	none	right rostral middle frontal	hypo	both within and beyond
15	25	m	none	unknown	left inferior parietal	distal hyper	only beyond

Table 8.1: Patient and FCD characteristics, and descriptions of the connectivity profiles. Aberrant connectivity profiles (compared to controls) are found in most cases; typically the abnormality in local functional connectivity extended beyond the structural lesion.
SF: seizure frequency; low signifies one seizure per month, high signifies multiple seizures per week.
IISS: inter ictal seizure spread; low signifies confined to one or several ipsilateral electrodes, high signifies including contralateral electrodes.
n.d.: none detected; no epileptiform activity found during EEG acquisition.

8.2.3 Neuroradiological examination

The structural scans were reviewed by a board certified neuroradiologist with >20 years of experience (PH) with the aim to localize the structural lesion. A spherical region of interest was placed at the center of the cortical abnormality on the T1-weighted scan. The radius of this sphere was tuned to comply most optimally with the structural boundaries of the cortical abnormality.

8.2.4 FCD local functional connectivity

The characterization of (abnormal) local functional connectivity around FCDs required several steps, see Figure 8.2. An important aspect was the mapping of all native space datasets to a common anatomical standard. This allowed for the derivation of homotopic normative connectivity profiles from the healthy controls to compare the FCD connectivity profiles to. Furthermore, functional connectivity as well as distance maps were to be calculated. It is assumed that locally, functional connectivity is mediated by juxtacortical short association fibers. As a surrogate for the length of these short fibers, the distance along the cortical surface (i.e. geodesic distance) was used to construct the required distance maps. Furthermore, functional connectivity maps were derived from preprocessed fMRI data in a seed-based approach. These were combined with the distance maps to calculate connectivity profiles, i.e. connectivity as a function of distance, which were finally used for statistical inference. These steps are summarized in Figure 8.2 and explained in detail below.

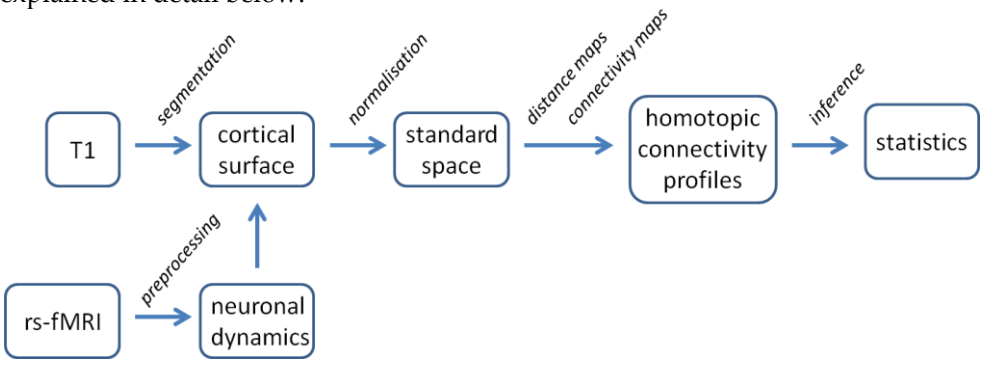

Figure 8.2: Resting-state fMRI processing pipeline. The cortical surface is segmented from the T1-weighted scan and the preprocessed fMRI data is mapped to the cortex. The gyral pattern is normalized and maps are derived for distance and functional connectivity to construct profiles of connectivity as a function of distance. These are investigated to find local abnormalities in patient functional connectivity.

8.2.4.1 Registering FCD locations to anatomical reference space

The Freesurfer software package (Dale, Fischl et al. 1999; Fischl, van der Kouwe et al. 2004) was used to tessellate the cortical surface from the T1-weighted scan; the resulting 3D triangular mesh consisted of approximately 300,000 vertices. For every patient, the dysplasia location was mapped to the nearest vertex (smallest Euclidian distance). Subsequently, the pattern of gyri and sulci was mapped to this cortical surface, and registered with Freesurfer's spherical standard space, which was subsequently warped to Freesurfer's standard anatomical space, see Figure 8.3. Effectively, this procedure maps the individual native space dysplasia locations to a common anatomical reference, suitable for between-subject homotopic comparison. It has been shown that gyral pattern based registration is more robust than conventional voxel-based approaches (Desikan, Segonne et al. 2006).

8.2.4.2 Geodesic distance

To investigate functional connectivity as a function of distance, the distance maps for the different dysplasia locations in standard space were determined. Assessment of distance maps in standard space compensates for inter-individual difference in the size and relative proportions of gyri and sulci. To construct these distance maps, for each dysplasia vertex, the shortest distance along the cortical surface to each other vertex was calculated, see Figure 8.4. For this, the exact geodesic algorithm for triangular meshes was used as described by Mitchell et al (Mitchell, Mount et al. 1987; O'Rourke 1999) in a Matlab implementation by Kirsanov, see for more information http://code.google.com/p/geodesic/.

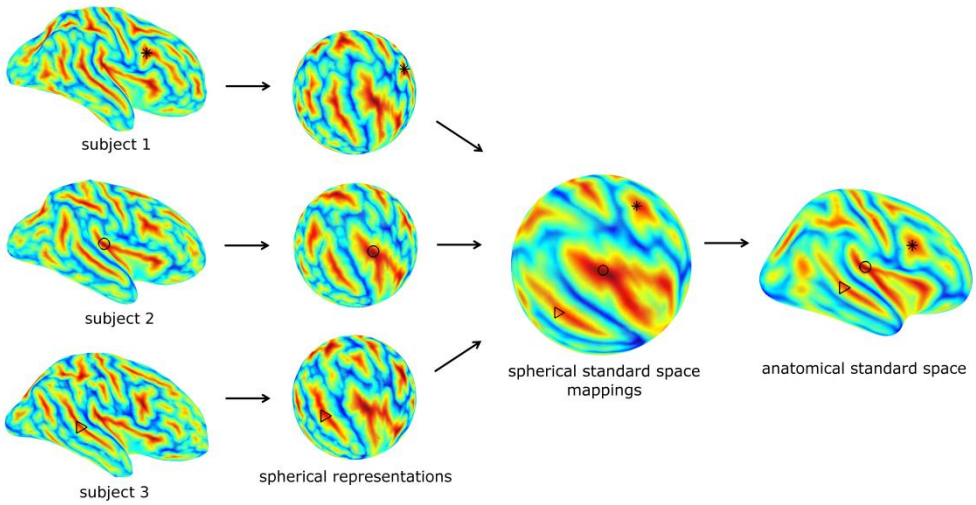

Figure 8.3: Inflated views of the pial surface of 3 representative subjects; the pattern of gyri/sulci is encoded in blue/red. Alternatively, these gyral patterns may be represented in spherical view. These spherical views can be mapped to a spherical standard space in Freesurfer, which is associated with an anatomical standard space. Data associated with the gyral pattern, such as cortical locations (black markers), are thus mapped to an anatomical standard to enable between subject comparisons.

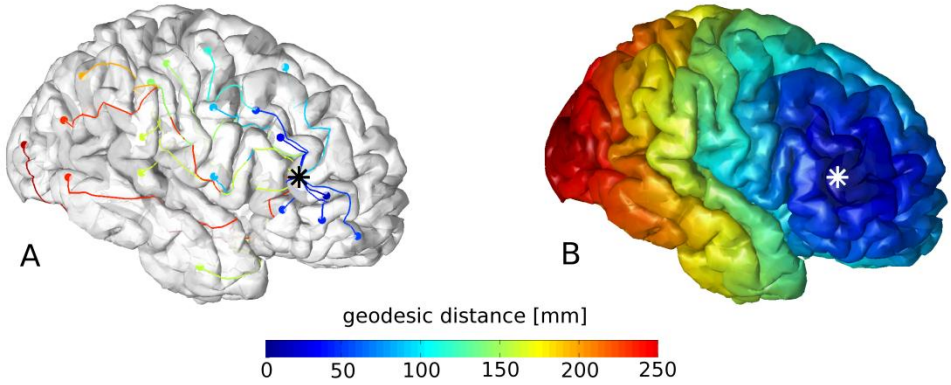

Figure 8.4: For the cortical location indicated by an asterisk (*), the shortest paths (along the cortex) to a number of other cortex vertices were determined and color coded by their path length in A; combining this for all cortex vertices yields the geodesic distance map in B.

8.2.4.3 fMRI preprocessing

The preprocessing of the fMRI data was performed using software tools from Statistical Parameteric Mapping (SPM8), FMRIB's Software Library (FSL 4.1.7) and Freesurfer (version 5.1.0). The two major steps are signal enhancement and projection of the data to the cortical surface.

8.2.4.4 Signal enhancement

First, to correct for head motion, all fMRI volumes were registered to the first dynamic scan using affine registration (6 degrees of freedom). Subsequently, the mean fMRI volume was calculated and used to affinely register the fMRI data to the T1-weighted scan.

Next, the fMRI data was deconfounded using linear regression. As nuisance regressors the movement parameters as derived in the previous step were used, as well as average white matter time series.

The aim of this step was to remove global confounds (such as scanner drift and breathing artifacts) from the data, without regressing out any of the neuronal signal fluctuations (Fox, Zhang et al. 2009; Smith, Miller et al. 2011). For this reason, the white matter masks (left and right hemisphere; derived from Freesurfer) were eroded by a single voxel to prevent the mixing in of gray matter signal due to partial volume effects of voxels at the gray matter-white matter interface.

Finally, band pass filtering was applied to confine the signal to the range of 0.01-0.1 Hz typically used in resting-state fMRI analyses (Zalesky, Fornito et al. 2010; Cocchi, Bramati et al. 2012; Hong, Zalesky et al. 2013).

8.2.4.5 Projecting resting-state data to the cortex

The preprocessed fMRI data was projected to the cortical surface using Freesurfer tools. This involves averaging the fMRI time-series over the cortex in the direction perpendicular to the surface for each vertex. Methodologically, this is similar to projecting conventional (voxel-based) activation maps to the cortical surface, only here it is part of the analysis pipeline rather than a visualization method.

To avoid artifacts at tissue interfaces (partial volume effects due to the proximity of white matter, CSF, or blood vessels), projections only included the cortical core (80% of the cortical thickness).

Finally, the surface-based data were spatially smoothed (over the surface) using a Gaussian kernel of full-width-at-half-maximum (FWHM) 10 mm.

8.2.4.6 Extraction of seed time series

For each patient, a seed time series was calculated by averaging the time series over all vertices within 5 mm geodesic distance of the dysplasia location. Using the same approach, homotopic time series were derived in all other subjects.

It is known that epileptiform spikes may induce additional BOLD fluctuations (Lopes, Lina et al. 2012).

Therefore, patient and controls seed time series were compared to detect increased signal variance in FCD time series using 2-sample Student's t-tests ($p<0.05$). The goal of this step was to exclude patients with spike-contaminated seed time series

from further analysis, since these may perturb the connectivity profiles as described below.

8.2.4.7 Derivation and comparison of local functional connectivity profiles

For each patient, the seed time series was correlated with those of all other vertices. The resulting connectivity map was combined with the associated geodesic distance map to assess functional connectivity as a function of distance: for concentric isobands on the distance map of width 2 mm, the average connectivity was calculated for the local environment in the range 2-40 mm. Similarly, homotopic connectivity profiles were derived in all other subjects.

For every patient, 2-sample Student's t-tests were used to compare the FCD connectivity profile to the homotopic normative connectivity profiles derived from the controls. Similarly, 2-sample Student's t-tests were employed to assess whether the homotopic connectivity profiles of the other patients (who had their dysplasia in a different location) were abnormal with respect to the normative connectivity profiles of the controls.

Connectivity abnormalities were considered relevant if deviations from the normative profiles were both significant ($p<0.05$) and robust, i.e. found over several consecutive isobands of distance.

8.3 Results

8.3.1 Major findings

In a single patient, the FCD time series showed increased signal variance ($p=0.01$), and this subject was excluded from further analysis.

In the healthy controls, gradually and consistently decreasing connectivity profiles were found, which varied with cortical location. In the majority of patients (14/16), the connectivity profile of their FCD was significantly disturbed with respect to these normative profiles. For 9/15 patients, connectivity was already disturbed within the FCD; for the remaining patient, connectivity was (also) disturbed beyond the structural margins of the lesion. These results are summarized in Table 8.1.

The distance between lesions in standard space was 66±28 mm. Homotopic connectivity profiles derived from other patients (i.e. beyond their own FCD) demonstrated no deviations from the norm at the group level. Aberrant FCD connectivity profiles both involved local hyper- and hypoconnectivity, as well as combinations, for an overview, see Table 8.1. Specific illustrative cases are discussed below.

8.3.2 Overall hypoconnectivity

For the same patient as in Figure 8.1 (patient 1; right insular FCD), a profile of overall hypoconnectivity was found, see Figure 8.5. Note that already within the structural lesion, functional connectivity was reduced with respect to the homotopic connectivity profiles derived in the controls. This patient had a high seizure frequency (multiple seizures per week) and high inter-ictal spread of epileptiform activity (i.e. including propagation to contralateral electrode).

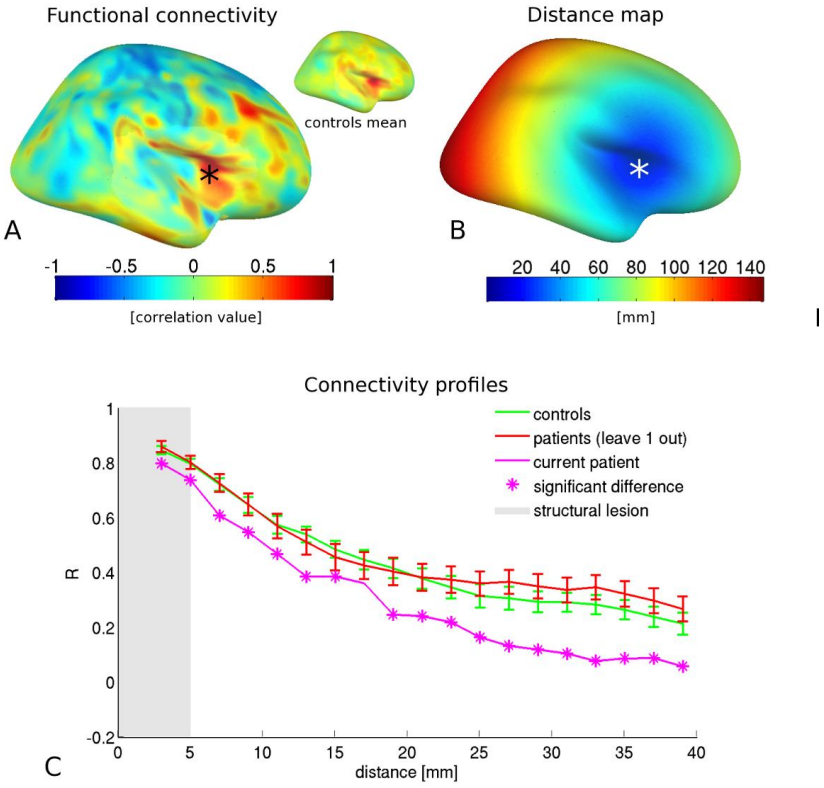

Figure 8.5: For patient 1, the lesion location and its connectivity map are given in A; the inset is the average homotopic connectivity map of the controls. The geodesic distance map for this location is given in B. By combining the connectivity and distance maps, connectivity profiles as depicted in C can be constructed. Average homotopic connectivity profiles for the controls and for the other patients (i.e. excluding patient 1) are also provided. The extent of the structural lesion on conventional MRI is shaded; connectivity values that are aberrant compared to the controls are indicated by an asterisk (*). Surface maps represent inflated views; in contrast, connectivity values and distance maps were assessed in native space. Error bars represent 1 standard error.

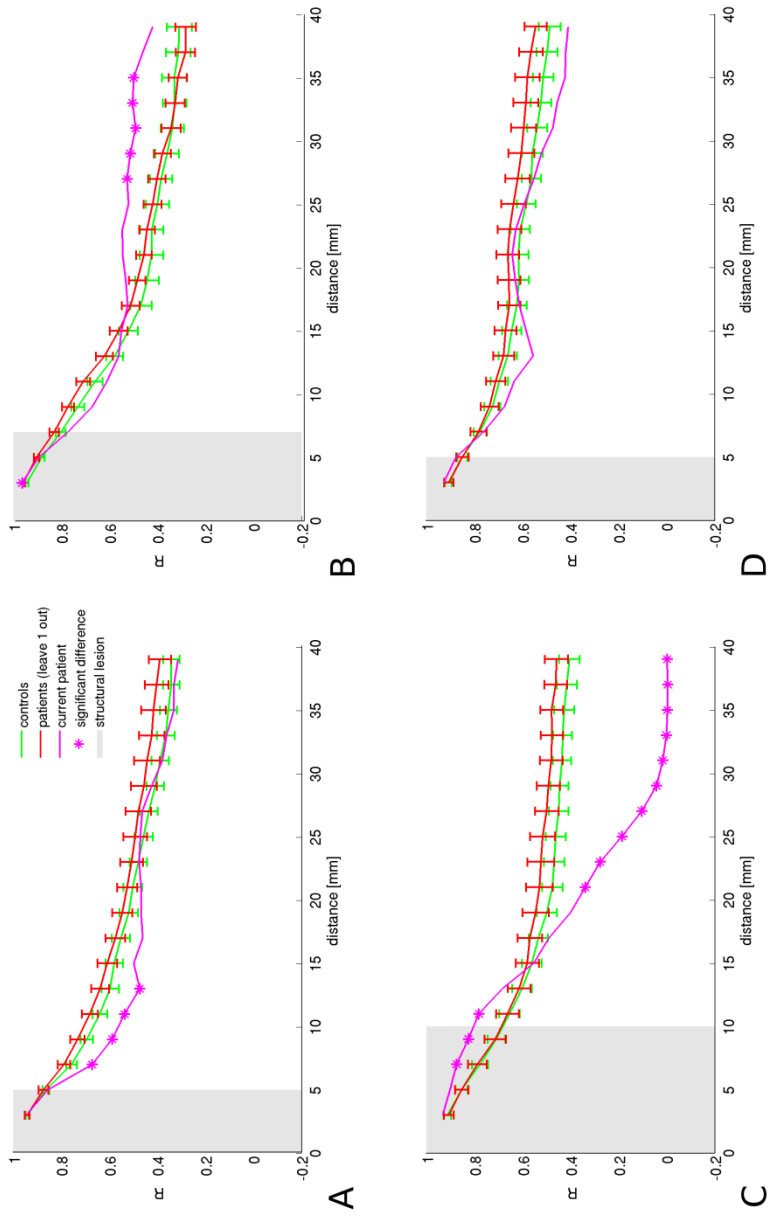

Figure 8.6: Different profiles of aberrant connectivity. In patient 2, transient hypoconnectivity is found directly beyond the lesion visible on conventional structural MRI (A). In patient 5, on the other hand, transient distal hyperconnectivity is found (B). In patient 11, a dual profile is found of hyperconnectivity within and directly beyond the structural lesion, and hypoconnectivity more distally (C). In a few patients, no aberrant connectivity values were found, such as in patient 4 (D). Error bars represent 1 standard error.

8.3.3 Transient hypoconnectivity

A similar but more subtle profile of aberrant connectivity was found in patient 2, see Figure 8.6A. This patient had a right superior frontal lesion and displayed reduced functional connectivity directly adjacent to the structural lesion, up to a distance of about 12 mm from the lesion center. This patient had a high seizure frequency. No statement can be made about interictal spread of epileptiform spikes since none were detected during EEG acquisition.

8.3.4 Distal hyperconnectivity

Also hyperconnectivity was found, for example in patient 5, who had a left postcentral lesion, see Figure 8.6B. Local connectivity was normal up to a distance of about 25 mm, i.e. well outside the boundary of the structural lesion. Beyond this distance, hyperconnectivity was found for about 10 mm. This patient had a low seizure frequency (about 1 seizure per month) combined with high interictal spread of epileptiform activity.

8.3.5 Proximal hyperconnectivity, distal hypoconnectivity

In patient 11, who had an FCD in the right supramarginal gyrus, connectivity was significantly increased up until 10 mm from the lesion center, and then transitioned into a profile of significant hypoconnectivity beyond the structural lesion, see Figure 8.6C. This patient had a high seizure frequency and no interictal spread of epileptiform activity.

8.3.6 No abnormalities

In patient 4, who had a right precentral FCD, no abnormalities were found in the connectivity profile, see Figure 8.6D. This patient combined a high seizure frequency with low interictal spread of epileptiform EEG-activity (i.e. confined to one or several ipsilateral electrodes).

Overall, note that on the group level, no aberrant connectivity profiles were found in the patients beyond their FCD location. This can be deduced from comparing the leave-one-out patient curves to the control curves in the aforementioned figures.

8.4 Discussion

In this study, we explored local functional connectivity of FCD lesions. Since these cortical malformations vary in location over patients, dedicated methodology for individual subject analysis was developed. This involved gyral pattern based registration of the dysplasia locations as well as the fMRI data to a common

anatomical standard, for comparison of patient connectivity profiles to homotopic normative profiles derived in healthy controls.

8.4.1 Major findings

Local connectivity profiles were abnormal in the majority of patients (13/15). Remarkably, these aberrant connectivity profiles represented hyperconnectivity, hypoconnectivity and combinations thereof. Typically, functional connectivity was (also) aberrant beyond the structural boundaries of the lesion (12/15 cases). Furthermore, patient connectivity profiles were normal at distal locations (i.e. at the FCD location of *other* patients).

8.4.2 Pathophysiological interpretation

The variable nature of the abnormalities in functional connectivity may suggest that different pathological mechanisms are at work, such as excitotoxic effects and the formation of local epileptic networks, causing hypo- and hyperconnectivity, respectively. The latter has been suggested as a mechanism to recruit non-dysplastic cortex in FCD seizure generation during sleep (Chassoux, Landre et al. 2012). These variable findings underline the heterogeneity of a clinical sample of FCD patients.

With respect to the extent of the functional connectivity abnormality, typically connectivity profiles were aberrant also beyond the MR-visible lesion (12/15), which is in line with histopathological findings (Hauptman and Mathern 2012). Further research is needed to establish whether the current findings translate to specific local microscopic tissue abnormalities.

8.4.3 Clinical outlook

In this exploratory study, no clear links were found between the type of aberrant connectivity profile and patient characteristics such as EEG findings, see Table 8.1. However, functional imaging has been linked to electrophysiology before, in studies were epileptiform spikes were mapped to the brain using simultaneously acquired EEG-fMRI (Jager, Werhahn et al. 2002; Thornton, Vulliemoz et al. 2011). Possibly more advanced EEG data, such as recorded from subdural electro grids, may help to relate the current functional connectivity findings to subject-specific electrophysiology.

Besides the aberrant FCD connectivity profiles established in the individual patients, we found that at the group level, patient connectivity profiles are normal beyond their dysplasia location (i.e. at the locations were *another* patient had a dysplasia). This suggests that in FCD-mediated epilepsy, functional connectivity is only locally disturbed. In line with this, FCD-related seizures are typically stereotyped, suggesting the involvement of well-localized brain regions

(Chassoux, Landre et al. 2012). This may also explain why focal resection may have such excellent seizure control outcome (Wang, Deans et al. 2013).

8.4.4 Methodological considerations

We investigated functional connectivity up to a range of 40 mm geodesic distance from the dysplasia center. This corresponds roughly to the extent of a gyrus, and resulted (for the controls) in gradually and consistently decreasing connectivity profiles, as expected. In the majority of the investigated patients, functional connectivity was disturbed right up to the end of this range, and beyond the border of the structural lesion. This may indicate abnormal distal connectivity; however, the investigation of connectivity between distributed regions as mediated by long-range connections is beyond the scope of this study.

It is remarked that the definition of the border of the structural lesion is not very accurate as the representations of an FCD by a spherical region of interest is a strong simplification. In any case, our preliminary findings suggest that in FCD the abnormality extends beyond the MR-visible lesion. As such, our findings might be of interest for surgical planning, as recent findings show that the identification and removal of as much aberrant cortex as possible improves seizure-free outcome (Hauptman and Mathern 2012; Wang, Deans et al. 2013).

For 9/15 patients, functional connectivity was already aberrant within the lesion, whereas in others the connectivity profile only became aberrant beyond the structural margins. Given what is said about the accuracy of the extent of the structural lesion, these differences may also arise from the definition of the seed time series, which was derived from all vertices within 5 mm (geodesic distance) from the lesion midpoint. At short distance and in large lesions, this comes down to assessing the (high) connectivity of the core of the lesion with its outer perimeter, whereas in small lesions, the (lower) connectivity with the surrounding tissue was calculated. We used variance analysis of the seed time series in an attempt to prevent connectivity profile differences to be driven by seed time series abnormalities. This led to the exclusion of a single patient, for which the seed time series may have been contaminated by spike-induced additional BOLD fluctuations.

8.4.5 Directional anisotropy of effects

In our approach we averaged functional connectivity values over concentric isobands on the geodesic distance map. With increasing distance from the dysplasia center, this lumps more and more distributed regions into a single connectivity value, gradually compromising the spatial precision of our approach. However, our work represents an exploratory study aimed at investigating homogenous local (rather than distributed distal) connectivity profiles. The exact extent of the local environment, preferably as a function of the location on the

cortex and taking into account local gyration, is an interesting subject for future research. Such approaches should confine the local analysis to e.g. single gyri in order not to cross functional boundaries.

In conclusion, local functional connectivity is disturbed in FCD, which may express as hyperconnectivity, hypoconnectivity or combinations, the histopathological and electrophysiological bases of which remain to be established. It was demonstrated that in FCD, local functional connectivity typically is aberrant also beyond the structural lesion, which may facilitate the delineation of the clinically relevant lesion beyond its structural boundaries on conventional MRI.

Acknowledgement

We would like to acknowledge Ester Peeters for data acquisition, Marc Geerlings for continuous soft- and hardware support, and the patients for their time and interest in our research. We would like to thank the Dutch Epilepsy Foundation for funding.

The funders had no influence on study design, patient inclusion, and data acquisition, nor on analysis or interpretation of the results.

References

Blumcke, I., M. Thom, et al. (2011). "The clinicopathologic spectrum of focal cortical dysplasias: a consensus classification proposed by an ad hoc Task Force of the ILAE Diagnostic Methods Commission." Epilepsia **52**(1): 158-74.

Chassoux, F., E. Landre, et al. (2012). "Type II focal cortical dysplasia: electroclinical phenotype and surgical outcome related to imaging." Epilepsia **53**(2): 349-58.

Cocchi, L., I. E. Bramati, et al. (2012). "Altered functional brain connectivity in a non-clinical sample of young adults with attention-deficit/hyperactivity disorder." J Neurosci **32**(49): 17753-61.

Dale, A. M., B. Fischl, et al. (1999). "Cortical surface-based analysis. I. Segmentation and surface reconstruction." Neuroimage **9**(2): 179-94.

Desikan, R. S., F. Segonne, et al. (2006). "An automated labeling system for subdividing the human cerebral cortex on MRI scans into gyral based regions of interest." Neuroimage **31**(3): 968-80.

Fischl, B., A. van der Kouwe, et al. (2004). "Automatically parcellating the human cerebral cortex." Cereb Cortex **14**(1): 11-22.

Fonseca Vde, C., C. L. Yasuda, et al. (2012). "White matter abnormalities in patients with focal cortical dysplasia revealed by diffusion tensor imaging analysis in a voxelwise approach." Front Neurol **3**: 121.

Fox, M. D., D. Zhang, et al. (2009). "The global signal and observed anticorrelated resting state brain networks." J Neurophysiol **101**(6): 3270-83.

Hauptman, J. S. and G. W. Mathern (2012). "Surgical treatment of epilepsy associated with cortical dysplasia: 2012 update." Epilepsia **53 Suppl 4**: 98-104.

Hofman, P. A., G. J. Fitt, et al. (2011). "Bottom-of-sulcus dysplasia: imaging features." AJR Am J Roentgenol **196**(4): 881-5.

Hong, S. B., A. Zalesky, et al. (2013). "Decreased functional brain connectivity in adolescents with internet addiction." PLoS One **8**(2): e57831.

Jager, L., K. J. Werhahn, et al. (2002). "Focal epileptiform activity in the brain: detection with spike-related functional MR imaging--preliminary results." Radiology **223**(3): 860-9.

Kassubek, J., H. J. Huppertz, et al. (2002). "Detection and localization of focal cortical dysplasia by voxel-based 3-D MRI analysis." Epilepsia **43**(6): 596-602.

Lee, S. K., D. I. Kim, et al. (2004). "Diffusion tensor MRI visualizes decreased subcortical fiber connectivity in focal cortical dysplasia." Neuroimage **22**(4): 1826-9.

Lopes, R., J. M. Lina, et al. (2012). "Detection of epileptic activity in fMRI without recording the EEG." Neuroimage **60**(3): 1867-79.

Mitchell, J. S. B., D. M. Mount, et al. (1987). "The discrete geodesic problem." SIAM J. Comput. **16**(4): 647-668.

O'Rourke, J. (1999). "Computational geometry column 35." Internat. J. Comput. Geom. Appl. **4--5**: 513-515.

Palmini, A., I. Najm, et al. (2004). "Terminology and classification of the cortical dysplasias." Neurology **62**(6 Suppl 3): S2-8.

Rastogi, S., C. Lee, et al. (2008). "Neuroimaging in pediatric epilepsy: a multimodality approach." Radiographics **28**(4): 1079-95.

Smith, S. M., K. L. Miller, et al. (2011). "Network modelling methods for FMRI." Neuroimage **54**(2): 875-91.

Taylor, D. C., M. A. Falconer, et al. (1971). "Focal dysplasia of the cerebral cortex in epilepsy." J Neurol Neurosurg Psychiatry **34**(4): 369-87.

Thornton, R., S. Vulliemoz, et al. (2011). "Epileptic networks in focal cortical dysplasia revealed using electroencephalography-functional magnetic resonance imaging." Ann Neurol **70**(5): 822-37.

Wang, D. D., A. E. Deans, et al. (2013). "Transmantle sign in focal cortical dysplasia: a unique radiological entity with excellent prognosis for seizure control." J Neurosurg **118**(2): 337-44.

Widjaja, E., S. Blaser, et al. (2007). "Evaluation of subcortical white matter and deep white matter tracts in malformations of cortical development." Epilepsia **48**(8): 1460-9.

Widjaja, E., S. Zarei Mahmoodabadi, et al. (2009). "Subcortical alterations in tissue microstructure adjacent to focal cortical dysplasia: detection at diffusion-tensor MR imaging by using magnetoencephalographic dipole cluster localization." Radiology **251**(1): 206-15.

Winston, G. P., C. Micallef, et al. (2013). "The value of repeat neuroimaging for epilepsy at a tertiary referral centre: 16 years of experience." Epilepsy Res **105**(3): 349-55.

Yagishita, A., N. Arai, et al. (1997). "Focal cortical dysplasia: appearance on MR images." Radiology **203**(2): 553-9.

Zalesky, A., A. Fornito, et al. (2010). "Network-based statistic: identifying differences in brain networks." Neuroimage **53**(4): 1197-207.

CHAPTER 9

General discussion

R.M.H. Besseling

Brain wiring and neuronal dynamics
advances in MR imaging of focal epilepsy

9.1 Thesis overview

In this thesis, we employed advanced MRI methods to detect abnormalities in brain structure and function in two different types of focal epilepsy. With respect to structural abnormalities, morphological analysis was applied to detect regions of aberrant cortex in rolandic epilepsy (RE). Moreover, high angular resolution diffusion weighted imaging (HARDI) and tractography were applied to detect abnormalities of brain wiring of structural white matter connections. Also functional MRI (fMRI) was used, to detect abnormalities in functional connectivity patterns of synchronous neuronal dynamics. The overall goal was to find neuroimaging correlates for RE-typical language impairments.

In addition and in a more explorative approach, we investigated local functional connectivity in focal cortical dysplasia (FCD) patients with the aim to improve the delineation of the clinically relevant (epileptogenic) cortical abnormality, beyond the structural lesion as visible on conventional MRI.

9.2 Reproducibility of structural connectivity

In order to appreciate the minimally detectable effect size of pathological change, insight is needed into the reproducibility of the applied techniques. Concerning functional connectivity, a robust set of large-scale resting state networks (RSNs) has been identified that is highly reproducible over subjects (Beckmann, DeLuca et al. 2005; Smith, Fox et al. 2009). These networks have been shown to be preserved even during sleep and under anesthesia, and represent sensitive markers of disease (Smith, Jenkinson et al. 2004; Filippini, MacIntosh et al. 2009; Woolrich, Jbabdi et al. 2009).

On the other hand, the reproducibility of structural connectivity is investigated to a lesser extent, especially regarding white matter bundle geometry (Ciccarelli, Parker et al. 2003; Heiervang, Behrens et al. 2006; Wakana, Caprihan et al. 2007). This forms the subject of Chapter 2.

For several major white matter tracts, measures that quantify structural connectivity were investigated, such as fractional anisotropy (FA) and apparent diffusion coefficient (ADC) as derived from diffusion tensor imaging (DTI), as well as tract density imaging (TDI) (Basser, Mattiello et al. 1994; Calamante, Tournier et al. 2010). Also the reproducibility of geometric measures was studied, such as tract morphology and volume. Nine healthy subjects were scanned twice in order to assess between-session and between-subject variability.

An important aspect of this study was spatial registration. Tract-specific seed and target regions needed to be registered from an anatomical standard space to the individual subjects. Subsequently, individual native space tract segmentations had to be mapped back to standard space to assess the

reproducibility of tract geometry. For this, non-linear registrations of FA maps were used. Since FA provides a rich contrast within the white matter, it is assumed to be very suitable for between-subject tractography registration.

Important insights from this study were that the reproducibility differs not only over the measures under investigation, but also over the various tracts we studied. For example, the reproducibility of tract segmentation was better for compact deep white matter sections than for those also including distal projections, and was higher in the corpus callosum than in the arcuate fasciculus. Furthermore, FA and ADC showed better reproducibility and higher between-subject discrimination than tract volume or TDI, and as a consequence may be more suitable to detect pathological abnormalities.

In the wider context of this thesis, this study served to get familiar with important concepts of neuroimaging, such as image alignment (to compensate for motion artifacts), advanced modeling (constrained spherical deconvolution (CSD) tractography (Tournier, Calamante et al. 2007)), spatial normalization and registration (to an anatomical standard), and quantification of connectivity measures. This resulted in a better understanding of the data, as well as an insight into the sources of error along the tractography pipeline in particular and in advanced neuroimaging methods in general.

9.3 Observations in rolandic epilepsy

After having addressed these methodological issues, the major part of this thesis is clinically oriented, and is primarily focused on finding structural and functional correlates for language impairment in children with rolandic epilepsy (RE).

9.3.1 Morphological findings

In Chapter 3, we investigated cortical thickness in a group of children with RE compared to healthy controls. In this study it was shown that children with RE demonstrate regions of reduced cortical thickness, notably in the left hemisphere and exceeding the rolandic (sensorimotor) cortex. Furthermore, more extensive and widely distributed cortical abnormalities were found when taking into account the effect of age, as the children with RE demonstrated gradual and progressive cortical thinning with age.

Note that typically, no specific macroscopic abnormalities are found in RE (Boxerman JL, Hawash K et al. 2007). In contrast, this study demonstrates that using dedicated quantitative analysis, subtle but significant morphological abnormalities of the cortex can be detected.

9.3.1.1 Distributed cortical abnormalities

An extensive body of neuropsychological literature exists on RE. These studies demonstrate that RE does not merely represent rolandic (sensorimotor) pathology such as seizures and problems in motor development (Overvliet GM, Aldenkamp AP et al. 2011), but also entails a range of neuropsychological problems, such as inattention, impulsivity, and a multitude of cognitive complaints (Massa R, de Saint-Martin A et al. 2001; Lindgren S, Kihlgren M et al. 2004; Duman, Kizilay et al. 2008; Kavros PM, Clarke T et al. 2008). It has been suggested that these problems imply dysfunction in several circuits distant from the rolandic focus (Massa R, de Saint-Martin A et al. 2001), which is in line with the distributed (rather than focal) nature of the cortical abnormalities we found.

More specifically, we predominantly found left-lateralized abnormalities, and in the fully developed brain, the left hemisphere is typically language dominant (Price CJ 2010). To be precise, the left inferior frontal, supramarginal and middle temporal cortices were involved, which are all known to have certain language functionality (Price CJ 2010). This is in accordance with the extensive literature on language impairment in RE (Lundberg S, Frylmark A et al. 2005; Monjauze C, Tuller L et al. 2005; Northcott E, Connolly AM et al. 2005; Papavasiliou A, Mattheou D et al. 2005; Clarke, Strug et al. 2007; Overvliet GM, Besseling RM et al. 2010; Monjauze C, Broadbent H et al. 2011).

9.3.1.2 Age effect and cortical development

Especially the effect of age on cortical thickness motivated speculations about the pathophysiological mechanisms that may be involved.

Normal brain maturation involves a phase of cortical thickening, followed by cortical thinning (Andersen 2003; Raznahan A, Shaw P et al. 2011). Since cortical thickness reflects the number of underlying fibers (Gong, He et al. 2012), this signifies an initial overshoot of connections, which is resolved later in development. The basis for this is a process called pruning, in which redundant connections are selectively removed under guidance of a variety of neuronal cues (Andersen 2003). Effectively, pruning improves the efficiency and efficacy of the network.

In the study on cortical thickness, we found reduced cortical thickness and gradual cortical thinning in the children with RE. On the other hand, the controls were in the transition from cortical thickening to thinning, which is normal for the age range under study (8-14 years) (Muftuler, Davis et al. 2011; Raznahan A, Shaw P et al. 2011). We speculated that these findings may represent cortical underdevelopment and early or accelerated cortical thinning in the patients. A potential mechanism is that in addition to the efficiency-driven pruning process, connections are unselectively removed due to pathological cues such ongoing

epileptiform activity. Obviously, this impacts network functionality, and thereby cognition.

9.3.1.3 Clinical outlook

In agreement with this, from EEG literature it has long been known that interictal spikes may reduce the amplitude and increase the latency of directly subsequent evoked potentials, transiently compromising local neuronal signaling (Shewmon and Erwin 1988; Seri, Cerquiglini et al. 1998). Taking this a step further, it has been suggested that excitotoxic effects of ongoing epileptiform activity may cause local cortical atrophy that permanently compromises network functionality in the RE-related Landau Kleffner syndrome (LKS) (Bourgeois and Landau 2004; Takeoka, Riviello et al. 2004; Fejerman N 2009). Similar mechanisms, although more subtle, may be at work in RE, and the topology of the observed morphological abnormalities is in agreement with impairments of the language network.

Note that observations of cortical thickness only provide an indirect window on the underlying network, and actually convey no information at all on electrophysiology. It would be interesting to know whether the observed cortical abnormalities coincide with regions of epileptiform activity. Dedicated approaches are needed to test this hypothesis, as standard surface EEG may lack sensitivity and spatial accuracy to detect these subtle and local events.

Furthermore, although this study demonstrated morphopathology of the language system, it leaves open the question why specifically the language network is compromised in RE.

9.3.1.4 Distributed pathology motivates network analysis

Most importantly, this study demonstrated that RE represents subtle but significant distributed morphological abnormalities of the language network, and is not merely a focal pathology. These observations naturally motivate dedicated investigations of the brain from a network perspective, and prompt studies of functional and structural connectivity. Such studies should also aim to find neuronal mechanism that link RE to language problems.

9.3.2 Lessons from functional imaging

Chapters 4 and 5 investigate RE from the perspective of functional connectivity. Chapter 4 applies a graph approach, in which nodes are defined from task fMRI and connectivity values (edges) are derived from correlation analysis of resting-state fMRI time series.

Because in RE the epileptic focus resides in the sensorimotor cortex, a well established motor task of finger tapping was employed to define the respective regions of interest (ROIs) (Biswal, Yetkin et al. 1995; Bandettini 2012). To establish

the link with language, word generation and reading tasks were employed to define ROIs with respect to expressive and receptive language, respectively.

9.3.2.1 Bilateral language processing

Based on previous findings of aberrant language laterality in childhood epilepsy (Liegeois, Connelly et al. 2004; Yuan, Szaflarski et al. 2006), a laterality analysis was applied to the language task data (Abbott, Waites et al. 2010). This demonstrated bilateral language processing in patients as well as controls, with only a slight predominance of the left hemisphere. In line with this, literature on brain development states that hemispheric specialization with respect to language is established from an initially bilateral language network (Kadis, Pang et al. 2011). This implies that in addition to the left-lateralized cortical abnormalities described in Chapter 3, contralateral homotopes of left-lateralized language-mediating regions may also be aberrant in RE. Indeed, it has recently been suggested that language network reorganization to the right hemisphere may play a role in RE (Vannest, Karunanayaka et al. 2009; Datta, Oser et al. 2013). To this end, in the current functional connectivity analysis, bilateral ROIs were included for language.

9.3.2.2 Reduced functional connectivity between motor and language areas

The connectivity analysis demonstrated reduced functional connectivity in RE between the left motor cortex and the right inferior frontal gyrus (IFG). The right IFG is the contralateral homotopic region of Broca's expressive language area in the left hemisphere (Catani, Jones et al. 2005; Tomasi and Volkow 2012). Because of the bilateral language activations patterns observed in this pediatric cohort, we interpreted this as reduced functional connectivity between the motor and the language system. The integrity of this connection seemed to be of relevance for language function, as lower connectivity values correlated with reduced language performance in the patients.

These findings provide a functional correlate for language impairment, as it was demonstrated that a connection between the sensorimotor (rolandic) cortex and the language network is impaired in RE, the strength of which correlates with language performance.

9.3.2.3 Generic investigation of the rolandic network

In this study, functional connectivity was assessed for a limited set of tasks and task fMRI derived ROIs. In Chapter 5, we attempted to develop a more generic approach by extracting the network of interest directly from resting-state data, which is assumed to reflect the functional repertoire of the brain in a more complete and unbiased sense (Beckmann, DeLuca et al. 2005; Smith, Fox et al. 2009; Smith 2012).

Independent component analysis (ICA) of resting-state data was employed to identify the spatio-temporal pattern that we termed the "rolandic network". This network was selected based on coverage of the bilateral rolandic cortices, but actually was more extensive; it additionally demonstrated intrinsic functional connectivity with the cerebellum and the bilateral supramarginal and superior temporal cortices.

This rolandic network was compared between patients and controls. Reduced functional connectivity was found in the patients for the left inferior frontal gyrus, which was identified as Broca's area by the expressive language task described in Chapter 4.

9.3.2.4 Integration of the motor and the language system

The extensive nature of the rolandic network (i.e. also beyond regions of purely sensorimotor nature), as well as its reduced functional connectivity with Broca's area, motivated a literature search on how the motor and the language system are related. An extensive body of work exists on this subject, and it is a matter that has recently regained interest in neuroimaging (Cappa and Pulvermuller 2012).

Several examples are given in the discussion of Chapter 5, among which a study by Pulvermuller et al., in which is shown that the perception of speech sounds most strongly activates the superior temporoparietal cortex (Wernicke's receptive language area), but shows differential activation in the motor cortex dependent on the specific articulator involved (i.e. lips and tongue area, respectively) (Pulvermuller, Huss et al. 2006).

In all, these studies demonstrate that the motor system is not only relevant for language in a straightforward way such as coordination of articulatory movement, but is also involved in purely cognitive aspects of language, such as comprehension.

9.3.2.5 Moto-lingual integration as a model for language problems in RE

This concept of moto-lingual integration seems key in explaining language impairment in RE, as it provides a pathway along which rolandic neuropathology (e.g. epileptiform activity) may impact the language network. Furthermore, the profound integration of the motor network with even cognitive aspects of language may explain the broad range of language impairments found in RE.

Note that the reduced integration between the motor network and the language system as reported in Chapter 4 actually directly translates to the current findings. However, the current study demonstrates that rather than considering the motor and the language systems as separate entities, they are to a certain extent an integrated unit, and an abnormality in one intrinsically may also affect the other.

9.3.2.6 Interpretation of resting-state networks

The network which we termed "rolandic" is actually part of a canonical set of large-scale ICA networks often described in the literature, and is usually referred to as the sensorimotor network (Beckmann, DeLuca et al. 2005; Smith, Fox et al. 2009). However, in Chapter 5 we argue that these ICA networks should not be termed based on a functional interpretation; instead, an anatomical description should be employed, based on which regions are involved. This helps to prevent biased functional interpretations of potential network abnormalities. The term "sensorimotor network" seems too narrow and ignores the inclusion of superior temporal and supramarginal cortices, which are not purely of sensorimotor nature. In the left hemisphere, these cortices have actually been attributed language functionality (Price CJ 2010).

9.3.2.7 Combing the functional findings

Comparing the two functional studies described in Chapters 4 and 5, the latter is more generic as it investigates functional connectivity for the rolandic network as a whole, rather than for a limited set of assumed regions of interest. Furthermore, Chapter 5 provides the additional insight of the fundamental integration of the motor network and the language system. In the preceding Chapter 4, this integration was only implicit, in the combined finding of reduced connectivity between the motor and the language system and the association between this reduction and lower language scores in the patients. As mentioned above, moto-lingual integration provides a useful model for understanding language problems in RE.

9.3.3 Structural connectivity correlates

Having thus established functional correlates for RE-related language impairment, in Chapter 6 we investigated whether associated abnormalities in structural connectivity of white matter bundles may also be found.

We employed Freesurfer to derive a parcellation of the gyral pattern and applied tractography to find to which other regions the rolandic parcels (i.e. bilateral pre- and postcentral gyri) connect. Profiles of high structural connectivity with ipsilateral rolandic parcels and supramarginal and superior temporal gyri were established. In addition, the precentral gyri showed strong connectivity with ipsilateral prefrontal regions, whereas the postcentral gyri were strongly connected to the ipsilateral superior parietal cortex.

For these robust and anatomically plausible connections, structural integrity was quantified by fractional anisotropy (FA), which is a measure for the within-voxel coherence of fiber orientation (i.e. "white matter integrity"). In methodological Chapter 2, we established that FA has a high reproducibility on the tract level, as well as provides good subject differentiation.

9.3.3.1 FA reduction for left-lateralized language connections

FA values were compared between groups, and significant differences entailed FA reductions in patients compared to controls. Notably, most aberrant connections were found in the left hemisphere, where they were also most pronounced. More specifically, in the left hemisphere FA was reduced for the connections between the left pre- and postcental gyri and the pars opercularis of the inferior frontal gyrus, and for the connection between the postcentral and the supramarginal gyri.

Moreover, for the connection between the left postcentral gyrus and the left pars opercularis, lower FA values were associated with lower core language scores in the patients.

The left pars opercularis is part of Broca's area, and the left supramarginal cortex roughly corresponds to Wernicke's receptive language area (Price CJ 2010). As a consequence, these findings represent reduced structural connectivity between the rolandic cortex and language areas in the left hemisphere. In addition, for the left inferior frontal gyrus, lower connectivity with the postcentral gyrus also corresponded with reduced language performance.

These findings are in agreement with the findings of reduced functional connectivity of the rolandic cortex with anterior language areas in Chapter 4 and 5.

9.3.4 Integrating brain structure and function

Finally, Chapter 7 integrates brain structure and function by assessing the correlation between structural and functional connectivity (SC and FC, respectively).

RE manifests during a critical phase of brain development in which SC and FC converge driven by a common maturation process of network optimization (Hagmann, Sporns et al. 2010; Supekar, Uddin et al. 2010). In other words, the brain infrastructure is being matched to the information traffic and vice versa, leading to an increased SC-FC correlation.

In addition to maturational effects, the SC-FC correlation may be affected by epileptic remodeling. For example, both reduced and increased SC-FC correlations have been reported in adults with idiopathic generalized epilepsy (Zhang, Liao et al. 2011; Liao, Zhang et al. 2013). The direction of the effect may depend on disease stage, among other factors (van Diessen, Diederen et al. 2013). In early stages, for example, only functional changes may have occurred yet. Thus, SC and FC are differentially impacted, and the SC-FC correlation is reduced. In later phases, both SC and FC may reflect extensive and concordant epileptic remodeling, which leads to an increased SC-FC correlation.

In Chapter 7, the SC-FC correlation was investigated in RE as a function of age. To test for separate structural or functional changes, graph theoretical measures of network organization were also studied for both SC and FC.

9.3.4.1 Maturational delay in structure-function correlation

A reduction in SC-FC correlation was found in the children with RE compared to the healthy controls. This did not seem to be caused by prominent network remodeling since no consistent effects were found with respect to structural or functional network organization. However, in the patients the SC-FC correlation significantly increased with age, whereas no such effect was found in the controls. We interpreted these results as a maturational delay in the SC-FC correlation in the children with RE. Possibly, SC and FC are already to a certain extent matched in the healthy controls, whereas in the children with RE, this process is still ongoing at the age range under investigation (8-14 year).

9.3.4.2 Localization the aberrant structure-function correlation

The above analyses were not only performed at the whole-brain level, but also for 5 sub-networks (modules) as identified from a modularity analysis of the average SC network of the controls. Similar effects as on the global level were found for a left and a right centro-temporal module, as well as for a medial parietal sub-network. In the latter, the reduction in SC-FC correlation was actually more pronounced than on the whole-brain level.

These medial parietal abnormalities may relate to the compromised visuo-spatial skills that have reported in RE (Pinton, Ducot et al. 2006; Volkl-Kernstock, Willinger et al. 2006).

More importantly, this medial parietal module provides an interface between the bilateral cento-temporal (rolandic) modules. Since these are the region from which the seizures originate in RE, our findings may reflect maturational delay in network development in (or near) epileptogenic cortex.

An important methodological consideration of this study is that the module structure employed to localize global effects may have been sub-optimal to detect aberrant sub-networks in RE. Dedicated investigation of the language network may have yielded more specific results, however probably at the cost of subjective choices concerning which nodes/connection to include in the analysis.

9.3.5 Overall insights for RE

Note that in RE, typically no lesions or other gross structural abnormalities are found upon neuroradiological examination of conventional MRI scans. It is therefore classified as a non-symptomatic localization-related epilepsy. In contrast, employing quantitative analysis, we demonstrated that abnormalities can be found with respect to cortical morphology, functional connectivity, white matter integrity, and the structure-function correlation. Moreover, all these abnormalities can, to a certain extent, be associated with type and severity of language impairments, which is a major component of the neuropsychological profile of impairment in RE (Overvliet GM, Besseling RM et al. 2010).

More specifically, our investigations into cortical morphology (Chapter 3) illustrated the distributed (rather than focal) character of RE, which motivated the application of connectivity analyses. From functional connectivity we learned that the motor and the language system are to a certain extent functionally integrated (Chapter 5). As a consequence, pathology in the rolandic cortex is likely to impact the language network as well. This is in line with our findings of reduced functional and structural connectivity (Chapter 4-6), and the associations between reduced connectivity and lower language performance we found in children with RE employing functional and structural data (Chapters 4 and 6, respectively). Finally, the investigations of SC-FC correlation (Chapter 7) suggest a maturational delay in network development, among others in centro-temporal (rolandic) cortex, and as such are in agreement with the abnormalities of cortical development reported in Chapter 3.

9.3.6 Methodological issues and directions for future research

The studies that were just discussed were designed to establish the link between RE and language impairment from a neuroimaging perspective. This is an important challenge, since in spite of all evidence, the non-benign character of RE is still under debate among clinicians (Hughes 2010). Within our group, important neuropsychological work has been done to establish that language impairment is an integrated aspect of RE (Overvliet GM, Besseling RM et al. 2010; Overvliet GM, Aldenkamp AP et al. 2011; Overvliet GM, Aldenkamp AP et al. 2011). This thesis aims to further elaborate this concept by providing underlying neuronal correlates of abnormalities in brain morphology and connectivity.

The studies presented here were described in a certain methodological order, which does not necessarily comply with the pathophysiological order of events. Most probably primary changes are of a reversible functional nature, and include subtle modifications of receptor expression patterns, neurotransmitter levels and synaptic densities. Structural connectivity will subsequently irreversibly change as a result of the altered network dynamics, and finally concordant morphological alterations will occur. The occurrence and timing of these neuropathological processes are important topics for future research.

Our work is on establishing neuronal correlates for language impairment, but is not aimed at exploring therapeutic options. A clinical debate is ongoing whether or not RE should be treated using anti-epileptic drugs (AEDs) (Hughes 2010). With the aim on seizure suppression, it is unclear whether this is desirable since seizures are typically mild and nocturnal and resolve spontaneously before the age of 16 years (Loiseau P and Duché B 1989; Panayiotopoulos, Michael et al. 2008). Moreover, AEDs may induce cognitive complaints and as such may offer no overall clinical improvement (Ijff and Aldenkamp 2013).

However, it has been argued that even subclinical epileptiform activity may have a detrimental effect on brain networks (Bourgeois and Landau 2004; Takeoka, Riviello et al. 2004). In line with this, it has been demonstrated that seizure-free siblings of children with RE (who do show ongoing EEG abnormalities) show impaired language performance (Clarke, Strug et al. 2007). Potentially the use of AEDs with the aim to suppress epileptiform activity (rather than seizures) is a useful therapeutic strategy, although at present still controversial (Arif, Buchsbaum et al. 2009; Porras-Kattz, Harmony et al. 2011). From a pathophysiological perspective, the suppression of epileptiform activity may reverse functional abnormalities, thus preventing subsequent permanent changes in structural connectivity and brain morphology. Timely onset of treatment (i.e. in the reversible phase) seems important in ensuring a normalization of the trajectory of brain development (Andersen 2003).

Longitudinal study designs seem essential in investigating the order of and interaction between changes in brain function, structure, and morphology (Rubinov, Sporns et al. 2009), and also to gain insight into how these changes are influenced by pharmacological intervention. Early inclusion, preferably before seizure onset (e.g. based on risk factors in the language profile; (Overvliet GM, Aldenkamp AP et al. 2011)), as well as sufficiently long follow up (until well after seizure remission) appear crucial for the success of such studies.

A further point of interest is the importance of the laterality of the abnormalities we described. The investigations of cortical thickness and structural connectivity suggested that especially the left hemisphere is affected in RE. However, one of the fMRI studies revealed bilateral language activation, as well as reduced functional connectivity in the right hemisphere (Chapter 4). Recent fMRI studies suggest reduced language lateralization and/or language network reorganization to the right hemisphere in RE (Vannest, Karunanayaka et al. 2009; Datta, Oser et al. 2013). Actually, this leaves unresolved in which hemisphere most (language-related) abnormalities are to be expected; abnormalities in both hemispheres should therefore be considered.

In this context, it seems likely that the laterality of the EEG abnormalities is of relevance, with stronger language network abnormalities and/or reorganization presenting in children with a left-lateralized epileptic focus (Liegeois, Connelly et al. 2004; Monjauze C, Broadbent H et al. 2011). However, it is well established that in RE the laterality (and severity) of the EEG abnormalities may dramatically change over time (Riva, Vago et al. 2007). In our clinical cohort, the EEG was assessed as part of the diagnostic work and not at the time of scanning. Since the majority of the children with RE (20/24) was right handed, primarily typical (left-lateralized) language processing may be assumed, although for future studies dedicated assessment of the current EEG status is warranted. For now, it seems likely that for the age range under study (8-14 years), brain abnormalities in

classical (left-lateralized) language areas as well as contralateral homotopic cortex may bear relevance for language impairment.

9.4 Aberrant functional connectivity in focal cortical dysplasia

Apart from the main body of work in this thesis on RE, also another cohort of focal epilepsy patients was studied, namely patients with focal cortical dysplasia (FCD).

Whereas in the chapters on RE the goal was to find neuronal correlates for language impairment, Chapter 8 on FCD has a more exploratory and descriptive nature. In contrast to RE, FCD is associated with structural brain lesions on conventional imaging, and the aim was to improve the characterization of these.

9.4.1 Clinically relevant versus MR-visible lesion

FCD often gives rise to medically refractory epilepsy, for which surgical resection of the cortical abnormality is a useful therapeutic option (Blumcke, Thom et al. 2011; Hauptman and Mathern 2012). Histopathological examinations of surgical specimens has demonstrated that surgery outcome with respect to seizure control is best when all aberrant cortex is removed (Hauptman and Mathern 2012). Even though FCDs can have clear features on conventional structural MRI, such as cortical thickening and blurring of the gray matter-white matter interface (Kassubek, Huppertz et al. 2002; Hofman, Fitt et al. 2011), it is not clear whether such macroscopic morphological characteristics are optimal to delineate the aberrant tissue. In other words, it is well possible that the clinically relevant abnormality of epileptogenic tissue exceeds the structural lesion as visible on conventional MRI.

9.4.2 Functional remodeling in relation to (micro)structural changes

Diffusion weighted imaging has already been applied to assess FCD microstructure and that of adjacent major white matter tracts (Lee, Kim et al. 2004; Widjaja, Blaser et al. 2007; Widjaja, Zarei Mahmoodabadi et al. 2009; Fonseca Vde, Yasuda et al. 2012).

Alternatively, fMRI provides information on gray matter neuronal activity (oxygen consumption), and functional connectivity may be employed to assess cortical (gray matter) abnormalities directly, rather than underlying white matter abnormalities. Furthermore, as functional and structural connectivity are mutually dependent (Rubinov, Sporns et al. 2009), functional remodeling is to be expected in relation to the already described (micro)structural changes (Widjaja, Zarei Mahmoodabadi et al. 2009; Wang, Deans et al. 2013).

In Chapter 8, functional connectivity is assessed as a function of the distance to the center of the structural lesion, and compared between patients and controls.

9.4.3 Homotopic comparison

An important methodological challenge is that FCD lesions may be located anywhere on the cortex. As a consequence, the applicability of group analyses based on spatial overlap of effects is limited. In Chapter 8, methodology is presented for inter-individual mapping of gyral patterns, which is partly based on the registration methods already explored in Chapter 2. Thus, local functional connectivity in the individual patient can be compared with homotopic connectivity profiles derived in the controls.

9.4.4 Aberrant functional connectivity profiles

In the patients, connectivity profiles were determined that were aberrant from the gradually decreasing homotopic connectivity profiles found in the controls. Both profiles of hyper- and hypoconnectivity were found, as well as combinations. In most cases, aberrant functional connectivity was also detected beyond the structural lesion. These extensive abnormalities of local functional connectivity may help to better delineate the clinically relevant cortical abnormality, i.e. (also) beyond the structural margins of the lesion.

9.4.5 Open issues

In this exploratory study, no clear associations were found between the type of aberrant connectivity profile and patient characteristics such as EEG findings. However, from EEG literature it has long been known that epileptiform spikes may acutely reduce the amplitude and increase the latency of local evoked potentials (Shewmon and Erwin 1988; Seri, Cerquiglini et al. 1998). It is not clear how such transient effects may influence ongoing neuronal signaling, although they may affect functional connectivity patterns. Potentially dedicated EEG assessment, e.g. employing subdural electrode grids, may help to establish the link between electrophysiology and functional imaging.

Furthermore, histopathological examination of surgical specimens is needed to investigate whether the observed abnormalities in functional connectivity translate to specific microscopic tissue abnormalities.

9.5 Overall conclusion

Taking the studies on RE and FCD together, the overall conclusion of this thesis is that neuronal correlates can be found for epilepsy characterized by focal seizures, and that these represent distributed abnormalities. Since the brain is a network, it indeed is unlikely that any abnormality of the brain is of a purely focal nature, and our findings are in line with this view.

For RE, in which no structural lesions are present, distributed abnormalities in cortical morphology as well as aberrant functional and structural connectivity link its epileptic focus in the rolandic cortex to impairments of the language system. More specifically, the functional architecture of the brain seems to facilitate propagation of rolandic pathology into the language system (Chapter 5). The combined findings probably reflect aberrant brain development (Chapter 3, Chapter 7).

For FCD and in a more explorative approach, it was demonstrated that abnormalities in functional connectivity may have a larger spatial extent than the structural lesion on conventional MRI, which may be relevant for surgical strategies.

References

Abbott, D. F., A. B. Waites, et al. (2010). "fMRI assessment of language lateralization: an objective approach." Neuroimage **50**(4): 1446-55.

Andersen, S. L. (2003). "Trajectories of brain development: point of vulnerability or window of opportunity?" Neurosci Biobehav Rev **27**(1-2): 3-18.

Arif, H., R. Buchsbaum, et al. (2009). "Patient-reported cognitive side effects of antiepileptic drugs: predictors and comparison of all commonly used antiepileptic drugs." Epilepsy Behav **14**(1): 202-9.

Bandettini, P. A. (2012). "Sewer pipe, wire, epoxy, and finger tapping: the start of fMRI at the Medical College of Wisconsin." Neuroimage **62**(2): 620-31.

Basser, P. J., J. Mattiello, et al. (1994). "MR diffusion tensor spectroscopy and imaging." Biophys J **66**(1): 259-67.

Beckmann, C. F., M. DeLuca, et al. (2005). "Investigations into resting-state connectivity using independent component analysis." Philos Trans R Soc Lond B Biol Sci **360**(1457): 1001-13.

Biswal, B., F. Z. Yetkin, et al. (1995). "Functional connectivity in the motor cortex of resting human brain using echo-planar MRI." Magn Reson Med **34**(4): 537-41.

Blumcke, I., M. Thom, et al. (2011). "The clinicopathologic spectrum of focal cortical dysplasias: a consensus classification proposed by an ad hoc Task Force of the ILAE Diagnostic Methods Commission." Epilepsia **52**(1): 158-74.

Bourgeois, B. F. and W. M. Landau (2004). "Landau-Kleffner syndrome and temporal cortical volume reduction: cause or effect?" Neurology **63**(7): 1152-3.

Boxerman JL, Hawash K, et al. (2007). "Is Rolandic epilepsy associated with abnormal findings on cranial MRI?" Epilepsy Research **75**(2-3): 180-185.

Calamante, F., J. D. Tournier, et al. (2010). "Track-density imaging (TDI): super-resolution white matter imaging using whole-brain track-density mapping." Neuroimage **53**(4): 1233-43.

Cappa, S. F. and F. Pulvermuller (2012). "Cortex special issue: Language and the motor system." Cortex.

Catani, M., D. K. Jones, et al. (2005). "Perisylvian language networks of the human brain." Ann Neurol **57**(1): 8-16.

Ciccarelli, O., G. J. Parker, et al. (2003). "From diffusion tractography to quantitative white matter tract measures: a reproducibility study." Neuroimage **18**(2): 348-59.

Clarke, T., L. J. Strug, et al. (2007). "High risk of reading disability and speech sound disorder in rolandic epilepsy families: case-control study." Epilepsia **48**(12): 2258-65.

Datta, A. N., N. Oser, et al. (2013). "Cognitive impairment and cortical reorganization in children with benign epilepsy with centrotemporal spikes." Epilepsia **54**(3): 487-94.

Duman, O., F. Kizilay, et al. (2008). "Electrophysiologic and neuropsychologic evaluation of patients with centrotemporal spikes." Int J Neurosci **118**(7): 995-1008.

Fejerman N (2009). "Atypical rolandic epilepsy." Epilepsia **50**(Suppl 7): 9-12.

Filippini, N., B. J. MacIntosh, et al. (2009). "Distinct patterns of brain activity in young carriers of the APOE-epsilon4 allele." Proc Natl Acad Sci U S A **106**(17): 7209-14.

Fonseca Vde, C., C. L. Yasuda, et al. (2012). "White matter abnormalities in patients with focal cortical dysplasia revealed by diffusion tensor imaging analysis in a voxelwise approach." Front Neurol **3**: 121.

Gong, G., Y. He, et al. (2012). "Convergence and divergence of thickness correlations with diffusion connections across the human cerebral cortex." Neuroimage **59**(2): 1239-48.

Hagmann, P., O. Sporns, et al. (2010). "White matter maturation reshapes structural connectivity in the late developing human brain." Proc Natl Acad Sci U S A **107**(44): 19067-72.

Hauptman, J. S. and G. W. Mathern (2012). "Surgical treatment of epilepsy associated with cortical dysplasia: 2012 update." Epilepsia **53 Suppl 4**: 98-104.

Heiervang, E., T. E. Behrens, et al. (2006). "Between session reproducibility and between subject variability of diffusion MR and tractography measures." Neuroimage **33**(3): 867-77.

Hofman, P. A., G. J. Fitt, et al. (2011). "Bottom-of-sulcus dysplasia: imaging features." AJR Am J Roentgenol **196**(4): 881-5.
Hughes, J. R. (2010). "Benign epilepsy of childhood with centrotemporal spikes (BECTS): to treat or not to treat, that is the question." Epilepsy Behav **19**(3): 197-203.
Ijff, D. M. and A. P. Aldenkamp (2013). "Cognitive side-effects of antiepileptic drugs in children." Handb Clin Neurol **111**: 707-18.
Kadis, D. S., E. W. Pang, et al. (2011). "Characterizing the normal developmental trajectory of expressive language lateralization using magnetoencephalography." J Int Neuropsychol Soc **17**(5): 896-904.
Kassubek, J., H. J. Huppertz, et al. (2002). "Detection and localization of focal cortical dysplasia by voxel-based 3-D MRI analysis." Epilepsia **43**(6): 596-602.
Kavros PM, Clarke T, et al. (2008). "Attention impairment in rolandic epilepsy: systematic review." Epilepsia **49**(9): 1570-1580.
Lee, S. K., D. I. Kim, et al. (2004). "Diffusion tensor MRI visualizes decreased subcortical fiber connectivity in focal cortical dysplasia." Neuroimage **22**(4): 1826-9.
Liao, W., Z. Zhang, et al. (2013). "Relationship between large-scale functional and structural covariance networks in idiopathic generalized epilepsy." Brain Connect **3**(3): 240-54.
Liegeois, F., A. Connelly, et al. (2004). "Language reorganization in children with early-onset lesions of the left hemisphere: an fMRI study." Brain **127**(Pt 6): 1229-36.
Lindgren S, Kihlgren M, et al. (2004). "Development of cognitive functions in children with rolandic epilepsy." Epilepsy Behav. **5**(6): 903-910.
Loiseau P and Duché B (1989). "Benign childhood epilepsy with centrotemporal spikes." Cleve Clin J Med **56**(Suppl Pt 1): S17-22; discussion S40-2.
Lundberg S, Frylmark A, et al. (2005). "Children with rolandic epilepsy have abnormalities of oromotor and dichotic listening performance." Dev Med Child Neurol **47**(9): 603-608.
Massa R, de Saint-Martin A, et al. (2001). "EEG criteria predictive of complicated evolution in idiopathic rolandic epilepsy." Neurology **57**(6): 1071-1079.
Monjauze C, Broadbent H, et al. (2011). "Language deficits and altered hemispheric lateralization in young people in remission from BECTS." Epilepsia **52**(8): e79-e83.
Monjauze C, Tuller L, et al. (2005). "Language in benign childhood epilepsy with centro-temporal spikes abbreviated form: rolandic epilepsy and language." Brain and Language **92**(3): 300-308.
Muftuler, L. T., E. P. Davis, et al. (2011). "Cortical and subcortical changes in typically developing preadolescent children." Brain Res **1399**: 15-24.
Northcott E, Connolly AM, et al. (2005). "The neuropsychological and language profile of children with benign rolandic epilepsy." Epilepsia **46**(6): 924-930.
Overvliet GM, Aldenkamp AP, et al. (2011). "Correlation between language impairment and problems in motor development in children with Rolandic epilepsy." Epilepsy & Behavior.
Overvliet GM, Aldenkamp AP, et al. (2011). "Impaired language performance as a precursor or consequence of Rolandic epilepsy?" Journal of the Neurological Sciences **304**(1): 71-74.
Overvliet GM, Besseling RM, et al. (2010). "Nocturnal epileptiform EEG discharges, nocturnal epileptic seizures, and language impairments in children: Review of the literature." Epilepsy Behav **19**(4): 550-558.
Panayiotopoulos, C. P., M. Michael, et al. (2008). "Benign childhood focal epilepsies: assessment of established and newly recognized syndromes." Brain **131**(Pt 9): 2264-86.
Papavasiliou A, Mattheou D, et al. (2005). "Written language skills in children with benign childhood epilepsy with centrotemporal spikes." Epilepsy & Behavior **6**(1): 50-58.
Pinton, F., B. Ducot, et al. (2006). "Cognitive functions in children with benign childhood epilepsy with centrotemporal spikes (BECTS)." Epileptic Disord **8**(1): 11-23.
Porras-Kattz, E., T. Harmony, et al. (2011). "Magnesium valproate in learning disabled children with interictal paroxysmal EEG patterns: Preliminary report." Neurosci Lett **492**(2): 99-104.
Price CJ (2010). "The anatomy of language: a review of 100 fMRI studies published in 2009." Ann N Y Acad Science **1191**: 62-88.

Pulvermuller, F., M. Huss, et al. (2006). "Motor cortex maps articulatory features of speech sounds." Proc Natl Acad Sci U S A **103**(20): 7865-70.

Raznahan A, Shaw P, et al. (2011). "How does your cortex grow?" Journal of Neuroscience **31**(19): 7174-7177.

Riva, D., C. Vago, et al. (2007). "Intellectual and language findings and their relationship to EEG characteristics in benign childhood epilepsy with centrotemporal spikes." Epilepsy Behav **10**(2): 278-85.

Rubinov, M., O. Sporns, et al. (2009). "Symbiotic relationship between brain structure and dynamics." BMC Neurosci **10**: 55.

Seri, S., A. Cerquiglini, et al. (1998). "Spike-induced interference in auditory sensory processing in Landau-Kleffner syndrome." Electroencephalogr Clin Neurophysiol **108**(5): 506-10.

Shewmon, D. A. and R. J. Erwin (1988). "The effect of focal interictal spikes on perception and reaction time. II. Neuroanatomic specificity." Electroencephalogr Clin Neurophysiol **69**(4): 338-52.

Smith, S. M. (2012). "The future of FMRI connectivity." Neuroimage **62**(2): 1257-66.

Smith, S. M., P. T. Fox, et al. (2009). "Correspondence of the brain's functional architecture during activation and rest." Proc Natl Acad Sci U S A **106**(31): 13040-5.

Smith, S. M., M. Jenkinson, et al. (2004). "Advances in functional and structural MR image analysis and implementation as FSL." Neuroimage **23 Suppl 1**: S208-19.

Supekar, K., L. Q. Uddin, et al. (2010). "Development of functional and structural connectivity within the default mode network in young children." Neuroimage **52**(1): 290-301.

Takeoka, M., J. J. Riviello, Jr., et al. (2004). "Bilateral volume reduction of the superior temporal areas in Landau-Kleffner syndrome." Neurology **63**(7): 1289-92.

Tomasi, D. and N. D. Volkow (2012). "Resting functional connectivity of language networks: characterization and reproducibility." Mol Psychiatry **17**(8): 841-54.

Tournier, J. D., F. Calamante, et al. (2007). "Robust determination of the fibre orientation distribution in diffusion MRI: non-negativity constrained super-resolved spherical deconvolution." Neuroimage **35**(4): 1459-72.

van Diessen, E., S. J. Diederen, et al. (2013). "Functional and structural brain networks in epilepsy: What have we learned?" Epilepsia **54**(11): 1855-65.

Vannest, J., P. R. Karunanayaka, et al. (2009). "Language networks in children: evidence from functional MRI studies." AJR Am J Roentgenol **192**(5): 1190-6.

Volkl-Kernstock, S., U. Willinger, et al. (2006). "Spacial perception and spatial memory in children with benign childhood epilepsy with centro-temporal spikes (BCECTS)." Epilepsy Res **72**(1): 39-48.

Wakana, S., A. Caprihan, et al. (2007). "Reproducibility of quantitative tractography methods applied to cerebral white matter." Neuroimage **36**(3): 630-44.

Wang, D. D., A. E. Deans, et al. (2013). "Transmantle sign in focal cortical dysplasia: a unique radiological entity with excellent prognosis for seizure control." J Neurosurg **118**(2): 337-44.

Widjaja, E., S. Blaser, et al. (2007). "Evaluation of subcortical white matter and deep white matter tracts in malformations of cortical development." Epilepsia **48**(8): 1460-9.

Widjaja, E., S. Zarei Mahmoodabadi, et al. (2009). "Subcortical alterations in tissue microstructure adjacent to focal cortical dysplasia: detection at diffusion-tensor MR imaging by using magnetoencephalographic dipole cluster localization." Radiology **251**(1): 206-15.

Woolrich, M. W., S. Jbabdi, et al. (2009). "Bayesian analysis of neuroimaging data in FSL." Neuroimage **45**(1 Suppl): S173-86.

Yuan, W., J. P. Szaflarski, et al. (2006). "fMRI shows atypical language lateralization in pediatric epilepsy patients." Epilepsia **47**(3): 593-600.

Zhang, Z., W. Liao, et al. (2011). "Altered functional-structural coupling of large-scale brain networks in idiopathic generalized epilepsy." Brain **134**(Pt 10): 2912-28.

Summary

The brain processes internal and external information by synchronization of neuronal activity within distributed networks. Epilepsy is a neurological disorder that is characterized by spontaneously occurring recurrent seizures and a more or less pronounced disturbance of this information processing. Seizures are associated with typical abnormalities on electroencephalography (EEG), and represent episodes of hypersynchronisation of hyperexcitable cortical neurons. The type and severity of the seizures depends on the location and extent of the aberrant cortex (epileptogenic zone), and to what extent the epileptiform activity spread over the brain.

Rolandic epilepsy (RE) is one of the most common childhood epilepsies and is characterized by centro-temporal spikes on EEG and mild seizures (i.e. short and with preserved consciousness), which are typically nocturnal. Over the last decade, RE has been associated with language impairments, which can clinically be of more relevance than the seizures. The aim of this thesis is to find neuronal correlates of aberrant brain connections that link the epileptic focus in the rolandic (sensorimotor) cortex to abnormalities in (distal) language areas, employing advanced magnetic resonance imaging (MRI) methods. The unveiling of the underlying brain abnormalities may provide new insights, in addition to the existing literature of largely neuropsychological nature.

In a quantitative morphological approach, Chapter 3 describes distributed reductions in cortical thickness in children with RE compared to healthy controls. Moreover, cortical thinning with age was found in the patients, but not in the controls. These effects were most prominent in the left hemisphere, and covered supramarginal, inferior frontal and middle temporal regions which are classically considered language-mediating. These findings demonstrate that RE is a distributed (rather than focal) pathology, and represent subtle morphopathology.

Concerning the neuropathological mechanism, cortical thinning is not a pathological effect per se. It may also represent a phase of normal brain development, in which redundant connections are removed from the initially overcomplete brain network to improve its efficiency and efficacy. This normal maturation effect would result in cortical thinning within the age range of this study (8-14 years) as well. However, since the controls were in the transition between cortical thickening and cortical thinning, we interpreted the persistent cortical thinning in the patients as pathological. Possibly, RE-related epileptiform activity causes additional and unselective removal of brain connections, which compromises network topology and thus cognition.

The finding that RE is a distributed (rather than focal) pathology motivated dedicated connectivity analyses to study the networks involved. Chapters 4 and 5 investigate neuronal dynamics using functional MRI. This led to the finding that in RE, functional connectivity is reduced between the rolandic cortex (epileptic focus) and classical language mediating regions (or contralateral homotopic cortex), notably Broca's area. These findings represent functional correlates for language impairment in RE. Moreover, in Chapter 4 reduced functional connectivity was associated with lower language performance in the patients.

An important generic insight from Chapter 5 is that the rolandic cortex and the language-mediating inferior frontal, supramarginal, and superior temporal cortices are to a certain extent integrated, also in the controls. Using independent component analysis (ICA), it was demonstrated that at the systems level, these regions all reside within the same spatio-temporal pattern of synchronous resting-state activity. Resting-state networks are assumed to consolidate and maintain the intrinsic functional architecture of the brain at rest. In RE, this moto-lingual integration is an important model to link rolandic (sensorimotor) abnormalities, such as epileptiform activity and seizures, to co-occuring language problems. In other words, rolandic neuropathology is expected to inherently affect the language network.

Having established functional correlates for language impairment in RE, Chapter 6 investigates tissue microstructure and structural connectivity employing high angular resolution diffusion weighted imaging (HARDI) and white matter fiber tractography. Patterns of high rolandic connectivity were found for inferior frontal, supramarginal, and superior temporal cortex, which were taken forward to further analysis. Connectivity abnormalities consistently represented reductions in fractional anisotropy (FA), which can be interpreted as decreased white matter integrity. Particularly the left supramarginal and inferior frontal gyri were affected. For the connection between the latter and the left postcentral gyrus, reduced connectivity was associated with lower language performance in the patients. These findings represent structural abnormalities of language-mediating white matter connections.

Finally, in Chapter 7 structural and functional connectivity (SC and FC, respectively) are combined in an investigation of the SC-FC correlation. During normal brain development, SC and FC converge, driven by a common maturation process of brain network optimization. The brain infrastructure is being matched to the information traffic and vice versa, which leads to an increased SC-FC correlation. In epilepsy, however, both reduced and increased SC-FC correlations have been reported, probably reflective of pathological changes in network integrity. To investigate to what extent functional and/or structural remodeling may manifest in RE, graph theoretical analyses of network organization was included.

A reduction in SC-FC correlation was found in patients compared to controls, most strongly for the youngest subjects and less so for the older children. Graph theoretical measures revealed no consistent abnormalities in structural or functional network organization. These findings were interpreted as a maturational delay in SC-FC convergence in the children with RE compared to the controls. Possibly in the controls SC and FC were already to a certain extent integrated, whereas in the patients this process was still ongoing in the age range under study (8-14 years). These effects were strongest for medial-parietal connections, which form an interface between the bilateral centro-temporal (rolandic) regions.

In addition to the investigations into neuronal correlates for language impairment in RE, a cohort of focal cortical dysplasia (FCD) patients was studied. FCD represent a congenital malformation of cortical development that is highly epileptogenic and often drug resistant. Surgical removal of the cortical abnormality can be a successful therapeutic strategy and requires accurate neuroimaging to delineate the lesion. However, histopathological examination of surgical specimens has demonstrated that the clinically relevant abnormality of epileptogenic cortex may exceed the macroscopic lesion as seen on conventional MRI.

In an exploratory approach, we investigated local functional connectivity of FCD lesions to characterize the adjacent cortex. For this, patient-specific FCD connectivity patterns were compared to homotopic local connectivity profiles derived from healthy controls.

Patient connectivity profiles represented significant hypoconnectivity, hyperconnectivity, and combinations. Typically, connectivity abnormalities were also found beyond the structural margins of the lesion. Dedicated electrophysiological and histopathological examinations are needed to validate whether these functional abnormalities translate to clinically relevant microstructural tissue abnormalities.

In conclusion, RE is characterized by distributed abnormalities in functional and structural connectivity, which provide a basis for dysfunction in distant circuits. Which networks are exactly affected depends on the intrinsic functional and/or structural architecture of the brain; in RE this typically concerns language problems. The combined findings reflect a process of aberrant brain maturation, among others a delayed convergence between brain network structure and function. Finally, the extensive nature of local functional abnormalities in FCD deserves further research, and may have important consequences for surgical planning.

Samenvatting

Het brein verwerkt interne en externe informatie door het synchroniseren van neuronale activiteit in gedistribueerde hersennetwerken. Epilepsie is een neuronale aandoening die gekenmerkt wordt door aanvallen en waarbij die informatieverwerking in meer of mindere mate verstoord is. Epileptische aanvallen gaan samen met typische verstoringen van het electroencephalogram (EEG) en zijn feitelijk episodes van hypersynchronisatie van hypersensitieve corticale neuronen. De soort en ernst van de aanvallen hangt af van de locatie en grootte van de corticale afwijking (epileptogene zone), en wordt ook bepaald door de mate waarin de epileptiforme activiteit spreidt over de rest van het brein.

Rolandische epilepsie (RE) is één van de meest voorkomende kinderepilepsiën, en wordt gekarakteriseerd door centro-temporale ontladingen op het EEG en relatief milde aanvallen (kort en met behoud van bewustzijn), die vaak 's nachts plaatsvinden. Gedurende de laatste jaren is het duidelijk geworden dat RE samengaat met cognitieve problemen die ernstiger kunnen zijn dan de aanvallen zelf. Doel van dit proefschrift is om met behulp van geavanceerde MRI technieken afwijkende hersenverbindingen op te sporen die het epileptische focus in de rolandische (sensomotorische) cortex linken aan afwijkingen van het taalnetwerk. Het opsporen van hersenafwijkingen die bij RE ten grondslag liggen aan de taalproblemen biedt nieuwe inzichten t.o.v. de neuropsychologische studies waarbij deze taalproblemen zijn aangetoond.

Hoofdstuk 3 is een kwantitatieve morfologische studie en beschrijft gedistribueerde afwijkingen in corticale dikte bij kinderen met RE ten opzichte van gezonde controlekinderen. Bovendien werden er progressieve afnames in corticale dikte gevonden bij de patiëntjes, maar niet bij de controles. Deze effecten traden vooral op in de linker hemisfeer, en betroffen supramarginale, inferieur frontale en midtemporale regio's die geassocieerd kunnen worden met taalfunctie. Deze bevindingen illustreren dat RE een gedistribueerde (i.p.v. focale) afwijking is en tonen subtiele morfopathologie van het brein aan.

Wat het neuropathologische mechanisme betreft is afname van de cortexdikte geen ziekteproces op zichzelf. In aanleg is het brein namelijk een overcompleet netwerk; tijdens de ontwikkeling verdwijnen overbodige hersenverbindingen om de efficiëntie en effectiviteit van dit netwerk te vergroten (het zogenaamde *pruning*). Ook deze normale ontwikkeling zou resulteren in een afname van corticale dikte binnen de leeftijdsrange van deze studie (8-14 jaar). Omdat we vonden dat de controles in de overgang van diktetoename naar dikteafname waren, interpreteerden wij de persisterende afname van de cortexdikte in de patiëntjes als pathologisch. Mogelijk zorgen epileptische

ontladingen ervoor dat er bij RE naast selectieve pruning ook willekeurig hersenverbindingen verdwijnen, waardoor de topologie van het netwerk en daarmee de cognitie wordt aangedaan.

De bevinding dat RE een gedistribueerd (i.p.v. focaal) karakter heeft is een reden voor de toepassing van connectiviteitsanalyses om de betrokken netwerken te bestuderen. De hoofdstukken 4 en 5 beschrijven patronen van fluctuaties in neuronale activiteit zoals bestudeerd middels functionele MRI. We vonden dat bij RE de functionele connectiviteit verminderd is tussen de rolandische cortex (epileptisch focus) en bekende taalgebieden (of contralaterale homotope cortex), met name het gebied van Broca. Deze bevindingen representeren functionele correlaten voor taalproblematiek bij RE. In hoofdstuk 4 bleek de gerapporteerde afname in functionele connectiviteit bovendien te correleren met lagere taalprestaties in de patiëntjes.

Een belangrijk algemeen inzicht uit hoofdstuk 5 is dat de rolandische cortex en belangrijke taalgebieden in de inferieur frontale, supramarginale en superieur temporale cortex op een bepaalde manier geïntegreerd zijn, ook bij de gezonde controlekinderen. Middels analyse van onafhankelijk componenten (*independent component analysis*; ICA) werd namelijk aangetoond dat in rust al deze gebieden op systeemniveau deel uitmaken van hetzelfde spatio-temporele patroon. Het wordt aangenomen dat zo'n zogenaamd *resting-state* netwerk de intrinsieke functionele architectuur van het brein voorstelt, en ervoor zorgt dat in rust de functionele samenhang tussen de betrokken gebieden onderhouden wordt. Bij RE is deze verstoorde integratie tussen de motorcortex en taalgebieden een belangrijk model om rolandische (sensomotorische) afwijkingen zoals epileptische ontladingen en aanvallen te linken met de taalproblemen die ook vaak gevonden worden. Met andere woorden, rolandische neuropathologie heeft inherent ook effect op het taalnetwerk.

Na het vaststellen van functionele correlaten voor taalproblematiek bij RE, behandelt hoofdstuk 6 het vinden van afwijkingen in witte stof microstructuur en abnormale structurele connectiviteit met behulp van hoog-angulaire resolutie diffusiegewogen beeldvorming (*high angular resolution diffusion weighted imaging*; HARDI) en tractografie. Patronen van hoge rolandische connectiviteit werden gevonden voor de inferieur frontale, supramarginale en superieur temporale cortex; deze verbindingen werden nader onderzocht. Connectiviteitsafwijkingen betroffen steeds afnames in fractionele anisotropie (FA), hetgeen kan worden geïnterpreteerd als afnames in witte stof integriteit. Vooral de supramarginale en inferieur frontale gyri van de linker hemisfeer bleken aangedaan. Voor de verbinding tussen die laatste en de linker postcentrale gyrus was bij de patiëntjes een lagere connectiviteit geassocieerd met een afname in taalprestatie. Deze bevindingen representeren structurele afwijkingen van witte stofbanen die van belang zijn voor taal.

Tot slot combineert hoofdstuk 7 structurele en functionele connectiviteit (SC en FC, respectievelijk) in een studie naar de SC-FC correlatie. Bij normale hersenontwikkeling convergeren SC en FC als gevolg van een gemeenschappelijk maturatieproces van netwerkoptimalisatie. De infrastructuur van het brein wordt als het ware afgestemd op het informatieverkeer en andersom, waardoor de SC-FC correlatie toeneemt. Bij epilepsie zijn echter zowel afnames als toenames in de SC-FC correlatie gevonden, waarschijnlijk als gevolg van pathologische veranderingen in de netwerkstructuur. Om te onderzoeken in welke mate functionele en/of structurele veranderingen op zichzelf een rol spelen bij RE, werd er bij deze sudie ook naar graaftheoretische maten van netwerkorganisatie gekeken.

Een afname van de SC-FC correlatie werd gevonden in de patiëntjes t.o.v. de controles, en in meerdere mate voor de jongere subjecten dan voor de oudere kinderen. Met graaftheorie werden geen consistente afwijkingen in structurele of functionele netwerkorganisatie gevonden. Deze bevindingen werden geïnterpreteerd als een ontwikkelingsachterstand in de SC-FC convergentie voor de kinderen met RE t.o.v. de controlekinderen. Mogelijk waren SC en FC bij de controles al min of meer op elkaar afgestemd, terwijl dit proces bij de patiëntjes nog bezig was binnen de leeftijdsrange die is onderzocht (8-14 jaar). Deze effecten waren het sterkst voor medio-parietale connecties die de beide centro-temporale (rolandische) regio's met elkaar verbinden.

Naast het onderzoek naar neuronale correlaten voor taalproblematiek bij RE werd ook een groep patiënten met focale corticale dysplasieën (FCD) bestudeerd. FCD is een aangeboren aanlegstoornis van de cortex die sterk epileptogeen is; de resulterende epilepsie laat zich vaak niet goed met medicijnen behandelen. Chirurgische resectie van de cortexafwijking kan een effectieve behandeling zijn en vereist nauwkeurige beeldvorming om het pathologische weefsel af te bakenen. Histopathologisch onderzoek aan resectiemateriaal laat echter zien dat de klinisch relevante afwijking (epileptogeen weefsel) groter kan zijn dan de macroscopische lesie zoals die op conventionele MRI wordt gezien.

In een exploratieve studie onderzochten wij de lokale functionele connectiviteit van FCD lesies met als doel de omliggende cortex te karakteriseren. Hiervoor werden patiënt-specifieke FCD connectiviteitspatronen vergeleken met homotope lokale connectiviteitspatronen zoals bepaald in gezonde controles.

Bij de connectiviteitspatronen van de patiënten was sprake van significante hypo- en hyperconnectiviteit, maar ook combinaties hiervan. Typisch was de connectiviteit ook afwijkend buiten de structurele grenzen van de lesie. Verder electrofysiologisch en histopathologisch onderzoek is vereist om te bepalen of deze functionele afwijkingen samengaan met klinisch relevante afwijkingen in de microstructuur van het weefsel.

Samenvattend kunnen we stellen dat RE samengaat met gedistribueerde afwijkingen in functionele en structurele connectiveit en aldus invloed kan hebben op distale neuronale circuits. Welke netwerken exact aangedaan zijn hangt af van de intrinsieke functionele en/of structurele architectuur van het brein; bij RE zijn dit met name taalproblemen. De gecombineerde bevindingen weerspiegelen een abnormale hersenontwikkeling, met name een achterstand in de convergentie tussen netwerkstructuur en –functie. Voor FCD is tot slot verder onderzoek nodig naar het uitgebreide karakter van lokale afwijkingen in functionele connectiviteit, aangezien dit belangrijke consequenties kan hebben voor de chirurgische planning.

Dankwoord

Best belangrijk, zo'n dankwoord... Zeker als je je realiseert dat dat het meest gelezen deel van je proefschrift is! En best lastig ook, want er zijn natuurlijk een boel mensen betrokken bij een promotie. Sommigen van (heel) dichtbij, anderen wat meer op afstand, en dat verandert bovendien in de loop van het project. Allemaal hebben ze op één of andere manier een rol gespeeld in de totstandkoming van dit boekje.

Prof Dr A. P. Aldenkamp, beste Bert, bedankt dat ik deel mocht uitmaken van jouw epilepsie imaginggroep. Met het focus op "niet doen wat technisch mogelijk, maar wat klinisch wenselijk is" stond de translatie van het onderzoek naar de klinische praktijk altijd hoog in het vaandel. Zeker voor iemand met een technische achtergrond zoals ik was dit een goede insteek om richting te geven aan het onderzoek.

Prof Dr Ir W. H. Backes, beste Walter, bedankt voor de fijne dagelijkse begeleiding. Kenmerkend voor je voortvarende stijl is dat je regelmatig binnenstormt en zegt: "Enne?" Afhankelijk van de context kan dit een veelvoud aan dingen betekenen, zoals: functioneert die nieuwe analyse nou, wat moeten we nog bespreken, heb je mijn mail gelezen, hoe schiet het op met het manuscript van het artikel, enzovoorts. Fijn dat je me steeds meer ruimte bood voor eigen ideeën, dat wekt vertrouwen en heeft tot mooie nieuwe inzichten geleid, bijvoorbeeld bij de ICA analyse. Gefeliciteerd dat je werklust en inzet nu zijn beloond met de titel van hoogleraar!

Dr J. F. A. Jansen, beste Jaap, ook jij hartstikke bedankt dat ik steeds bij je kon aankloppen. Je bent snel van begrip en kritisch, en wist zo uitstekend te duiden waar het onderzoek rammelde, en welke analyses anders of beter moesten. Je weet de dingen altijd duidelijk uit te leggen, ook in het Engels, en dit is de leesbaarheid van de artikelen zeker ten goede gekomen.

Dr P. A. M. Hofman, beste Paul, in een multidisciplinair team mag een klinische begeleider natuurlijk niet ontbreken. Tijdens de besprekingen met Walter en Jaap voorzag jij ons altijd van de juiste klinische perspectieven, en hetzelfde gold voor je feedback op de manuscripten: bedankt daarvoor!

Beste Geke, jij was gedurende de eerste 2 jaar mijn klinische buddy, en door jouw neuropsychologisch onderzoek staat nu vast hoe belangrijk de rol van taalproblematiek is bij rolandische epilepsie. Op die manier heb je de weg vrijgemaakt voor mijn neuroimaging werk naar welke veranderingen in de hersenen daaraan ten grondslag liggen. Ik denk niet alleen graag terug aan de gezellige ritten naar Kempenhaeghe, maar ook aan de stevige discussies die we hadden, en die soms aan de REL studie een heel andere betekenis gaven...

Ook de neuroimaging aio's wil ik bedanken; eerst was dat alleen Maarten, die inmiddels alweer zo'n 2 jaar als postdoc in Genève werkt, maar inmiddels zijn er een aantal "brainiacs" bijgekomen: Harm, Frank, Tamar en May. Ik vond jullie fijne roomies, en vond het leuk om met jullie van gedachten te wisselen over analysemethodes en breinfunctie, en programmeerfrustraties te delen. Ik wens jullie veel succes met jullie eigen onderzoek.

Verder wil ik Jos en Marc vermelden, aan wie ik menige (domme?) scripting vraag heb gesteld, en die ook meer dan eens van hun stoel moeten zijn gevallen als ze zagen hoeveel gigabyte ik die dag weer had weggeschreven. Zonder jullie geweldige IT kennis en mooie cluster van workstations stond mijn laptop misschien zelfs nu nog te ratelen op de eerste analyse...!

Natuurlijk wil ik ook de andere stafleden en aio's van radiologie bedanken voor de samenwerking en de goede sfeer. Prof Dr Joachim Wildberger wil ik ervoor bedanken dat ik op deze fijne afdeling een werkplek mocht hebben.

Van de afdeling Neurologie wil ik Dr Mariëlle Vlooswijk bedanken, die vanuit haar eigen onderzoek naar netwerkproblemen bij epilepsie altijd veel interesse had in mijn werk. Prof Dr Hans Vles wil ik bedanken voor zijn kinderneurologische expertise, en de opbouwende feedback en uitdagende vragen n.a.v. de verschillende manuscripten. Neuroradioloog Christianne Hoeberigs wil ik bedanken voor haar aandeel in het beoordelen van de imaging van de FCD patiënten.

Vanuit Kempenhaeghe wil ik Dr Anton de Louw en Saskia Ebus bedanken voor hun klinische EEG kennis, toch een onmisbare expertise voor wie epilepsie bestudeert.

Daarnaast ook Prof Dr Paul Boon, naast Bert hoofd van de afdeling O&O (onderzoek en ontwikkeling). Paul, jij stond wat verder van mijn onderzoek af en zag de voortgang met name tijdens de promovendidagen, maar dit was altijd met gemeende interesse, ik heb dat als zeer motiverend ervaren.

Ook Esther Peeters mag hier niet onvermeld blijven, met wie ik menige gezellige vrijdag achter de scannerconsole heb doorgebracht. Ik bewonder hoe goed je de kinderen op hun gemak kon stellen en hoe soepel het scannen vervolgens verliep. Het gaat je goed op je nieuwe werkplek bij Scannexus!

Verder wil ik de Kempenhaeghse aio's bedanken voor de al genoemde en interessante promovendidagen, maar ook de gezellige etentjes na afloop. Met name noem ik Sylvie, die in elk artikelmanuscript altijd weer taal- en spelfouten wist te vinden waar iedereen al meerdere keren overheen gelezen had.

Ook de studenten en klifio's die onderzoek bij ons deden wil ik bedanken; Rachelle, Marloes, Eduard, Sri, Helen en Lisanne. Sorry dat ik jullie vragen vaak met een (of meerdere) tegenvragen beantwoordde, maar hé, zo werkt wetenschap: dé manier bestaat niet, en alleen met verschillende perspectieven op hetzelfde probleem kom je uiteindelijk verder. Ik hoop dat jullie er een boel van geleerd hebben; ik in elk geval wel.

Dan zijn er nog de onderzoekers van buiten de eigen groep; Miriam, Dennis, Jan, Elisabeth, Desiree, Martijn en Anja met wie ik met veel plezier de ISMRM Benelux 2012 heb georganiseerd. Furthermore, I'd like to mention the researchers who again and again proved challenged by an interesting question in their e-mail, and who especially at the beginning of my research helped me to get a grip on the field. I'd especially like to acknowledge Alexander Leemans and Donald Tournier for their help.

Ook wil ik alle kinderen, ouders en volwassenen bedanken die aan onze studies deelnamen. Zonder jullie geen data, en zonder data geen analyses. Bedankt voor jullie tijd en interesse in ons onderzoek, we hebben er een boel van geleerd!

Verder wil ik pap, mam en Michel bedanken. Ondanks dat jullie niet alle details van mijn onderzoek even goed snapten, zijn jullie een vaste factor in mijn leven en steunden jullie mij in mijn keus te gaan promoveren. Dat voelt voor jullie misschien vanzelfsprekend, maar dit is wat mij betreft dé plek om daar dankjewel voor te zeggen!

En het is wat cliché, maar laat ik dan toch maar eindigen met Birgit. Lieve meid, bedankt dat jij er bent en dat we het zo fijn hebben samen. Bedankt ook, dat ik af en toe mocht zeuren als een script na het weekend bleek te zijn vastgelopen, of als een analyse domweg niks opleverde. Inmiddels ken je die aio-frustraties zelf maar al te goed, maar uiteindelijk zul je net als ik kunnen zeggen: het is volbracht!

René Besseling
Maastricht, januari 2014

Curriculum Vitae

René Besseling was born on October 10, 1984, in Maastricht. After secondary school (St Maartens College, gymnasium), he studied Biomedical Engineering at the Eindhoven University of Technology. He passed his propaedeutic year cum laude and his bachelor phase with great appreciation. Under supervision of Prof Peter Hilbers (Biomedical Engineering) and Dr Massimo Mischi (Electrical Engineering), he graduated with great appreciation on prostate cancer detection and grading from dynamic contrast-enhanced ultrasound. This work resulted in his first conference contribution (IEEE EMBS 2009), and may have kindled his interests in scientific research.

After graduation, René further pursued his scientific career at the epilepsy research group of Prof Bert Aldenkamp. Located at the department of Radiology of the Maastricht University Medical Center and in close collaboration with Epilepsy Center Kempenhaeghe in Heeze, he studied functional and structural brain connectivity in epilepsy using advanced MRI methods. Under supervision of Prof Aldenkamp, Dr Walter Backes, Dr Jaap Jansen and Dr Paul Hofman, this led to numerous contributions to international scientific conferences. In 2012, he was co-organizer of the ISMRM Benelux Chapter annual meeting in Leuven. Furthermore, his work resulted in several scientific publications, which form the basis for the thesis that lies in front of you.

Having to commute back and forth to Eindhoven for the first 1.5 years of his PhD project, René loves that he can now cycle to work. However, he is very fond of vintage cars, especially the Renault 4 model, of which he owns several that he restores and repairs himself. Furthermore, he is active as tenor and board member in the Maastricht University Choir.

List of publications

First author:

1. *Reduced structural connectivity between sensorimotor and language areas in rolandic epilepsy*, **René M. H. Besseling**, Jacobus F.A. Jansen, Geke M. Overvliet, Sylvie J.M. van der Kruijs, Saskia C.M. Ebus, Anton de Louw, Paul A.M. Hofman, Johannes S.H. Vles, Albert P. Aldenkamp, Walter H. Backes
   PLoS ONE 2013; 8(12): e83568. doi: 10.1371 /journal.pone.0083568
2. *Aberrant functional connectivity between motor and language networks in rolandic epilepsy*, **René M.H. Besseling**, Geke M. Overvliet, Jacobus .F.A Jansen, Sylvie J.M. van der Kruijs, Johannes S.H. Vles, Saskia C.M. Ebus, Paul A.M. Hofman, Anton de Louw, Albert P. Aldenkamp, Walter H. Backes,
   Epilepsy Research 2013; 107, 253-262
3. *Reduced functional integration of the sensorimotor and language network in rolandic epilepsy,* **René M.H. Besseling**, Jacobus F.A. Jansen, Geke M. Overvliet, Sylvie J.M. van der Kruijs, Johannes S.H. Vles, Saskia C.M. Ebus, Paul A.M. Hofman, Anton de Louw, Albert P. Aldenkamp, Walter H. Backes,
   NeuroImage Clinical 2013; 2, 239–246
4. *Early onset of cortical thinning in children with rolandic epilepsy,* Geke M. Overvliet & **René M.H. Besseling**, Jacobus F.A. Jansen, Sylvie J.M. van der Kruijs, Johannes S.H. Vles, Paul A.M. Hofman, Saskia C.M. Ebus, Anton de Louw, Albert P. Aldenkamp, Walter H. Backes,
   NeuroImage Clinical 2013; 2, 434–439
5. *Tract Specific Reproducibility of Tractography Based Morphology and Diffusion Metrics,* **Besseling RM**, Jansen JF, Overvliet GM, Vaessen MJ, Braakman HM, Hofman PA, Aldenkamp AP, Backes WH,
   PLoS ONE 2012; 7(4): e34125. doi:10.1371/journal.pone.0034125

Co authorship:

1. *Clinical evaluation of language fundamentals in Rolandic epilepsy, an assessment with CELF-4*, Overvliet GM, **Besseling RM**, van der Kruijs SJ, Vles JS, Backes WH, Hendriksen JG, Ebus SC, Jansen JF, Hofman PA, Aldenkamp AP,
   Eur J Paediatr Neurol. 2013; 17(4) 390-396
2. *Correlation between language impairment and problems in motor development in children with rolandic epilepsy,* Overvliet GM, Aldenkamp AP, Klinkenberg S, Nicolai J, Vles JS, **Besseling RM**, Backes W, Jansen JF, Hofman PA, Hendriksen J,
   Epilepsy Behav. 2011; 22(3): 527-531.
3. *Association between frequency of nocturnal epilepsy and language disturbance in children,* Overvliet GM, **Besseling RM**, Vles JS, Hofman PA, van Hall MH, Backes WH, Aldenkamp AP,
   Pediatr Neurol. 201; 44(5): 333-339
4. *Nocturnal epileptiform EEG discharges, nocturnal epileptic seizures, and language impairments in children: review of the literature,* Overvliet GM, **Besseling RM**, Vles JS, Hofman PA, Backes WH, van Hall MH, Klinkenberg S, Hendriksen J, Aldenkamp AP,
   Epilepsy Behav. 2010;19(4): 550-558

In submission:

1. *Abnormal profiles of local functional connectivity proximal to focal cortical dysplasias,*
   René M.H. Besseling, Jacobus F. A. Jansen, Anton de Louw, Mariëlle C.G. Vlooswijk, M. Christianne Hoeberigs, Albert P. Aldenkamp, Walter H. Backes, Paul A.M. Hofman
2. *Delayed convergence between brain network structure and function in rolandic epilepsy,* **René M. H. Besseling**, Jacobus F.A. Jansen, Geke M. Overvliet, Sylvie J.M. van der Kruijs, Saskia C.M. Ebus, Anton de Louw, Paul A.M. Hofman, Johannes S.H. Vles, Albert P. Aldenkamp, Walter H. Backes